

Open Research Online

The Open University's repository of research publications and other research outputs

Laser-induced transient absorption spectroscopy of phthalocyanine dyes

Thesis

How to cite:

Stringer, Mark Richard (1985). Laser-induced transient absorption spectroscopy of phthalocyanine dyes. PhD thesis The Open University.

For guidance on citations see [FAQs](#).

© 1985 The Author



<https://creativecommons.org/licenses/by-nc-nd/4.0/>

Version: Version of Record

Link(s) to article on publisher's website:

<http://dx.doi.org/doi:10.21954/ou.ro.0000f804>

Copyright and Moral Rights for the articles on this site are retained by the individual authors and/or other copyright owners. For more information on Open Research Online's data [policy](#) on reuse of materials please consult the policies page.

oro.open.ac.uk

D 65066/86
UNRESTRICTED

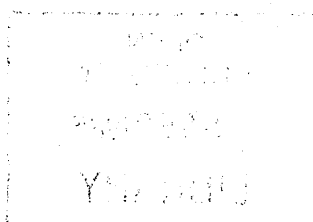
LASER-INDUCED TRANSIENT ABSORPTION
SPECTROSCOPY OF PHTHALOCYANINE DYES

A THESIS PRESENTED TO THE PHYSICS DEPARTMENT
OF THE OPEN UNIVERSITY AS PARTIAL FULFILMENT
OF THE DEGREE OF DOCTOR OF PHILOSOPHY.

by

MARK RICHARD STRINGER B.Sc

JANUARY 1985



Date of submission: Jan '85
Date of award: 24.6.85

ProQuest Number: 27775879

All rights reserved

INFORMATION TO ALL USERS

The quality of this reproduction is dependent on the quality of the copy submitted.

In the unlikely event that the author did not send a complete manuscript and there are missing pages, these will be noted. Also, if material had to be removed, a note will indicate the deletion.



ProQuest 27775879

Published by ProQuest LLC (2020). Copyright of the Dissertation is held by the Author.

All Rights Reserved.

This work is protected against unauthorized copying under Title 17, United States Code
Microform Edition © ProQuest LLC.

ProQuest LLC
789 East Eisenhower Parkway
P.O. Box 1346
Ann Arbor, MI 48106 - 1346

ABSTRACT

This work reports a further investigation into the spectroscopic properties of phthalocyanine dyes in solution. The technique of nanosecond kinetic spectrophotometry was applied, with excitation at both the fundamental ruby laser output wavelength (694 nm) and the second harmonic (347 nm); corresponding in energy to the first and second excited singlet states respectively of several of the phthalocyanine compounds. The resultant transient absorption spectra indicate that the same laser-induced intermediates - those that can be identified as the lowest excited states of singlet and triplet multiplicity - are produced following excitation at either wavelength. However, the transient response also displays a marked perturbation from that characteristic of a 'simple' energy redistribution process; a perturbation that is deduced to be a consequence of both the high intensity of laser excitation and the tendency of the phthalocyanine dyes to form molecular aggregates.

Further evidence is proposed regarding the 'anomalous blue fluorescence' reported from this type of compound, with particular emphasis placed upon the need for a high degree of solute purity.

PREFACE AND ACKNOWLEDGEMENTS

This thesis is arranged in such a way as to fulfil two objectives. The first of these is to describe a program of research, including:

- a) The experimental techniques adopted.
- b) The data obtained.
- c) The conclusions reached in the light of previous work of a similar nature.

The secondary objective is to provide a background against which this specific area of research can be highlighted. For this reason, the opening chapter is the most general; outlining the relevance of both 'continuous' and time-resolved spectroscopic methods in the study of the electronic structure of organic molecules.

Chapter 2 is specific in describing the construction and parameters of the principal experimental arrangement - nanosecond-laser kinetic spectrophotometry - whereas Chapter 3 concentrates upon the structure and spectroscopic properties of one particular group of organic compounds - the phthalocyanine dyes.

The results of the experimental work performed are set out in Chapter 4, with Chapter 5 reserved for the discussion of these results and the exposition of conclusions.

I offer thanks to the entire Physics discipline for allowing me to pursue this research, but I must single out my supervisor, Dr. Keith Hodgkinson, as worthy of special praise; his advice and patient encouragement have been invaluable. I am also grateful to the Chemistry department for the use of some of their equipment and particularly to Dr. David Roberts and Dr. John Coyle for their helpful instruction on matters foreign.

I would not have done without the help and hindrance of the Physics technicians and I certainly would not have done without the financial assistance provided by the Open University - many thanks.

Finally, I am grateful to Pam Taylor who has 'processed' this jumble of long and unusual words and symbols in a manner worthy of better publications.

CONTENTS

	Page
CHAPTER 1 SPECTROSCOPIC METHODS	1
1 ELECTRONIC STRUCTURE AND ABSORPTION	2
(i) Classification of electrons and orbitals	2
(ii) Types of absorption transition	4
2 TRANSITION PROCESSES BETWEEN π -ELECTRON STATES	6
(i) Selection rules	6
(ii) Absorption	8
(iii) Radiative de-excitation	9
(iv) Radiationless transitions	10
(v) Rate parameters	11
3 'CONTINUOUS' SPECTROSCOPY	13
(i) Preamble	13
(ii) Absorption spectroscopy	13
(iii) Fluorescence spectroscopy	16
(iv) Phosphorescence spectroscopy	18
4 TIME-RESOLVED SPECTROSCOPY	19
(i) Preamble	19
(ii) Flash photolysis - principles and advances	20
(iii) Current trends	24
CHAPTER 2 NANOSECOND-LASER KINETIC SPECTROPHOTOMETRY	26
1 EXPERIMENTAL ARRANGEMENT	27
(i) Preamble	27
(ii) Laser excitation	27
(iii) Pulsed Xenon arc-lamp	31

(iv) Optical arrangement	33
(v) Photodetection	36
(vi) System timing	38
2 ANALYSIS OF DATA	38
(i) Reading the polaroids	38
(ii) Transient optical density	40
 CHAPTER 3 PHTHALOCYANINE DYES	 44
1 INTRODUCTION	45
2 MOLECULAR STRUCTURE AND LIGHT ABSORPTION	46
(i) The phthalocyanine unit	46
(ii) Molecular-orbital analyses	47
3 SPECTROSCOPIC OBSERVATIONS OF PHTHALOCYANINES	51
(i) Ground-state absorption	51
(ii) Fluorescence spectra	54
(iii) Time-resolved fluorescence	59
(iv) Stimulated emission	60
(v) Phosphorescence	62
(vi) Saturable absorption	63
(vii) Transient absorption	64
4 SUMMARY	71
 CHAPTER 4 RESULTS	 73
1 INTRODUCTION	74
(i) Experimental procedure	74
(ii) Sample purification	75
(iii) Solution chemistry	75

2	VANADYL PHTHALOCYANINE	76
(i)	Ground-state absorption	76
(ii)	VOPc in toluene . λ_{ex} 694 nm	77
(iii)	VOPc in toluene . λ_{ex} 347 nm # 1	78
(iv)	Fluorescence spectra	78
(v)	VOPc in toluene . λ_{ex} 347 nm # 2	79
(vi)	VOPc in nitrobenzene . λ_{ex} 347 nm	80
(vii)	Summary	80
3	ALUMINIUM PHTHALOCYANINE CHLORIDE	82
(i)	Ground-state absorption	82
(ii)	AlPcCl in ethanol . λ_{ex} 694 nm	83
(iii)	AlPcCl in ethanol . λ_{ex} 347 nm # 1	85
(iv)	Fluorescence spectra	86
(v)	AlPcCl in ethanol . λ_{ex} 347 nm # 2	86
(vi)	Summary	88
4	COPPER PHTHALOCYANINE	90
(i)	Ground-state absorption	90
(ii)	CuPc in 1-chloronaphthalene . λ_{ex} 694 nm	90
(iii)	CuPc in 1-chloronaphthalene . λ_{ex} 347 nm	91
(iv)	Fluorescence spectra	92
(v)	Summary	92
5	ZINC PHTHALOCYANINE	94
(i)	Ground-state absorption	94
(ii)	ZnPc in ethanol . λ_{ex} 347 nm # 1	94
(iii)	Fluorescence spectra	95
(iv)	ZnPc in ethanol . λ_{ex} 347 nm # 2	95
(v)	Summary	96
6	MAGNESIUM PHTHALOCYANINE	97
(i)	Ground-state absorption	97

(ii) MgPc in ethanol . λ ex 347 nm # 1	97
(iii) Fluorescence spectra	98
(iv) MgPc in ethanol . λ ex 347 nm # 2	99
(v) Summary	100
7 METAL-FREE PHTHALOCYANINE	101
(i) Preamble	101
(ii) Ground-state absorption	102
(iii) H ₂ Pc in 1-chloronaphthalene . λ ex 694 nm	102
(iv) H ₂ Pc in toluene . λ ex 347 nm	102
(v) H ₂ Pc in o-xylene . λ ex 694 nm	103
(vi) H ₂ Pc in o-xylene . λ ex 347 nm	104
(vii) Summary	104
8 MISCELLANY	106
(i) Effect of temperature upon the ground-state absorption of H ₂ Pc in toluene.	106
(ii) Effect of temperature upon the ground-state absorption of AlPcCl in ethanol.	107
(iii) Effect of temperature upon the ground-state absorption of ZnPc ethanol.	107
(iv) Effect of concentration upon the ground-state absorption of ZnPc in ethanol.	108
(v) Effect of concentration upon the ground-state absorption of MgPc in ethanol.	108
(vi) Summary	109
CHAPTER 5 DISCUSSION AND CONCLUSIONS	112
1 SATURATION	113
2 TRANSIENT RESPONSE	114
3 'RED' FLUORESCENCE	119

4	'BLUE' FLUORESCENCE	120
5	SUMMARY AND TIPS FOR FUTURE WORK	122
Appendix 1 : Phthalocyanines in use		126
Appendix 2 : Intensity dependance of transient optical density		131
Appendix 3 : Phthalocyanines - a collection of transient absorption spectra		133
Appendix 4 : Solute purification		134
References		136

CHAPTER 1

SPECTROSCOPIC METHODS

1.1 ELECTRONIC STRUCTURE AND ABSORPTION

1.1(i) Classification of electrons and orbitals

The fundamental element of organic chemistry is the carbon atom. The electronic structure of organic compounds is determined by the manner in which this element participates in molecular bonding, and the three types of bonding arrangement that can be distinguished may be explained in terms of the concept of hybridization.(1)

The ground-state electronic configuration of the carbon atom is denoted as $1s^2 2s^2 2p^2$. However, upon forming compounds one of the electrons in a 2s atomic orbital is promoted to a 2p orbital and the electronic configuration becomes $1s^2 2s^1 2p^3$. The formation of three types of hybrid arrangement are thus possible, involving the participation of two, three, or all four of the valence electrons; mixing the single 2s electron orbital with one, two, or all three of the 2p orbitals generates sp (digonal), sp^2 (trigonal) and sp^3 (tetragonal) hybridization respectively.

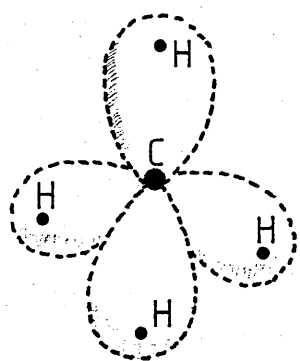
In the latter scheme, four identical hybrid orbitals are produced that are directed towards the corners of a regular tetrahedron centred on the carbon nucleus. These are termed σ (sigma)-orbitals and are occupied by σ -electrons. This type of orbital can associate with the orbitals of other atoms to produce σ -bonds, and those compounds in which each

carbon atom forms four bonds of σ -type are said to be saturated (such as methane CH_4 [Fig.1.1(a)], ethane C_2H_6). A σ -bond is treated as being localised about the axis between the bonded atomic nuclei and the probability distribution of each σ -electron is rotationally symmetric about the bond.

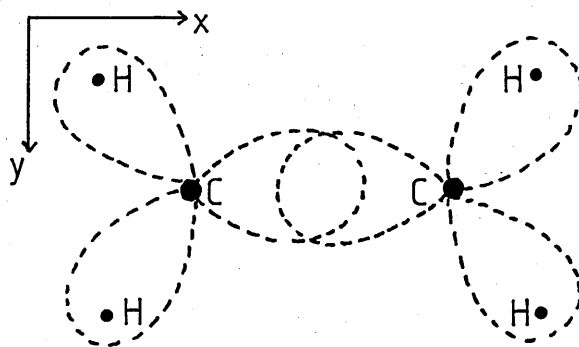
In sp^2 hybridization, three equivalent σ -orbitals are produced that lie in the same plane and are inclined at 120° to each other. It is this arrangement that forms the structure of ethylene, which is the simplest unsaturated - or conjugated - compound [Fig.1.1(b)], and also accounts for the hexagonal ring structure of benzene, the prototype of the aromatic hydrocarbons.

The remaining p-atomic orbital associated with each carbon atom is unchanged by this hybridization and in contrast to the σ -orbitals, the wavefunction is perpendicular to the molecular plane. Electrons in such orbitals are designated π (pi)-electrons. In an unsaturated compound the π -orbital of each carbon atom can interact to produce π -bonds. However, the π -electrons can be treated as being delocalised to form π -molecular orbitals and, as shown in Fig.1.2, the maximum charge density of this type of orbital lies above and below the molecular plane.

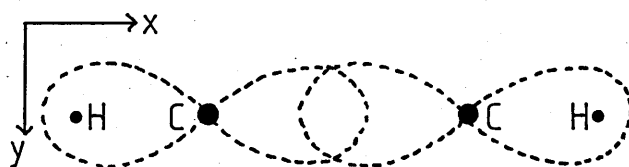
In the third arrangement, sp hybridization, two equivalent σ -orbitals are produced that are directed at 180° to each other. This configuration accounts for the linear structure



(a) Methane

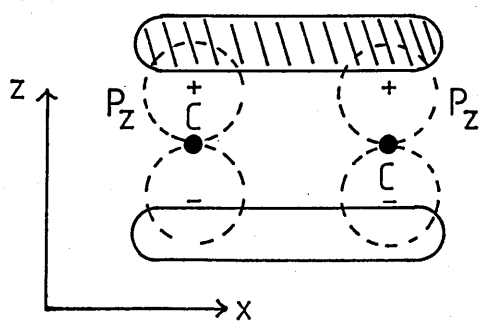


(b) Ethylene

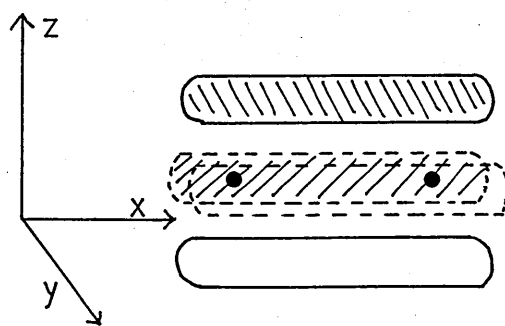


(c) Acetylene

Fig.1.1: The formation of σ -bonds.



(a) Ethylene



(b) Acetylene

Fig.1.2: The formation of π molecular orbitals.

of molecules such as acetylene [Fig.1.1(c)]. As well as the localised C-C and C-H σ -bonds, the two remaining π -orbitals associated with each carbon atom may be paired to produce orthogonal π -molecular orbitals (Fig.1.2(b)).

In addition to the arrangement of σ and π -electrons, in some compounds (notably those containing elements of group V, VI or VII of the periodic table) there are non-bonding valence shell electrons (n) which are not involved in bonding relationships and can be regarded as being localised on their atomic nuclei.

1.1(ii) Types of absorption transition

It is the absorption of the appropriate wavelength of electromagnetic radiation that induces transitions from one molecular energy state to another and the possible electronic transitions are shown in Fig.1.3.(2)

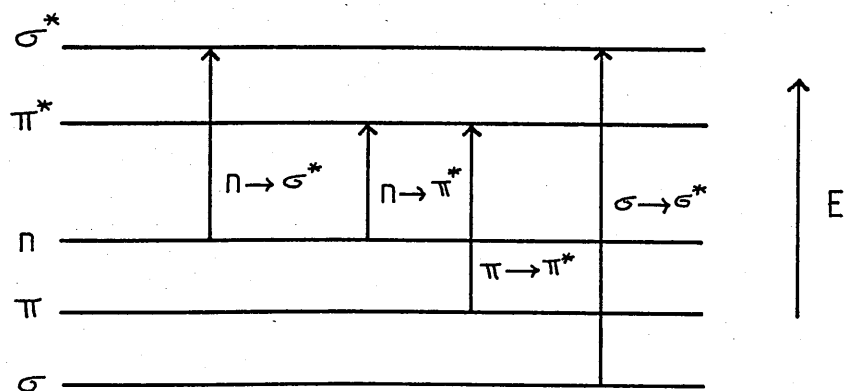


Fig.1.3

Types of absorption transition

The σ -electrons are tightly bound and thus form the lowest energy electronic state. The delocalised π -electrons are less tightly bound, and the non-bonding electrons (if any are present) have an energy that is the same as that of electrons occupying the corresponding atomic orbitals on the isolated atom. The highest energy absorption transition is clearly between the bonding and anti-bonding - or excited - state of σ -type, denoted as $\sigma \rightarrow \sigma^*$. Many saturated molecular systems allow such transitions, which correspond to the absorption of electromagnetic radiation in the ultra-violet region of the spectrum, of such short wavelength that the absorption can only be recorded by using a spectrograph that can be evacuated to eliminate absorption by atmospheric oxygen.(3) It is the transmission of visible and near u-v radiation and the chemical stability of many saturated compounds that allows their use as spectroscopic solvents (e.g. n-heptane, methyl-cyclohexane).

It is the $\pi \rightarrow \pi^*$ transitions that are common in conjugated compounds and these occur at longer wavelengths than the corresponding $\sigma \rightarrow \sigma^*$ transitions. In general, the greater the number of atoms involved in the formation of such a molecule, the greater is the shift of the principal absorption to longer wavelengths.(4) Organic dyes, which have a strong absorption in the visible region of the spectrum, usually consist of a long-chain π -electron system.

The delocalisation of the π -electrons implies that each

electron has a large freedom of motion. It is under this assumption that one type of theoretical model - a free-electron molecular orbital [FEMO] model - can often be applied to the π -electronic states of conjugated and aromatic compounds. An example of such a model applied to one specific group of compounds - the phthalocyanine dyes - is detailed in Chapter 3.

Since the initial step in a photophysical or photochemical process is usually a photon-induced π - π^* transition, it is important to consider the energy redistribution processes involving these electronic states.

1.2 TRANSITION PROCESSES BETWEEN π -ELECTRON STATES

1.2(i) Selection rules

An electronic state is characterised⁽⁵⁾ by the parameters of energy, multiplicity and symmetry (which, in centro-symmetric molecules includes parity). When a molecule absorbs a photon, its energy increases by an amount equal to that of the photon. This is expressed by the relation:

$$E = h\nu = \frac{hc}{\lambda} \quad (1.1)$$

where h is Planck's constant, ν and λ are the frequency and wavelength of the radiation respectively and c is the velocity of light.

The multiplicity, symmetry and parity determine the selection

rules which dominate the probability of transition.

Multiplicity describes the total spin angular momentum in the system and is given by:

$$\text{Multiplicity} = 2S + 1 \quad (1.2)$$

where S is the sum of the spin angular momentum components.

In an unexcited molecule, which has an even number of π -electrons in the ground state, the electrons are paired in accordance with the Pauli exclusion principle to produce a total spin of zero. Thus the multiplicity of such a state is unity and the state is termed a singlet. If the π -electron is excited with no reversal in its spin direction then the resultant excited state is also a singlet. If however, the electron undergoes a reversal of spin upon excitation, then an excited triplet state is produced. The multiplicity selection rule dictates that transitions between electronic states of different multiplicity are forbidden.

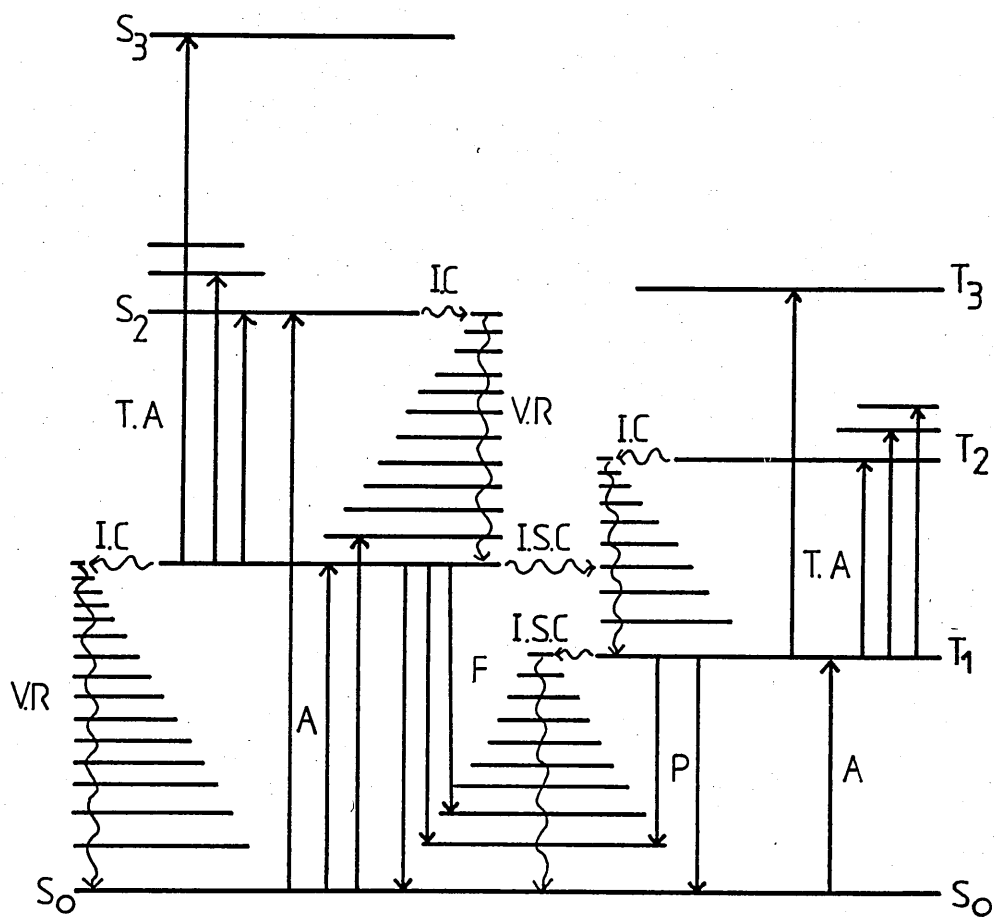
Similarly, transitions between electronic states of the same molecular symmetry are forbidden. In addition, in centrosymmetric molecules, where the states are labelled either as even (g:gerade) or odd (u:ungerade) parity (depending upon whether the wavefunction associated with the electronic state is symmetric or antisymmetric with respect to reflection in the centre of gravity of the molecule), the parity selection rule dictates that transitions between electronic states of the same parity ($g \rightarrow g$, $u \rightarrow u$) are forbidden.

The fact that many 'forbidden' transitions are observed with finite intensity in many molecules is due to intra-molecular or inter-molecular perturbations. Thus singlet-triplet transitions may be enhanced by the presence of paramagnetic substances (such as O_2) or if the molecule or its environment contains heavy atoms. Also, molecular vibrations and interactions with adjacent states distort the symmetry and parity of the higher electronic states, introducing an element of 'allowedness' of transition.

The relative energy spacing of the ground and excited molecular energy levels is represented on a Jablonski diagram [Fig.1.4]. The triplet state is always lower in energy than the corresponding singlet state as a consequence of a molecular analogue of Hunds rule.⁽⁶⁾ Vibrations of the atomic nuclei making up the molecular skeleton may also be induced and the energy levels associated with these quantised molecular vibrations are shown. It is necessary to include in a complete description the rotational levels also, but their energy spacing are too small to be represented on this diagrammatic scale; the notation of photophysical processes is commonly simplified by specifying only the electronic and vibrational changes - so called 'vibronic' transitions.

1.2(ii) Absorption

A molecule is excited from a lower to a higher electronic state by the absorption of a photon at the appropriate



A: Absorption
 F: Fluorescence
 P: Phosphorescence
 ISC: Inter-Sytem Crossing
 IC : Internal Conversion
 VR: Vibrational Relaxation
 T.A: Transient Absorption

Fig. 1.4

Jablonski diagram

energy. In the absence of any external perturbation, the Boltzmann equation (equation 1.3) predicts that at room temperature, the lowest vibrational level of the ground electronic state has a far greater population than any other state:

$$\frac{N_2}{N_1} = e^{-(E_2-E_1)/kT} \quad (1.3)$$

where N_1 , N_2 are the populations of vibrational levels of energy E_1 , E_2 respectively.

$$E_2 - E_1 \approx \frac{1}{8} \text{ eV}$$

and $kT \approx \frac{1}{40} \text{ eV} \quad (\text{at } 300^\circ\text{K}).$

Therefore the population of the first 'hot' vibrational level is about e^{-5} times of the lowest. It is for this reason that the absorption of radiation is assumed to occur from the state S_{00} into one of the vibronic levels S_{pn} , the exact level depending upon the energy of the photons.

Absorption from $S_{00} \rightarrow T_{qm}$ may occur but as discussed previously, it is a spin-forbidden transition and is generally a factor of $\approx 10^8$ less intense than singlet-singlet absorption. Such absorption lies to longer wavelengths (visible and near i.r.).

1.2(iii) Radiative de-excitation

A molecule may lose energy by undergoing a transition from a higher to a lower vibronic state with the emission of a

photon. Such a radiative transition between states of the same multiplicity is called fluorescence; between states of different multiplicity it is called phosphorescence. Again, the spin-forbidden transition of phosphorescence is much less intense than the highly allowed fluorescence transition. The failure to observe radiative transitions from higher electronic states (S_p , T_q) led to the formulation of Kashas' rule (7) which states that, in a complex molecule, emission occurs from the lowest excited electronic state of a given multiplicity (S_1 or T_1). Exceptions to Kashas' rule are not unknown (8), nevertheless it will be assumed here that radiative transitions do occur from the lowest vibrational level of the first excited electronic state to a vibrational level of the ground state.

1.2(iv) Radiationless transitions

A transition which occurs between isoenergetic vibrational levels of different electronic states takes place with no emission of photons. Such a transition between states of the same multiplicity is termed internal conversion, between states of different multiplicity; inter-system crossing. Internal conversion occurs very rapidly between upper excited states, accounting for the lack of emission from the upper states, whereas the internal conversion transition $S_1 \rightarrow S_0$ is so much slower that fluorescence can compete. The inter-system crossing process from the singlet to triplet manifold (normally $S_1 \rightarrow T_1$) is also competitive with fluorescence.

These transitions are often preceded by thermal activation of the initial electronic state and/or followed by vibrational relaxation of the final electronic state.

1.2(v) Rate parameters

The probability of a uni-molecular process is independent of time and is expressed as a first-order rate parameter k (in units of s^{-1}). If a molar concentration of $[X^*]$ moles l^{-1} of an excited molecule decays by a uni-molecular process, then the rate of decay of $[X^*]$ is given by:

$$\frac{-d[X^*]}{dt} = k_x [X^*]. \quad (1.4)$$

It is often implied that there are no 'instantaneous' processes, but this is not so - absorption transitions are immeasurably fast in principle. Following excitation into a high vibronic energy level ($S_{00} \rightarrow S_{pn}$), the excess energy is rapidly degraded by a combination of internal conversion and vibrational relaxation until the lowest vibrational level of S_1 is reached - in keeping with Kasha's principle. The combined rate parameter for this process may be expressed as k_{ic} ($\approx 10^{12} s^{-1}$). From the level S_{10} , the three processes of fluorescence to the ground state, internal conversion/vibrational relaxation to the ground-state and inter-system crossing to the triplet state are competing processes and have comparable rate parameters, i.e. $k_f \approx k_{ic}$

$\approx k_{isc} (\approx 10^8 \text{ s}^{-1})$. The reason why $k_{ic}' \gg k_{ic}$ is that the higher excited electronic states are separated by a smaller energy gap than that between the first excited state and the ground-state. The radiationless relaxation process is strongly dependent upon the energy gap between the electronic states involved, with the transition probability decreasing as this energy difference increases.

Transitions from the lowest triplet state (phosphorescence and inter-system crossing to the ground state) have much smaller rate parameters, $k_p \approx k_{isc} (\approx 10^3 - 10^{-1} \text{ s}^{-1})$, since they are spin-forbidden. Therefore, translating these rate parameters into excited state lifetimes by the simple relation:

$$\tau = \frac{1}{\Sigma k} \quad (1.5)$$

it is clear that triplet states have a relatively long natural lifetime ($\approx 10 - 10^{-3} \text{ s}$). Not only does this mean that it is possible to build up an appreciable population within the triplet state, but also that within this lifetime the excited molecule may undergo some chemical reaction within its environment. This is the basis of photochemistry.

Therefore both conventional spectroscopic methods and a means of monitoring transient phenomena are necessary in providing a full description of the excited states of a molecular species.

1.3 'CONTINUOUS' SPECTROSCOPY

1.3(i) Preamble

The present theories concerning the electronic structure of molecules, as only briefly described here, derive from the accumulation of vast amounts of empirical data, much of which has been provided by the three standard spectroscopic techniques employing a continuous light source as excitation: absorption, fluorescence and phosphorescence spectroscopy. It is useful to consider what information these techniques can provide and what their limitations are, particularly when compared to time-resolved studies.

1.3(ii) Absorption spectroscopy

An absorption spectrum is completely described by a plot of absorption intensity against wavelength. Ultra-violet and visible spectroscopy is usually performed using a commercial double-beam spectrometer with the molecular samples in solution. The graphical output shown in Fig.1.5 comprises an absorption band system corresponding to a number of vibronic transitions. Such an envelope of vibronic bands is referred to as the Franck-Condon envelope, this follows from the principle developed by Franck and Condon which states that, because the time required for an electronic transition is negligible compared with that of nuclear motion, the most probable vibronic transition is one involving no change in

nuclear co-ordinates.⁽⁹⁾ Also the most intense band is called the Franck-Condon maximum. If this coincides with the 0-0 band, then it indicates that the nuclear configuration of the excited state is similar to that of the ground-state (Fig.1.5(a)). For molecules in which the Franck-Condon maximum is displaced with respect to the 0-0 transition, the nuclear configuration of the excited state is displaced relative to the ground-state (Fig.1.5(b)). The wavelengths at which the vibronic bands are to be found indicate not only their energies above the ground state, but also the relative energy separation of the vibrational levels of the excited state.

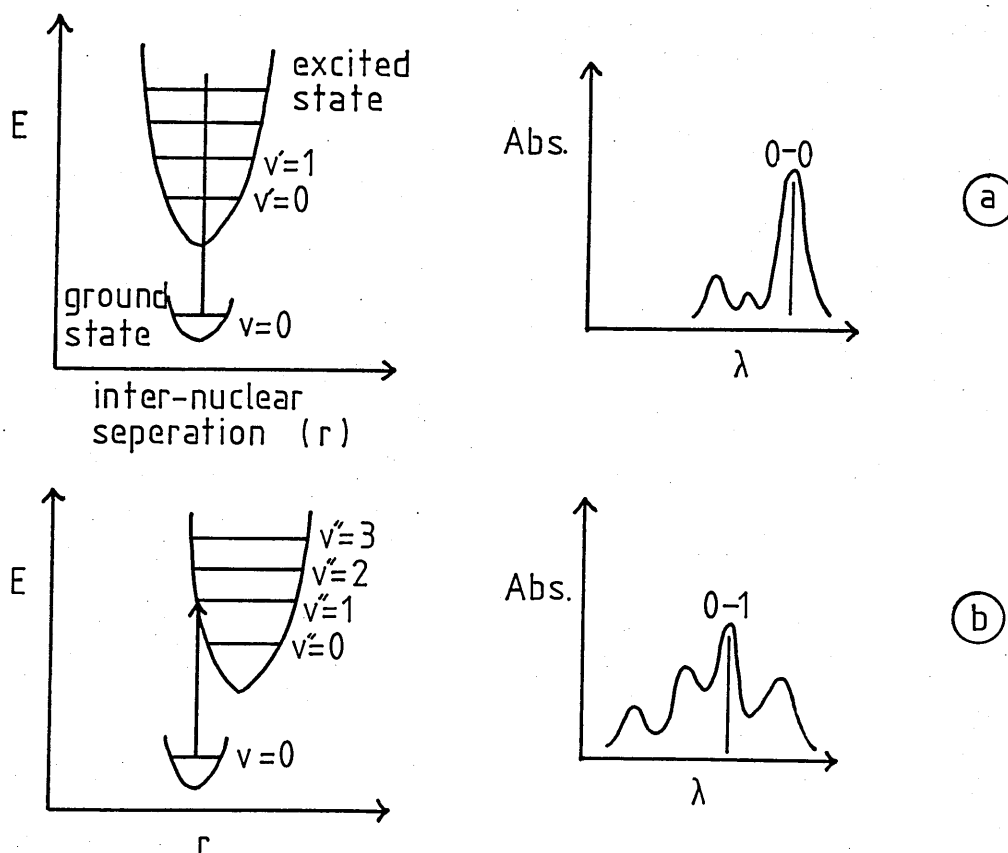


Fig.1.5

Dependence of absorption maximum upon nuclear geometry.

Absorption intensity is usually plotted in units of optical density or as the extinction coefficient. These parameters are related by the Beer-Lambert law:

$$I_t = I_0 10^{-\epsilon c l} \quad (1.6)$$

where I_0 , I_t are the incident and transmitted light intensity.

ϵ = decadic molar extinction coefficient.

c = concentration of absorbing species.

l = optical path length.

rearranging:

$$\text{optical density} = \log I_0/I_t = \epsilon c l \quad (1.7)$$

According to this equation the optical density of a solution should remain constant as long as the product of concentration and path length remain constant. However, the extinction coefficient quite often varies with concentration of the solute due to molecular association, or it may be inaccurately recorded due to fluorescence emission or poor solvent transmission.

An alternative measure of absorption intensity is the oscillator strength:

$$f = 4.3 \times 10^{-9} \int \epsilon d\bar{\nu} \quad (1.8)$$

where $\int \epsilon d\bar{\nu}$ is the area under a curve of extinction coefficient plotted against wavenumber $\bar{\nu}$ ($= \frac{1}{\lambda} \text{ cm}^{-1}$). The rate constant for emission from an excited state is related to the oscillator strength by:

$$k_e = \frac{2 f \bar{\nu}_0^2}{3} \quad (1.9)$$

where $\bar{\nu}_0$ is the wavenumber corresponding to the maximum of absorption. Therefore it is possible to estimate the emissive lifetime of an excited state by the intensity of its absorption band.

1.3(iii) Fluorescence spectroscopy

A fluorescence emission spectrum is a plot of emission intensity as a function of wavelength, for a fixed excitation wavelength and intensity. Normally fluorescence transitions occur between the lowest vibrational level of the first excited state and the vibrational levels of the ground state. Therefore information is gathered about the energy separation of the ground and first excited electronic state and also that of the vibrational modes of the ground state. This is particularly useful when the usual techniques of the characterisation of vibrational energy levels, i.e. infra-red and Raman spectroscopy, are not applicable, for instance when a molecule lacks a permanent dipole moment.

The Franck-Condon principle applies to the emission process as well as to absorption, and maximum intensity of absorption and fluorescence occur when the overlap integral between the wavefunctions of the initial and final state is large. The difference in position of the maximum of emission and of the zero-zero transition on a wavelength scale is the "Stokes

shift" and is a measure of the change in geometry between the two states involved in the transition. Provided the vibrational frequencies of the excited state are similar to those of the ground-state, the normal fluorescence spectrum and the absorption spectrum have a mirror-image relationship.⁽¹⁰⁾ This is illustrated in Fig.1.6 for an anthracene solution.

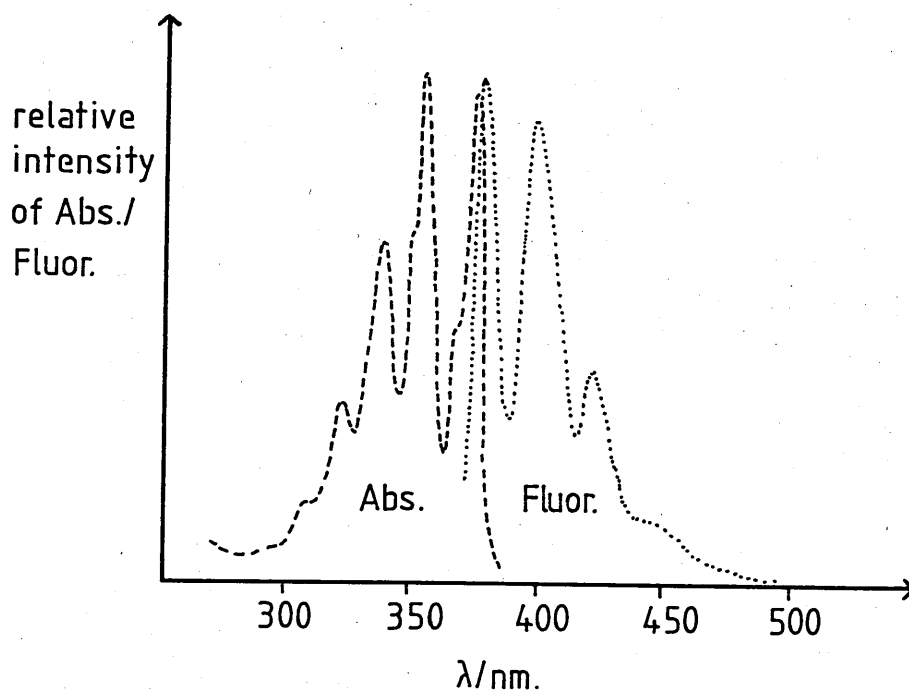


Fig.1.6: Anthracene in ethanol: mirror-image relationship.

A fluorescence excitation spectrum is a plot of fluorescence emission intensity (at a fixed emission wavelength) as a function of excitation wavelength. The observed spectrum varies with the sample extinction coefficient i.e. it will have the same appearance as the absorption spectrum. An advantage of excitation spectroscopy over standard absorption spectroscopy is the greater sensitivity of the luminescent technique, allowing observations of excitation spectra at concentrations too low to be measured accurately by

absorption.

1.3(iv) Phosphorescence spectroscopy

It was Lewis et al. (11) who determined that the long-lived luminescence that is observed from some organic compounds originates from the lowest triplet state. It was demonstrated (12) that such molecules irradiated in a rigid glass medium show both phosphorescence and paramagnetic susceptibility due to the parallel spin alignment of the excited and ground-state electrons. Both radiative and non-radiative $T_1 \rightarrow S_0$ relaxation are spin-forbidden processes which results in a long triplet lifetime; therefore the triplet state is susceptible to the presence of impurities which take part in bimolecular quenching processes. For this reason, phosphorescence is usually studied in a clear rigid glass at 77°K which serves to inhibit diffusion. Since the phosphorescence emission bands may overlap slightly with the fluorescence bands, the technique of phosphorimetry is used to separate the two processes. A phosphorimeter uses a chopped excitation beam and also chops the output in such a way that the excitation and detected emission are out of phase. This allows the phosphorescence intensity to be monitored over a period when the short-lived fluorescence has decayed to zero. The measurement of phosphorescence lifetimes is also possible.

The phosphorescence emission spectrum is a plot of emission

intensity as a function of wavelength, monitored at a fixed excitation wavelength and intensity. It allows the determination of the energy of the first excited triplet state and has vibrational structure corresponding to transitions $T_{10} \rightarrow S_{0n}$.

A phosphorescence excitation spectrum is equivalent to the $S_{00} \rightarrow T_{1M}$ absorption, though it requires the use of an intense excitation source. The technique is much less susceptible to errors due to residual impurities than is direct $S_0 \rightarrow T_1$ spectroscopy.

1.4 TIME-RESOLVED SPECTROSCOPY

1.4(i) Preamble

The description of phosphorescence spectroscopy suggests that it is not a truly continuous method of analysis in that the chopping of the excitation beam provides a means of producing a train of pulses, the temporal width of the pulses depending on the speed of revolution of the chopper. This enables the measurement of phosphorescence lifetimes and is an example of the fundamental criterion in transient spectroscopy, i.e. to be able to monitor short-lived events in a molecular system, the excitation which produces the transient species should be of shorter duration than the event itself. In effect, the system is excited and the relative concentrations of the transients created are plotted as a function of time, either

by monitoring the luminescence or by following the time-history of some other physical property.

Although the study of luminescence has been common since last century, using spark sources for excitation, a new-era of time-resolved spectroscopy was stimulated by the development of high intensity flash-lamps that went hand-in-hand with the development and progress of the flash photolysis technique.

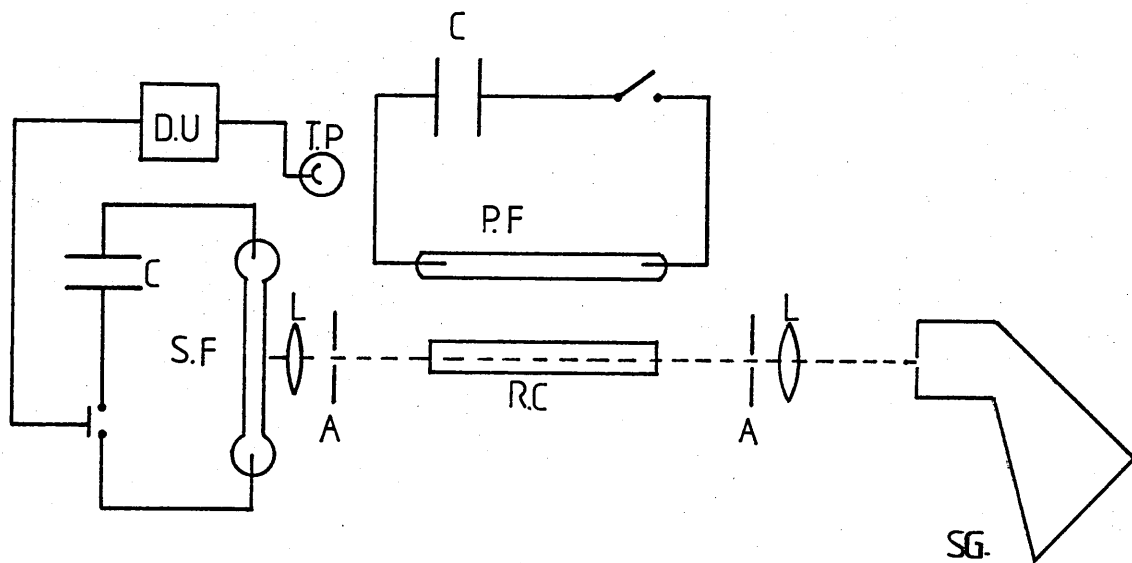
1.4(ii) Flash photolysis: principles and advances

Flash photolysis is a technique in which a high intensity pulse of light generates transient species in sufficient concentration that they may be detected by their absorption spectrum. Different forms of the technique have been developed; all rely upon the flash generation of transients, but the recording of the resultant absorption varies in each case. In FLASH SPECTROSCOPY (Fig.1.7(a)) the excitation flash generates the transient species and their absorption spectrum is recorded using light from a short-duration, less intense flash - the spectroscopic flash. This light passes through the sample to a spectrograph where the photographic plate records the light intensity as a function of wavelength. In this way a complete transient absorption spectrum is recorded at a set time interval after excitation. By varying the delay between the excitation and spectroscopic flashes the relative intensity of absorbance over the complete spectrum may be recorded as a function of time.

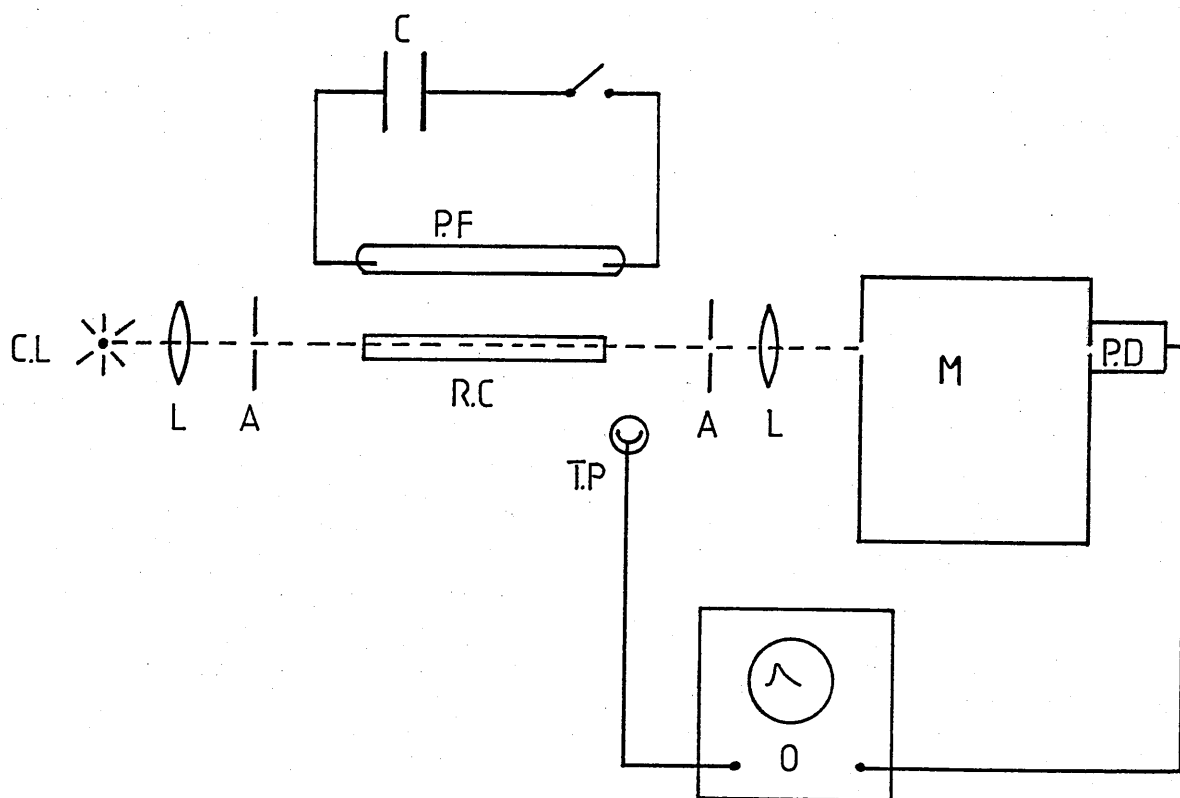
Fig. 1.7

Abbreviations

A	:	Aperture
C	:	Capacitor
C.L	:	Continuous Lamp
D.U	:	Delay Unit
L	:	Lens
M	:	Monochromator
O	:	Oscilloscope
P.D	:	Photo-Detector
P.F	:	Photolysis Flashlamp
R.C	:	Reaction Cell
S.F	:	Spectroscopic Flashlamp
S.G	:	Spectrograph
T.P	:	Trigger Photocell



a) Flash Spectroscopy



b) Kinetic Spectrophotometry

In KINETIC SPECTROPHOTOMETRY (Fig.1.7(b)) the excitation flash generates the transient species and their decay kinetics are monitored at a single wavelength using a continuous light source. The light passes through the sample to a monochromator/photodetector/oscilloscope combination where the photodetector responds to the light intensity as a function of time and its output signal is displayed by the oscilloscope. In this way a complete time profile of the transient species is recorded at a set wavelength. In order to build up a complete transient absorption spectrum, many readings must be taken at closely spaced wavelength intervals. In order to achieve simultaneous spectral and temporal resolution following a single excitation flash, the RAPID-SCAN (14) method may be adopted. This combines the objectives of both flash spectroscopy and kinetic spectrophotometry. The apparatus includes a steady monitoring source as well as a means of rapidly scanning either the spectral or the time 'axis' - such as a rotating or oscillating mirror in the dispersion equipment. If the detection system consists of a spectrograph and photographic plate, the entire spectrum can be monitored over a range of times by one scan of the mirror. In combination with the monochromator and photodetector it is necessary to scan repeatedly over the desired range of wavelengths at a rate determined by the period of revolution of the mirror.

Whichever method of analysis is chosen, the time resolution

of the experiment is determined by the duration of the excitation flash. Early flash photolysis arrangements (15,16) used flash-lamps discharged from large banks of capacitors which produced an intense, though long-duration ($\approx 1\text{ms}$) output. Subsequent developments in flash lamp design and in discharge circuits reduced the duration of the flash to 10^{-5} sec (17,18), while maintaining sufficient intensity to produce reasonable transient concentration. Further reductions of gas discharge output duration to $\approx 10^{-9}$ (19) provided an excitation source which became useful in the measurement of fluorescence lifetimes and for characterising instrument response functions but have too low an intensity to be used in flash photolysis. Thus the flash photolysis technique was restricted to the study of transients with lifetimes $\geq 1\mu\text{s}$. This includes transient absorption from the lowest triplet state (T_1) of many organic molecules. (20,21)

With the development of the Q-switched solid-state laser (22,23) came an improvement in the time resolution of the flash photolysis technique by a factor of several hundred. The ruby laser (fundamental wavelength 694.3nm) and neodymium:glass laser (1060nm) were found to be capable of delivering high intensity outputs in 10-30ns. However these two wavelengths are longer than that of the principal absorption band of most organic molecules. For this reason many workers utilized the phenomenon of harmonic generation which occurs when laser radiation is passed through a non-linear crystal such as KDP. In this way, nanosecond flash

photolysis experiments were performed which used the frequency-doubled ruby laser (347nm)(24,25) and the frequency quadrupled Nd:glass laser(26) (265nm) as excitation source. Much of the early work concentrated upon the study of transient absorption from the lowest excited singlet state (S_1) of organic compounds and such transitions highlight the advantages of time-resolved spectroscopy over conventional techniques. Since the ground state (S_0) in these molecules is of even (g) parity, the most intense absorption bands are those corresponding to transitions to states of odd (u) parity, i.e. $S_0(g) \rightarrow S_1(u)$. Transitions from S_0 to excited states of even parity have a much lower probability and are less intense or absent from the spectrum. However transitions $S_1(u) \rightarrow S_p(g)$ are not parity forbidden so that such short-lived absorption provides a means of characterising excited states not accessible directly from the ground state.

An example of a particular limitation of ground state absorption spectroscopy is that the u-v cutoff of many solvents occurs between 200nm and 300nm which prevents the accurate detection of absorption bands which lie to shorter wavelengths. Using the state S_1 as a temporary 'base' for absorption allows access to the higher energy excited states.

The advantages of a laser source over a flash-lamp in a flash photolysis apparatus are not restricted to the improvement in time resolution. The monochromatic nature of a laser beam

ensures that all the excitation energy is concentrated at one very narrow band of wavelengths compared to the 'wasteful' white light produced by flash lamps. Also the collimation of the laser beam allows the sample to be remote from the laser source, whereas, the need to collect the maximum excitation light from flash lamps results in their proximity to the sample chamber.

1.4(iii)Current trends

The development of mode-locked lasers (27,28) shortly after the introduction of nanosecond lasers provided a further improvement in time resolution of the excitation source. The generation of light pulses lasting only several picoseconds presented the possibility of following the initial energy redistribution processes subsequent to excitation. As a consequence this improvement also stimulated the development of light detectors of improved time resolution and of new principles in the monitoring of ultra-fast processes. Picosecond spectroscopy is now established in many laboratories, with the dye laser, synchronously pumped by a c-w mode-locked ion laser, having evolved as the most versatile source of excitation. In combination with the streak camera it is possible to monitor, in real time, fluorescence emission with a time resolution of lps or less.(29) Using pump and probe methods, transient absorption/bleaching can be monitored with a time resolution determined by the temporal width of the laser pulse, as can

such gated emission studies as frequency up-conversion.(30)

It must be emphasised that by no means all of the transient species monitored by time-resolved spectroscopy are those described by unimolecular physical processes. The first flash photolysis experiments were developed specifically for the study of free-radicals created by the disruption of molecular bonds, and subsequent improvements in time resolution have made available a wealth of information on a variety of transient processes in physics, chemistry and biology.(31-33)

The availability of conventional and nanosecond (excimer laser) flash photolysis equipment as commercial packages is evidence enough that the development and widespread use of picosecond techniques has not made these 'slower' methods redundant. Each method is particularly suited to a certain type of study though it is evident that much of the glamour of laser spectroscopy lies with those in the 'picosecond club'.

In an attempt to redress the balance, this work concentrates upon the use of a nanosecond source - a Q-switched ruby laser - as the excitation in a kinetic spectrophotometry arrangement.

CHAPTER 2

NANOSECOND-LASER KINETIC SPECTROPHOTOMETRY

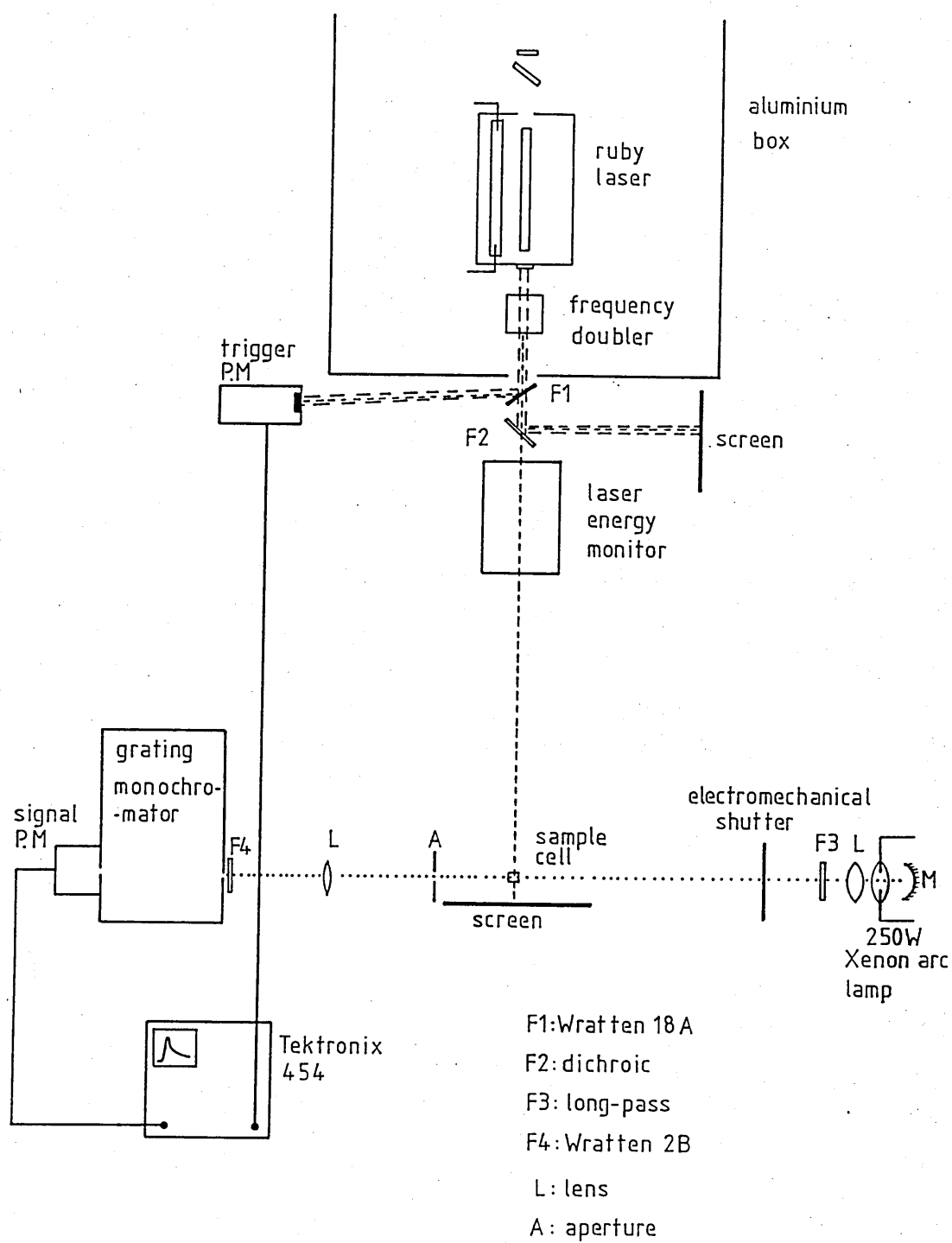


Fig.2.1: Experimental Arrangement (λ_{ex} 347nm.)

2.1 EXPERIMENTAL ARRANGEMENT

2.1(i) Preamble

The experimental arrangement [Fig.2.1] is an adaption of that used by Hodgkinson (1972)⁽³⁴⁾ and De-Silva (1976).⁽³⁵⁾ The excitation source is a Q-switched ruby laser and the output at either the fundamental wavelength (694.3nm) or the second-harmonic wavelength (347.1nm) may be used. The monitoring light is provided by a pulsed xenon arc-lamp.

2.1(ii) Laser excitation

The ruby laser consists of a 6-inch long, 5/8-inch diameter ruby rod, positioned along one of the foci of a highly reflective elliptical chamber [Fig.2.2].

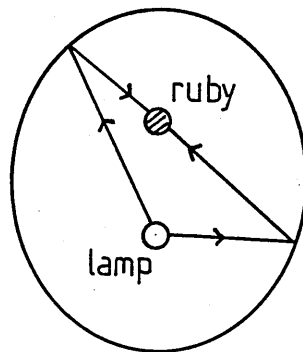


Fig. 2.2

Elliptical pumping chamber

A linear xenon flash-lamp lies along the other focus of the ellipse, parallel to the ruby rod. This flash lamp is the

pumping source and it is supplied with electrical energy by a large bank of capacitors (1800 μ f) charged to a voltage of around 2.2kV. The energy discharged through the lamp per flash is given by:

$$E = \frac{1}{2} CV^2 \approx 4400 \text{ J} \quad (2.1)$$

The pumping flash has a half-height duration of 1.5 ms as shown in Fig.2.4(a).

The flash-lamp and ruby rod are both cooled by a continuous flow of distilled, deionized water in order to prevent damage by heat generated during the intense light flash.

The ruby rod forms the active medium of the laser, while the optical resonant cavity, which is necessary to provide the feedback which promotes laser action, is formed using a dielectric mirror at the non-output end of the laser and a quartz etalon (14% reflective at 694.3nm) as the output coupler [Fig.2.3]. The cavity is relatively lossy and since

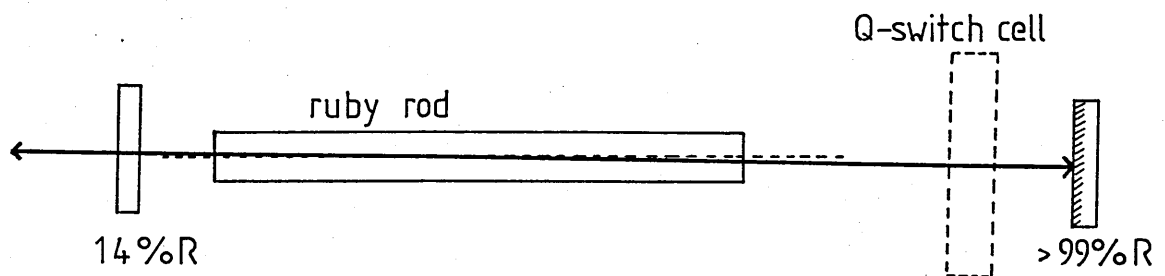


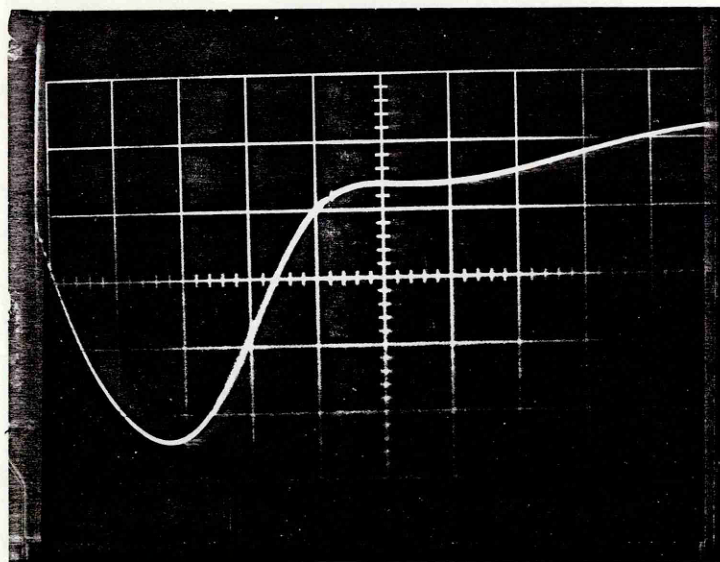
Fig.2.3:Optical resonant cavity.

ruby is a three level laser medium, in which more than half the ground state atoms need to be excited in order to generate a population inversion, it is clear why a high pumping energy is required for the lasing threshold to be reached.

The laser light passing through the output reflector following flash-lamp pumping consists of an envelope of 'spikes' which are random in energy and separation [Fig.2.4(b)]. The irregularity and total time duration of this normal-mode laser pulse would seriously limit the usefulness of the laser as a spectroscopic source if it were not for the technique of Q-switching, in which the laser is able to produce a high-power, short duration - or "giant"-pulse.

A passive Q-switch is used in this laser system; a solution of vanadyl phthalocyanine (VOPc) dissolved in nitrobenzene is contained in a 1-cm path-length quartz cell which is placed in the optical resonant cavity between the rear reflector and the end of the ruby rod. As this solution absorbs light strongly at 694.3nm (concentration adjusted to allow 40% transmittance), oscillation within the resonant cavity is inhibited, with the result that a much higher than normal population inversion is built up within the ruby rod. As soon as the ruby starts to emit coherent light, the solution bleaches, i.e. becomes highly transmitting at the ruby laser output wavelength and a giant pulse results. Fig.2.4(c)

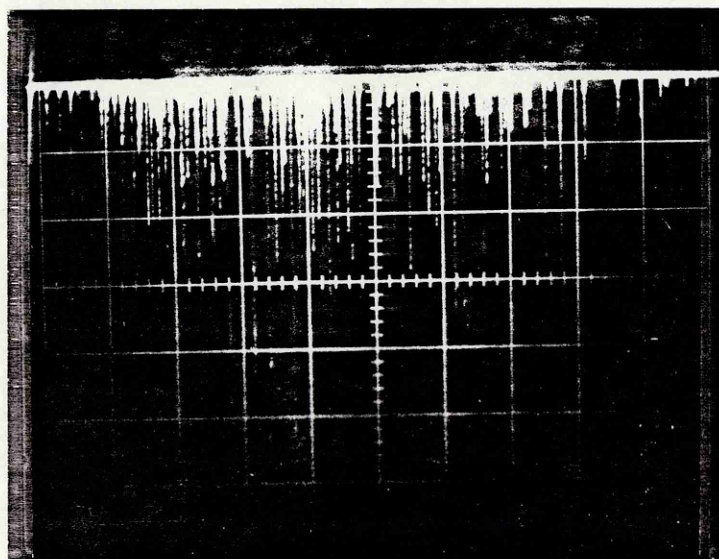
(a)



Xenon
flash-lamp
output.

0.5 ms/div

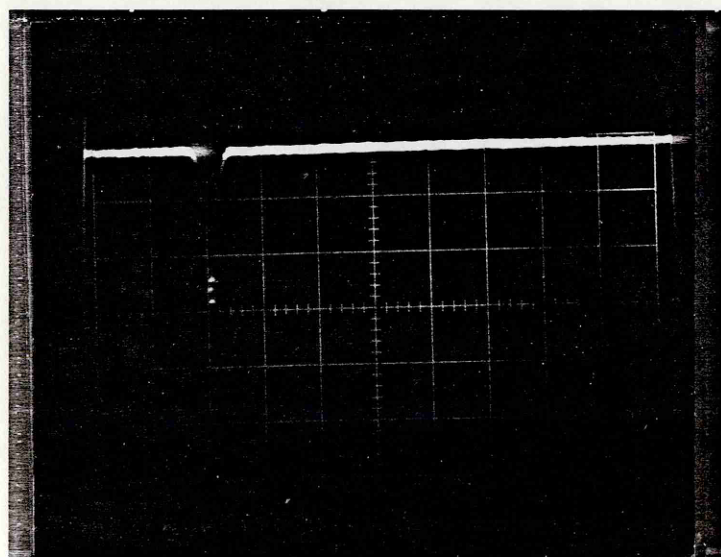
(b)



normal-mode
laser pulse.

0.2 ms/div

(c)



Q-switched
laser pulse.

50 ns/div

Fig. 2.4

shows the laser pulse to have a half-width of 15ns and the energy output at 694.3nm is highly reproducible and greater than 1 J. It is important that the end faces of the ruby rod are not parallel with the resonator reflectors, otherwise "pre-lasing" occurs; this has the effect of broadening the Q-switched laser pulse.⁽³⁶⁾ Therefore the rod is slightly angled within the resonant cavity.

As mentioned in the previous chapter, the principal absorption band of most organic molecules lies in the blue or near u-v region of the spectrum. This means that excitation at the ruby laser fundamental wavelength is normally impractical - this was certainly the case for many of those compounds which were the subject of investigation in the early nanosecond laser photolysis experiments. However, by placing a frequency-doubling crystal in the path of the laser beam, a fraction of the 694.3nm light can be converted to the 2nd harmonic wavelength of 347.1nm, with which it is possible to excite many molecular species. This technique has been widely adopted and the materials normally used for frequency-doubling are crystals of the Pottassium Dihydrogen Phosphate (KDP) family. In fact two different types of crystal have been used in this work: preliminary experiments were carried out using an angle-tuned, 2-inch long, 1-inch square aperture KDP crystal; higher conversion efficiencies ($\approx 15\%$) were achieved by using a temperature-tuned Rubidium Dihydrogen Arsenate (RDA) crystal, which is reported to be the most efficient crystal for the frequency - doubling of ruby laser

light when 90° phase-matched at 92°C.(37)

This work reports the study of transient absorption by phthalocyanine molecules following laser excitation. This group of molecules has characteristic absorption bands in the near u-v and red regions of the spectrum - in most cases conveniently situated to allow excitation at either 694.3 nm or 347.1 nm to create different initial excited states. The intensity of the fundamental excitation beam is varied using a filter of copper sulphate solution. A combination of Wratten 18A colour filter and dichroic beam-splitter is used to isolate the 2nd harmonic beam and prevent transmission of the fundamental wavelength. Approximately 100 mJ of 347.1 nm radiation is available for excitation.

2.1(iii)Pulsed Xenon arc-lamp

When monitoring small changes in optical transmission on a nanosecond time scale a high intensity light source is necessary to provide an adequate signal to noise ratio at the detector and to reduce the relative effect of fluorescence. Many previous nanosecond kinetic arrangements have employed a linear xenon flash-tube as the analysis source.(34,35,38,39) The monitoring light used in this system is provided by a constantly running Xenon arc-lamp operated in the pulsed mode.(40) An arc-lamp has the advantage of providing a smaller source of light than a flash-tube, which enables a higher efficiency of light collection by the optical system.

A circuit block diagram of the arc-lamp power supply is shown in Fig.2.5. The D.C. supply provides a continuous

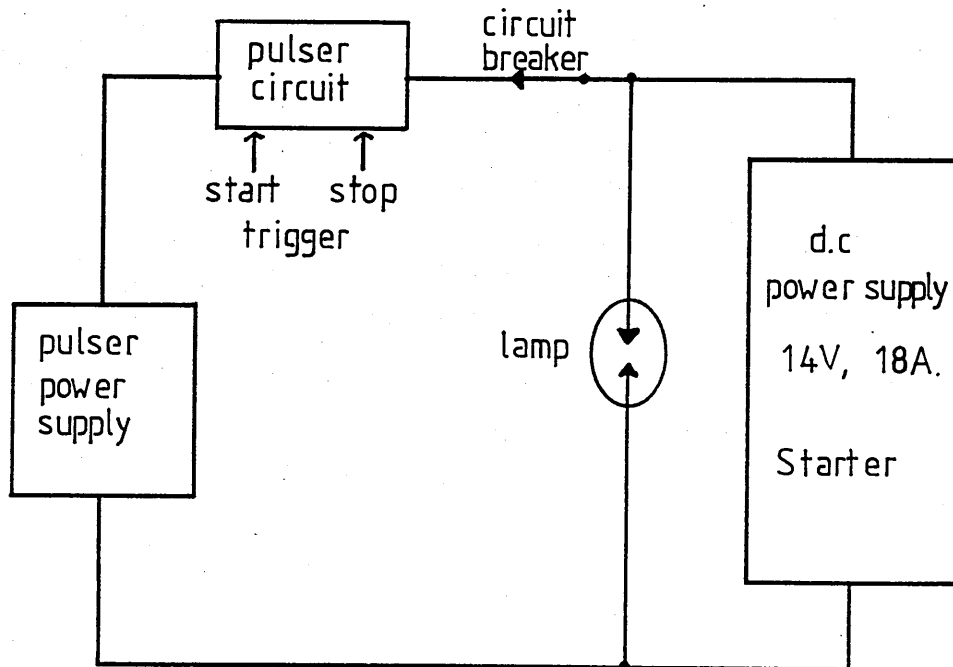


Fig. 2.5

Arc-lamp power supply

18A at 14V to the lamp. Using a pulser unit, an extra capacitor discharge is applied to the lamp which results in a large increase in radiance, particularly in the u-v where output is relatively low under D.C. conditions. The high intensity light pulse remains approximately constant for up to a millisecond [Fig.2.6] after which the lamp returns to normal D.C. operation.

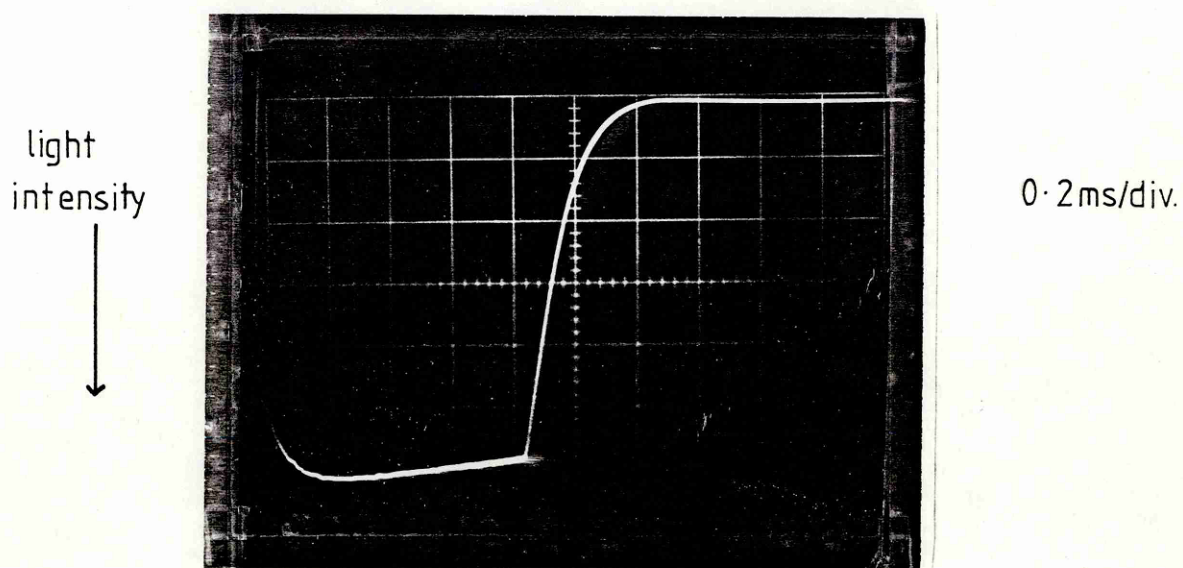


Fig. 2.6
Xenon arc-lamp pulse

2.1(iv) Optical arrangement

Transient absorption measurements are usually made with the laser light incident upon the sample cell either at a right-angle to, or collinear with the monitoring light beam (Figs. 2.7(a) and 2.7(b) respectively). All results reported

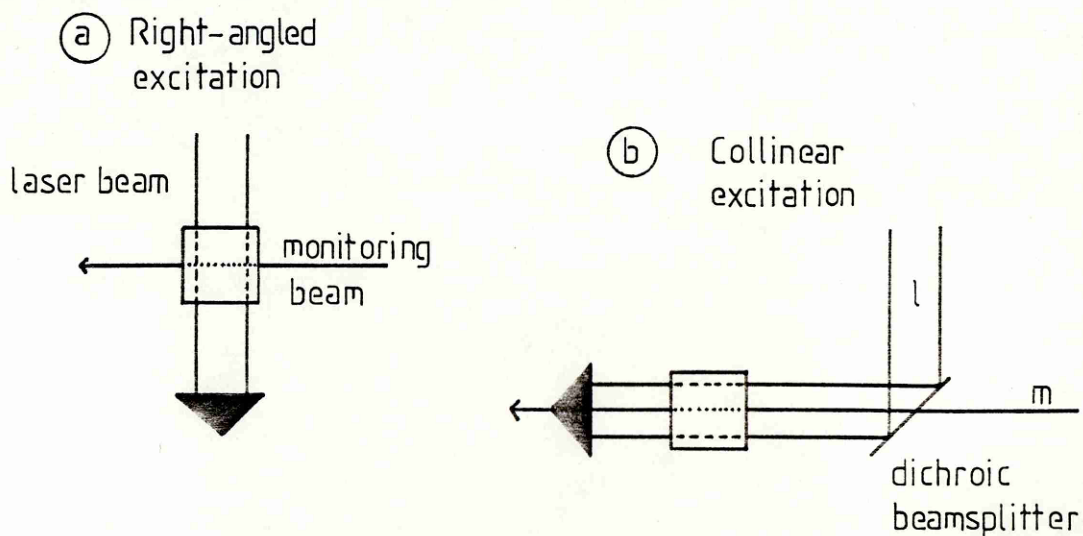


Fig. 2.7

here were obtained using the right-angled method; disadvantages of the collinear method include a loss of laser and/or monitoring light at the beam-splitter and the possibility of a high level of scattered laser radiation reaching the detector.

Fig.2.8 shows the full optical arrangement. The laser beam, although mildly diverging is unfocussed because a high energy density in the sample can lead to a spurious transient decay brought about by concentration gradients, biphotonic processes or local thermal effects. First-order rate constants are unaffected by concentration gradients, but second-order processes are concentration dependant. Hence sample solutions should be sufficiently dilute to maintain uniform concentration along the cell length.⁽³⁶⁾

Bebelaar⁽³⁹⁾ concluded that if the concentration of the sample can be made such that the optical density at the exciting wavelength ≈ 0.4 , then the right-angled method of excitation is advantageous. For single-pass arrangements a compromise must be made between the maximum yield of transients and their homogeneous distribution. If the optical density is too high, all the transients are produced at the front-face of the sample - if it is too low, not enough transients are created to yield an adequate transient absorption signal.⁽⁴¹⁾ For samples with an optical density > 0.4 , Bebelaar recommends the collinear arrangement.

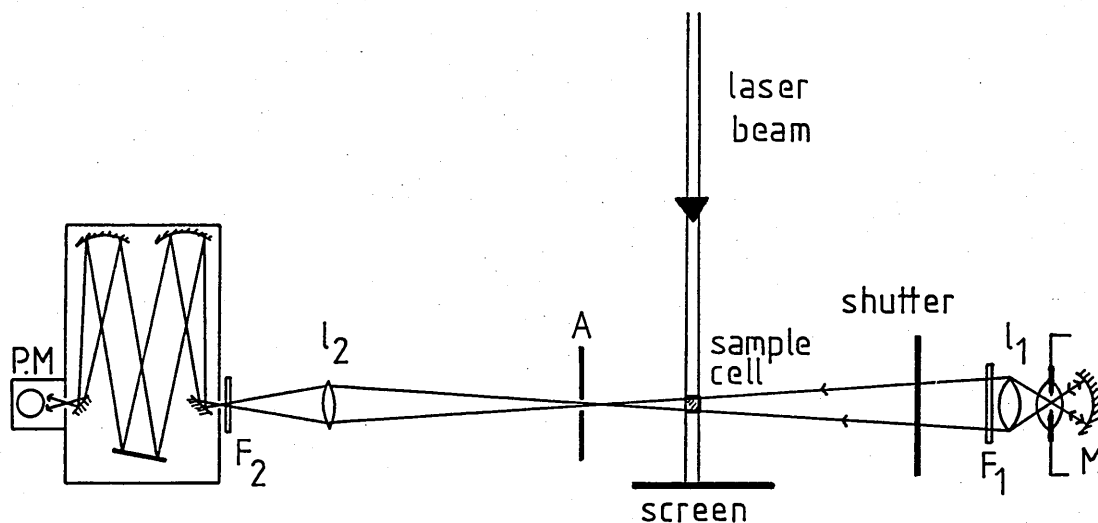


Fig. 2.8: Optical arrangement (not to scale).

After passing through the sample, the monitoring beam is apertured to ensure that the light collected by lens l_2 is that which has passed through the laser irradiated volume of the sample. This lens focuses the light onto the slits of a Hilger and Watts (D330) monochromator equipped with a 1200 lines/mm plane grating blazed at 500 nm. The aperture and separation of l_2 from the sample cell also serve to reduce the amount of fluorescent light that reaches the monochromator. The detection of 2nd-order diffracted light when monitoring at longer wavelengths is prevented by a long-pass filter (F_1), and scattered laser radiation at 347.1 nm is effectively removed at the monochromator entrance-slit by a Wratten 2B (F_2). With this optical arrangement an adequate light throughput can be achieved using a slit-width of 0.4 mm \rightarrow 0.5 mm (\approx 1 nm \rightarrow 1.3 nm resolution).

2.1(v) Photodetection

Kinetic spectrophotometry involves the detection of a fast, small change, in the intensity of a quasi-D.C. light level. A side-window photomultiplier (P.M.) tube (type 1P28 or similar) is normally used⁽⁴²⁻⁴⁵⁾ when monitoring transient absorption in the visible and near infra-red regions of the spectrum. In order to minimize photocathode shot-noise during the measurement, the P.M.cathode current, I_c , should be as large as possible without exceeding the linear operating range of the tube. If all the P.M. tube dynode stages were to be used in the amplification of the cathode current (typically between $10\mu\text{A}$ and $50\mu\text{A}$ ^(42,46)) then the resulting anode current would be well in excess of manufacturers' operating specifications. For this reason, and because each dynode introduces some noise and non-linearity into the signal, the minimum number of dynodes should be used that provides an adequate output signal.

Fig.2.9 shows the layout of the circuit used to deliver power to the P.M. tubes used in this work and it includes many of the features stressed by Fenster et al.⁽⁴⁷⁾ to extend linear operation. It is a six-stage arrangement with a potential divider chain used to branch off voltages to individual dynodes. The signal is collected at two dynodes (6 and 7) connected together with the unused dynodes connected and biased at -47 V with respect to the collecting dynodes.

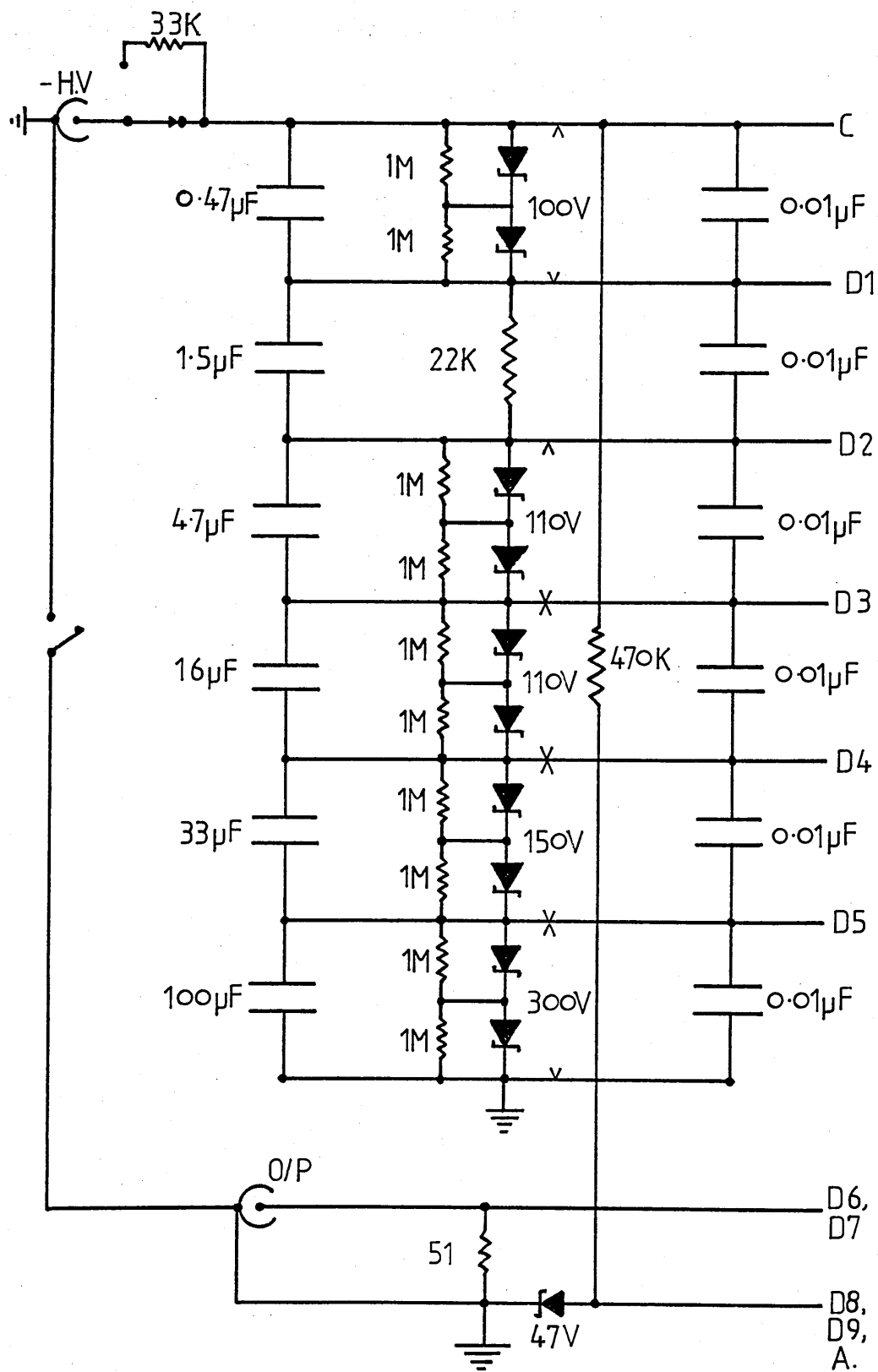


Fig. 2.9

P.M. TUBE POWER-SUPPLY

The overall gain of the photomultiplier is controlled by changing the gain at the first stage since small changes in this voltage alters the overall gain significantly with no loss of linearity. All stages were decoupled twice, first by high-value storage capacitors to ensure linear operation over the full millisecond of operation of the arc-lamp pulse, and second by low-inductance ceramic disc capacitors (located at the P.M. tube socket) to maintain high-frequency response. The recharging time constants of the larger storage capacitors between the final dynode stages are very much shorter than the time between successive Xenon arc-lamp pulses.

Data was collected using two separate P.M. tubes in different wavelength regions:

300 nm - 600 nm EMI 9664B (Trialkali photocathode)
600 nm - 800 nm HAMMAMATSU R666(S) (GaAs
photocathode)

The current generated by the P.M. tube is converted into a voltage signal by the $51\ \Omega$ resistor at the anode and a $50\ \Omega$ feed-through terminator at the far- end of the signal cable. This is fed directly into a Textronix 454 oscilloscope which is operated in the single-sweep mode. The oscilloscope trace is recorded on 20 000 ASA Polaroid film using a Tektronix C31 oscilloscope camera.

The linearity of the EMI 9664B P.M. tube was measured in a

Tube Voltage: -824V

λ : 460nm.

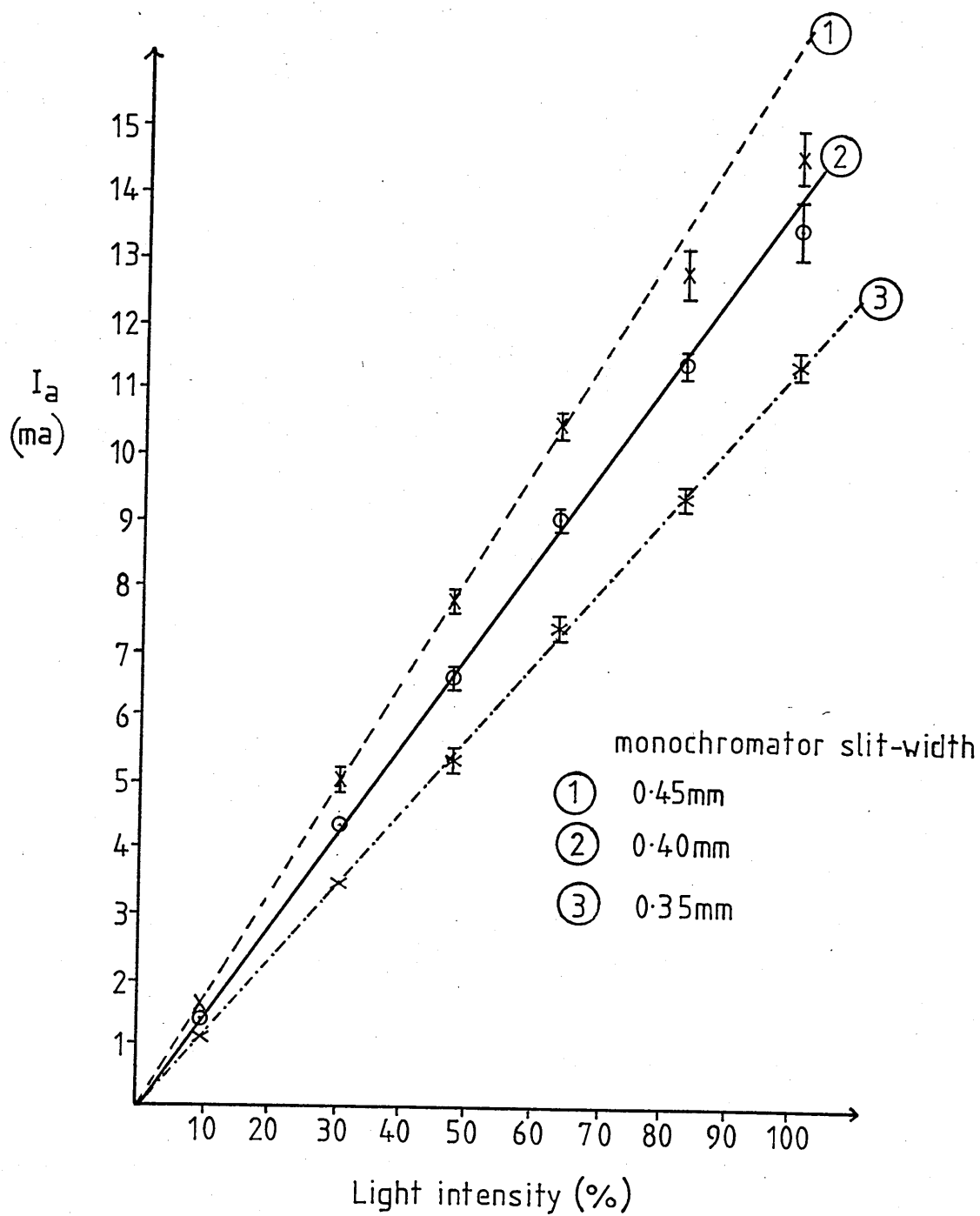


Fig.2.10

Linearity of EMI 9664B PM Tube.

region of high light intensity using calibrated neutral density filters and as can be seen in the graph of Fig.2.10, the combination of this tube and the power supply described can provide over 12mA before non-linearity occurs.

2.1(vi) System timing

Fig.2.11 shows the relative timing sequence used to produce the transient absorption signals on the oscilloscope screen. It is important that the laser light is incident upon the sample at a time when the arc-lamp pulse has levelled off at maximum intensity. This is achieved by operating the lamp pulses with a signal derived from the laser trigger unit with a suitable delay interposed. The oscilloscope sweep is initiated by a voltage pulse from the trigger photomultiplier (EMI 9664B) responding to a reflected portion of laser light. This P.M. tube is operated with a high cathode-anode voltage (1kV) in order to produce a steep, reliable trigger pulse. The use of a large trigger signal allows the oscilloscope trigger-level to be set high in order to protect against spurious triggering from the large noise spike which accompanies the firing of the laser.

2.2 ANALYSIS OF DATA

2.2(i) Reading the polaroids

Each photograph carries the following information:

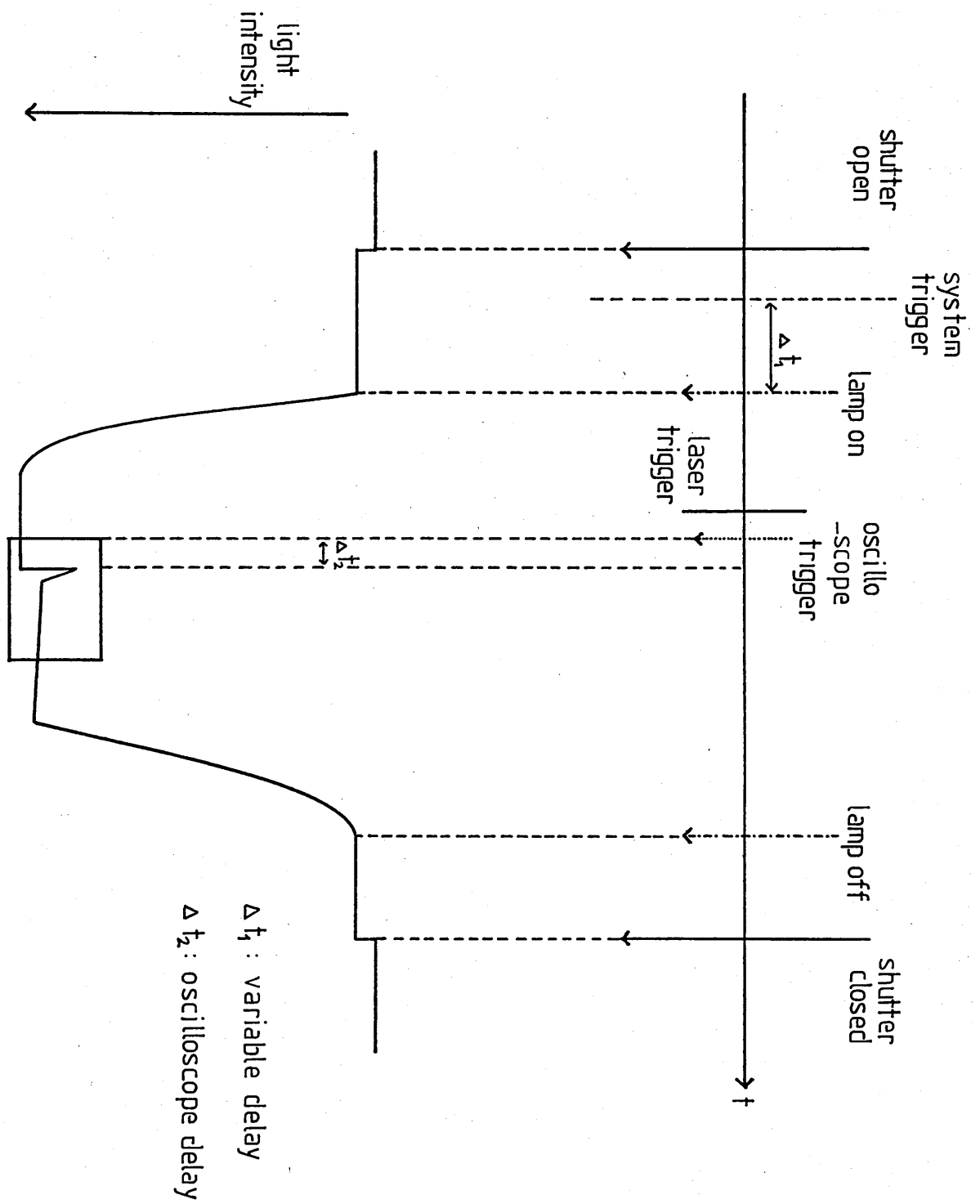


Fig. 2.11

System Timing

- 1) Fluorescence trace; mV/div, ns/div. Laser intensity.
- 2) Transient absorption/bleaching; mV/div, ns/div. Laser intensity.
- 3) Baseline offset (mV).
- 4) Wavelength (nm).

Fig.2.12 shows typical data for a number of conditions. In a region of moderate fluorescence, the correct transient absorption value can be found by addition of the fluorescence intensity at time t to the measured value of the absorption intensity at the same time. This is shown in Fig.2.12(a) with

$$I_t(t) = I_m(t) + |I_f| \quad (2.2)$$

where I_t = true transient absorption signal.

I_m = measured transient absorption signal.

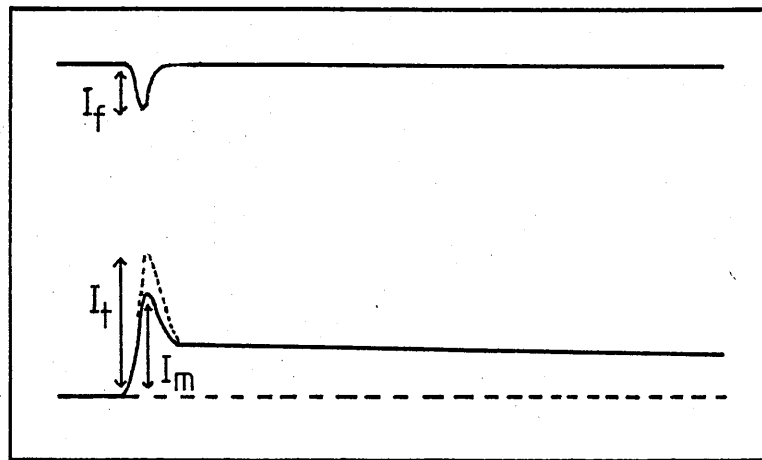
$|I_f|$ = magnitude of fluorescence signal.

If the fluorescence is strong (2.12(b)) the initial part of the transient absorption will be measurable as a reduction in the apparent fluorescence intensity below the base-line.

Equation 2.2 still applies though the parameter $I_m(t)$ will be negative for much of the duration of the fluorescence emission.

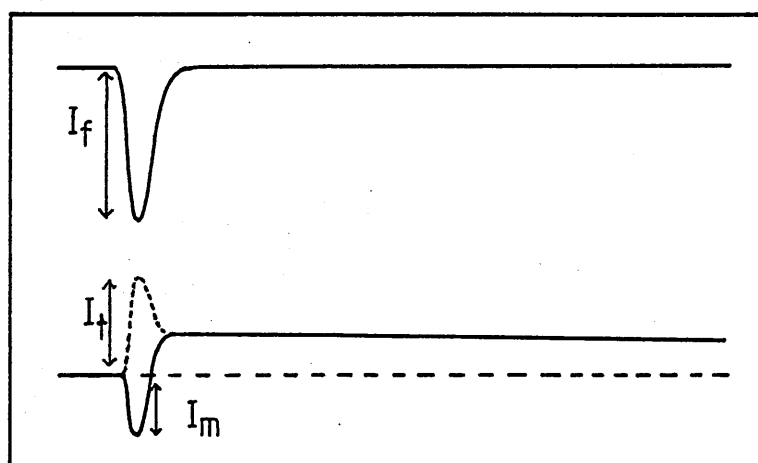
In a region of strong ground-state absorption, the monitoring light intensity reaching the P.M. tube is less than it would be in the absence of a sample. On exciting with the laser, the ground-state population is depleted and the transmission

(a)



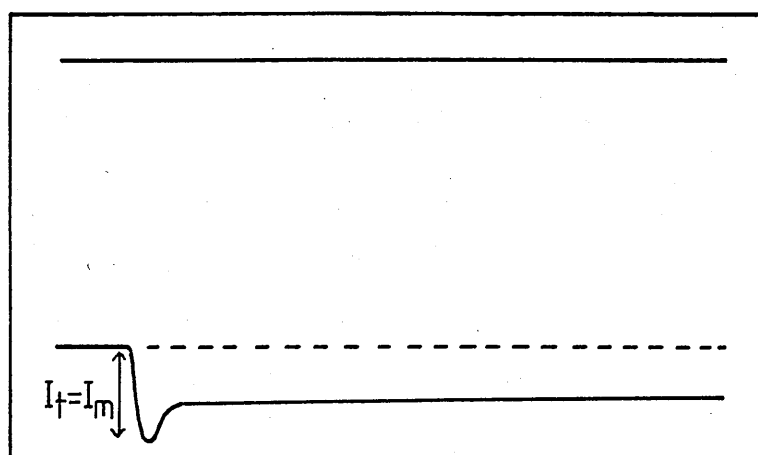
moderate
fluorescence

(b)



intense
fluorescence

(c)



ground-state
depletion

Fig. 2.12

Transient response for different conditions

of monitoring light increases. This bleaching effect is represented in Fig.2.12(c) and the contribution of absorption by the transient species cannot be measured solely from the information provided on the photographs. One of the techniques mentioned in the next section must be adopted in the case of significant ground-state absorption.

2.2(ii) Transient optical density

Fig.2.13 illustrates the passage of monitoring light through the sample prior to and following laser excitation. From

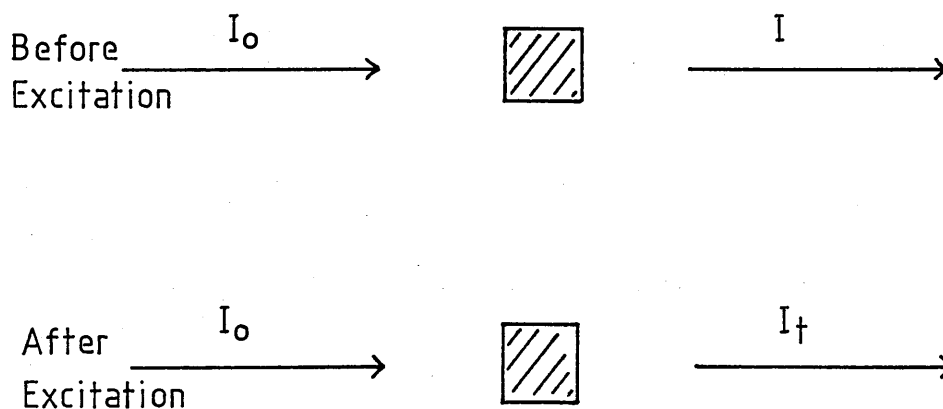


Fig.2.13

Passage of monitoring light.

Beer's law, the optical density prior to excitation is given by:

$$O.D_B = \epsilon_g C_0 l = \log I_0 / I \quad (2.3)$$

where ϵ_g = ground-state extinction coefficient.

C_o = molar concentration of ground-state.

After excitation:

$$O.D_A = \epsilon_g C_g l + \epsilon_t C_t l = \log I_o / I_t \quad (2.4)$$

where C_g = concentration of molecules remaining in the ground-state.

C_t = concentration of transient species.

ϵ_t = extinction coefficient of transient species.

$$\text{Clearly} \quad : C_o = C_g + C_t \quad (2.5)$$

The difference in optical density before and after excitation is given by:

$$\Delta O.D_t = O.D_A - O.D_B = C_t l (\epsilon_t - \epsilon_g) = \log I / I_t \quad (2.6)$$

Since the photo-multiplier voltage deflection is proportional to the light intensity:

$$\Delta O.D_t = \Delta \epsilon_t C_t l = \log \frac{V_o}{V_o - \Delta V_t} \quad (2.7)$$

where $\Delta \epsilon_t = (\epsilon_t - \epsilon_g)$.

ΔV_t = change in voltage at time t .

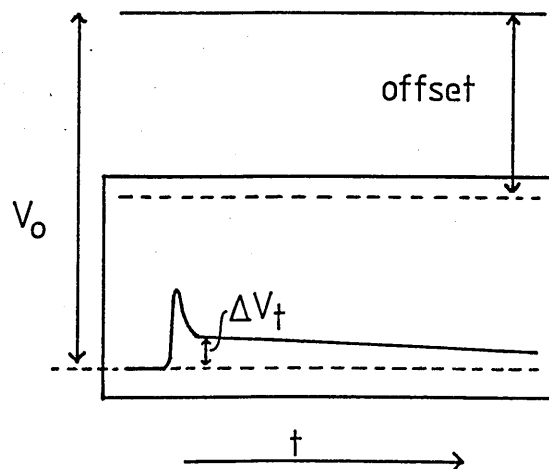


Fig.2.14

Thus as shown in Fig.2.14 the photographs provide the information necessary to calculate the difference in optical density between the ground-state absorption and the absorption by the transient species. In many cases it is desirable to be able to calculate the absolute value of the transient extinction coefficient. For example, in order to determine the quantum yield of inter-system crossing (Φ_{isc}) from S_1 to T_1 using the "comparative technique" of Amand and Bensasson⁽⁴⁸⁾ it is necessary to know the value of the triplet extinction coefficient, ϵ_T . The methods suggested to obtain this parameter include that of "singlet depletion", that of "complete conversion", and the "energy-transfer" method.^(42,49) However, all of these require the prior knowledge of the molar concentration of the ground-state and while this usually presents no problem, in cases where a solute is relatively insoluble in a solvent, difficulties can arise.

The compounds studied in this work - the phthalocyanine dyes - are not easily solvated in certain solvents, particularly those solvents which transmit u-v light. For this reason the method of preparation of the solution precludes the determination of the molar concentrations. Also transient absorption measurements were made in regions of high ground-state absorption. Therefore, the spectra presented in this work represent the "difference" optical density (Δ O.D) as a function of wavelength. Only an estimate of the amplitude of transient absorption in a region of ground-state absorption

can be made, and this requires the knowledge of the ground-state absorption spectrum.

CHAPTER 3

PHTHALOCYANINE DYES

3.1 INTRODUCTION

Phthalocyanine dyes were the first new class of coloured organic compound to be synthesised this century. The initial discoveries of a molecule of this type occurred by chance (50-52) but it was Linstead et al. (53-55) who applied the name and determined the structure of the parent compound - metal-free phthalocyanine - and several metal derivatives. Their size, planarity and similarity of structure to that of the naturally occurring porphyrin compounds was confirmed by the x-ray crystallographic studies of Robertson and Woodward. (56,57)

The properties of the phthalocyanines have been the subject of many investigations. Their chemical and thermal stability as well as their characteristic light absorption has allowed a wide variety of applications, from paint pigments to photosensitizers in solar energy storage (Appendix 1).

This work is mainly concerned with the transient light absorption process which occurs following laser excitation of phthalocyanine compounds in solution. Therefore, this chapter aims to describe the structure of the phthalocyanines, in particular to account for their characteristic light absorption, and to highlight the most important concepts and data discussed in the extensive literature dealing with their spectroscopic properties. Such a background serves to emphasise how these compounds have

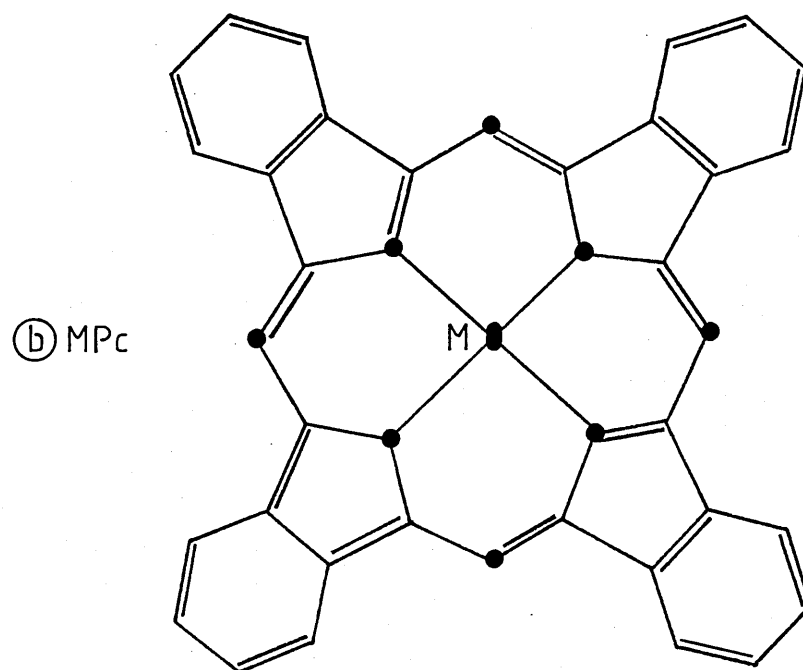
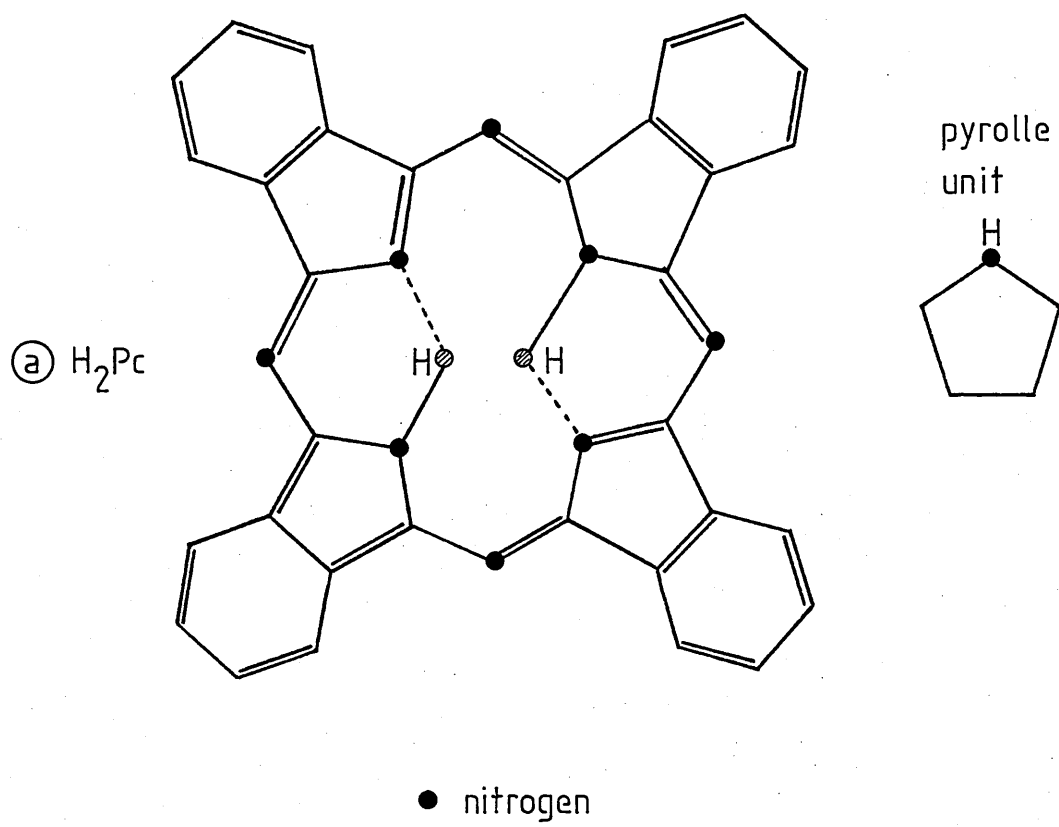


Fig. 3.1

found so many applications, and also to justify continued study.

3.2 MOLECULAR STRUCTURE AND LIGHT ABSORPTION

3.2(i) The phthalocyanine unit

The structures of the parent compound, metal-free phthalocyanine (H_2Pc), and a metal derivative (MPc) are shown in Fig.3.1. Each is composed of four pyrrole units interconnected by nitrogen bridges with a benzene ring fused to each pyrrole unit; this then forms a planar, 40-atom, conjugate ring system. The effect upon the structure of substituting the central hydrogen atoms by a metal atom is to increase the molecular symmetry.

The similarity in structure of the phthalocyanines and the porphyrins is illustrated by Fig.3.2 which shows the porphin

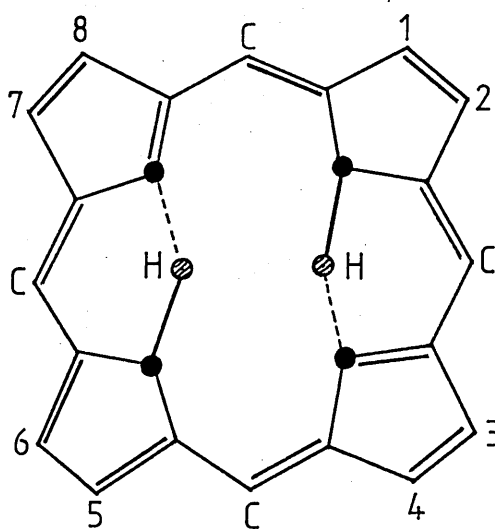
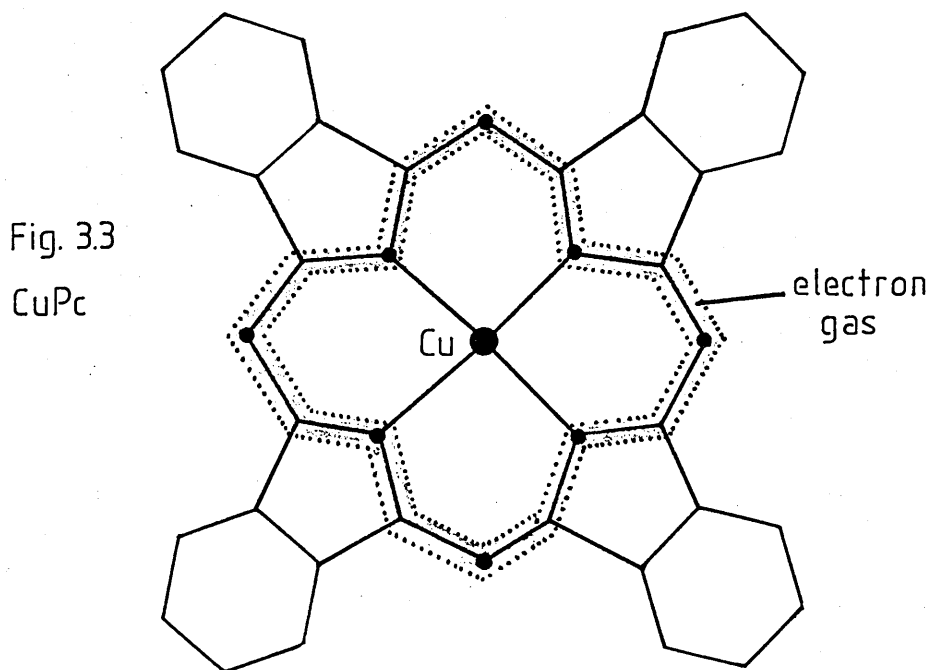


Fig.3.2: Porphin ring.

ring. In fact the phthalocyanines are only one of many groups of compound which can be formed by substitution around this porphin ring. Replacement of the four methine carbons (C-H) by 'aza' nitrogen atoms and addition of four benzene rings at positions 1,2; 3,4; 5,6; 7,8 produces the tetraazatetrabenzporphins - the structural name for phthalocyanines.

3.2(ii) Molecular-orbital analyses

The reason for the intense light absorption by phthalocyanines in the red and near u-v parts of the spectrum has been the subject of several theoretical analyses. The earliest molecular orbital treatment of a phthalocyanine is that by Kuhn (1948).⁽⁵⁸⁾ This free-electron model of (in this case) CuPc is worth considering in that it is reasonably successful in predicting the location of the principle absorption bands and it contains much that has a simple physical 'feel'.



The molecular frame of CuPc is shown in Fig.3.3. In Kuhn's analysis the benzene rings are considered as separate resonance systems and are neglected. Thus the colour of the molecule is assumed to be due to the "electron gas" formed from 9 π -electron pairs, extending over the 16-membered ring indicated. As a further approximation, the potential variations around the ring are also neglected allowing the state of each π electron to be described by a wavelength given by:

$$\lambda = \frac{h}{mv} \quad (3.1)$$

where m is the electron mass.

v is the electron velocity.

An integer number of waves must extend over the perimeter, thus:

$$\lambda = \frac{L}{n} \quad (3.2)$$

where $L = 16l$ (and l is the N-C bond length)

$n = 0, 1, 2, \dots$

Therefore the energies of the electron states are given by:

$$E_n = \frac{mv^2}{2} = \frac{h^2 n^2}{2mL^2}$$

and since two electron states exist for each value of n , (corresponding to two alternative arrangements of nodes and antinodes of the wavefunction around the molecular perimeter) the same energy must be assigned to each state.

In 1958 Kuhn modified his model⁽⁵⁹⁾ by taking into account that the inner ring around which the π -electrons are assumed

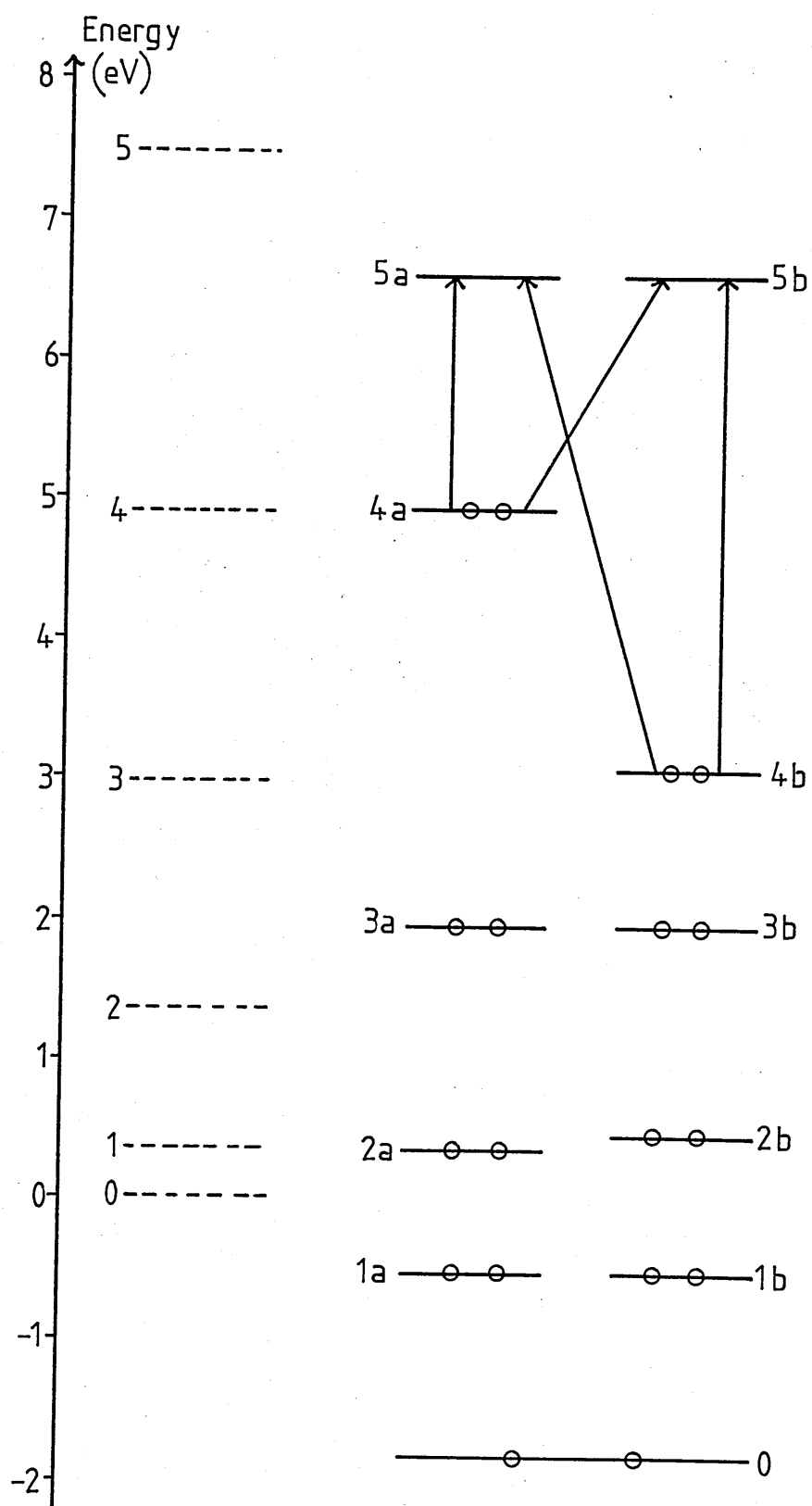


Fig.3.4

Free-electron orbital energies for CuPc.

free to move is formed from nitrogen as well as carbon atoms. Since a nitrogen atom has a greater electronegativity than a carbon atom, the potential-well in which the electrons move is not constant as had previously been assumed and each free electron is perturbed. Fig.3.4 shows the corrected and uncorrected values of the electron orbital energies for CuPc obtained using this model. The 18 π -electrons are arranged two at each orbital, with one orbital for the ground-state and two orbitals for higher states; hence the first vacant orbitals are the ones for $n = 5$. Thus, the first allowed electronic transitions are $\Psi_{4a} \rightarrow \Psi_{5a,b}$ and $\Psi_{4b} \rightarrow \Psi_{5a,b}$ which correspond to the absorption of light at 690 nm and 340 nm respectively. Kuhn's model also predicts a doubling of the absorption bands in metal-free phthalocyanine because the state 5b is expected to be lower than that of 5a - a consequence of the reduction of molecular symmetry. The metal phthalocyanines are indeed characterised by an intense absorption band centred around 350 nm (the Soret or B band) and another even more intense band between 650 nm and 700 nm (the Q band). Metal-free phthalocyanine differs in having an intense doublet between 650 nm and 700 nm.

An alternative theoretical approach was pursued by Chikayama et al.⁽⁶⁰⁾ who calculated the electronic energy levels of H₂Pc by a linear combination of atomic orbitals (LCAO) - molecular orbital approximation. They observed some disagreement with published absorption data which, they suggested, arose from inadequate assumptions concerning the

position of the central hydrogen atoms. Chen⁽⁶¹⁾ obtained the π -molecular orbitals of H_2Pc by Huckel-type calculations. He specifically compared a localised hydrogen scheme, in which each hydrogen atom is assumed to bond directly to two opposite nitrogens [Fig.3.5(a)], with a shared hydrogen model, where each hydrogen is assumed to be shared by two neighbouring nitrogens in the form of a hydrogen bond [Fig.3.5(b)]. The latter assumption seems the more successful in predicting the observed absorption wavelengths.

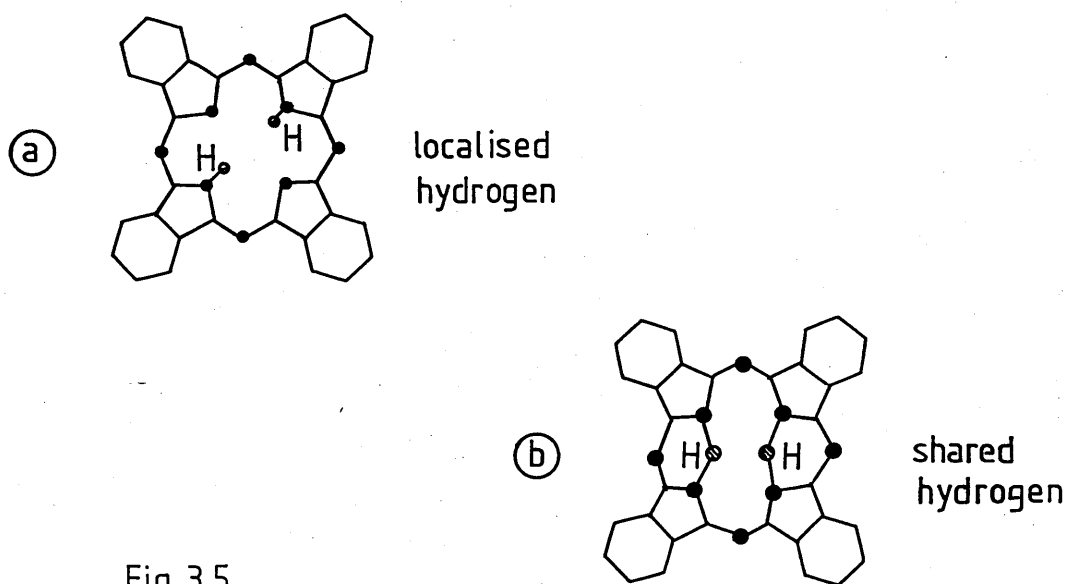


Fig.3.5

The semi-empirical molecular orbital study of Henrikson and Sundbom⁽⁶²⁾ suggests that in the region of the Soret band, there are three allowed $\pi \rightarrow \pi^*$ absorption transitions and also the lowest $n \rightarrow \pi^*$ transition. Such a transition arises from the excitation of the lone-pair electrons of the bridge nitrogens. According to their calculations, many transitions

are expected to occur at higher energies than the Soret band including both $\pi \rightarrow \pi^*$ and $n \rightarrow \pi^*$ transitions.

3.3 SPECTROSCOPIC OBSERVATIONS OF PHTHALOCYANINES

3.3(i) Ground-state absorption

The observation that the absorption spectra of metal-free and metal phthalocyanines in solution show well defined bands situated between 600 nm and 700 nm was first reported by Anderson et al.⁽⁶³⁾ Their results indicate the dependence of the position of the absorption maximum upon the central metal atom. Estigneev and Krasnovskii⁽⁶⁴⁾ point out the similarity of the absorption spectrum of MgPc to that of chlorophyll (a magnesium porphyrin) and also show that the positions of the absorption peaks vary with solvent.

Assour and Harrison⁽⁶⁵⁾ measured the absorption of $10^{-5}M$ solutions of H_2Pc and $CuPc$ in 1-chloronaphthalene [Fig.3.6]. These spectra portray absorption from the lowest vibrational level of the ground electronic state to the vibrational levels of the first excited electronic state ($S_{00} \rightarrow S_{1n}$).

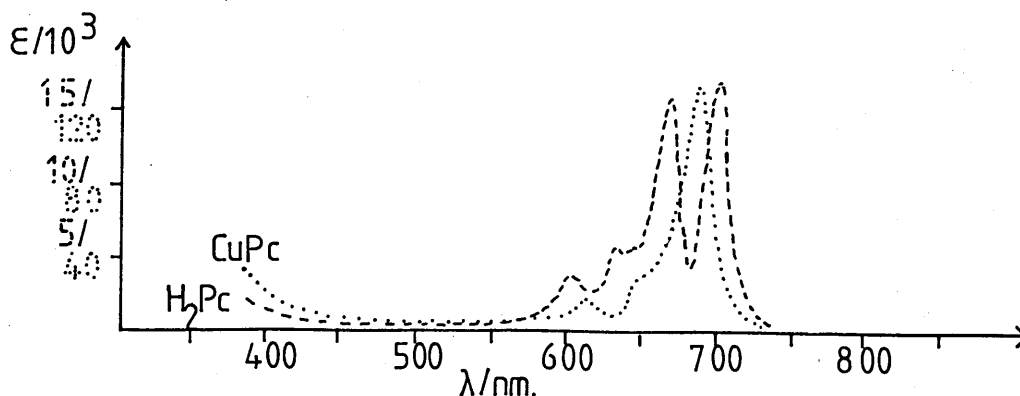


Fig.3.6: Absorption spectra of H_2Pc , $CuPc$ in 1-chloronaphthalene.

The longest wavelength absorption peak (a doublet in the case of H_2Pc) corresponds to the purely electronic transition $S_{00} \rightarrow S_{10}$. It is emphasised that the amplitudes of the extinction coefficients are lower limits due to the supposed presence of solid-phase colloidal particles.

Spectra recorded with the sample in the vapour phase are free from the effects of a solvent and from self-association. Eastwood et al.⁽⁶⁶⁾ and Edwards and Gouterman⁽⁶⁷⁾ report vapour absorption spectra for metal-free phthalocyanine and a number of metal derivatives [Table 3.1]. Compared to solution spectra, the vapour absorption bands have an increased half-width and are shifted to higher energies. Also, new bands are evident in the u-v region of the spectrum that had not previously been observed in solution studies.

Table 3.1 Absorption peaks of phthalocyanine vapours and solutions

Compound T°C/Solvent		Absorption band (nm.)				
		Q(0-0)	B	N	L	C
H ₂ Pc	(a) 470 vapour	686				
	(b) { 503 vapour 24 1-chloro	686 698.5	340	280,270	240	220,210
MgPc	(a) 535 vapour	665				
	(b) { 570 vapour 24 1-chloro	666 678	332	280.5		
CuPc	(a) 510 vapour	656				
	(b) { 531 vapour 24 1-chloro	657.5 678	325	276	240.5	218
ZnPc	(a) 530 vapour	660				
	(b) 556 vapour	661	326.5	276	240	220
	(a) 24 1-chloro	672				
VOPc	(b) { 495 vapour 24 1-chloro	671 700	333 346.5	280 290	243.5	220
(a) Ref. 66.						
(b) Ref. 67.						

The tendency of porphyrin and phthalocyanine compounds to form molecular aggregates when in solution was pointed out by Lebedev and Nasonov.⁽⁶⁸⁾ They observed a change in the spectra of several derivatives of aluminium phthalocyanine following an increase in temperature. A broad absorption with slight peaks at around 590 nm and 830 nm at 20°C was replaced by a narrow, intense band centred at 694 nm, characteristic of the monomer, when the temperature was raised to 100°C. Similarly Britt and Moniz⁽⁶⁹⁾ noted that for a solution of H₂Pc in 1-chloronaphthalene, the two absorption peaks in the red part of the spectrum behaved

differently and the spacing between them varied with increasing temperature. McVie⁽⁴²⁾ heated the same solution from 20-40°C and claimed that the two absorption peaks were replaced by a single peak at 679nm with enhanced intensity. This behaviour was attributed to the breakdown of aggregates or dimers.

Abkowitz and Monohan⁽⁷⁰⁾ propose that the polymorphism of phthalocyanine crystalline solids may be paralleled in solution by a tendency to form molecular aggregates. They observed, for CuPc and VOPc, using benzene and tetrahydrofuran as solvents, evidence of self-association by the appearance in the absorption spectrum of new bands as the dye concentration was increased. Deviations from Beer's law corresponded to contributions from both monomers and dimers and a monomer/dimer equilibrium was suggested in the 10^{-6} to 10^{-3} M range, with complexing more dominant in less polar solvents.

3(ii) Fluorescence spectra

Early observations of fluorescence emission from phthalocyanine compounds include those of Becker and Kasha⁽⁷¹⁾ who recorded the fluorescence maxima of H₂Pc (691.8 nm), MgPc (670.5 nm) and ZnPc (673.1 nm), all in EPA glass at 77°K. Subsequently Allison and Becker⁽⁷²⁾ observed the intensity of fluorescence from ZnPc to be approximately twice that from the first fluorescence band (541.7 nm) of Zn meso

porphyrin. This is indicative of the different ways that molecules of similar structure lose their excess energy to regain equilibrium.

A fluorescence emission spectrum of H_2Pc in 1-chloronaphthalene is shown in Fig.3.7. Peaks corresponding to

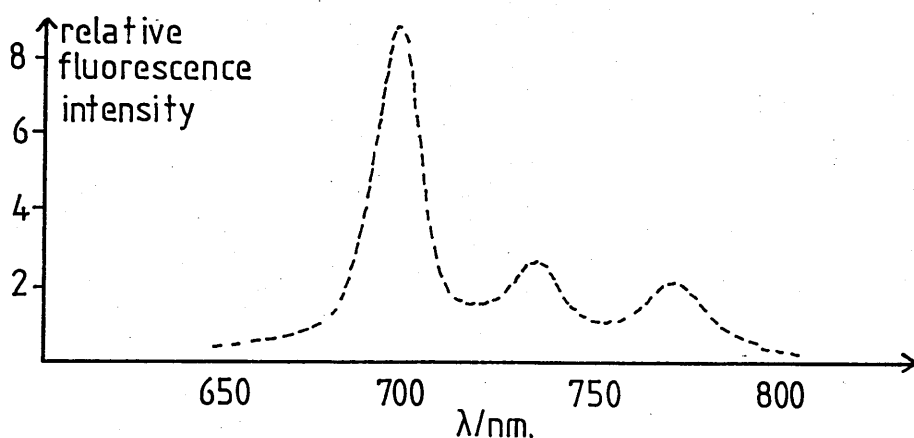


Fig.3.7: Fluorescence spectrum of H_2Pc in 1-chloronaphthalene. (65)

transitions $S_{10} \rightarrow S_{0n}$ can be seen at 699 nm, 735 nm and 777.5 nm. The separation of the vibrational bands is equivalent to $\approx 740 \text{ cm}^{-1}$ which compares well with the infra-red spectra of Sidorov. (73)

A comparison of vapour phase to solution fluorescence spectra shows the same differences as was evident in the absorption spectra, i.e. the peaks become wider and are blue shifted (66) [Table 3.2]. Significantly, no emission is observed from $CuPc$ vapour or, according to Vincett et al., (74) from $CuPc$ or $VOPc$ in solution.

Table 3.2 Fluorescence peaks of phthalocyanine vapours and solutions

Compound	T°C / solvent	Principal fluorescence band
		(nm.)
H ₂ Pc	24, 1-chloronaphthalene	705
	470, vapour	686
MgPc	24, 1-chloronaphthalene	682
	535, vapour	670
ZnPc	24, 1-chloronaphthalene	690
	530, vapour	665

Fluorescence, attributed to a transition from the upper vibrational levels of the first excited electronic state (S_{1n}) was recorded by Menzel et al.⁽⁷⁵⁾ for solutions of PdPc, RhPc, H₂Pc and MgPc in 1-chloronaphthalene at 77°K. It was concluded that in the metal-free compound and in those with a light central metal atom (such as MgPc), the dominant radiationless de-excitation of S_{1n} takes place by internal conversion to S_0 for all but the zero-point vibrational level of S_1 . For those compounds containing heavier atoms, internal conversion is slower than the vibrational relaxation process, so inter-system crossing to the lowest triplet level dominates from the lower vibrational levels of S_1 . This type of emission was also observed from H₂Pc and MgPc by Yoshino et al.⁽⁷⁶⁾ Both groups used a high-intensity argon-ion laser as the excitation source.

Rieckhoff and Voigt's⁽⁷⁷⁾ review once again points out the lack of emission from CuPc and VOPc and adds CoPc to the list of 'weak or non-fluorescent phthalocyanines'. A dependence of fluorescence emission upon solvent, temperature and

concentration is proposed - the latter accounted for by dimer formation. Huang and Sharp⁽⁷⁸⁾ provide evidence of aggregate formation producing emission from VOPc in 1-chloronaphthalene. The dimer fluorescence was observed to the high energy side of the expected monomer fluorescence peak, whereas emission from heavier aggregates was said to occur on the low energy side.

Several publications have dealt with an 'anomalous' fluorescence in the blue-violet region of the spectrum, which in some cases has been said to originate from the second excited singlet state of the phthalocyanine compound. Gibbs,⁽⁷⁹⁾ upon irradiating a solution of AlPcCl in 1-chloronaphthalene with the high-intensity 694 nm output of a Q-switched ruby laser, observed emission with a spectrum which roughly mirrored the Soret absorption band, with a Stokes shift of 1600 cm^{-1} . However, excitation with a low intensity light source failed to produce such emission, even with direct Soret absorption. It was therefore claimed that the state S_2 was populated by strong absorption of laser light from $S_0 \rightarrow S_1$ followed by transient absorption from $S_1 \rightarrow S_2$ during the laser pulse. Szabo and Erickson⁽⁸⁰⁾ reported the same effect in the same solution, although attempts to monitor any such emission from VOPc proved inconclusive in both nitrobenzene and perspex hosts.

Hodgkinson⁽³⁴⁾ recorded emission from VOPc in toluene in the blue-violet region of the spectrum using both conventional

fluorescence techniques and 2nd-harmonic ruby laser excitation. A fluorescence excitation spectrum showed a peak in the same region of the spectrum as the Soret absorption band, however the fluorescence emission peaks were seen to occur at a slightly lower energy (375 nm, 391 nm (max) and 408 nm). Thus it was speculated that the emission could originate from S_2 or from a high vibrational level of S_1 - or from an impurity. In good agreement were the results of Da-Silva,⁽³⁵⁾ who plotted the fluorescence emission of VOPc in toluene using second-harmonic ruby laser excitation. Peaks were located at 370 nm, 390 nm (max) and 410 nm. Also, for H_2Pc in toluene excited at 340 nm, a strong peak was observed at ≈ 390 nm.

Muralidharan et al.⁽⁸¹⁾ investigated the luminescence of $RhPc(CH_3OH)Cl$ in methanol. It was observed that when irradiated with light of $\lambda_{ex} \leq 400$ nm, a broad emission was produced with $\lambda_{max} \approx 420$ nm, which at 77° K showed some structure. An excitation spectrum indicated that this emission could not be associated with a radiative transition from the lowest singlet or triplet electronic states. The same group further reported a violet emission from phthalocyanines of Al (III), Co (III) and Ru (II), and evidence from a study of transient processes within $RhPc(CH_3OH)X$ [with $x = Cl^-$, Br^- and I^-] led to the attribution of such emission to the relaxation of an upper excited state of the triplet manifold.⁽⁸²⁾

3.3(iii)Time-resolved fluorescence

Table 3.3 contains the 'red' fluorescence decay times of a number of phthalocyanine compounds. Most of the data was obtained by monitoring the fluorescence in real time following irradiation by a ruby laser pulse (nanosecond or picosecond). However, the results of Dmetrievsky et al.(83) were obtained using the phase fluorimetry technique. They compared the results using hexane/dioxane solutions to those obtained in glass-like solutions at -180°C and found a 30% increase in lifetime in the latter media.

Mack(85) observed that not only are the location of the absorption peaks solvent dependant, but also the fluorescence lifetimes. However a variation in concentration of AlPcCl showed no effect upon the lifetime.

Table 3.3 Fluorescence decay times

Compound (ref)	Solvent	Lifetime (ns)
H ₂ Pc (83)	Hexane/dioxane	6.7
MgPc (83)	Hexane/dioxane	6.5
MgPc (84)	1-chloronaphthalene	9
ZnPc (83)	Hexane/dioxane	3.9
AlPcCl (85)	Ethanol	10.1
AlPcCl (85)	Methanol	10.3
AlPcCl (85)	1-chloronaphthalene	8
AlPcCl (86)	1-chloronaphthalene	6-7
AlPcCl (84)	1-chloronaphthalene	5
AlPcCl (87)	1-chloronaphthalene	11.72

Harrison and Kosonocky(88) and Guiliano and Hess(89) mention the observation of a 'delayed' red fluorescence from H₂Pc

following high intensity ruby laser excitation, with a 40 ns half-life reported in each case. Such a delayed emission may result from the excitation of the triplet state during laser irradiation with a subsequent repopulation of the state S_1 . Britt and Moniz⁽⁶⁹⁾ suggest that variations in the fluorescence decay time within the concentration range 10^{-6} M - 10^{-4} M may be due to the formation of dimers upon laser irradiation.

3.3(iv) Stimulated emission

It was Sorokin et al.⁽⁹⁰⁾ who first demonstrated laser action in an organic dye when, irradiating a solution of AlPcCl in ethyl alcohol with the 694 nm output of a Q-switched ruby laser, they observed a coherent output at 755 nm. Subsequent work⁽⁹¹⁾ showed the solvent dependence of the lasing wavelength:

Table 3.4 Laser action with ruby laser pumping

AlPcCl in :	λ max. Abs. (nm)	λ_L (nm)
Ethyl alcohol	670.0	755.5
1-Propanol	670.5	755.0
DMSO	677.0	761.5
Ethylene Glycol	681.5	763.0

The lasing wavelength coincides with the most prominent (and longest wavelength) vibronic fluorescence band. However, when AlPcCl was dissolved in methyl alcohol, no laser emission could be induced.

Gibbs and Kellock (92) observed laser action from AlPcCl in 1-chloronaphthalene at 708 nm following ruby laser excitation, which corresponds to the $S_{10} \rightarrow S_{00}$ transition. Any transition to a vibrational level of the ground-state could not be stimulated in this solvent. The presence of dimers is suggested as a possible reason why AlPcCl does not show laser action in certain solvents.(69) Unsuccessful attempts to produce stimulated emission from MgPc in acetone, ethanol and pyridine are reported, whilst efficient coherent output has been observed(93) for MgPc in quinoline at 759 nm.

Lin(94) observed superradiant laser emission at 690 nm when a solution of AlPcCl in methanol was pumped with a pulsed nitrogen laser. Thus excitation to the second excited singlet state is followed by laser output corresponding to the transition $S_{10} \rightarrow S_{00}$. Kugel(95) et al. also used nitrogen laser pumping to obtain laser action from a number of phthalocyanines [Table 3.5].

Table 3.5 Laser action with nitrogen laser pumping

Compound	Conc./Solvent	λ_L (nm)	$\Delta\lambda_L$ (nm)
AlPcCl	1×10^{-3} M Et OH	753.3	1.5
		685.7	1.6
	1×10^{-3} M Pyridine	761.6	1.4
		692.6	4.4
	2.5×10^{-3} M Pyridine	690.1	2.8
GcPcCl	2.8×10^{-4} M Pyridine	694.0	1.8
MgPc	1.2×10^{-3} M Pyridine	688.2	4.0
	5×10^{-4} M D.M.F.	682.5	3.0
ZnPc	5×10^{-4} M Pyridine	686.0	2.7
	1.4×10^{-4} M Pyridine	684.9	2.4

AlPcCl is seen to emit coherent light at two wavelengths simultaneously. The short and long wavelength lasing bands correspond to transitions to the ground state and to a vibrational level of the ground state respectively. The relative intensities of the two lasing bands are sensitive to concentration with the long wavelength band favoured at high concentration. This is believed to be a consequence of self-absorption of the short-wavelength emission.

3.3(v) Phosphorescence

Although it was Reickhoff and Voigt⁽⁷⁷⁾ who first reported a broad structureless emission from low-temperature solutions of H₂Pc (maximum emission at 810 nm - 820 nm) and several M-Pc's (880 nm - 950 nm), the first clear assignment of this type of emission as T₁ → S₀ phosphorescence was subsequently made by Vincett et al.⁽⁷⁴⁾

Solov'ev et al.⁽⁹⁶⁾ investigated the effect on the phosphorescence emission of substituting onto the porphin ring. It was found that benzosubstitution, while strongly affecting the ground-state absorption spectrum, produces the same $S_1 - T_1$ energy gap as in simple metal porphyrins. However aza-substitution was found to increase the energy gap from $\approx 3000 \text{ cm}^{-1}$ to $\approx 5000 \text{ cm}^{-1}$.

3.3(vi) Saturable absorption

The use of phthalocyanine compounds dissolved in organic solvents as a repeatable Q-switch element of a ruby laser was first put into practice by Sorokin's group.⁽²³⁾ The solutions, H_2Pc or $AlPcCl$ in 1-chloronaphthalene, or $VOPc$ in nitrobenzene, were seen to act as saturable absorbers with the bleaching process based upon the saturation of the $S_0 \rightarrow S_1$ absorption transition. The metal phthalocyanine Q-switch solutions were able to effect the production of a laser pulse 20 ns or less in duration, whereas the metal-free solution produced a broader pulse.

Armstrong's study⁽⁹⁷⁾ of saturable absorption showed that, at low light levels, both of these MPc solutions behave as linear attenuators. However, at higher intensities of ruby laser irradiation ($\approx 10^4 - 10^5 \text{ W/cm}^2$) a non-linear increase in transmission occurs until the totally bleached state is reached. Double laser pulse experiments indicated that the lowest triplet state may be significantly populated and could

remain so for up to $1\mu\text{s}$. The role of the triplet state during the bleaching process was mooted by Guiliano and Hess⁽⁸⁹⁾ with regard to the need for a rapid recovery from the bleached state for a dye to be useful as a mode-locking element. Hercher et al.⁽⁹⁸⁾ concluded that the phthalocyanines act as energy switches with relatively long relaxation times and exhibit two types of residual loss. That due to excited singlet absorption precludes the use of the solutions as Q-switches at high intensities. The long-lived triplet absorption precludes their use as mode-locking dyes.

A range of 22 different phthalocyanines and naphthalocyanines were studied as Q-switches by Gryanov et al.⁽⁹⁹⁾ It was once again pointed out that the position of the absorption maximum depends upon the nature of the central metal atom, the ligand and the solvent. The energy output of a ruby laser was found to be greater for those substances in which the ground-state absorption maximum lies close to the laser line. Batashev et al.⁽¹⁰⁰⁾ showed that when the phthalocyanine ring is substituted to form brominated derivatives, the absorption maximum moves into the near I.R. region of the spectrum, which allowed their use as a Q-switch element in a Nd:glass laser (λ_L 1060 nm).

3.3(vii) Transient absorption

The technique of conventional flash photolysis was well

established when Livingston and Fujimori⁽¹⁰¹⁾ adopted it as a method of recording transient absorption in a sample of MgPc in pyridine. The transient spectrum showed maxima at 410 nm and 470 nm, decreasing in amplitude towards the red region of the spectrum, which was assigned to absorption by the lowest triplet state of the molecule. A depletion of the entire ground-state absorption band was also recorded.

Using similar methods, Villar and Lindquist⁽¹⁰²⁾ plotted the transient absorption spectrum of H₂Pc in 1-chloronaphthalene. The main absorption was between 400 nm and 580 nm (λ_{max} 484 nm), with a decrease in ground-state absorption between 600 nm and 730 nm. The amplitude of the transient absorption reached its maximum at a moderate excitation intensity. An increase in flash energy could not increase the transient absorption. At 25°C, the decay of the transient species follows first-order kinetics corresponding to a lifetime of $\approx 170 \mu\text{s}$ in outgassed solution (concentration range $0.1 - 5 \times 10^{-6} \text{ M}$). However, at 55°C the initial decay is much faster, though with a decrease in concentration the rate of decay once more tends towards that at 25°C. This is claimed as evidence for a triplet-triplet annihilation process.

Tsvirko et al.⁽¹⁰³⁾ recorded transient absorption throughout the visible region of the spectrum, with a maximum at 470 nm, for pyridine solutions of MgPc and ZnPc. A combined study of the decay kinetics of the transient absorption and the phosphorescence emission of porphyrin compounds confirmed

that such absorption is indeed from the lowest triplet state.

In 1964, Kosonocky et al.⁽³⁸⁾ performed what must be considered as one of the earliest laser flash photolysis experiments. The recovery of ground-state absorption following Q-switched ruby laser excitation of a solution of H₂Pc in 1-chloronaphthalene was monitored and a lifetime of 1 μ s recorded for non-outgassed solution, which was seen to increase to 150 μ s in a deoxygenated sample. Recovery from the bleached state was also determined for CuPc in 1-chloronaphthalene (50 ns) and VOPc in toluene (20 ns).⁽¹⁰⁴⁾

The suitability of phthalocyanines for ruby laser excitation stimulated a series of similar studies: Spaeth and Sooy⁽¹⁰⁵⁾ observed a strong, broad, triplet-triplet absorption centred between 470 nm and 500 nm in solutions of H₂Pc, AlPcCl, CrPc, MgPc and MbPc. They also alluded to an additional broad peak located at \approx 640 nm in some of the spectra. Muller⁽¹⁰⁶⁾ observed the depletion of the complete ground-state absorption band of H₂Pc in 1-chloronaphthalene and new absorption bands appeared, corresponding to two absorption components. The spectrum of the long-lived component was found to agree with previously reported triplet absorption and the transient had a time dependence that was strongly sensitive to oxygen content (decay time varied from 350 ns \rightarrow 100 μ s). The short-lived component was observed in the 580 nm \rightarrow 620 nm region and its decay agreed with that of the observed fluorescence. Similar results were obtained for

MgPc.

Hodgkinson⁽³⁴⁾ was the first to study the transient absorption of phthalocyanine compounds using frequency-doubled ruby laser excitation i.e. directly populating the second excited singlet state. Both a short-lived and a long-lived decay component were reported in a sample of VOPc in toluene and when the same compound was dissolved in nitrobenzene, the transient absorption showed a fast rising edge followed by a strong ingrowth extending over tens of microseconds. It was tentatively suggested that the short-lived transient may have been due to excited singlet or triplet absorption, whilst the strong ingrowth could be a result of solute-solvent complex formation. Using the same equipment, Da-Silva⁽³⁵⁾ recorded a short-lived peak in the transient spectrum of H₂Pc in toluene at ≈ 540 nm. The spectrum of VOPc in toluene shows a broad peak at ≈ 490 nm with slight peaks at 575 nm and 600 nm.

McVie⁽⁴²⁾, using 694 nm-ruby laser photolysis, once again studied the triplet states of H₂Pc and CuPc in 1-chloronaphthalene. Both spectra show transient maxima in the region of 480 nm. The decays correspond to half-lives of 130 μ s (H₂Pc) and 35 ns (CuPc). Also determined were the absolute values of the triplet energy levels:

$$E_T (\text{H}_2\text{Pc}) = 120 \text{ k J mol}^{-1}, E_T (\text{CuPc}) = 150 \text{ k J mol}^{-1}$$

and the quantum yields of conversion to the triplet states:

$$\Phi_T (\text{H}_2\text{Pc}) = 0.14$$

$$\Phi_T (\text{CuPc}) = 0.70.$$

Studies of concentrated solutions (5×10^{-5} M) of CuPc and H₂Pc produced similar results, with a decay including both short-lived (100 ns) and longer-lived (2.5 μ S) components, which disappeared upon heating to be replaced by transients of triplet character. These transients may be explained by the presence of microcrystalline particles since the longer-lived species (which were not affected by the presence of oxygen) occurred when the phthalocyanines were dispersed in a variety of solvents in which they are insoluble. It is proposed that the transient absorption was associated with the formation of excitons within and on the particle surface, by laser excitation.

The primary photophysical processes for 1-chloronaphthalene solutions of AlPcCl, GaPcCl and InPcCl were characterised by Brannon and Magde⁽⁸⁷⁾ using a number of techniques including picosecond "pump and probe" in which they utilized a mode-locked ruby laser. The data is summarised in Table 3.6

Table 3.6 Transient parameters (i)

Compound	Φ_T	Φ_{ic}	Φ_f	τ_F ns.	τ_O ns.
AlPcCl	0.4 ± 0.08	0.0	0.58 ± 0.04	6.8 ± 0.6	11.7
GaPcCl	0.7 ± 0.10	0.0	0.31 ± 0.43	3.8 ± 0.3	12.1
InPcCl	0.9 ± 0.12	0.07	0.031 ± 0.004	(0.37)	(12)

This confirms the usual heavy-atom effect on the efficiency of intersystem crossing, though no such relation is obvious for the yield of internal conversion.

Pyatosin and Tsvirko⁽¹⁰⁷⁾ investigated the spectra and kinetics of triplet absorption of H₂Pc, AlOHPC, GaPcCl and VOPc using both 694 nm and 347 nm laser flash photolysis which they claim produces identical results. The characteristics of the absorption spectra are listed in Table 3.7.

Table 3.7 Transient parameters (ii)

Compound	Solvent	$\lambda_{\text{max}} S_0 \rightarrow S_1$ (nm)	$\lambda_{\text{max}} T_1 \rightarrow T_q$ (nm)	τ_T nS.
H ₂ Pc	1-chloro.	699	480	800
GaPcCl	chlorobenzene	690	490	370
VOPc	chlorobenzene	692	490	35
AlOHPC	o-dichlorobenzene	694	495	540

It was found that outgassing the solutions increased the triplet state lifetimes in all cases except VOPc. Despite the diffuse nature of the triplet absorption, the effect of the metal atom upon the position of the transient absorption was judged to be similar to the displacement of the ground-state absorption peak.

The work of Jacques and Braun⁽¹⁰⁸⁾ concentrates upon a comparison of transient absorption by solutions subject to low and high intensity laser (694 nm) excitation. The variation of the transient optical density as a function of laser intensity was analysed (Appendix 2) to yield the triplet extinction coefficient, ϵ_T , and the quantum yield of inter-system crossing, Φ_{isc} , for H₂Pc and ZnPc. It was found

that only for laser pulse energies of less than 2 m J are the experimental results in agreement with theory.

They report the transient spectrum of H₂Pc in 1-chloronaphthalene to have a maximum of 480 nm and depletion in the ground-state absorption band. The transients decay with first-order kinetics corresponding to a half-life of 125 μ S. All of which is in good agreement with previous work.

At low laser intensity, ($I < 2$ m J):

$$\epsilon_T (480 \text{ nm}) = 18,000 \pm 2000 \text{ M}^{-1} \text{ cm}^{-1}.$$

$$\Phi_{isc} = 0.17 \pm 0.03.$$

At higher intensities (up to ≈ 400 m J) a graphical extrapolation indicates a value of $\epsilon_T \approx 37,000 \text{ M}^{-1} \text{ cm}^{-1}$ which is the same as that reported by McVie⁽⁴²⁾ who also used high intensity excitation. Similarly for ZnPc in 1-chloronaphthalene, at low laser intensity:

$$\epsilon_T = 16,000 \pm 3000 \text{ M}^{-1} \text{ cm}^{-1}.$$

$$\Phi_{isc} = 0.65 \pm 0.04.$$

whereas the high-intensity data implies $\epsilon_T \approx 34,000 \text{ M}^{-1} \text{ cm}^{-1}$.

In an attempt to separate the light-absorbing molecules from each other, the phthalocyanines were mixed with an emulsion of oil and water. It was found that this microheterogeneous phase showed the same transient characteristics and the calculated parameters do not differ significantly from those obtained in homogeneous solution. However, the oscillograms revealed a distinct additional absorption as the laser

intensity was increased - with no simple kinetic involved. Since similar oscillograms to those obtained are compared to those found when working with colloidal systems, the results are explained by the presence of aggregates in both homogeneous solutions and microheterogeneous phase.

Appendix 3 contains some of the transient absorption spectra described here.

3.4 SUMMARY

The chapter is not a comprehensive survey of all spectroscopic observations of phthalocyanines since important features are neglected. Such data includes solid-phase spectra of thin-film structures and of crystals. Also omitted are the highly structured fluorescence spectra obtained either by using supersonic free jets⁽¹⁰⁹⁾ or by solvation of phthalocyanines in alkane matrices at low temperatures - shpolskii spectra.⁽¹¹⁰⁾

Similarly the areas discussed are by no means all-inclusive, the aim being to provide an outline of the type of spectroscopic investigations to which phthalocyanine compounds in solution have been subject, and a comparison of the resultant information.

The following chapter is concerned in part with a comparison of the transient absorption by solutions subject to 694 nm or

347 nm laser irradiation. These wavelengths correspond to an initial excitation into the first and second excited singlet states respectively of many phthalocyanine compounds and such a comparison is useful in providing information into molecular energy redistribution processes. Moreover, since the tendency to form molecular aggregates has been stressed and in particular since the transient absorption at high intensity excitation is said to be perturbed by such aggregates, the extent to which the unimolecular photophysical processes are followed is of interest.

Also, further information on the 'anomalous' 'blue' fluorescence of some phthalocyanines is discussed.

CHAPTER 4

RESULTS

4. INTRODUCTION

4.1(i) Experimental procedure

All of the transient absorption data presented in this chapter was obtained using the nanosecond kinetic spectrophotometric apparatus described in Chapter 2. The ground-state absorption spectra were recorded using three types of instrument: Pye Unicam models SP8500 and SP8100 and a Beckman model 20. Fluorescence spectra were obtained either by monitoring the light output following 347 nm. laser excitation, or by using an Applied Photophysics fluorimeter. The latter was equipped with a 250 W Xenon arc-lamp, an EMI 9813 KB photomultiplier tube and an Ortec 9315 photon counter.

Oxygen is efficient in quenching photo-excited states - a process which greatly reduces the excited state lifetime. For this reason transient absorption was studied using deoxygenated solutions. Two methods of de-oxygenation were attempted: 1) Purging with pure nitrogen, 2) A "freeze-pump-thaw" technique. In effect the latter technique was found to be the more reliable, for although nitrogen purging has been used in many previous instances, the adaptation used here was not successful in preventing the readmission of oxygen into the solution during the course of the experiment. Therefore, all spectra presented in this work were obtained using solutions deoxygenated by the freeze-pump-thaw technique.

4.1(ii) Sample purification

The phthalocyanine compounds were obtained from:

Eastman Organic Chemicals Inc.

Koch-Light Laboratories Ltd.

Spectroscopic solvents were obtained from:

B.D.H. Chemicals Ltd.

Aldrich Chemical Co. Inc.

Koch-Light (Genzyme Ltd.)

Prior to preparation of a solution, the solvent was, where necessary, purified by distillation - the level of impurity monitored by laser-induced fluorescence response. The solute was either used as received, or one of two methods of purification adopted. The details of these are given in Appendix 4 and are referred to in the text as methods A and B. The ground-state absorption spectrum is used as a measure of solution purity.

4.1(iii) Solution chemistry

Phthalocyanine compounds are insoluble in many organic solvents and studies of these compounds in solution have been limited to those few solvents (particularly 1-chloro-naphthalene) in which a moderate solubility is achieved. This situation is exacerbated by the desire to use a solvent

that does not absorb a significant quantity of light in the near u-v part of the spectrum. This is important because a comparison of the transient absorption process subsequent to fundamental and frequency-doubled laser excitation requires the same mode of energy input into the chromophore. A significant absorption of laser light at 347 nm by the solvent may introduce a transient response such as energy transfer from solvent to solute, solvent-solute complex formation or transient absorption by the solvent itself. Evidence of this latter process is presented in this work.

Two solvents which do not absorb a significant quantity of light at 347 nm and in which certain phthalocyanines are able to dissolve to a reasonable extent are ethanol and toluene. However, the method of solution preparation, which involves periodic gentle heating over a number of days, has prevented any determination of concentration.

4.2 VANADYL PHTHALOCYANINE

4.2(i) Ground-state absorption

The ground-state absorption spectra for two solutions of VOPc in toluene and one solution of VOPc in nitrobenzene are shown in Fig.4.1. Solution (1) was purified by method A, solution (2) by method B (Appendix 4).

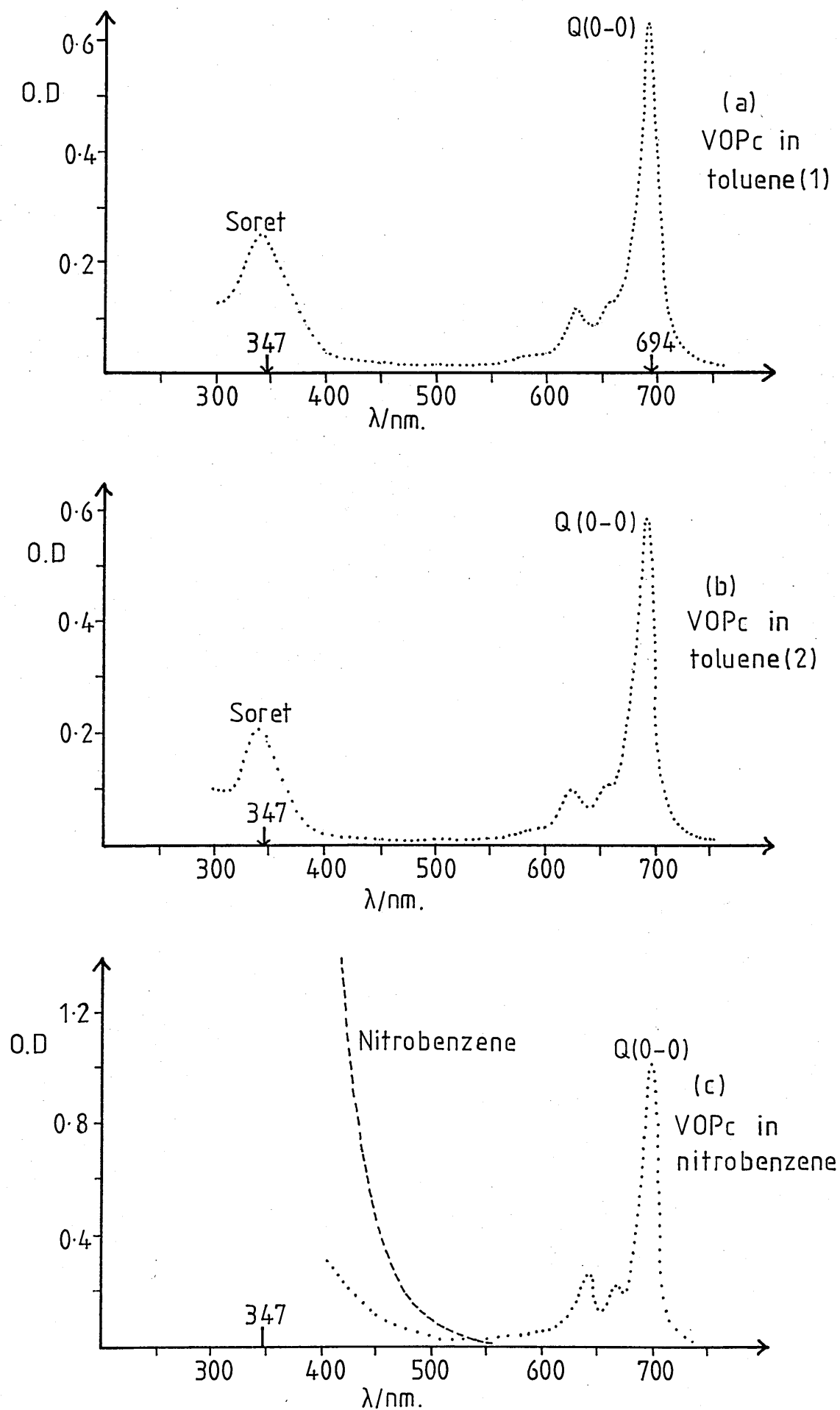


Fig.4.1: Ground-state absorption spectra.

4.2(ii) VOPc in toluene . λ_{ex} 694 nm

Transient spectra of solution (1) of VOPc in toluene are shown in Fig.4.2. The spectra represent the difference in absorption between a total ground-state population and a mixture of ground-state and transient species at times corresponding to the maximum of the 694 nm laser pulse ($t = 0$) and $t = 10$ ns, 20 ns after the laser maximum.

At $t = 0$ and $t = 10$ ns the spectra are almost identical in shape and amplitude, with transient absorption in the visible region and a maximum absorption at 480 nm. Also, there is strong ground-state depletion across the whole of the Q-absorption band between 610 nm and 730 nm, and at wavelengths shorter than 375 nm - corresponding to the Soret absorption transition. At $t = 20$ ns the shape of the spectrum is the same but the amplitude of absorption and depletion is reduced.

The transient response is illustrated in Fig.4.3 and the decays at 480 nm and 700 nm are plotted in Fig.4.4. From this graph, the lifetime of the transient species at these two wavelenths is calculated to be:

$$\tau_{480} = 11.6 \pm 2.1 \text{ ns}$$

$$\tau_{700} = 9.7 \pm 1.0 \text{ ns}$$

Fig. 4.2

Transient difference spectra of VOPc in toluene (1).

Spectra plotted at $t = 0$: --X---X---X--

$t = 10\text{ns}$:•.....•.....•.....

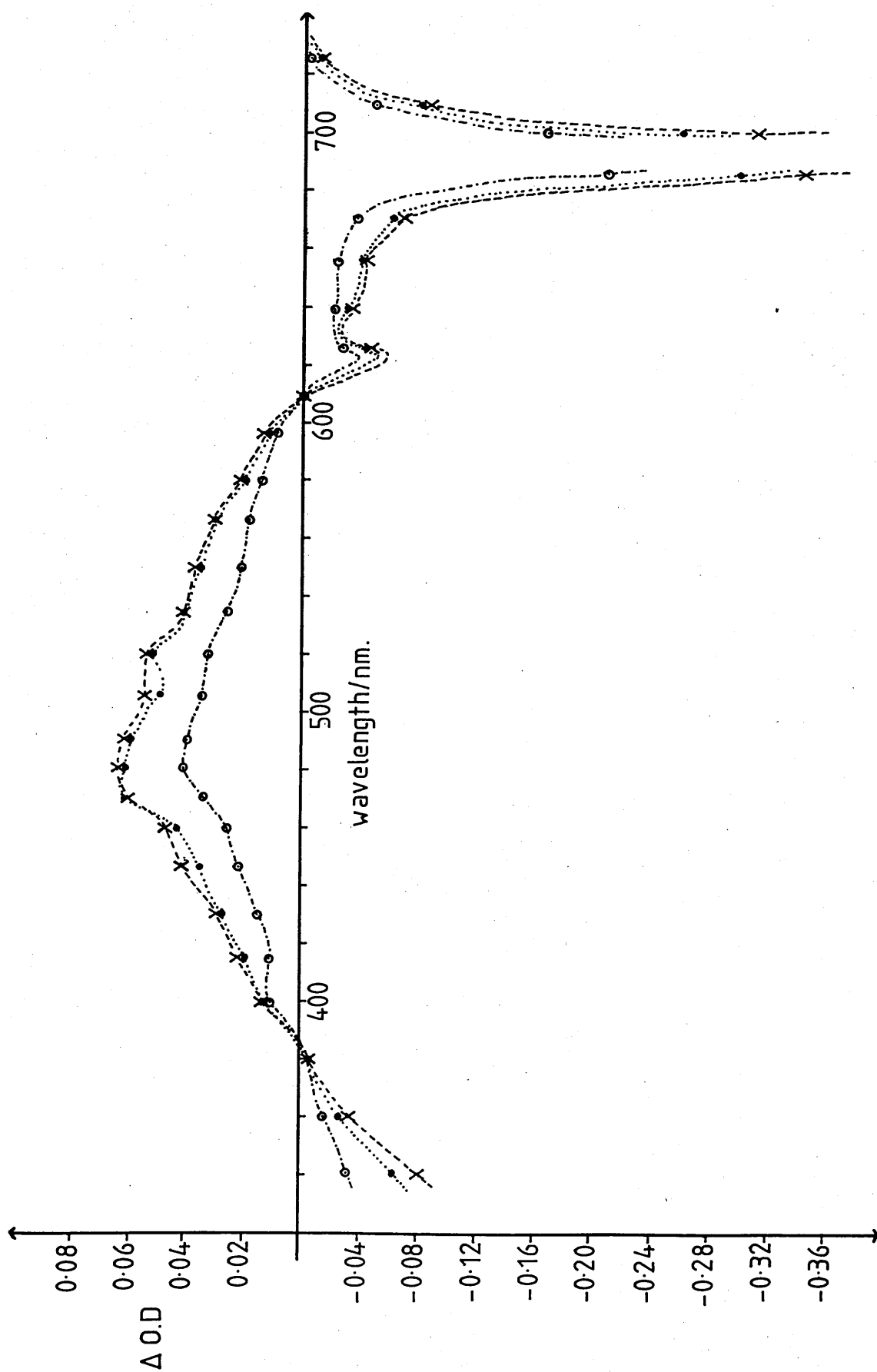
$t = 20\text{ns}$: ---○---○---○---○---

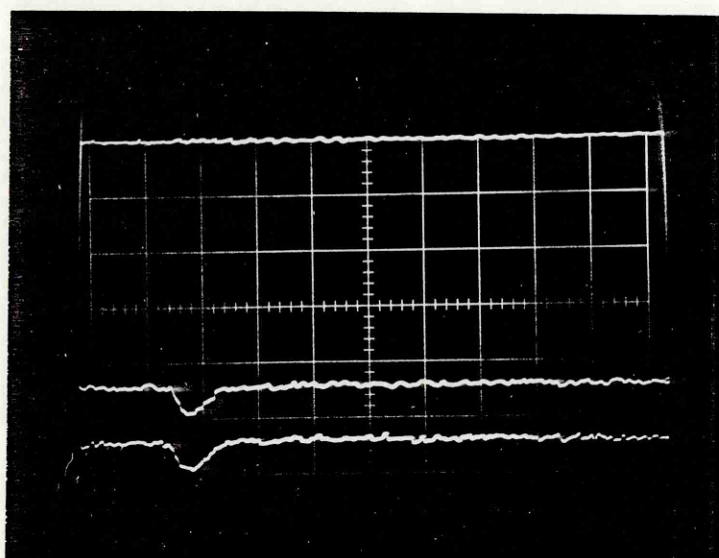
$\lambda_{\text{ex}} = 694\text{nm}$

Monochromator resolution = 1.04nm

Photomultiplier tube bias = -822V

Fig. 4.2

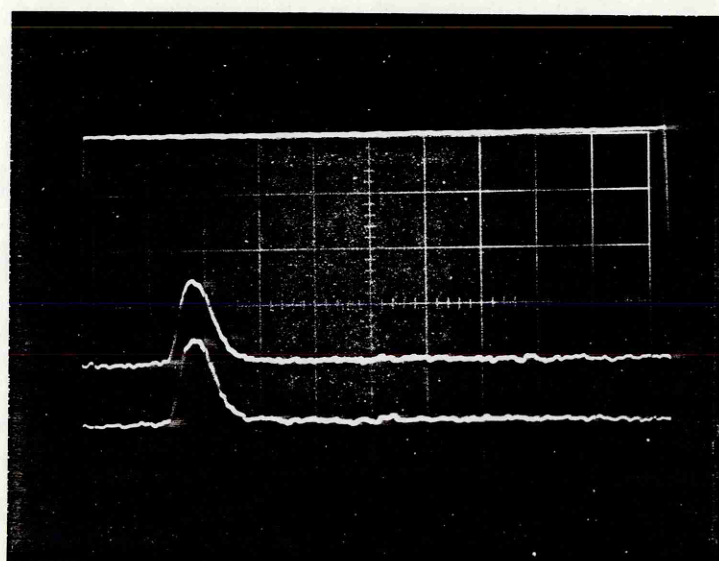




360nm.

10mv/div

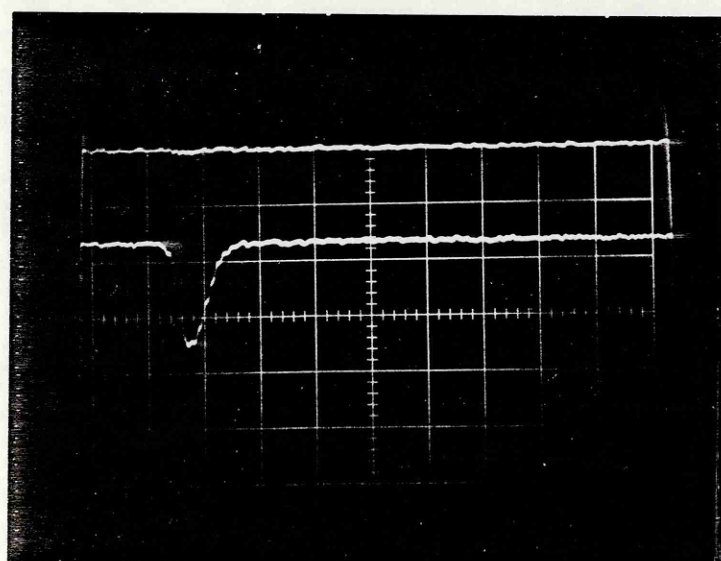
50ns/div



480nm.

20mv/div

50ns/div



700 nm.

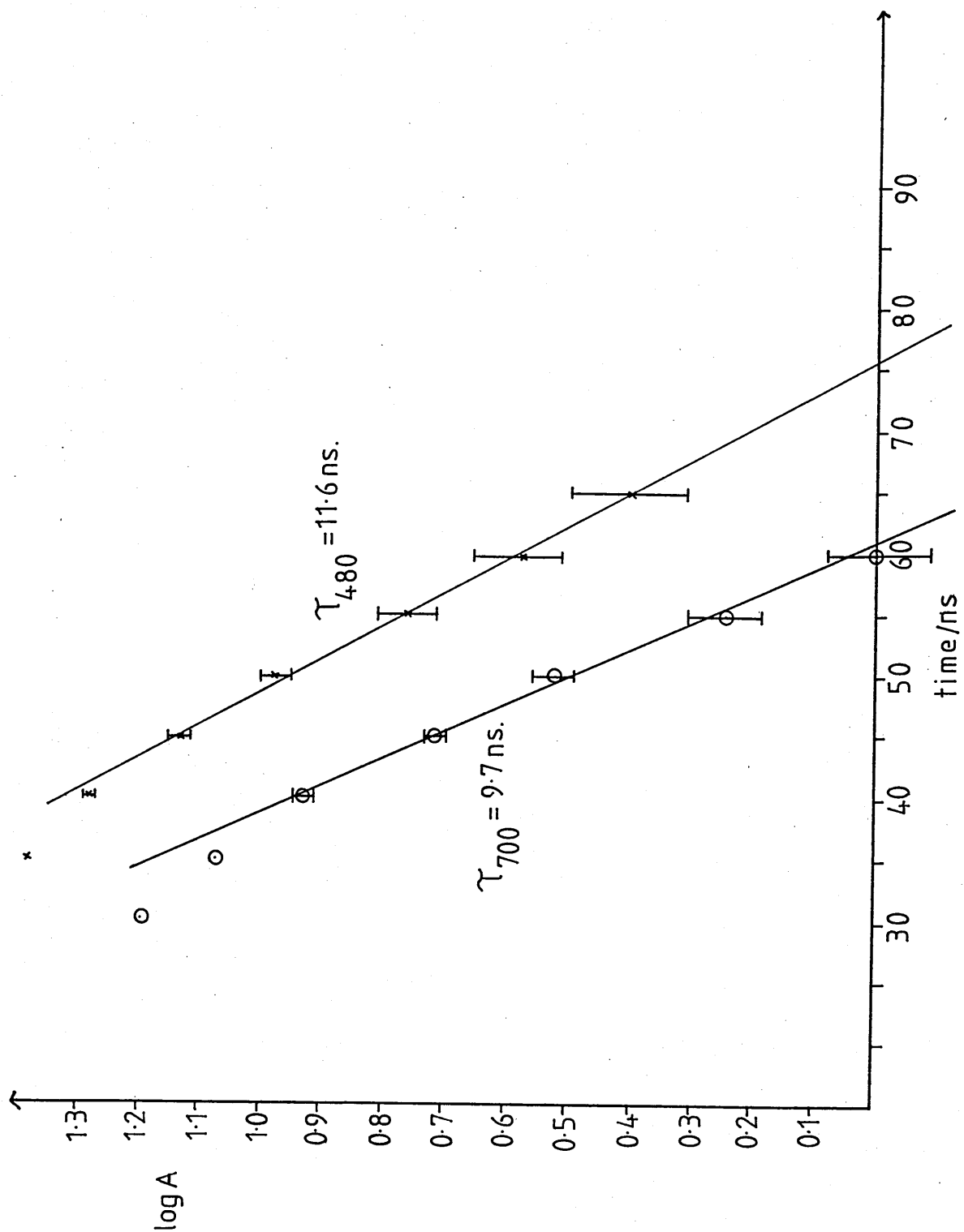
10 mv/div

50ns/div

Fig. 4.3: VOPc in toluene. λ_{ex} 694nm.

Fig. 4.4

Semi-log plots for VOPc in toluene. $\lambda_{\text{ex}} 694 \text{ nm}$.



4.2(iii) VOPc in toluene . λ_{ex} 347 nm. # 1

The transient spectra of solution (1) of VOPc in toluene at times $t = 0$, 10 ns and 20 ns after the maximum of the laser pulse are shown in Fig.4.5. The spectrum at $t = 0$ has a strong absorption in the visible with a small peak at 405 nm and a maximum absorption at ≈ 500 nm. Strong ground-state depletion is evident between 610 nm and 730 nm and at wavelengths shorter than 390 nm.

The amplitude of transient absorption and depletion decreases with time; in particular the peak at 405 nm become less well defined. The transient response is illustrated in Fig.4.6 and the decays at 490 nm and 700 nm plotted in Fig.4.7. The lifetime of the transient species at these two wavelengths is calculated to be:

$$\tau_{490} = 10.1 \pm 0.5 \text{ ns}$$

$$\tau_{700} = 8.4 \pm 0.7 \text{ ns}$$

Laser excitation is shown to induce a 'blue' fluorescence with a maximum yield at ≈ 390 nm.

4.2(iv) Fluorescence spectra

A fluorescence spectrum of solution (1) of VOPc in toluene using arc-lamp excitation at ≈ 347 nm is shown in Fig.4.8(a). The peak lies at 388 nm. Monitoring the emission at this wavelength and scanning the excitation wavelength produced

Fig. 4.5

Transient difference spectra of VOPc in toluene (1).

Spectra plotted at $t = 0$: --X--X--X--

$t = 10\text{ns}$:•.....•.....•.....

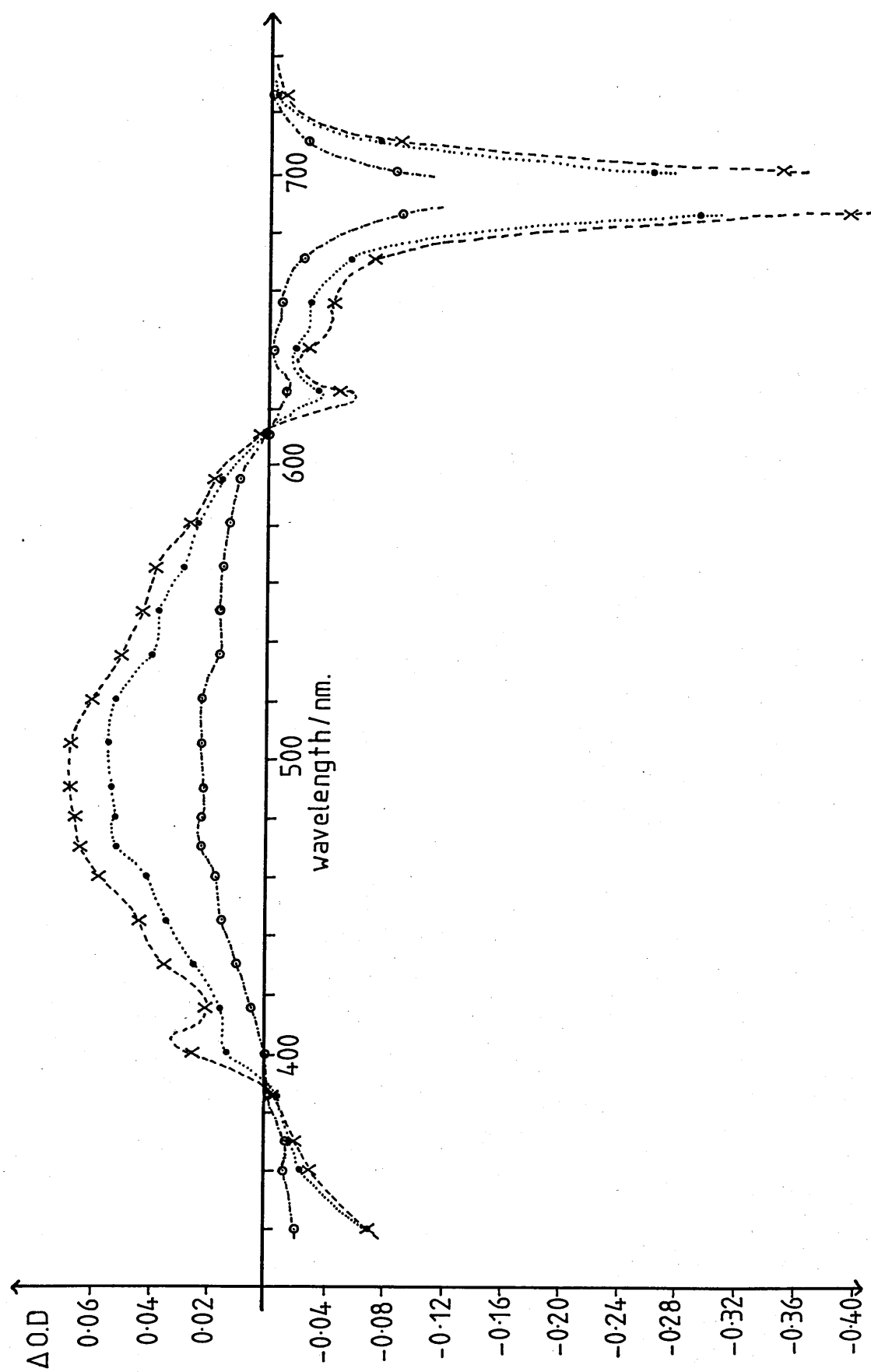
$t = 20\text{ns}$: ----○-----○-----○-----

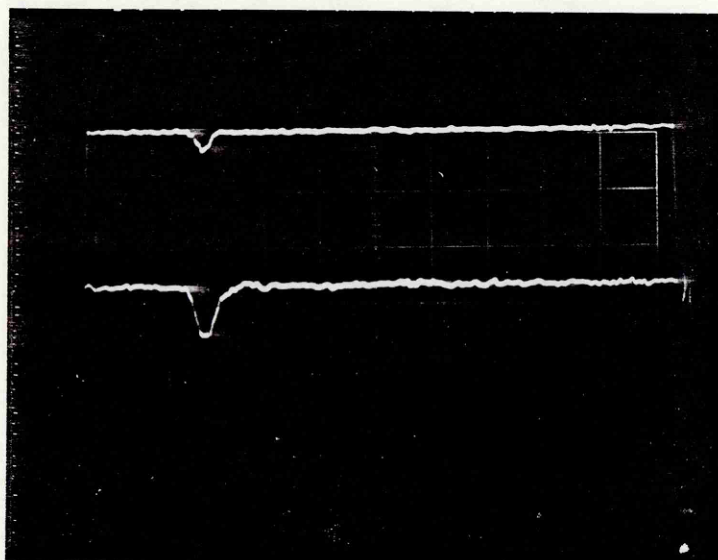
$\lambda_{\text{ex}} = 347\text{nm}$

Monochromator resolution = 1.04nm

Photomultiplier tube bias = -822V

Fig. 4.5

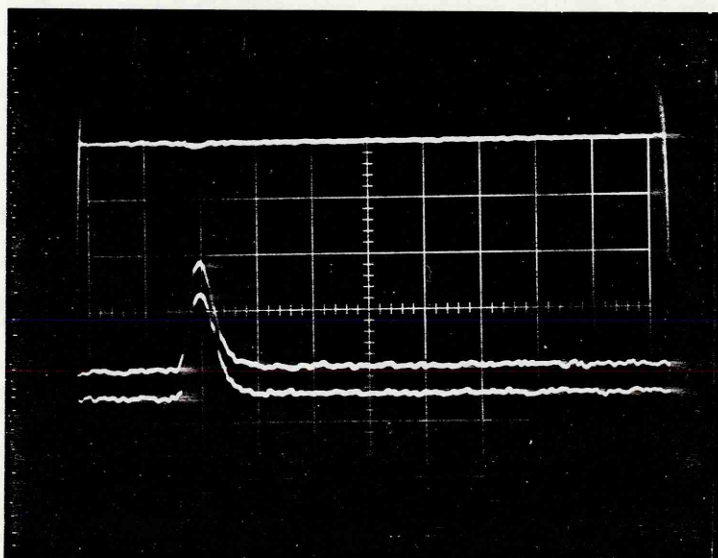




340 nm.

10mv/div

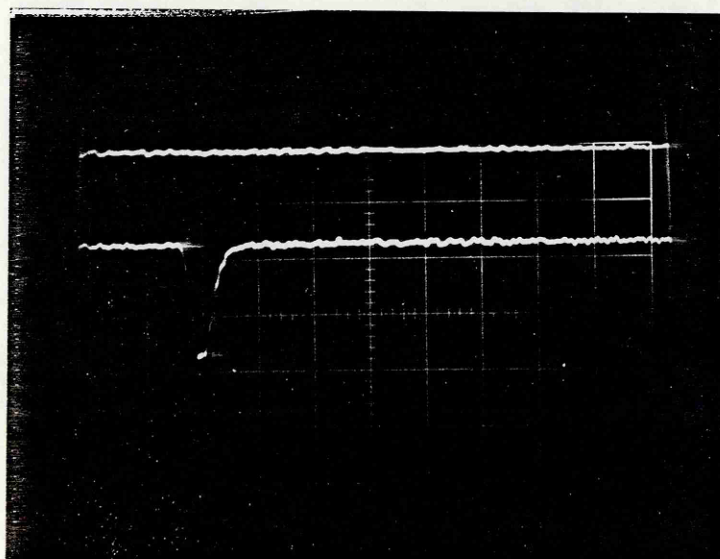
50ns/div



490 nm.

20mv/div

50ns/div



700 nm.

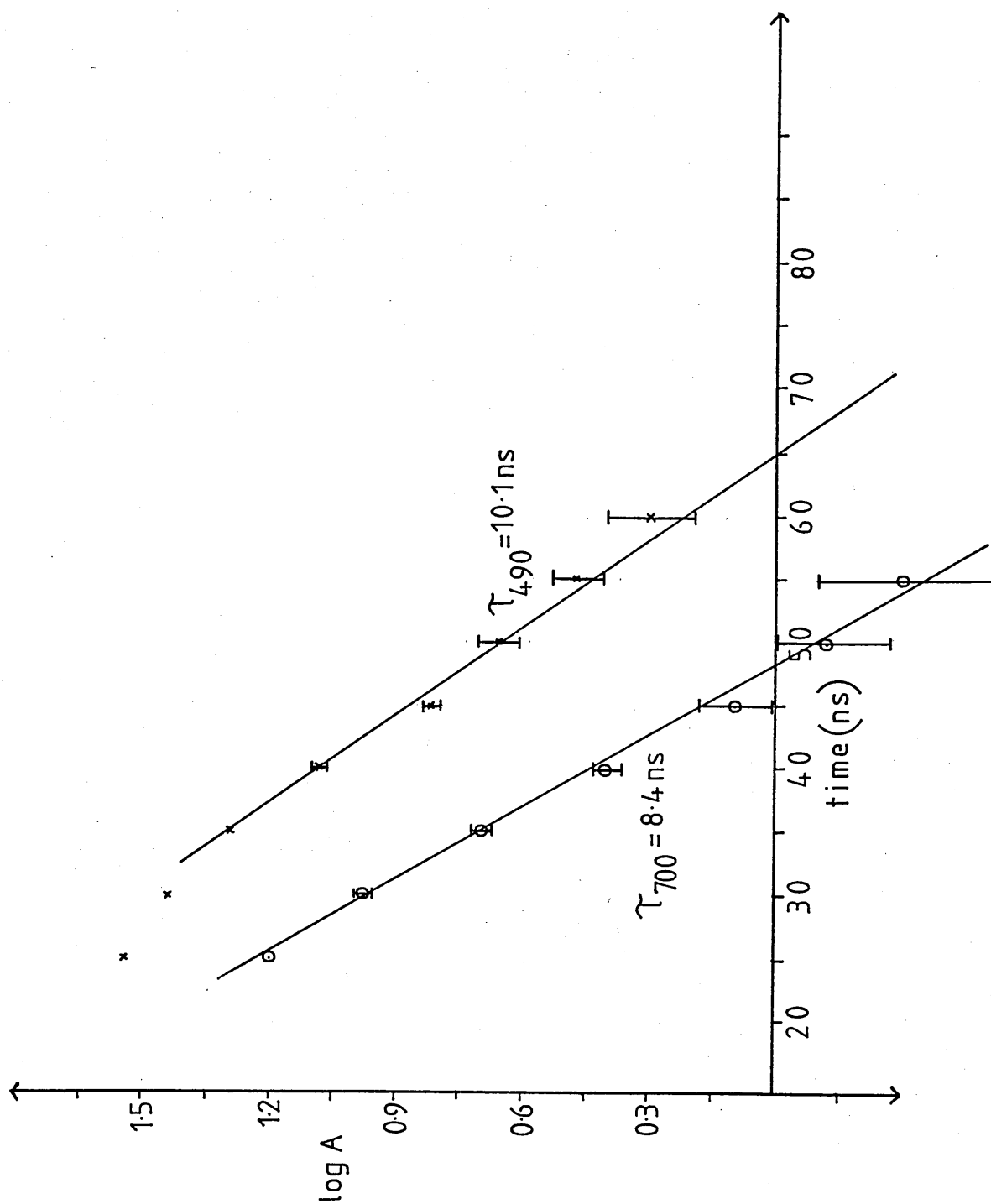
10mv/div

50ns/div

Fig. 4.6 VOPc in toluene λ_{ex} 347nm. # 1

Fig.4.7

Semi-log plots for VOPc in toluene (1). $\lambda_{ex}=347\text{nm}$.



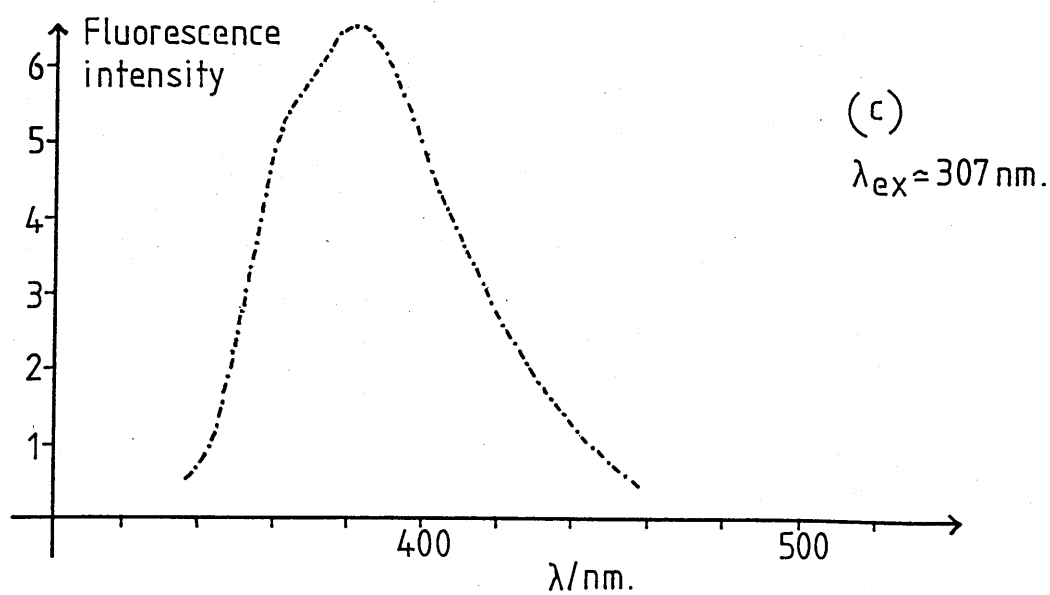
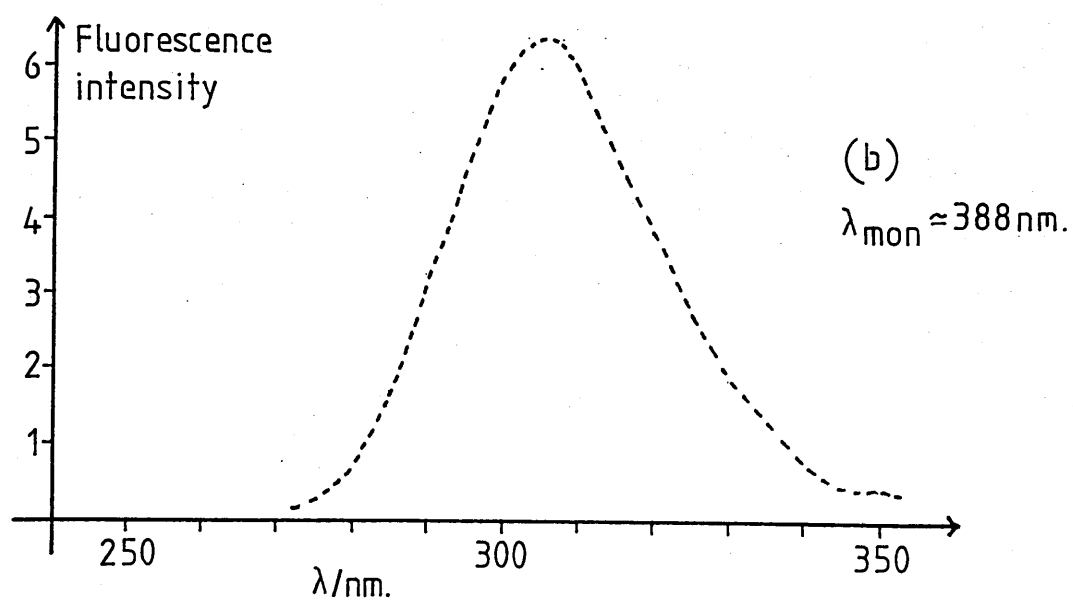
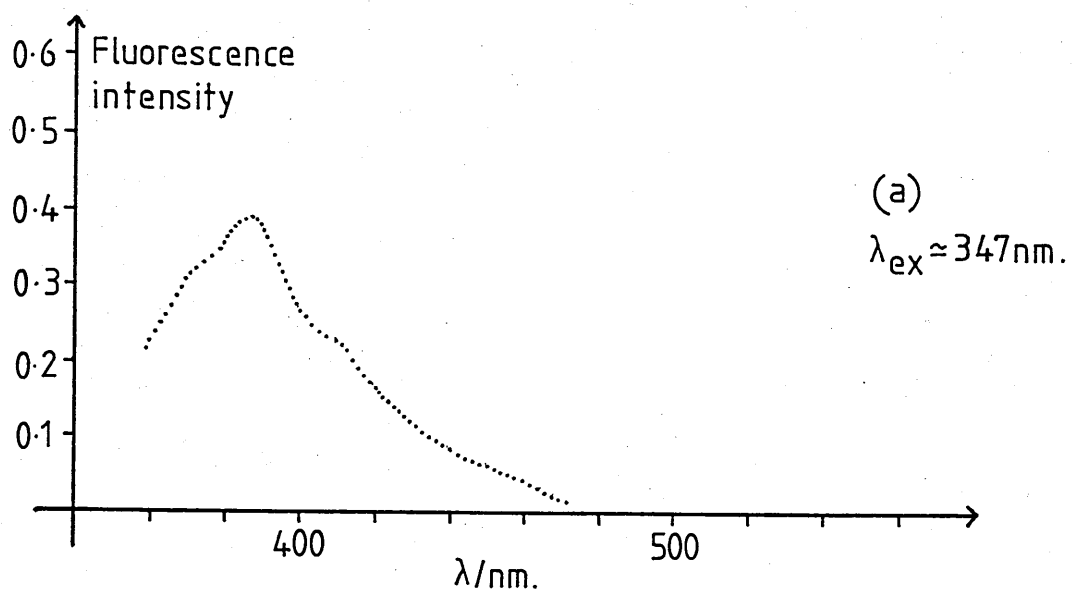


Fig.4.8: Fluorescence spectra of VOPc in toluene(1).

the spectrum of Fig.4.8(b) which has a single peak centred at 307 nm.

The fluorescence spectrum λ_{ex} 307 nm [Fig.4.8(c)] shows a much increased emission ($\times 17$) and a slight shift of the peak to 380 nm.

4.2(v) VOPc in toluene . λ_{ex} 347 nm. # 2

The transient spectra of solution (2) of VOPc in toluene at times $t = 0, 10 \text{ ns}, 20 \text{ ns}$ after the maximum of the laser pulse are shown in Fig.4.9. The shape of the spectra are very similar to those obtained using solution (1). The only slight differences are that the maximum of transient absorption lies at 490 nm, the small peak in the blue/near u-v lies at 400 nm and the depletion of the Soret absorption band does not yield a negative signal until 380 nm. Also, due to the lower concentration of solution (2), the amplitudes of transient absorption and depletion are not so large as in the former case.

The transient response is illustrated in Fig.4.10 and the decays at 500 nm and 700 nm plotted in Fig.4.11. The lifetime of the transient species at these two wavelengths is calculated to be:

$$\tau_{500} = 11.3 \pm 0.8 \text{ ns}$$

$$\tau_{700} = 8.0 \pm 0.9 \text{ ns}$$

Fig. 4.9

Transient difference spectra of VOPc in toluene (2).

Spectra plotted at $t = 0$: --*---*---*--

$t = 10\text{ns}$:•.....•.....

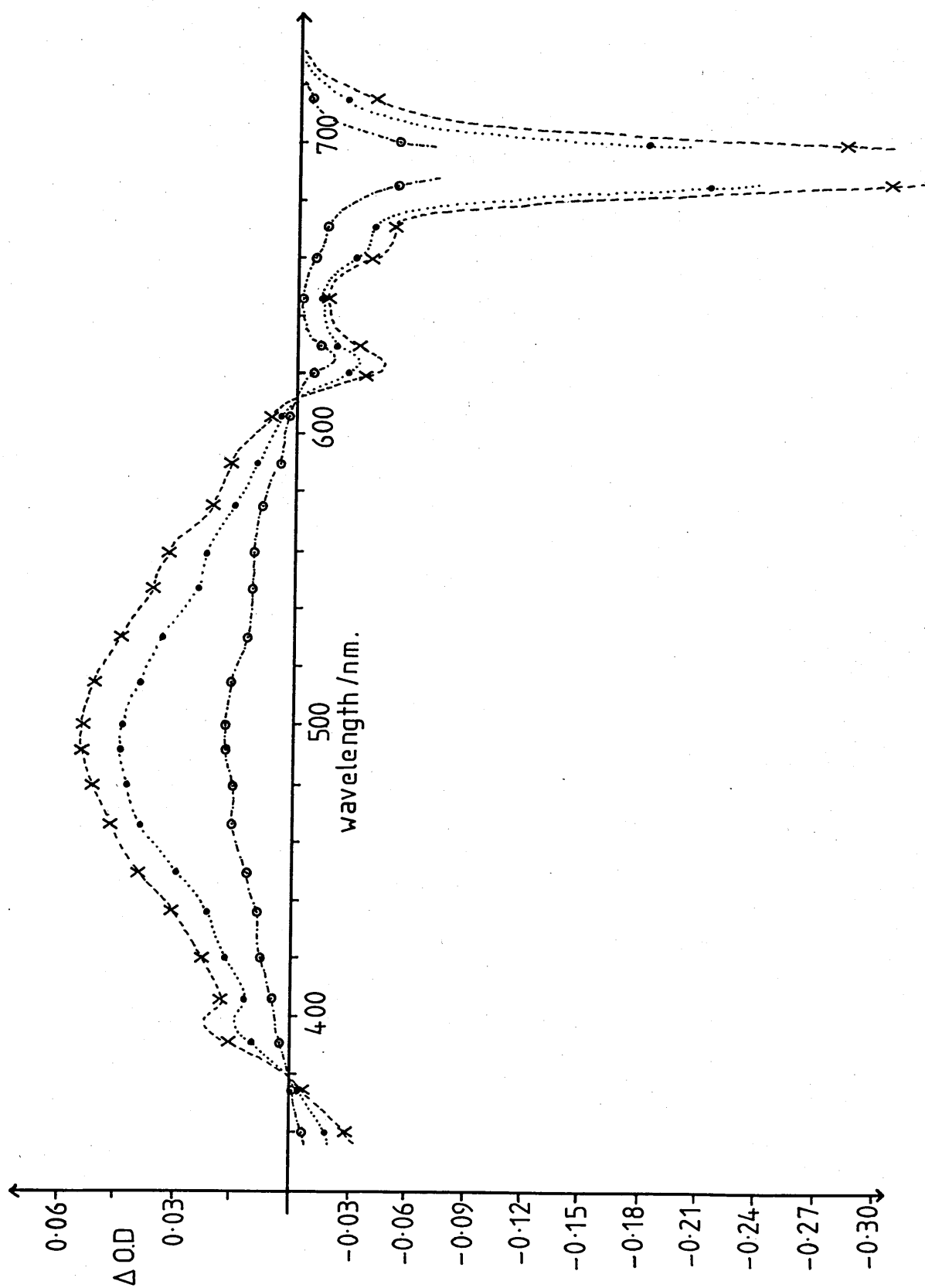
$t = 20\text{ns}$: ---○---○---○---

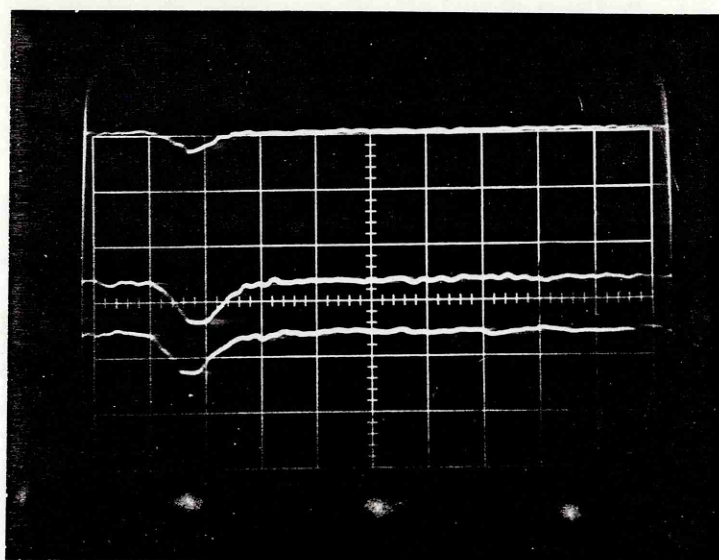
$\lambda_{\text{ex}} = 347\text{nm}$

Monochromator resolution = 1.17nm

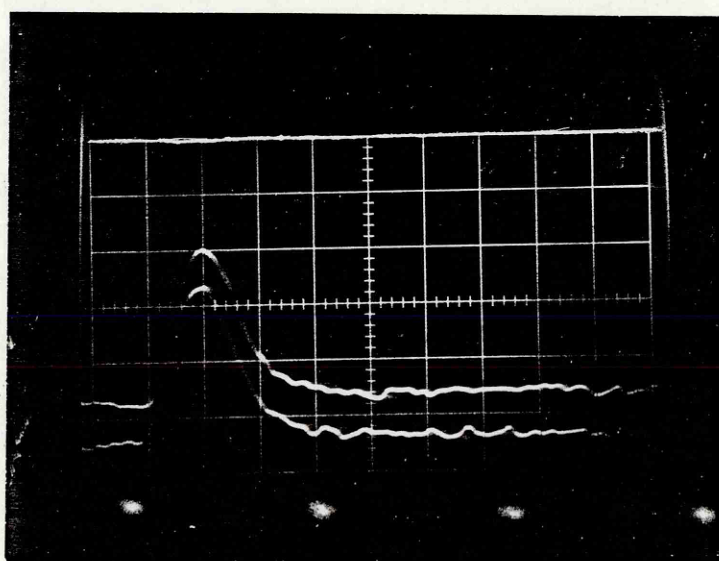
Photomultiplier tube bias = -820V

Fig. 4.9

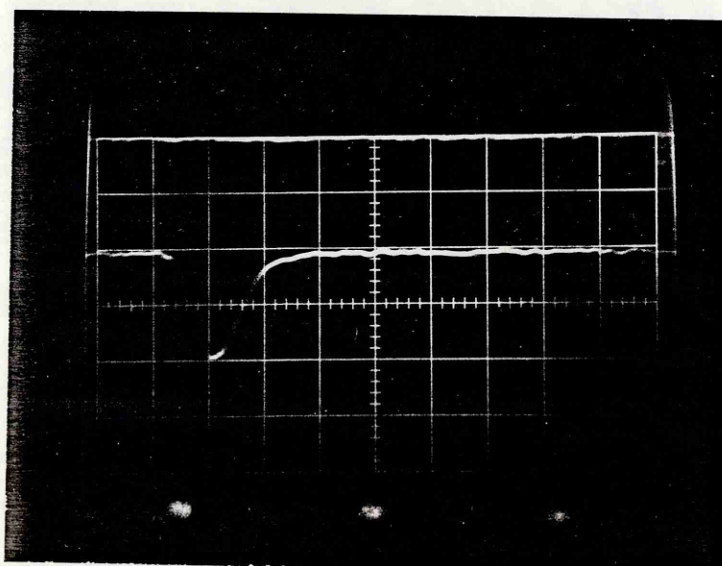




360nm
10mv/div
20ns/div



500nm.
10mv/div
20ns/div

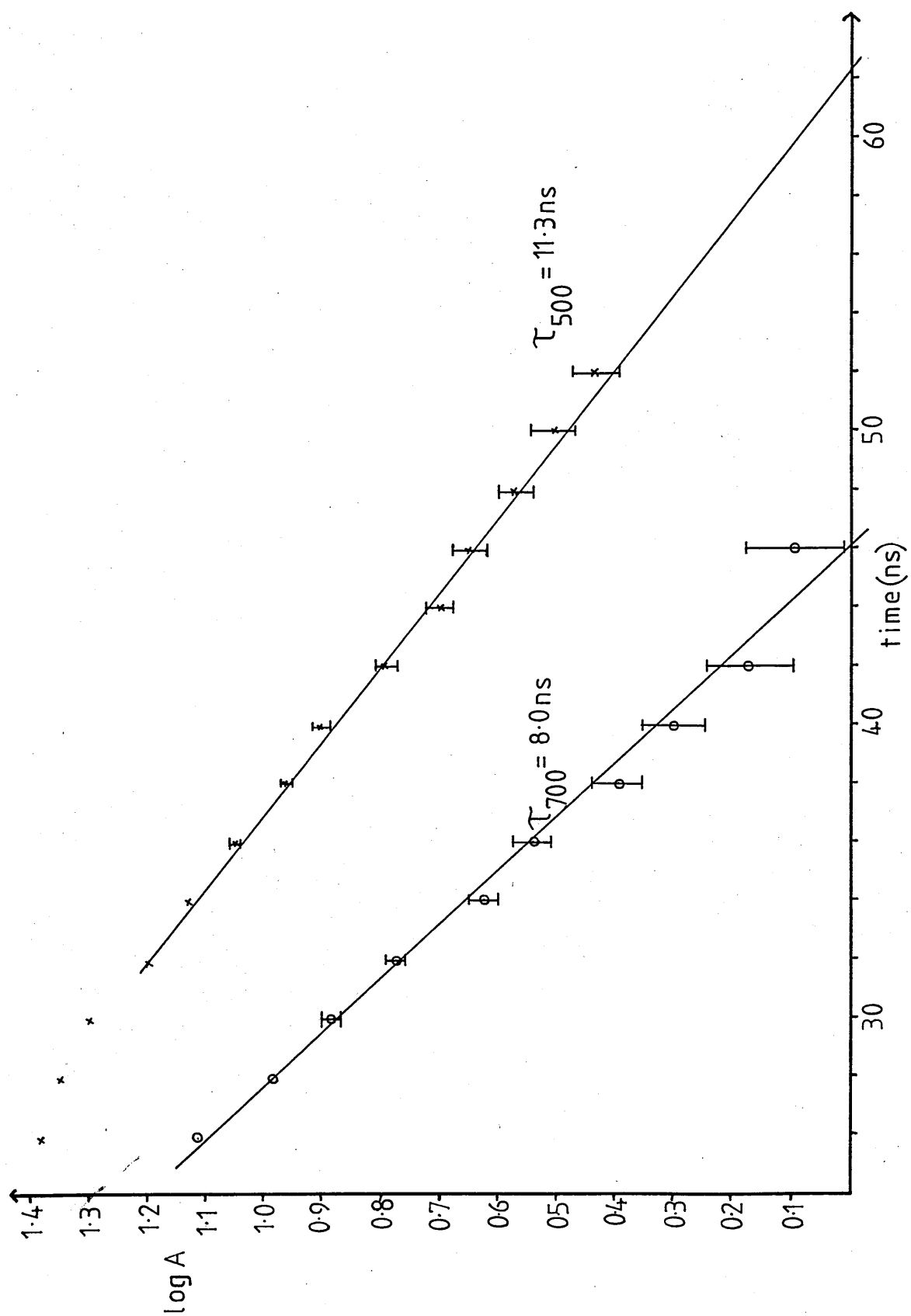


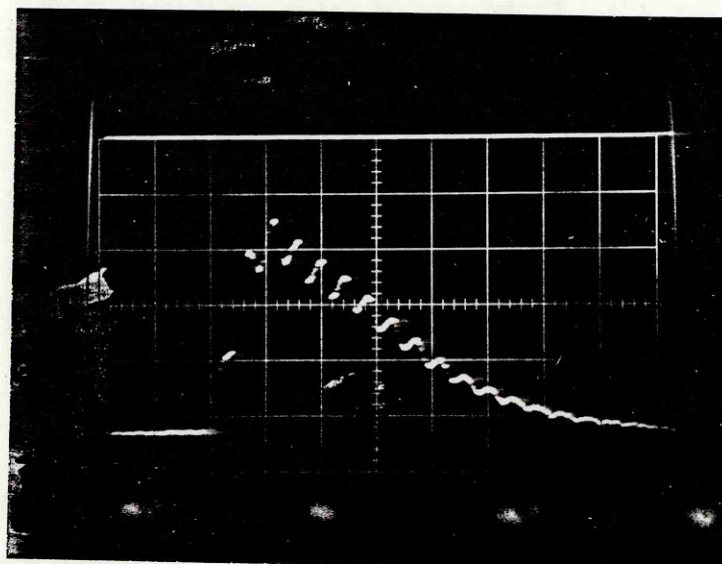
700nm.
10mv/div
20ns/div

Fig. 4.10: VOPc in toluene. λ_{ex} 347nm. # 2

Fig. 4.11

Semi-log plots for VOPc in toluene (2) $\lambda_{\text{ex}} 347\text{nm}$.



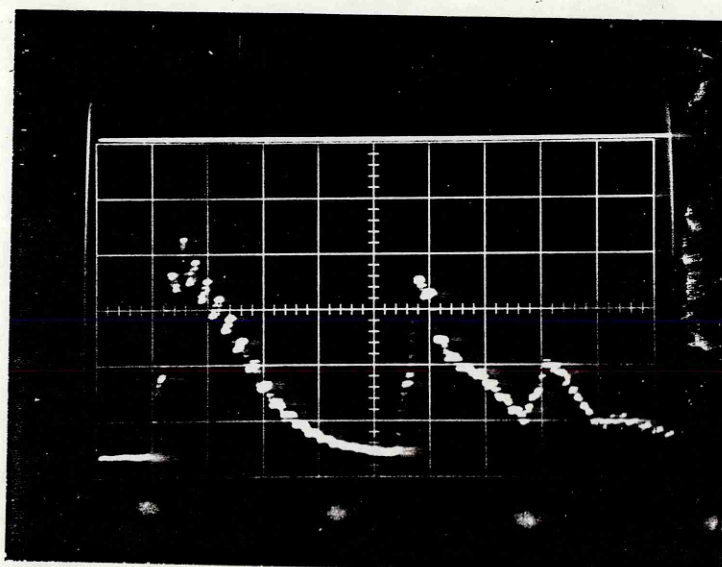


490nm.

20mv/div

1 μ s/div

not
outgassed

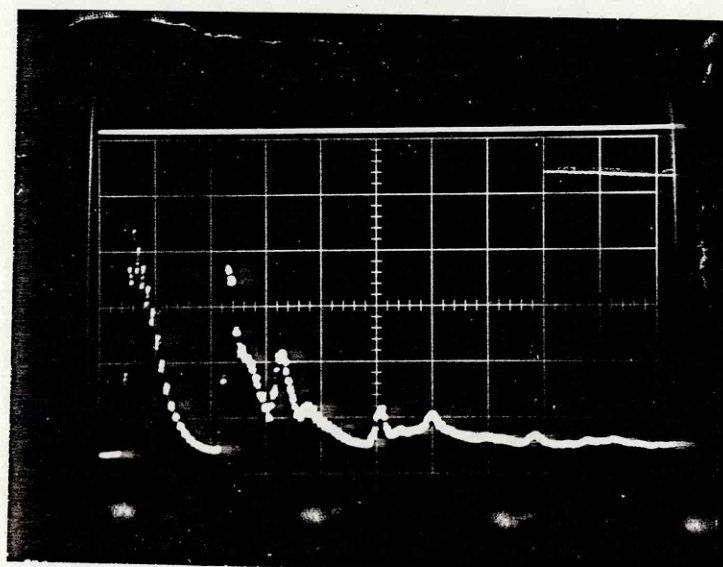


490nm.

20mv/div

2 μ s/div

not
outgassed



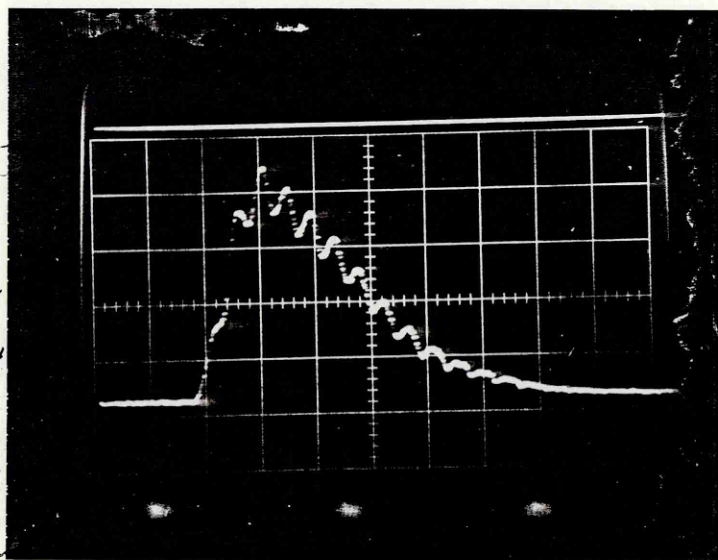
490nm.

20mv/div

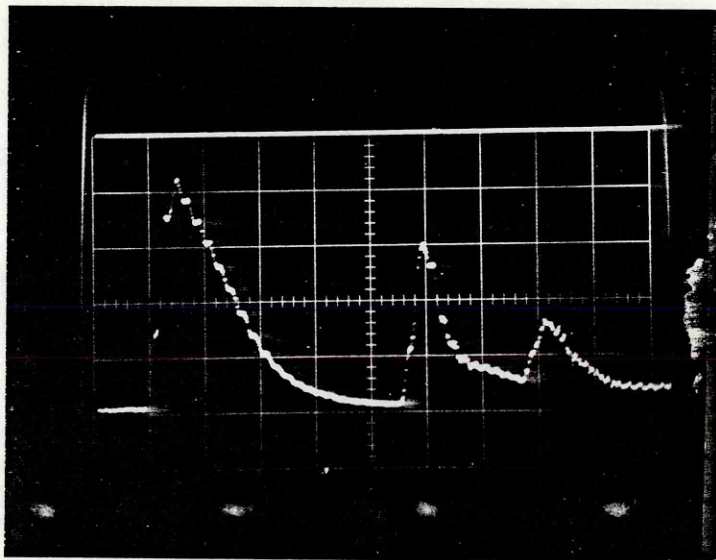
5 μ s/div

outgassed

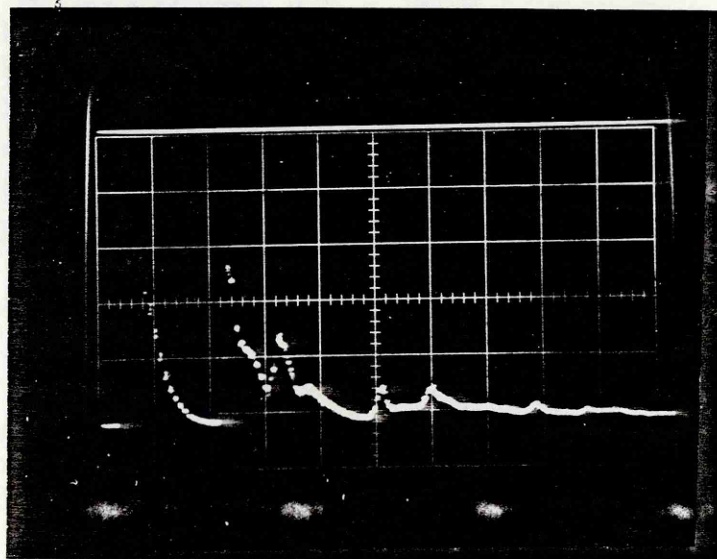
Fig.4.12 : VOPc in nitrobenzene. λ_{ex} 347nm.



490 nm.
20 mv/div
1 μ s/div
not
outgassed



490 nm.
20 mv/div
2 μ s/div
outgassed



490 nm.
20 mv/div
5 μ s/div
outgassed

Fig.4.13: Nitrobenzene. λ_{ex} 347 nm.

4.2(vi) VOPc in nitrobenzene . λ_{ex} 347 nm

The transient absorption at 490 nm of a solution of VOPc in nitrobenzene subject to 347 nm laser excitation is shown in Fig.4.12. The absorption does not set-in until approximately 1800 ns after the laser pulse and a series of decays are observed. Not all the absorptions are the same in shape as the leading one though the 'irregularity' is reproducible. The transient response appears unaffected by the presence of oxygen.

Fig.4.13 shows that the same transients are generated in a solution of nitrobenzene. Therefore this absorption is not a property of VOPc.

4.2 (vii) Summary

A comparison of the two sets of spectra obtained using 347 nm excitation shows a good agreement, although the amplitude of response of solution (2) is lower due to lower concentration. This may also be the reason for the slight differences observed, i.e. the slight shift of the small 'peak' and the onset of Soret band depletion to marginally shorter wavelengths. There is an indication that this region of ground-state depletion partially masks a near u-v transient absorption, of which this small peak is the long wavelength part.

Such behaviour is not obvious in the spectra obtained using 694 nm laser light, but otherwise they appear very similar to each other. All the spectra are also very similar to those reported as the triplet-triplet absorption of VOPc in 1-chloronaphthalene by McVie (694 nm),⁽⁴²⁾ and Pyatasin and Tsvirko (347 nm).⁽¹⁰⁷⁾

In considering the transient lifetimes, the convolution of the laser pulse with short-lived decay is significant. However it can be seen that the response subsequent to excitation into the first excited singlet state indicates that the maximum amplitude of transient absorption is not reached until after the maximum of the laser pulse. This is why the spectra at $t = 0$ and $t = 10$ ns are almost identical. In contrast the transient response to excitation into the second excited singlet is rapid. The two sets of decay times relating to this condition are comparable, but those obtained using red excitation have a slightly longer duration. There also seems to be a consistent pattern in that the decay of the transient absorption in the visible region of the spectrum appears slightly longer than that of the recovery from ground-state depletion. These lifetimes are comparable to the 15 ns decay time for this solution estimated by De-Silva,⁽³⁵⁾ but are shorter than the 20 ns recovery time obtained by Kosonochy and Harrison⁽¹⁰⁴⁾ and the triplet lifetime of 35 ns reported by Pyatosin and Tsvitko⁽¹⁰⁷⁾ for VOPc in 1-chloronaphthalene.

It is notable that the blue fluorescence observed from solution (1) is completely absent in solution (2), although there is a slight impurity emission from toluene. This is a consequence of the different effects of the two purification procedures on the solute and explanations are suggested in the conclusions (Chapter 5).

The action of 347 nm laser light on a solution of VOPc in nitrobenzene was reported by Hodgkinson⁽³⁴⁾ to induce an unusual transient absorption. It is likely that this effect was due to the action of the solvent. However the decay profile was not irregular in the same way as that presented here; in addition there was no delay between the laser pulse and the onset of transient absorption.

In common with many other previous observations, or lack of them, no fluorescence was recorded from the lowest excited singlet state for any of these VOPc solutions.

4.3 ALUMINIUM PHTHALOCYANINE CHLORIDE

4.3(i) Ground-state absorption

The ground-state absorption spectra for two solutions of AlPcCl in ethanol are shown in Fig.4.14. In solution (1), the solute is not purified whereas that of solution (2) is purified by method B.

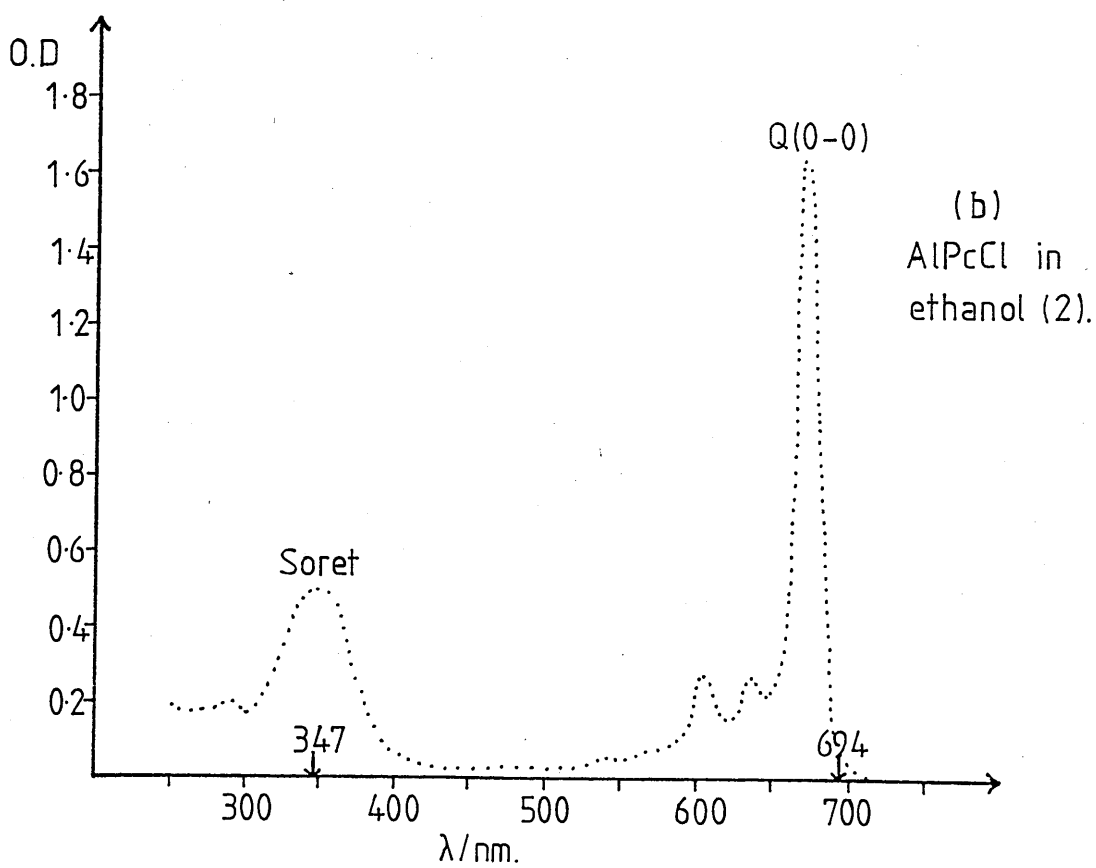
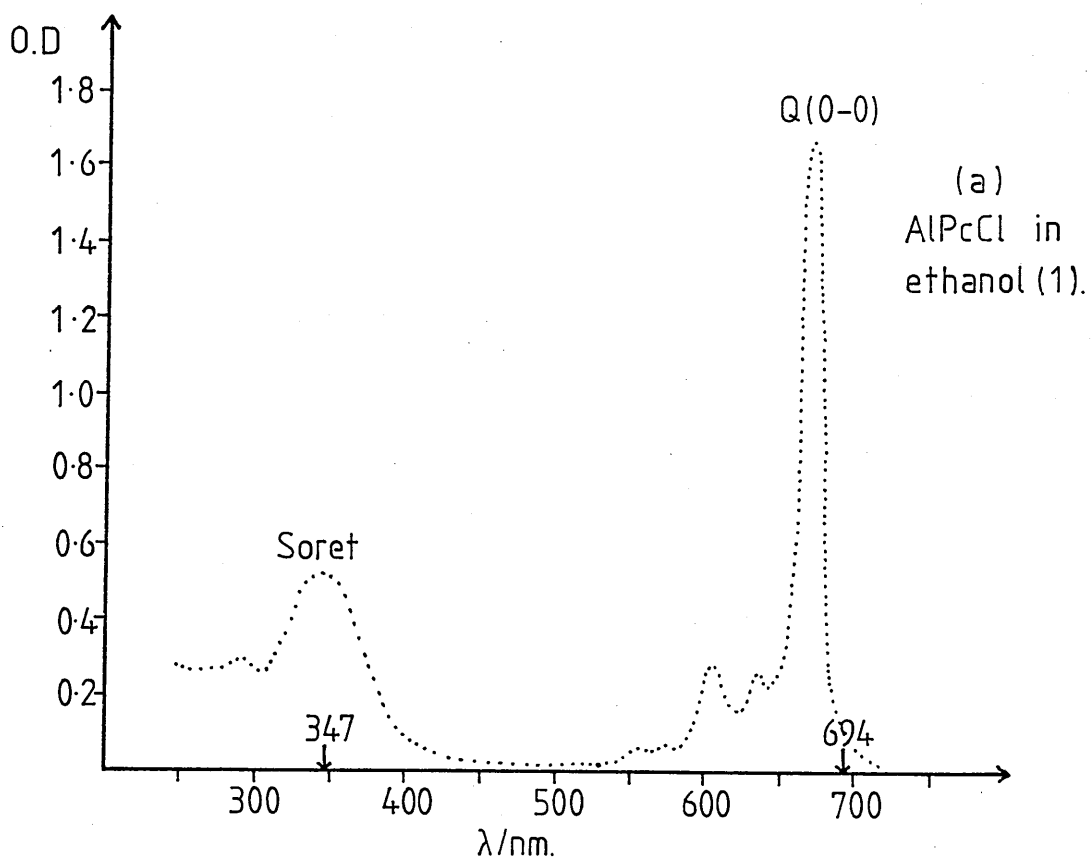


Fig.4.14: Ground-state absorption spectra.

4.3(ii) AlPcCl in ethanol . λ_{ex} 694 nm

The transient spectra of solution (1) of AlPcCl in ethanol at times $t = 0, 20 \text{ ns}, 100 \text{ ns}$ and 350 ns after the maximum of the 694nm laser pulse are shown in Fig.4.15. The spectrum at $t = 0$ shows a shoulder at 400 nm and an absorption throughout most of the visible with a broad peak centred on 490 nm. Between 580 nm and 640 nm there is an indication of a strong absorption component which is significantly masked by the disappearance of the ground-state absorption spectrum. At $t = 20 \text{ ns}$ this component appears slightly reduced although the transient absorption over the rest of the spectrum is greater than at $t = 0$ and the shoulder previously observed at 400 nm has developed into a small peak.

The overall shape of the spectra at $t = 100 \text{ ns}$ and 350 ns is similar to those for the earlier times although the visible absorption is broader and the main peak not so sharp. Also there is a more rapid fall-off in amplitude approaching 600 nm. It is notable that the amplitude of transient absorption increases between $t = 100 \text{ ns}$ and $t = 350 \text{ ns}$.

All the spectra show the effects of ground-state depletion at wavelengths longer than 595 nm and shorter than 375 nm corresponding to short and long wavelength edges respectively of the two ground-state absorption bands.

The transient response at 490 nm can be seen to better effect

Fig. 4.15

Transient difference spectra of AlPcCl in ethanol (1).

Spectra plotted at $t = 0$: -x-x-x-

$t = 20\text{ns}$:•.....

$t = 100\text{ns}$: --o--o--o--o--o--

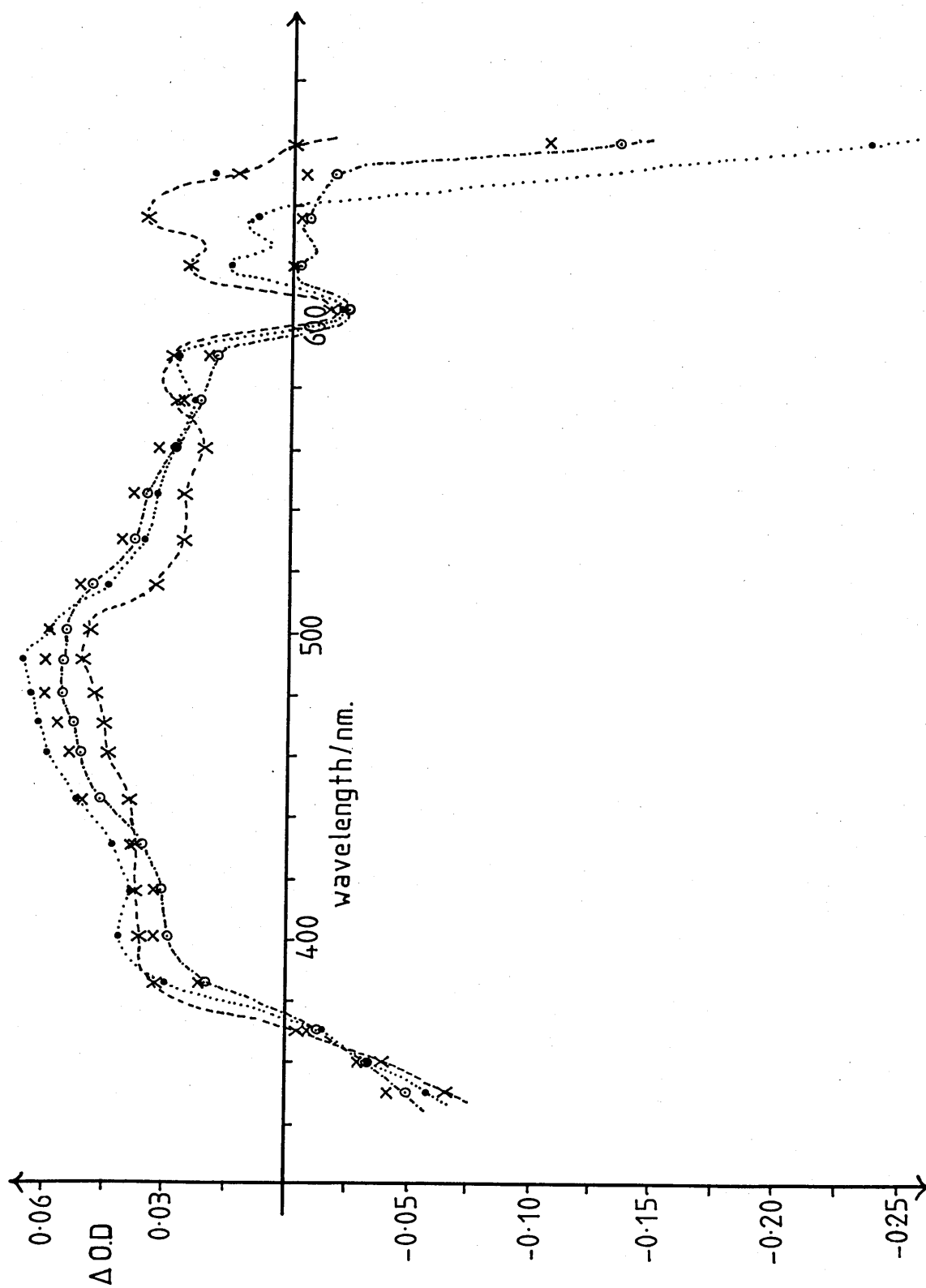
$t = 350\text{ns}$: x x x

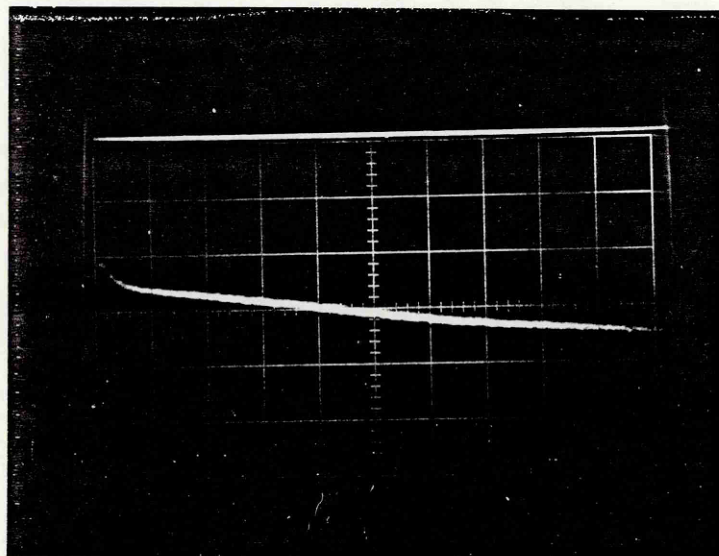
$\lambda_{\text{ex}} = 694\text{nm}$

Monochromator resolution = 1.04nm

Photomultiplier tube bias = -822V.

Fig.4.15

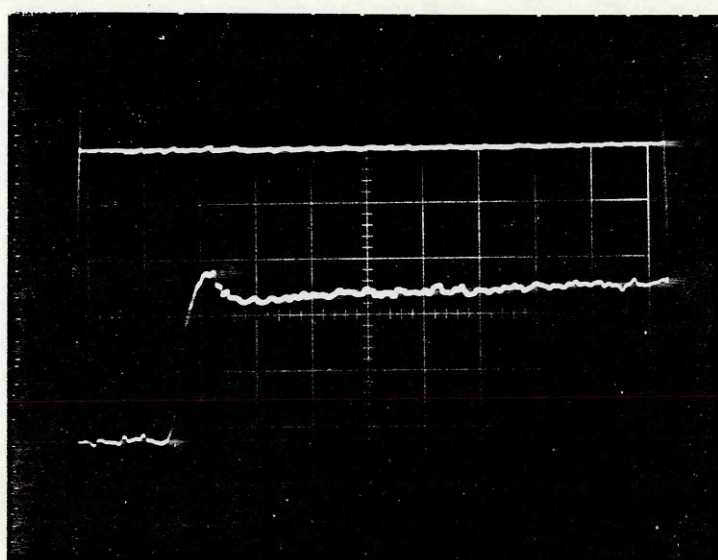




480 nm.

10mv/div

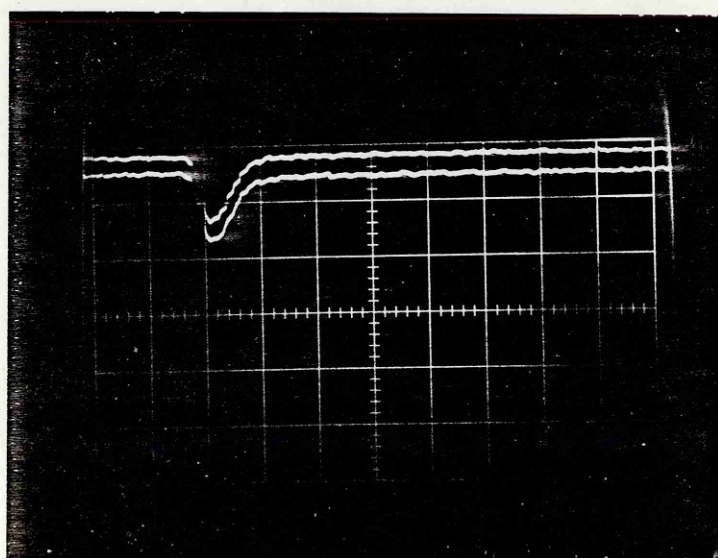
5 μ s/div



490 nm.

10mv/div

50ns/div



660 nm.

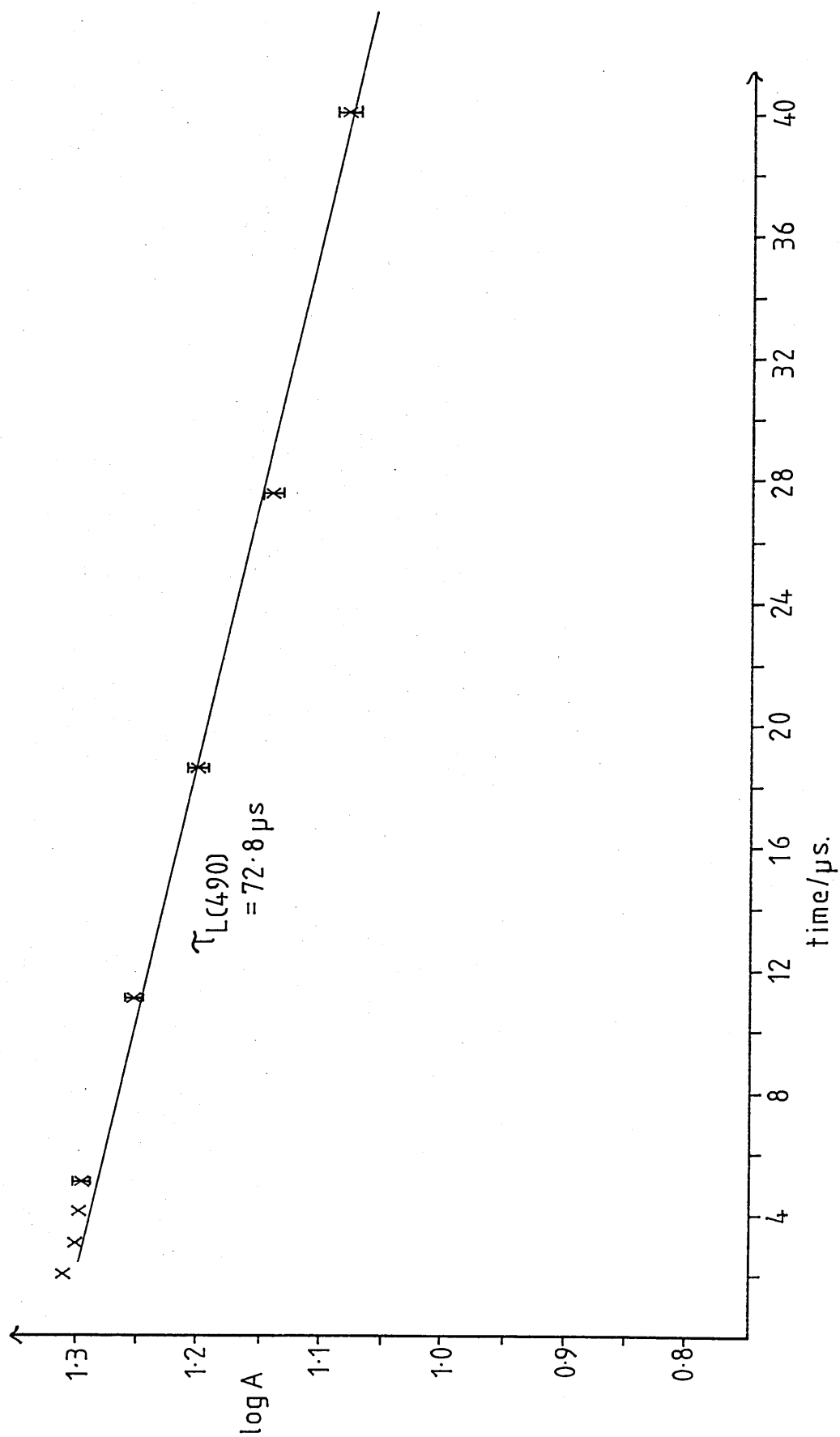
10mv/div

50ns/div

Fig. 4.16: AlPcCl in ethanol. λ_{ex} 694 nm.

Fig. 4.17

Semi-log plot for AlPcCl in ethanol, $\lambda_{\text{ex}} 694\text{nm}$.



in Fig.4.16. The kinetics are not simple, with the initial absorption component preceding another which grows in over the subsequent 500 ns. This in turn can be seen on a longer time-scale to decay to a longer-lived transient. The decay of this final component is plotted in Fig.4.17 and the lifetime calculated to be:

$$\tau_L(490) = 72.8 \pm 4.8 \mu s$$

A fluorescence emission occurs in the red part of the spectrum between 670 nm and 635 nm. The decaying edge of this fluorescence is longer than that of the laser pulse and the lifetime at 660 nm is calculated from Fig.4.18 to be:

$$\tau_F(660) = 14.0 \pm 1.5 \text{ ns}$$

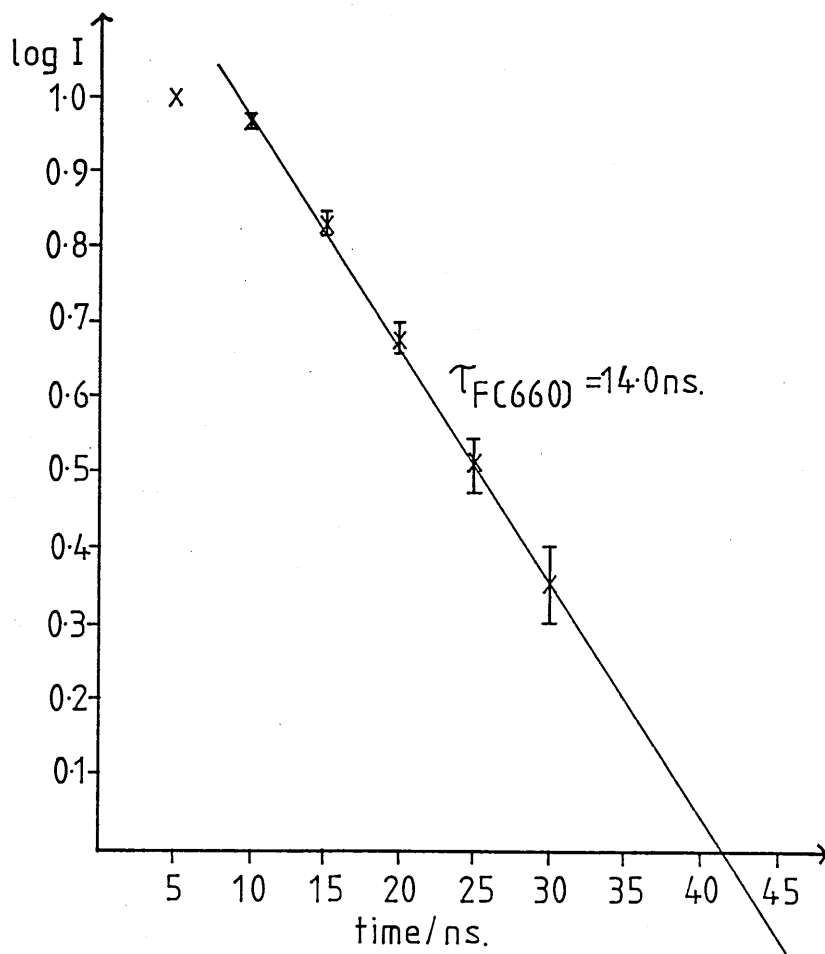


Fig.4.18: Semi-log plot for AlPcCl in ethanol. $\lambda_{ex} 694 \text{ nm.}$

4.3(iii) AlPcCl in ethanol . λ_{ex} 347 nm # 1

The transient spectra of solution (1) of AlPcCl in ethanol at times $t = 0$, 20 ns and 350 ns after the maximum of the 347 nm excitation are shown in Fig.4.19. At $t = 0$, there is an absorption in the near u-v with a peak at 395-400 nm and a broad peak of slightly greater intensity centred on 470-480 nm. In addition there is a clear indication of a region of strong transient absorption between 580 nm and 640 nm although eaten into by ground-state depletion. By 20 ns the regions of absorption in this red band and at ≈ 400 nm are reduced by proportionally more than that at the absorption maximum of 480 nm. Similarly at 350 ns the visible transient absorption shows the same overall shape but represents a slightly lower amplitude of response.

Ground-state depletion is evident in all spectra at wavelengths longer than 595 nm and shorter than 380 nm.

The decay profiles (Fig.4.20) indicate that at 470 nm there is a short-lived component followed by more than one longer-lived component. Although the decays are not obviously simple exponentials, lifetimes for each component have been estimated (Fig.4.21) and are suggested as being:

$$\tau_1 (470) = 359 \pm 238 \text{ ns}$$

$$\tau_2 (470) = 35.9 \pm 8.6 \text{ } \mu\text{s}$$

$$\tau_3 (470) = 70.7 \pm 2.9 \text{ } \mu\text{s}$$

Fig. 4.19

Transient difference spectra of AlPcCl in ethanol (1).

Spectra plotted at $t = 0$: -x--x--x-

$t = 20\text{ns}$:●.....●.....

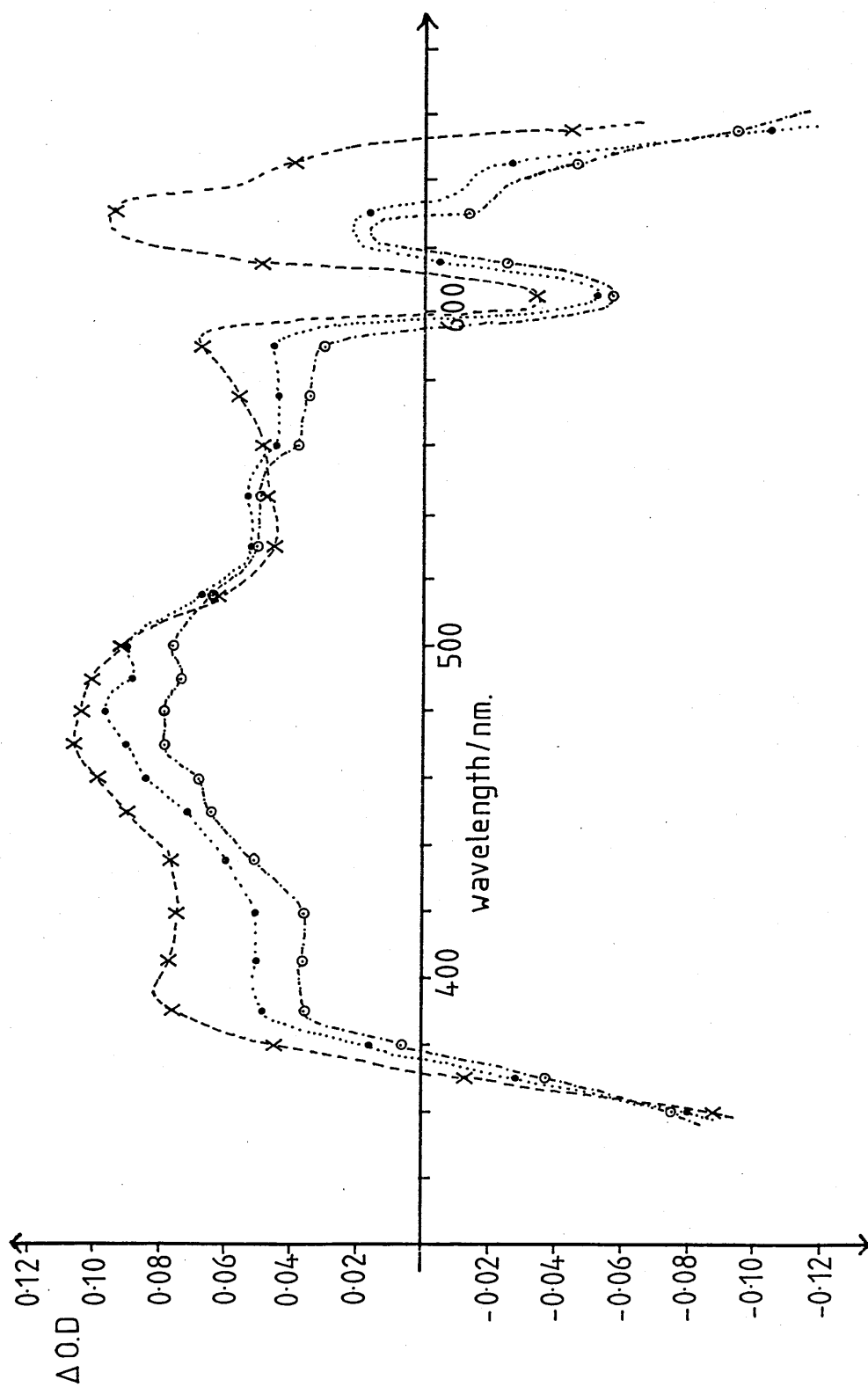
$t = 350\text{ns}$: ---○---○---○---

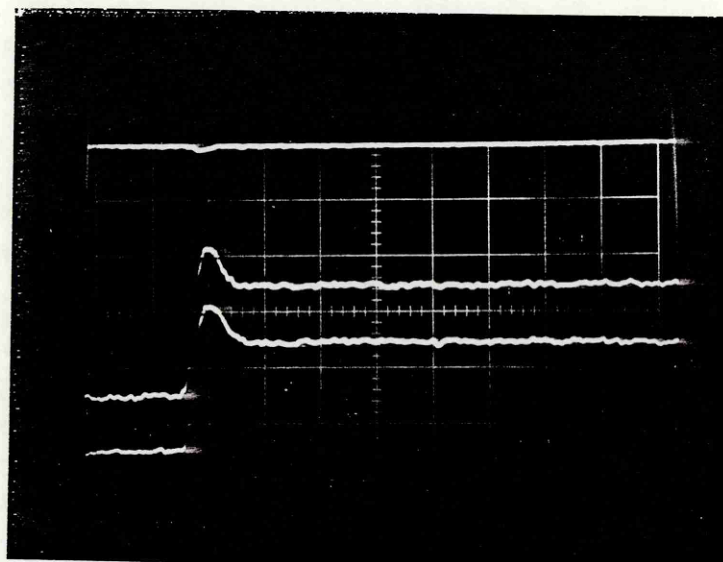
$\lambda_{\text{ex}} = 347\text{nm}$

Monochromator resolution = 1.04nm

Photomultiplier tube bias = -822V

Fig. 4.19

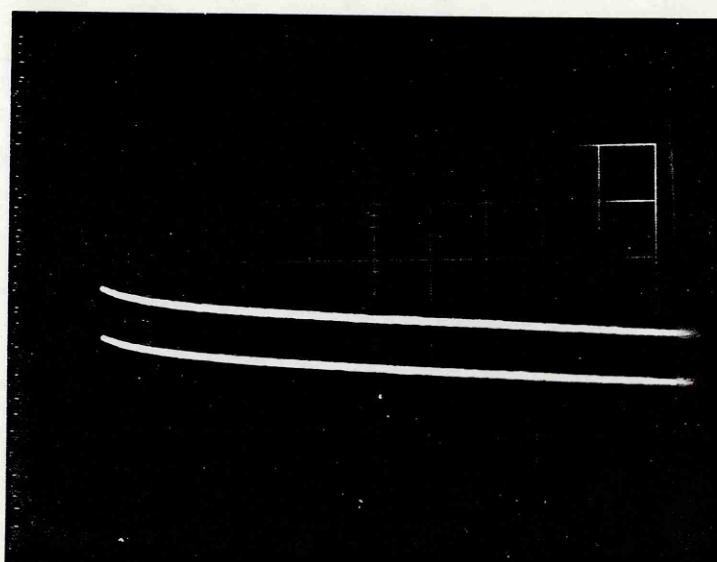




470nm.

20mv/div

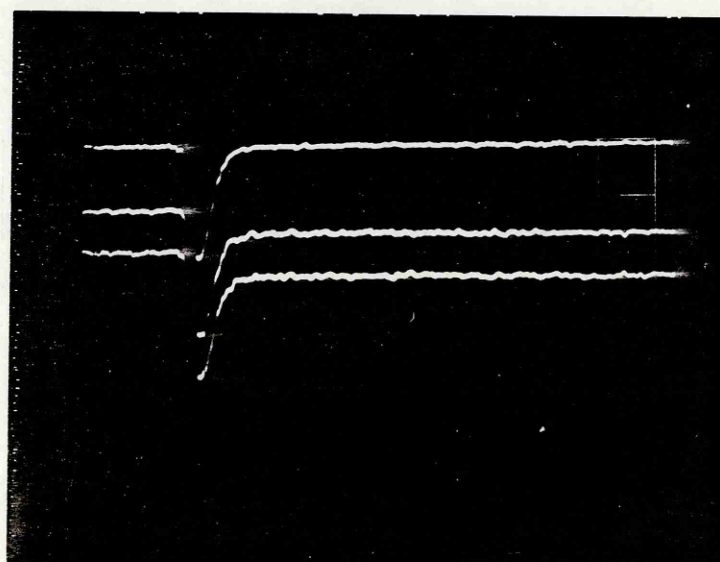
50ns/div



470nm.

20mv/div

5 μ s/div



655nm.

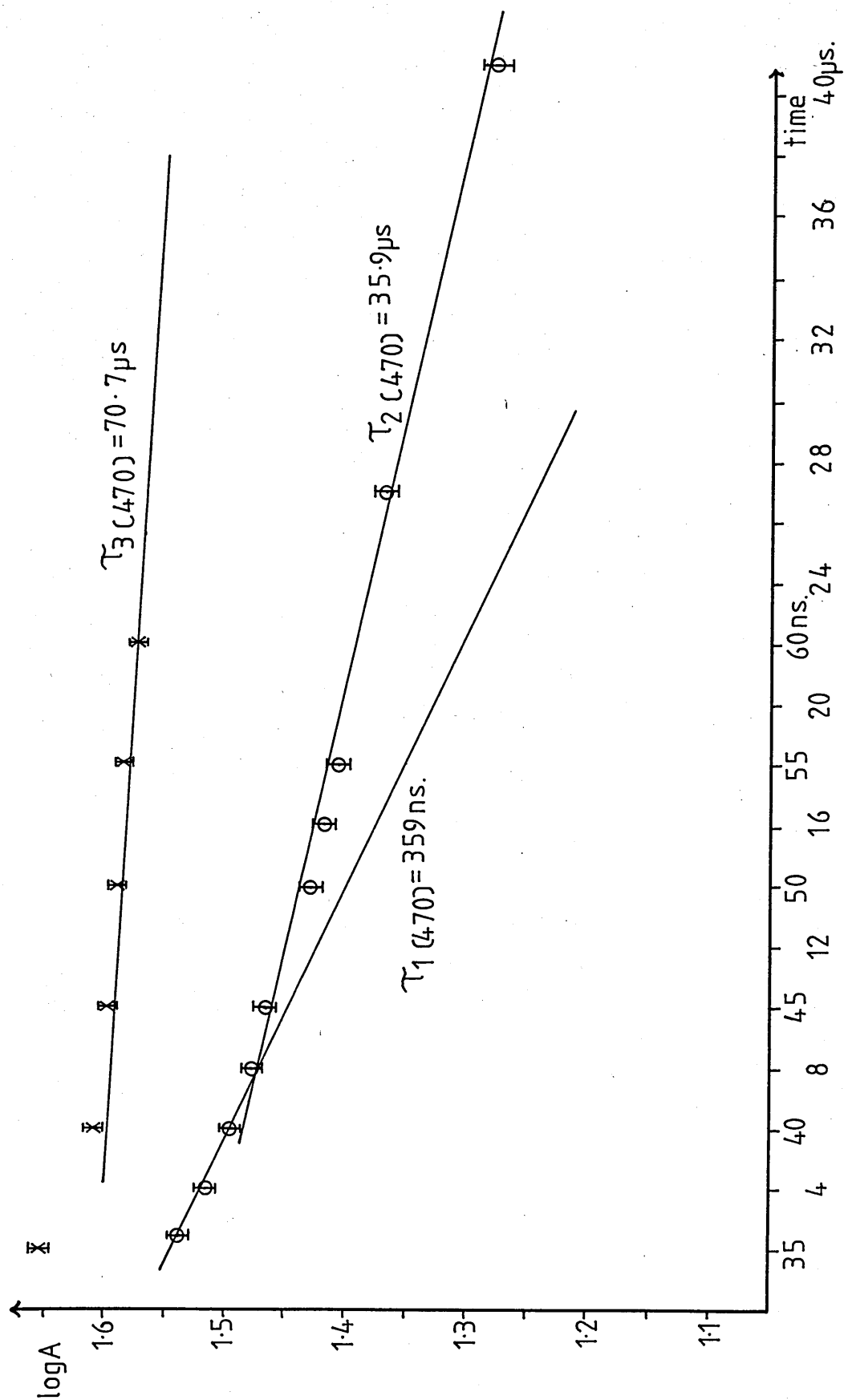
10mv/div

50ns/div

Fig. 4.20: AlPcCl in ethanol. λ_{ex} 347nm.# 1

Fig. 4.21

Semi-log plots for AlPcCl in ethanol (1) $\lambda_{\text{ex}} 347 \text{ nm}$.



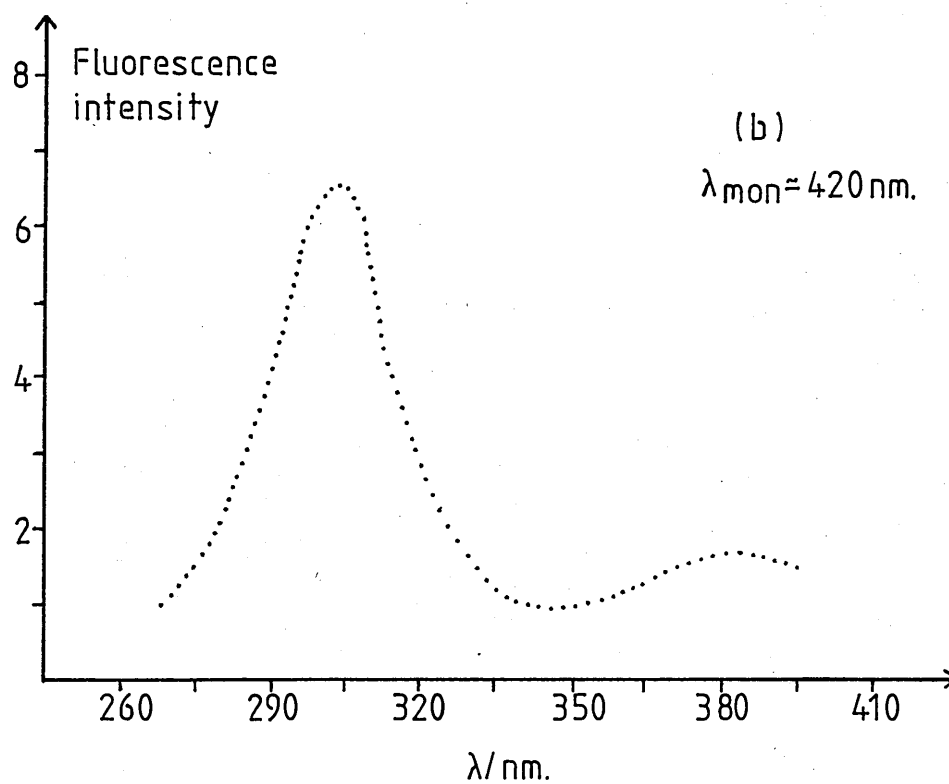
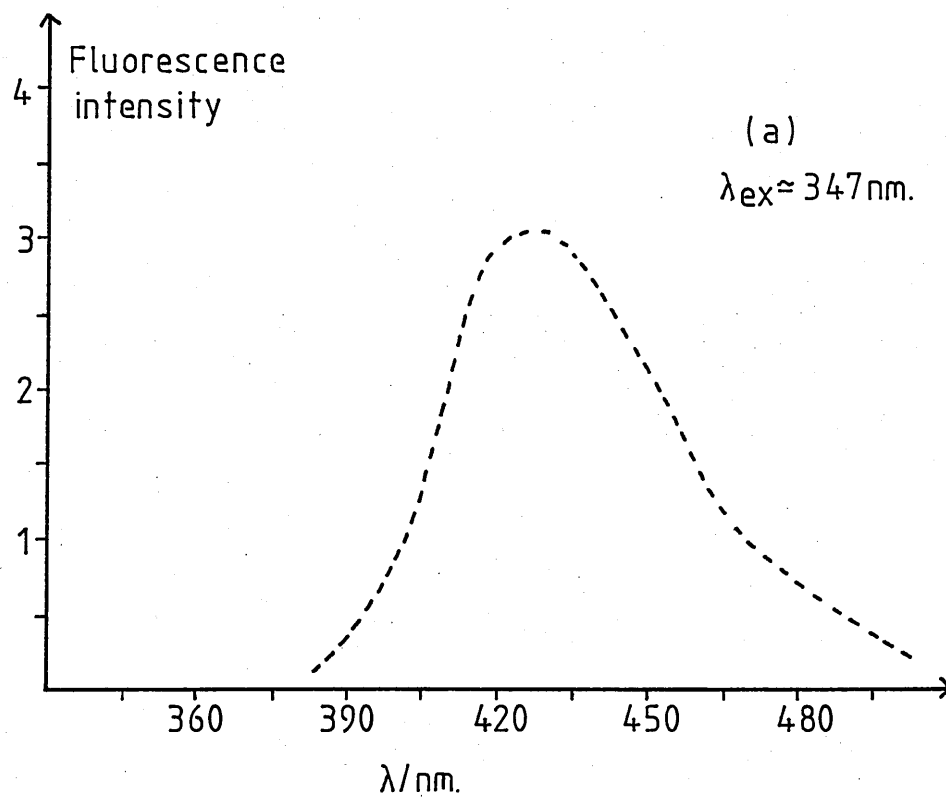


Fig.4.22: Fluorescence spectra of AlPcCl in ethanol (1).

Red fluorescence is observed between 655 nm and 630 nm. Also emitted is a weak blue fluorescence which is broad band and has a wide peak at ≈ 430 nm.

4.3(iv) Fluorescence spectra

A fluorescence spectrum of solution (1) of AlPcCl in ethanol using arc-lamp excitation at ≈ 347 nm is shown in Fig.4.22(a). In agreement with the laser-induced emission, the spectrum shows a broad-band fluorescence of low intensity with a rounded peak 420-430 nm. The fluorescence excitation spectrum (λ_{mon} 420 nm) of Fig.4.22(b) shows a single band corresponding to a maximum of absorption at 300 nm.

4.3(v) AlPcCl in ethanol . λ_{ex} 347 nm # 2

The transient spectra of solution (2) of AlPcCl in ethanol at times $t = 0, 20$ ns and 350 ns after the maximum at the 347 nm laser light are shown in Fig.4.23. They show the features outlined using solution (1) to good effect. In particular, the short-lived transient absorption band in the region of 'red' ground-state absorption is well defined and would appear to have a maximum at 610-620 nm. Also the absorption component in the near u-v shows a prominent peak at all three instants.

Fig. 4.23

Transient difference spectra of AlPcCl in ethanol (2).

Spectra plotted at $t = 0$: --X---X---X--

$t = 20\text{ns}$:•.....

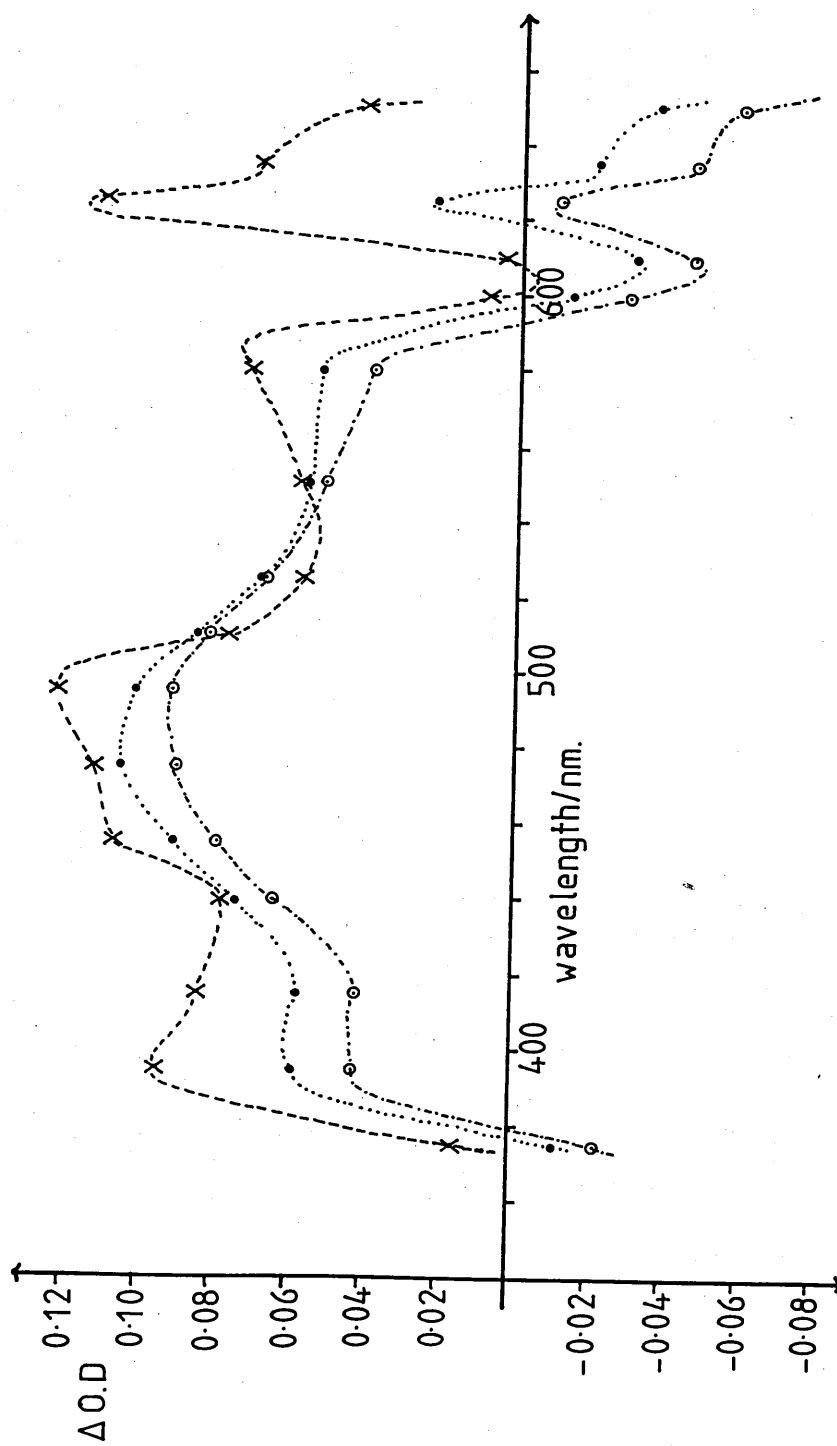
$t = 350\text{ns}$: --○---○---○---

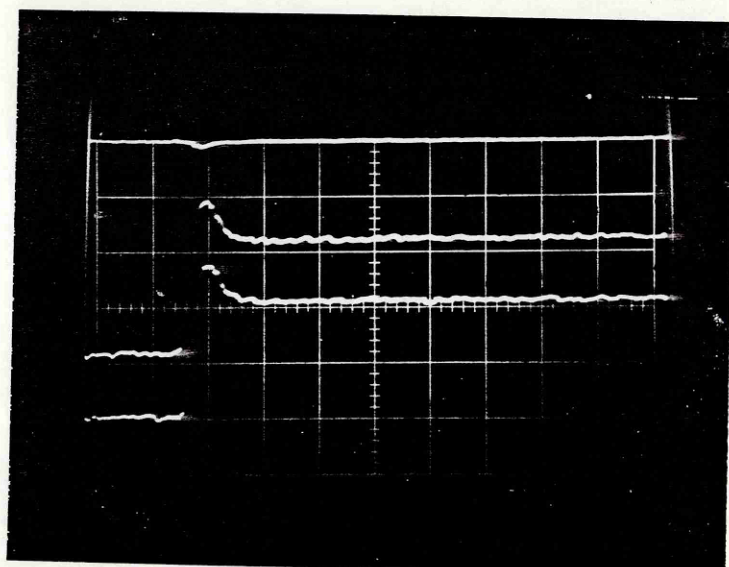
$\lambda_{\text{ex}} = 347 \text{ nm}$

Monochromator resolution = 1.04nm

Photomultiplier tube bias = -821V

Fig. 4.23

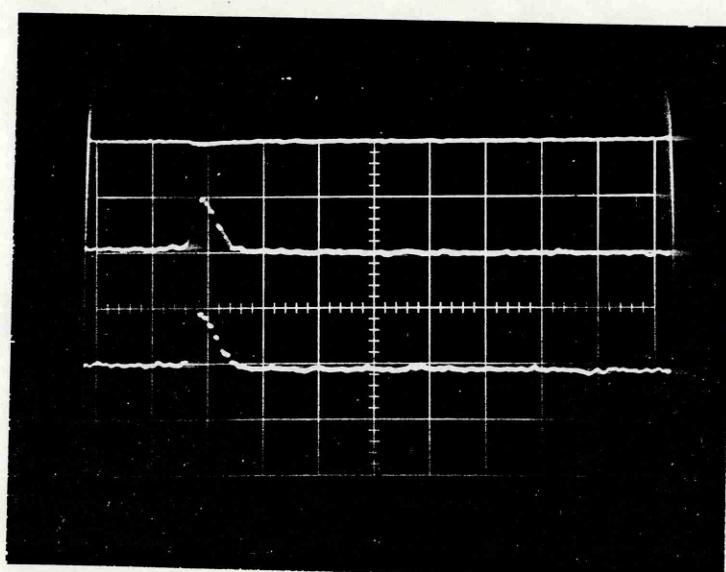




475 nm.

20 mv/div

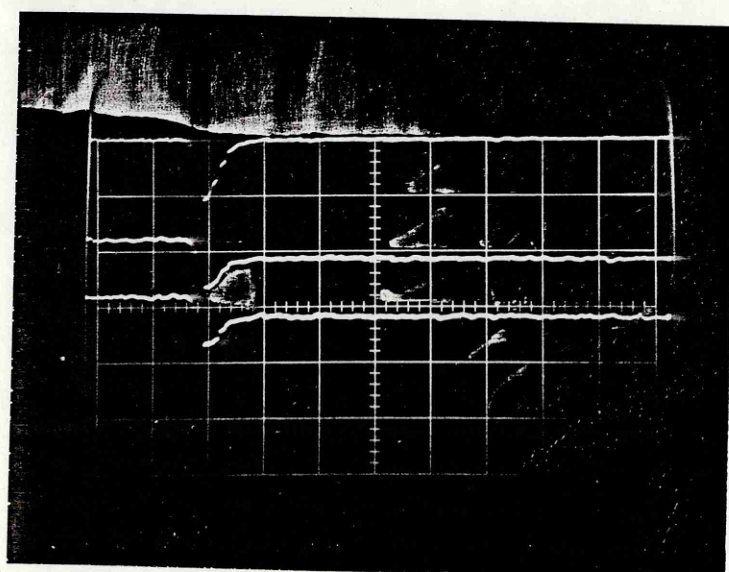
50 ns/div



625 nm.

10 mv/div

50 ns/div



650 nm.

10 mv/div

50 ns/div

Fig. 4.24: AlPcCl in ethanol. λ_{ex} 347 nm. #2

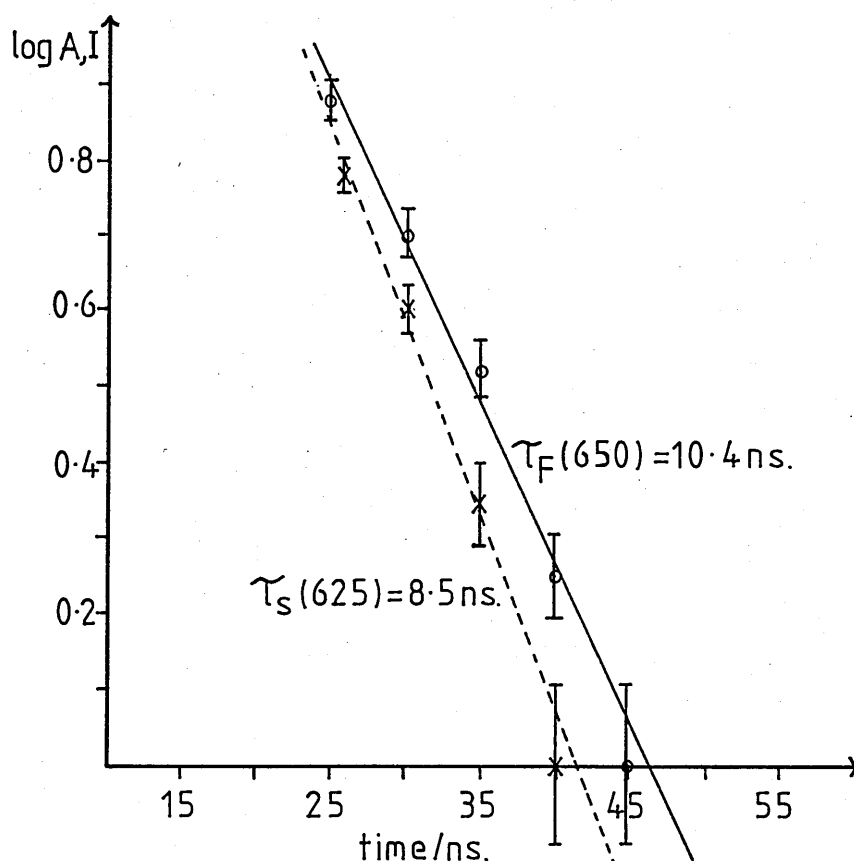


Fig. 4.25: Semi-log plots for AlPcCl in ethanol(2). $\lambda_{\text{ex}} 347 \text{ nm.}$

Decay profiles are shown in Fig. 4.24, including both the short-lived component at 625 nm and the red fluorescence at 650 nm. The lifetimes for these features are calculated from the graph of Fig. 4.25 to be:

$$\tau_F(650) = 10.4 \pm 1.3 \text{ ns}$$

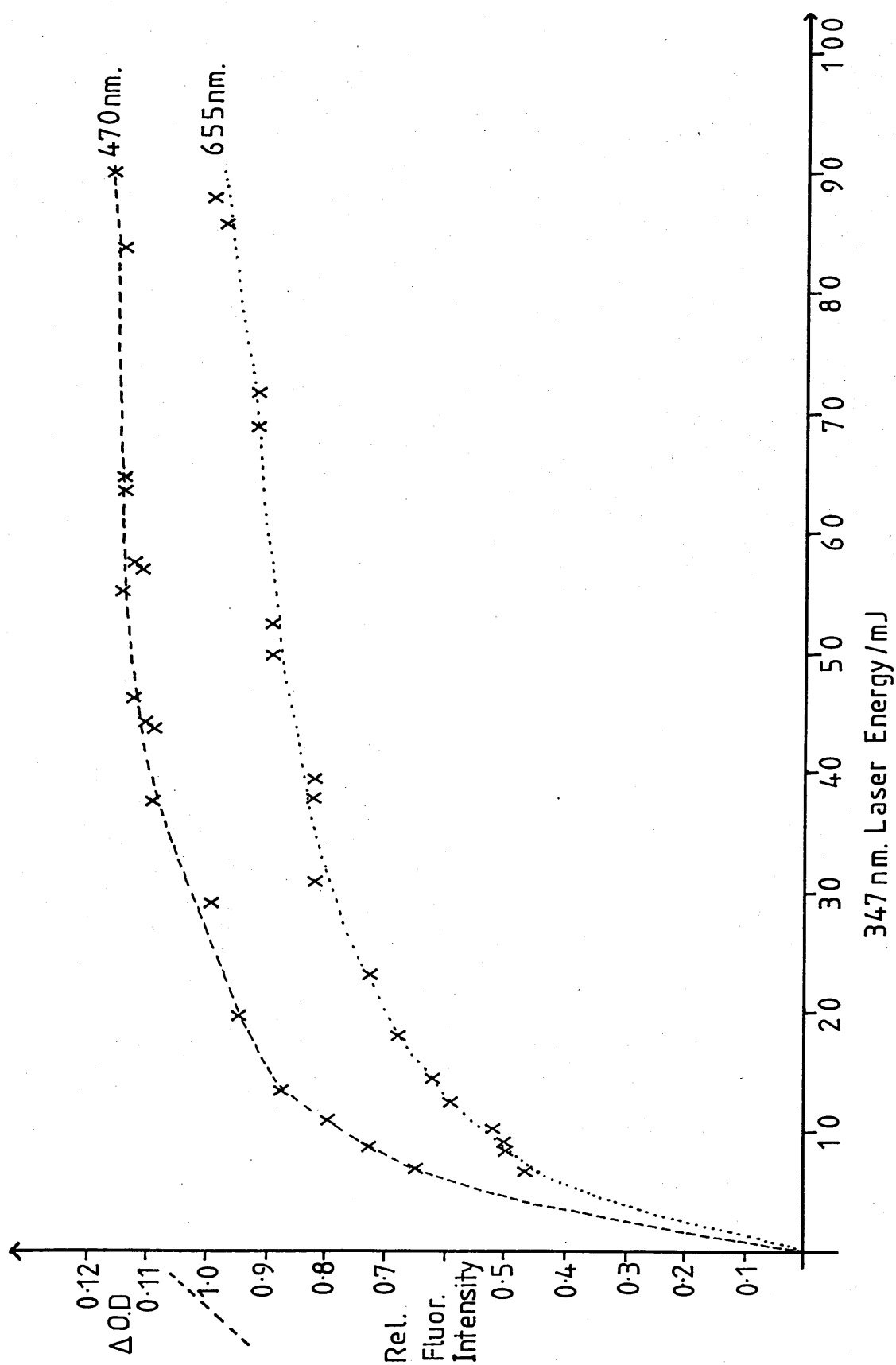
$$\tau_S(625) = 8.5 \pm 0.5 \text{ ns}$$

The 'blue' fluorescence from this solution is very weak.

The amplitudes of transient absorption at 470 nm and fluorescence at 655 nm were recorded as a function of 347 nm laser intensity and the results are shown in Fig. 4.26.

Fig. 4.26

AlPcCl in ethanol: saturation of response.



4.3(vi) Summary

The two solutions studied using second harmonic ruby laser excitation can be seen to have almost identical transient spectra. The only obvious difference is the degree of 'structure' in the visible absorption peak at $\approx 490\text{--}500\text{ nm}$. Also, the spectra obtained using the fundamental laser wavelength have the same overall shape. However, one significant departure is that the size of the transient absorption at zero-time, i.e. corresponding to the maximum of the 694 nm laser pulse, is less than that at subsequent times. This indicates a growing-in of the initial transient response - a behaviour not paralleled when excitation is directly into the second excited singlet state.

The peak situated at $\approx 400\text{ nm}$ is well defined and may represent the long-wavelength section of a wider transient absorption band in the near ultra-violet partially masked by the depletion of the Soret absorption band.

In all cases there is evidence of a short-lived absorption occurring between 580 and 640 nm , the lifetime of which is calculated as 8.5 ns . It must be emphasised that this is not the same transient that forms the initial component in the visible region of the spectrum and has an estimated decay time of $\approx 359\text{ ns}$. Although the decay scheme does not seem to follow simple exponentials, it was possible to obtain the

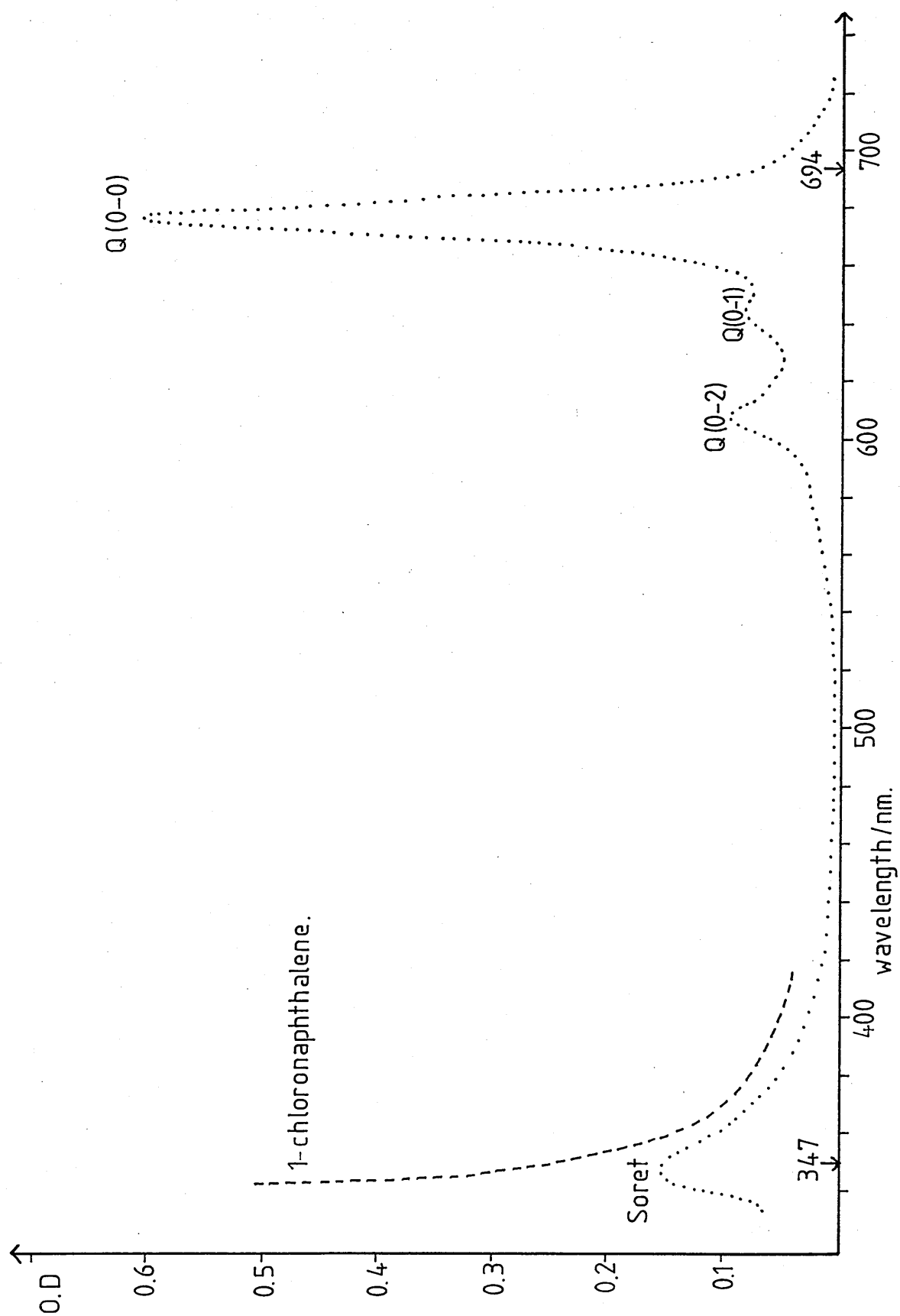
lifetime of the longest-lived components subsequent to each type of excitation. That these values, 72.8 μ s (694 nm) and 70.7 μ s (347 nm) are in good agreement indicates the same mode of decay.

A red fluorescence is evident from both solutions; at wavelengths which are shorter than the 694 nm excitation and which correspond to higher energies than the lowest vibrational level of the first excited singlet state. The lifetime of this red fluorescence was found to be longer using the 694 nm laser light, (14 ns compared to 10.4 ns for 347 nm excitations).

The 'blue' fluorescence, weakly emitted from solution (1) following 347 nm excitation is much reduced in the case of solution (2).

Fig.4.26 shows the saturation of transient absorption at 470 nm with increasing laser intensity. It can be seen that only for laser pulse energies of less than 20 m J does an increase in intensity result in a significant increase in the amplitude of transient absorption and a plateau is reached at \approx 45 m J. A similar effect is observed for the fluorescence response at 655 nm.

Fig.4.27: Ground-state absorption of CuPc in 1-chloronaphthalene.



4.4 COPPER PHTHALOCYANINE

4.4(i) Ground-state absorption

The ground-state absorption spectrum of a solution of CuPc in 1-chloronaphthalene is shown in Fig.4.27. The solute was not purified.

4.4(ii) CuPc in 1-chloronaphthalene . λ_{ex} 694 nm

The transient spectra of CuPc in 1-chloronaphthalene at times $t = 0$, 20 ns and 100 ns after the maximum of the 694 nm laser excitation are shown in Fig.4.28. At $t = 0$, 20 ns the spectra are almost identical in shape and amplitude, with a shoulder at 400 nm and a broad absorption in the visible with a maximum at 480-500 nm. By 100 ns the transient has decayed to produce a low amplitude response. Depletion of the ground-state absorption bands occurs at wavelengths shorter than 370 nm and between 600 and 700 nm.

Decay profiles at 490 nm and 670 nm are shown in Fig.4.29 and the lifetimes are calculated from the graph of Fig.4.30 to be:

$$\tau_{490} = 45.6 \pm 3.8 \text{ ns}$$

$$\tau_{670} = 34.2 \pm 1.3 \text{ ns}$$

The admission of oxygen into the solution is shown to effect a slight reduction of the decay time at 670 nm.

Fig. 4.28

Transient difference spectra of CuPc in 1-chloronaphthalene.

Spectra plotted at $t = 0$

$t = 20\text{ns}$

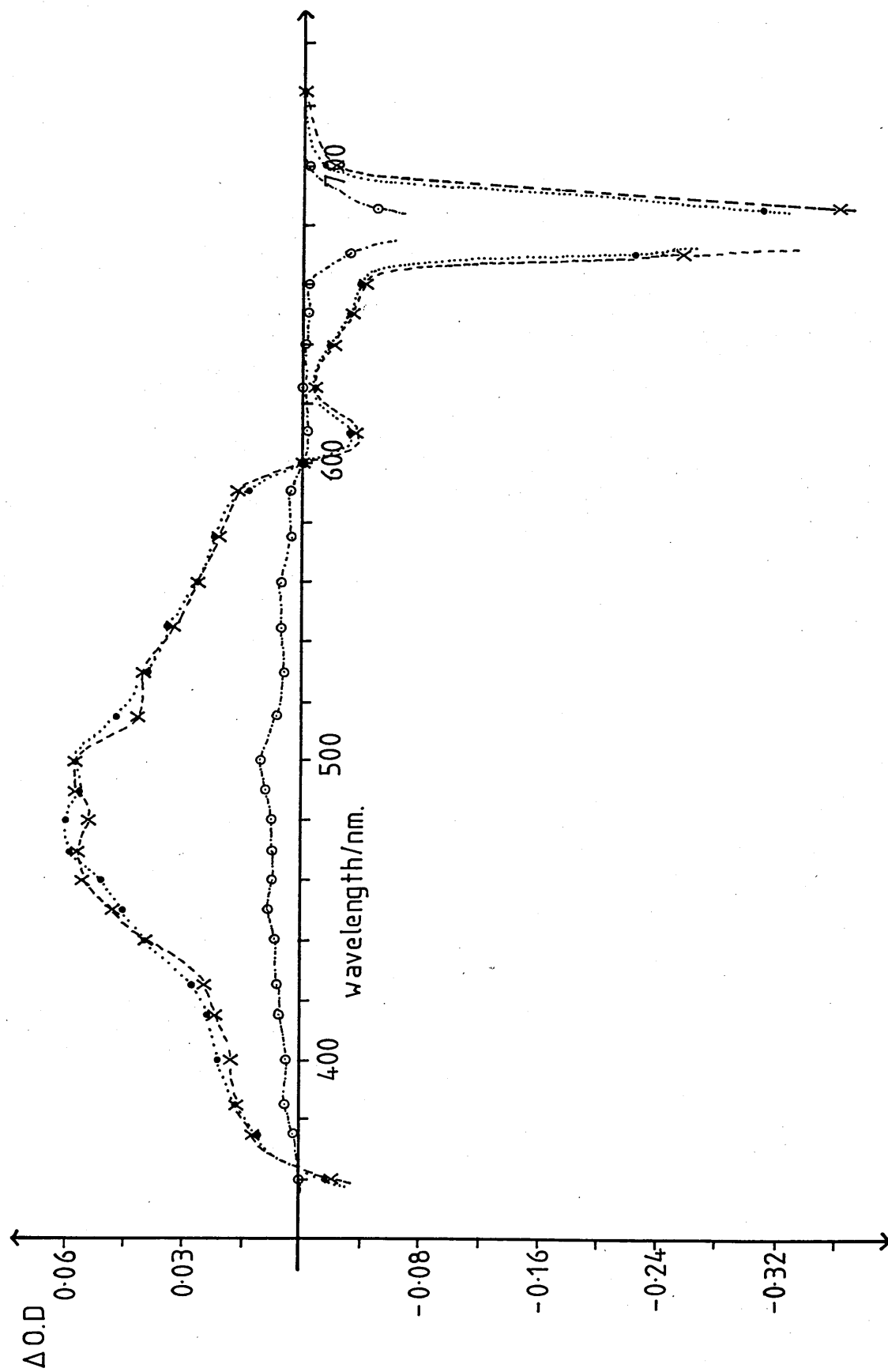
$t = 100\text{ns}$

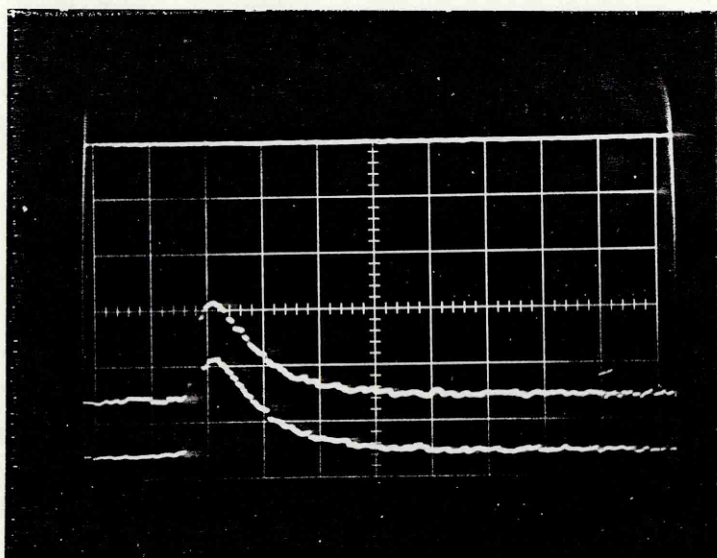
$\lambda_{\text{ex}} = 694\text{nm}$

Monochromator resolution = 1.04nm

Photomultiplier tube bias = -820V

Fig.4.28

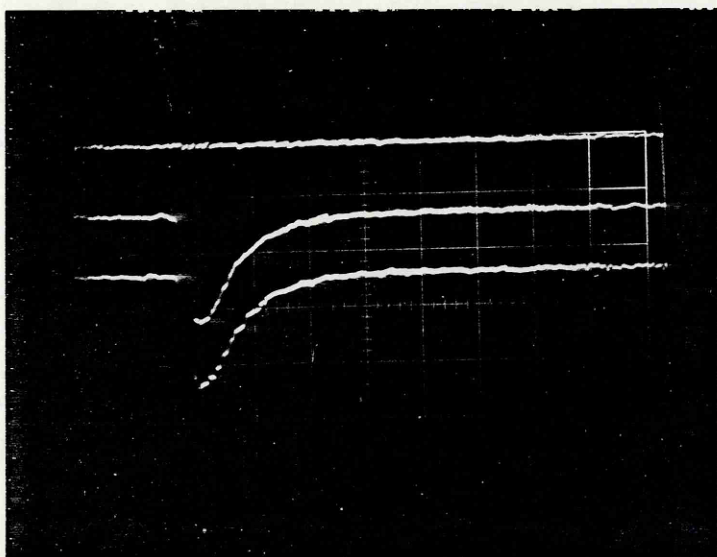




490 nm.

20 mv/div

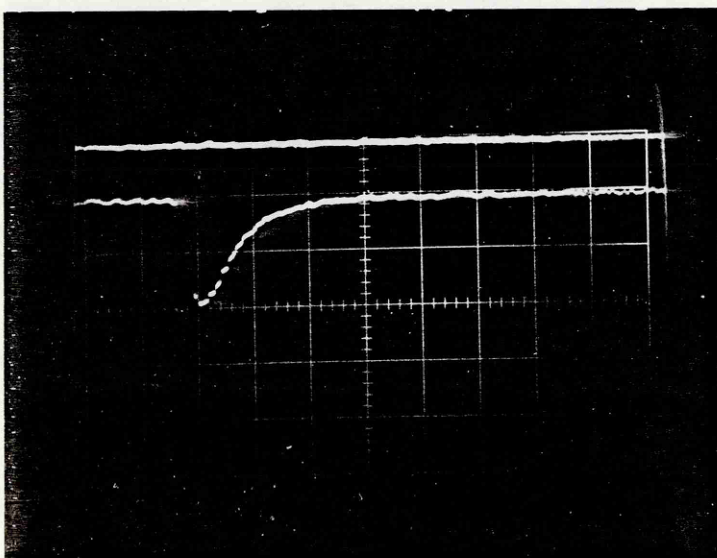
50 ns/div



670 nm.

10 mv/div

50 ns/div



670 nm.

10 mv/div

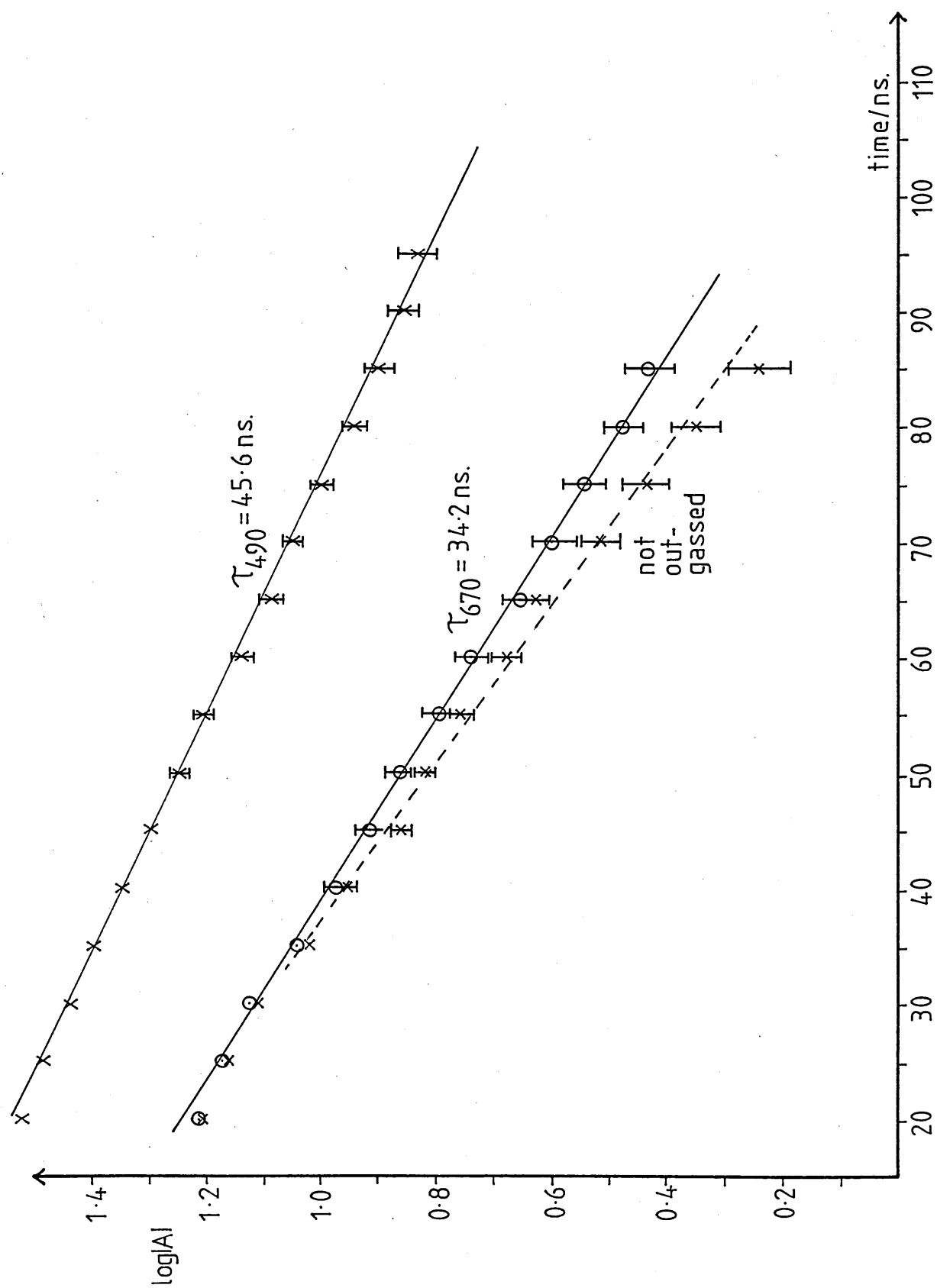
50 ns/div

not
outgassed

Fig. 4.29: CuPc in 1-chloronaphthalene. λ_{ex} : 694 nm.

Fig. 4.30

Semi-log plots for CuPc in 1-chloronaphthalene. $\lambda_{\text{ex}} 694 \text{ nm}$.



4.4(iii)CuPc in 1-chloronaphthalene . λ_{ex} 347 nm

The transient spectra of CuPc in 1-chloronaphthalene at times $t = 0, 20 \text{ ns}, 100 \text{ ns}$ and 350 ns after the peak of the 347 nm laser pulse are shown in Fig.4.31. They show the edge of a strong absorption in the blue-violet part of the spectrum and a small, short-lived peak at $\approx 470 \text{ nm}$. There is a gradual decrease in absorption amplitude throughout the visible until $\approx 600 \text{ nm}$ where the effects of the depletion of the Q-absorption band of CuPc takes over.

The transient spectra of 1-chloronaphthalene only, under the same conditions, are shown in Fig.4.32. The two sets of spectra have a similar appearance throughout most of the region studied. However, a striking difference is the almost constant positive absorption by 1-chloronaphthalene across the red part of the spectrum.

The similarities and differences in response of 1-chloronaphthalene with and without CuPc present is illustrated in Fig.4.33 by decay profiles at 480 nm and 670 nm. The differences between the two sets of spectra are emphasised by a simple subtraction to produce Fig.4.34 which represents the effect of the CuPc.

The main peak of this absorption lies at 460 nm and the shape of the spectrum appears slightly distorted, as well as displaced negatively with respect to the zero of absorption.

Fig. 4.31

Transient difference spectra of CuPc in 1-chloronaphthalene.

Spectra plotted at $t = 0$

$t = 20\text{ns}$

$t = 100\text{ns}$

$t = 350\text{ns}$

$\lambda_{\text{ex}} = 347\text{nm}$

Monochromator resolution = 1.04nm

Photomultiplier tube bias = -820V

Fig. 4.31

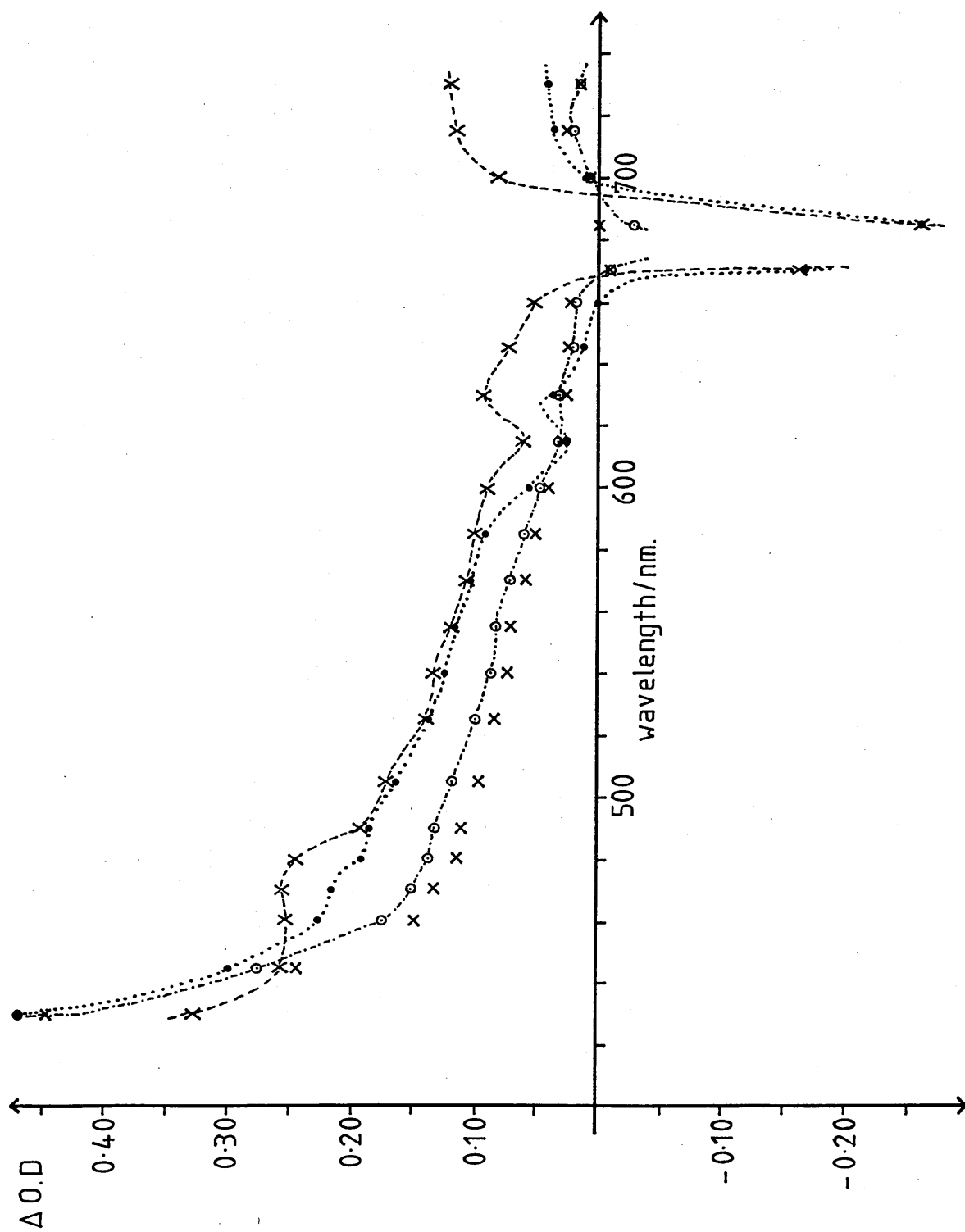


Fig. 4.32

Transient difference spectra of 1-chloronaphthalene.

Spectra plotted at $t = 0$

$t = 20\text{ns}$

$t = 100\text{ns}$

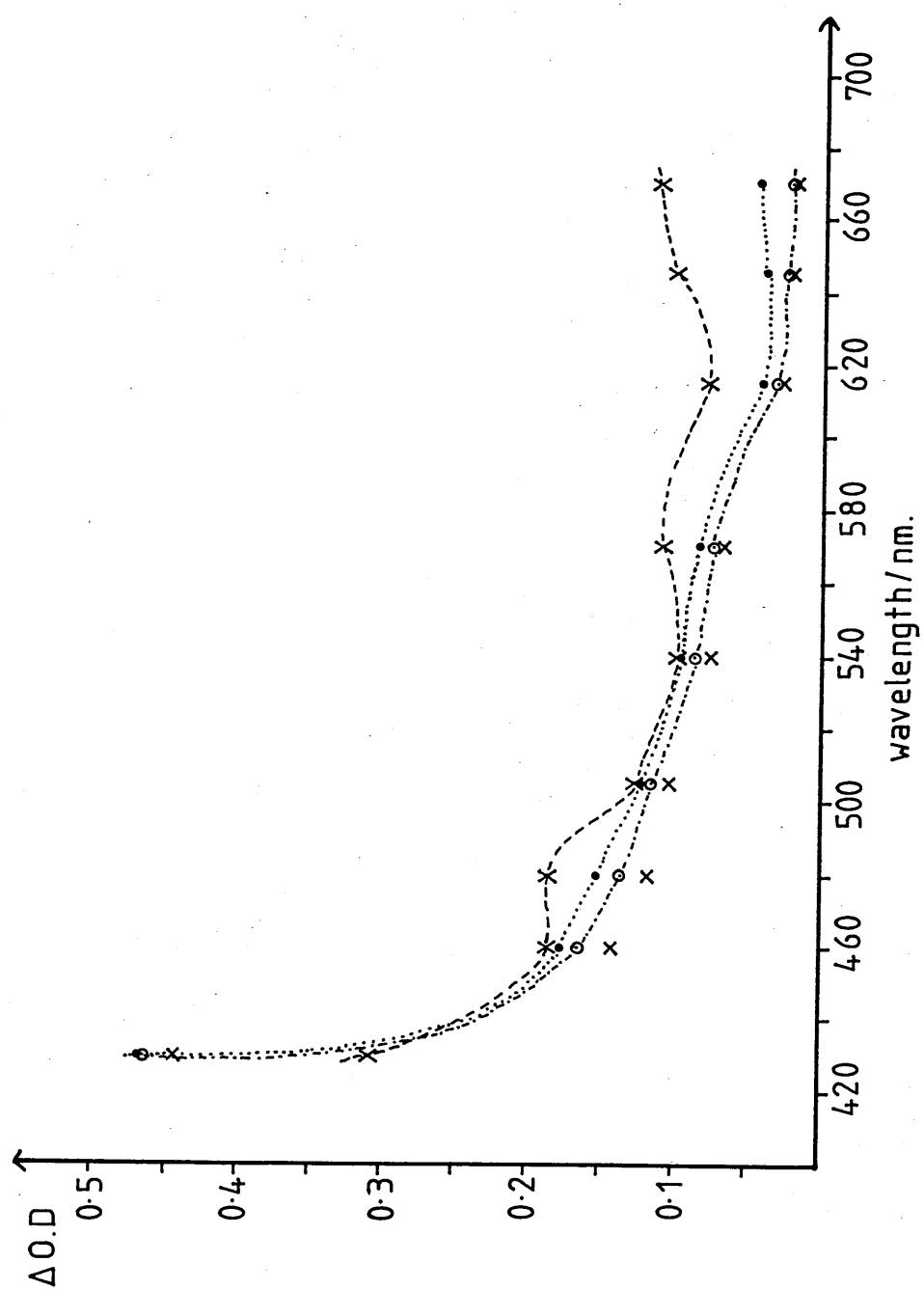
$t = 350\text{ns}$

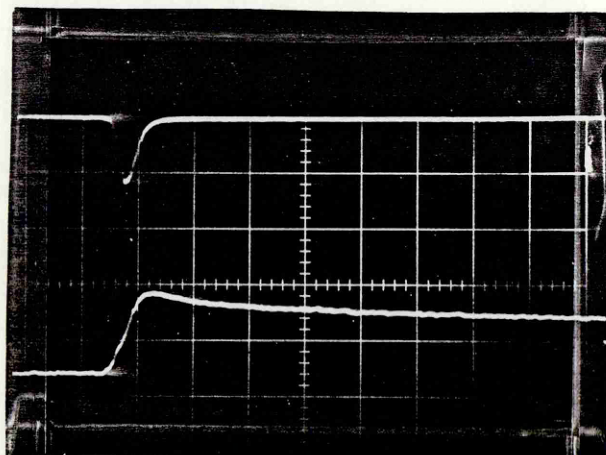
$\lambda_{\text{ex}} = 347\text{nm}$

Monochromator resolution = 1.04nm

Photomultiplier tube bias = -820V

Fig.4.32





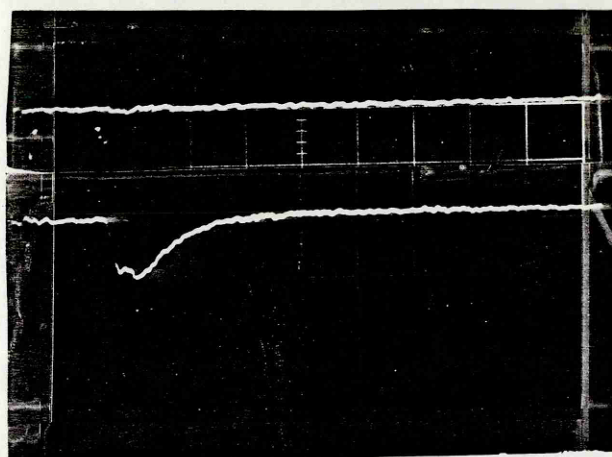
480 nm.

50mv/div.

50ns/div.

with

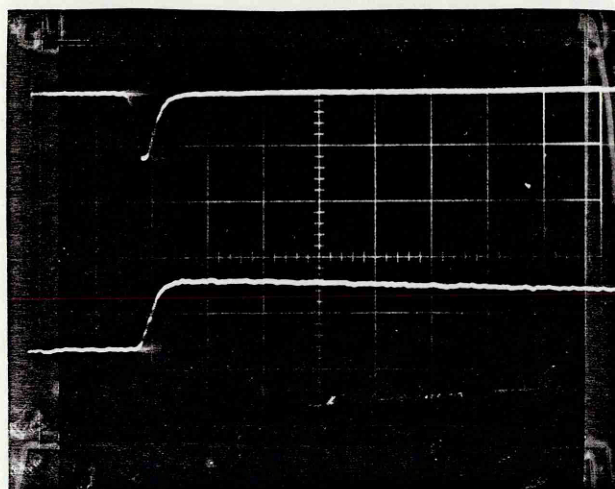
CuPc



670 nm.

10mv/div.

50ns/div.



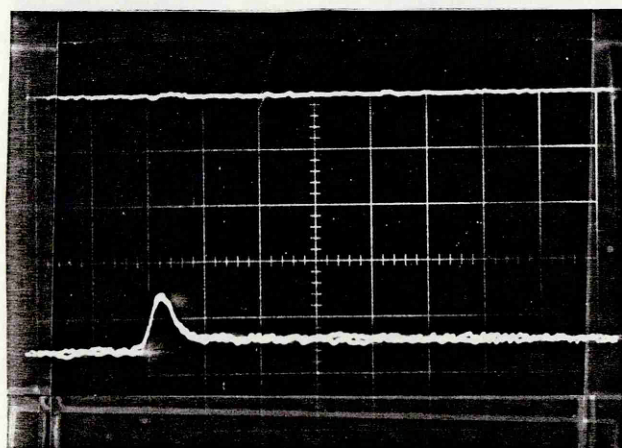
480nm.

50mv/div.

50ns/div.

without

CuPc



670nm.

10mv/div.

50ns/div.

Fig.4.33: 1-chloronaphthalene. λ_{ex} 347nm.

Fig.4.34

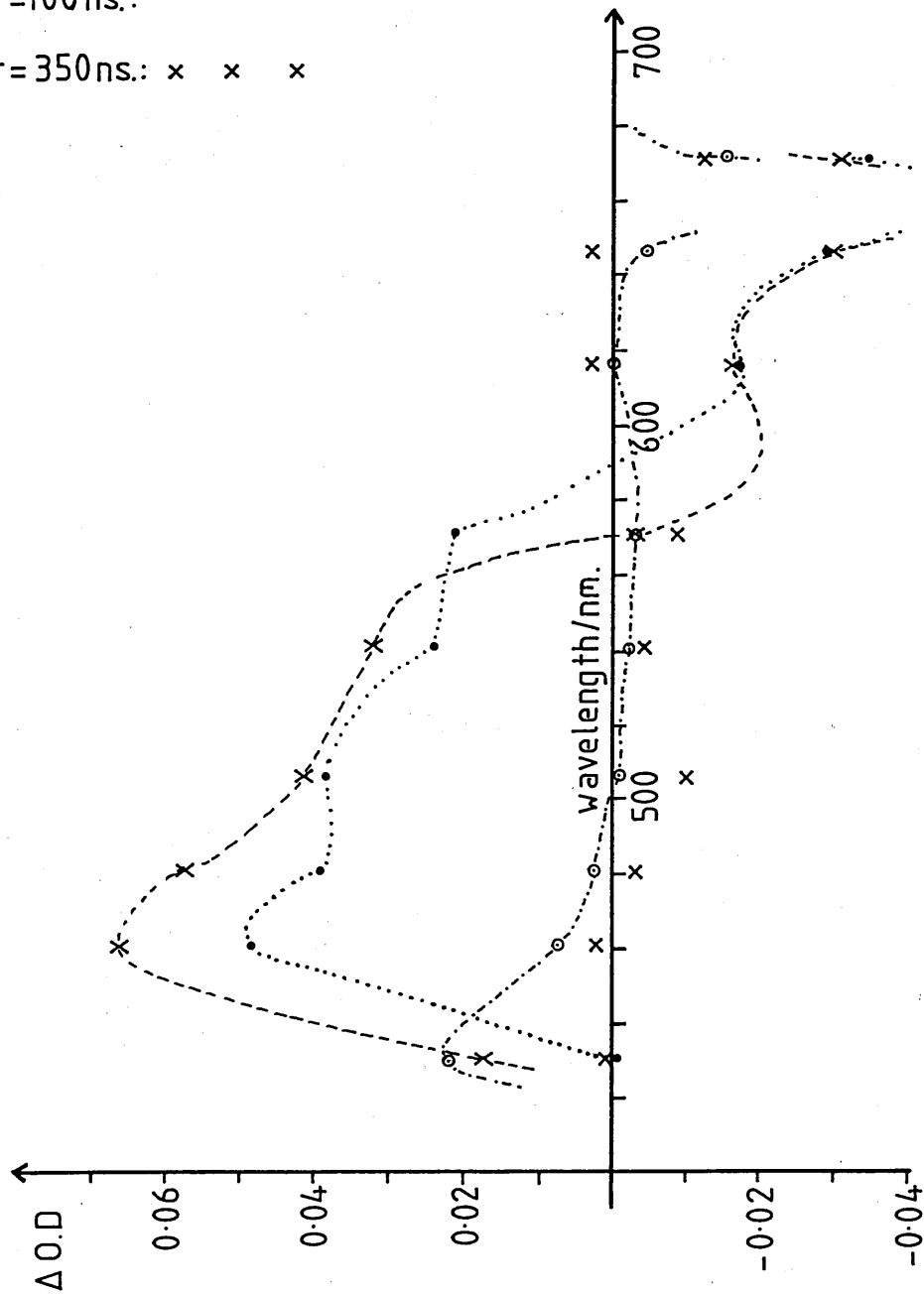
Transient response of CuPc.

$t=0$: -x---x-x-

$t=20\text{ ns.}$: ······

$t=100\text{ ns.}$: - - - - -

$t=350\text{ ns.}$: x x x



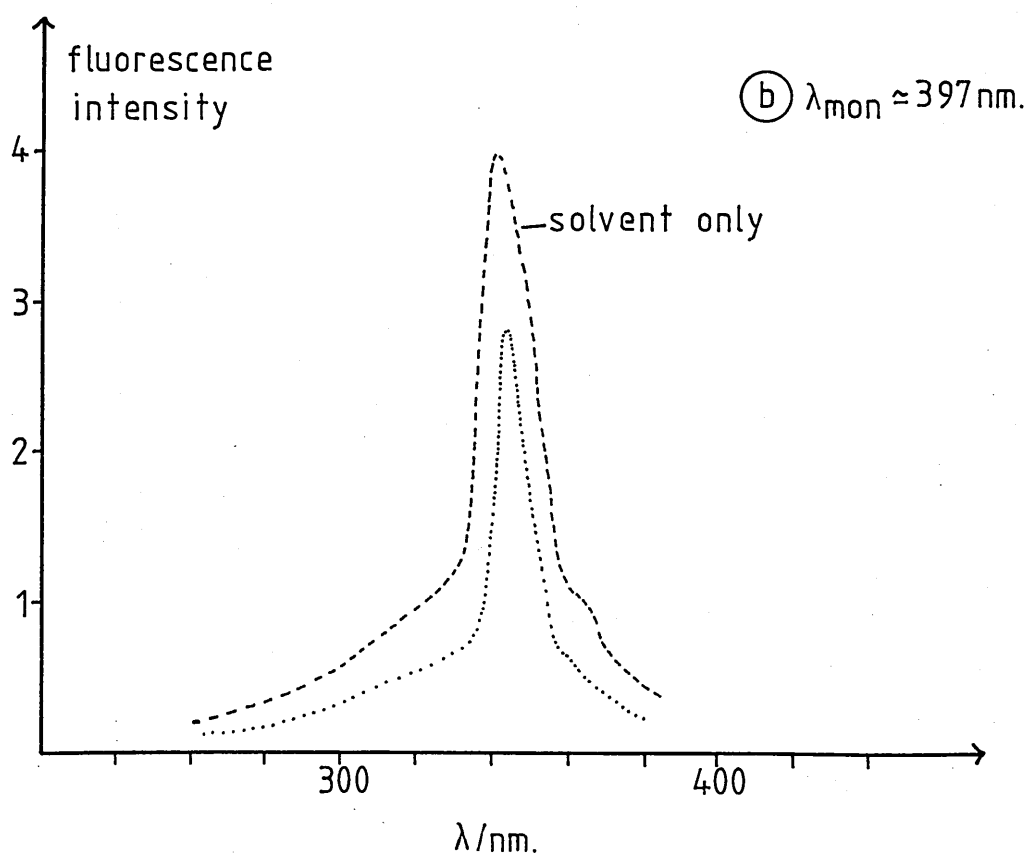
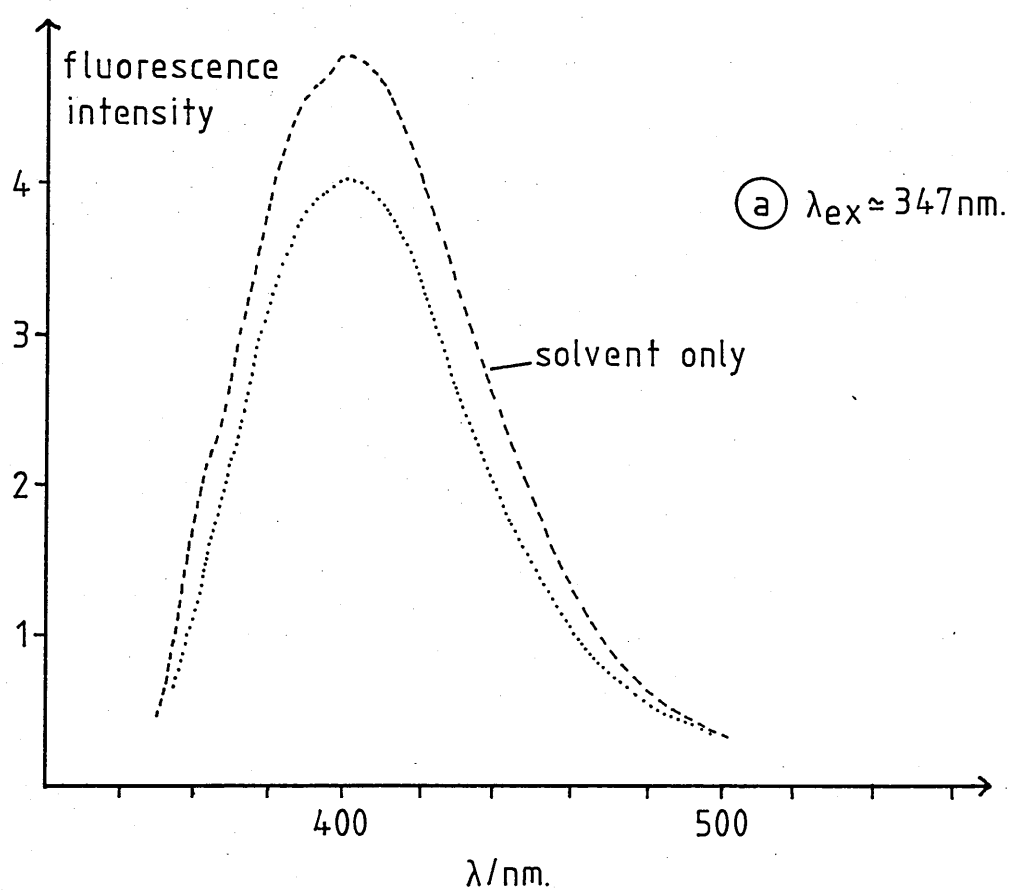


Fig.4.35: Fluorescence of CuPc in 1-chloronaphthalene.

It can be seen that, compared to the large amplitude of transient absorption by 1-chloronaphthalene, the effect of the CuPc is relatively small.

Measurement at wavelengths shorter than 430 nm was precluded by the very intense fluorescence in this region of the spectrum.

4.4(iv) Fluorescence spectra

The fluorescence emission spectra of 1-chloronaphthalene and CuPc in 1-chloronaphthalene, obtained using arc-lamp excitation at 347 nm, are shown in Fig.4.35(a). Both solutions have a single broad band with a maximum at 397 nm. The fluorescence excitation spectra monitored at this wavelength (Fig.4.35(b)) each have a single sharp peak at 343 nm which tails off to shorter wavelengths. These results show that the fluorescence yield is greater from the solution in which CuPc is not present.

4.4(v) Summary

The observation that the transient spectra induced by excitation at 694 nm have identical amplitude at $t = 0, 20$ ns, indicates a growing-in of the initial transient response. The location and shape of the transient absorption is in agreement with that presented as triplet absorption by McVie.⁽⁴²⁾ It is of interest that the decay of the transient

absorption in the visible region of the spectrum (45.6 ns) is longer than that of the recovery from ground-state depletion (34.2 ns). It is also notable that these figures can be compared to the triplet lifetime of 35 ns reported by McVie, and the time required for recovery from the bleached state of 50 ns reported by Harrison and Kosonocky⁽⁸⁸⁾ (albeit the wrong way round!).

It can be seen from Fig.4.27 that the solvent, 1-chloronaphthalene, absorbs light strongly in the near u-v part of the spectrum. Thus it may be assumed that a large proportion of the 347 nm laser light serves to excite the solvent. Undoubtedly the transient absorption by the solution of CuPc in 1-chloronaphthalene is in the main due to the response of the solvent. This is supported by the evidence of Nouchi⁽¹¹¹⁾ who reported a main transient absorption peak at 420 nm for 1-chloronaphthalene in ether/pentane at 77°K. However, the difference between the two sets of transient spectra obtained with and without CuPc present (Fig.4.34), indicates that the absorption due to the phthalocyanine compound subsequent to laser excitation is separable from that of the solvent. This suggests that there is no solute/solvent complex formation.

However, the observation that the 'baseline' of the transient absorption due to CuPc lies below the zero of the ordinate implies that the addition of the compound has a quenching effect upon the transient absorption of the solvent.

Similarly, the reduction of solvent fluorescence upon addition of the solute implies a quenching of the laser-induced excited state of 1-chloronaphthalene. A mechanism for this quenching is discussed in Chapter 5.

4.5 ZINC PHTHALOCYANINE

4.5(i) Ground-state absorption

The ground-state absorption spectra of two solutions of ZnPc in ethanol are shown in Fig.4.36. Solution (1) was purified by method A, solution (2) by method B.

4.5(ii) ZnPc in ethanol . λ_{ex} 347 nm # 1

The transient spectra of solution (1) of ZnPc in ethanol at times $t = 0$, 20 ns and 350 ns after the 347 nm laser peak are shown in Fig.4.37. The spectrum at $t = 0$ shows a small peak at 400 nm and a broad, slightly structured absorption throughout the visible with a maximum at 470 nm, which gradually declines towards the red part of the spectrum. At 20 ns and 350 ns the spectra are similar in form but do not appear as structured and show a greater amplitude than that recorded at zero-time.

The decay profiles at 470 nm are shown in Fig.4.38; the transient which grows in over the 500 ns subsequent to the initial rising edge decays into a longer-lived transient. It

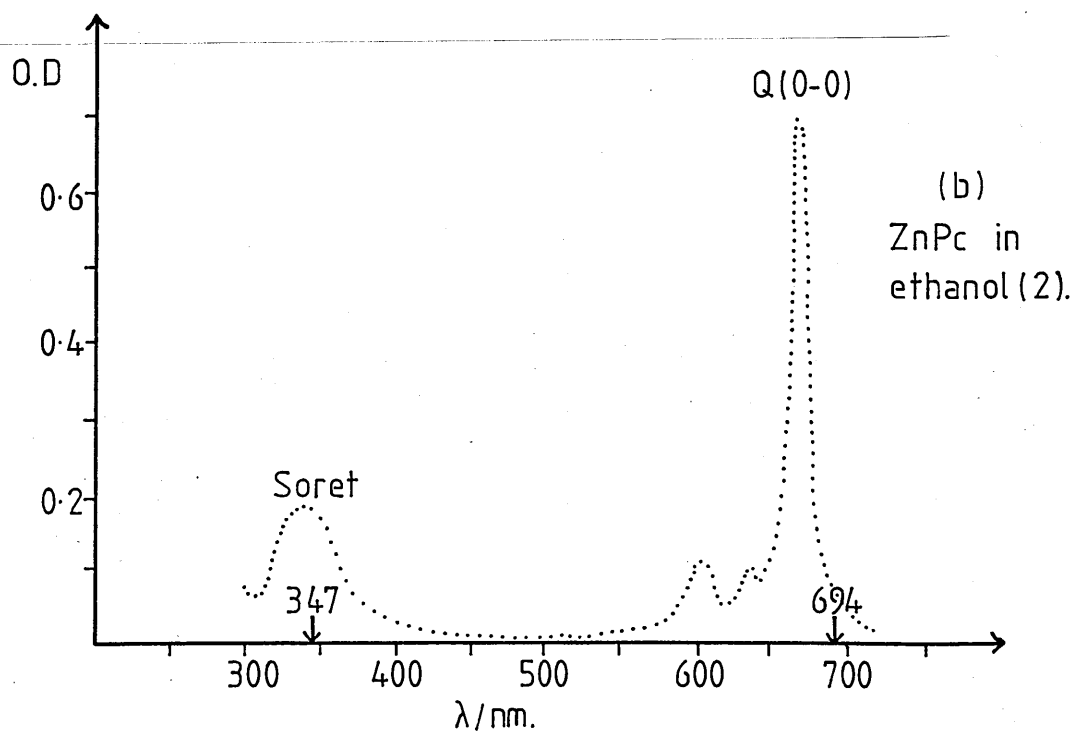
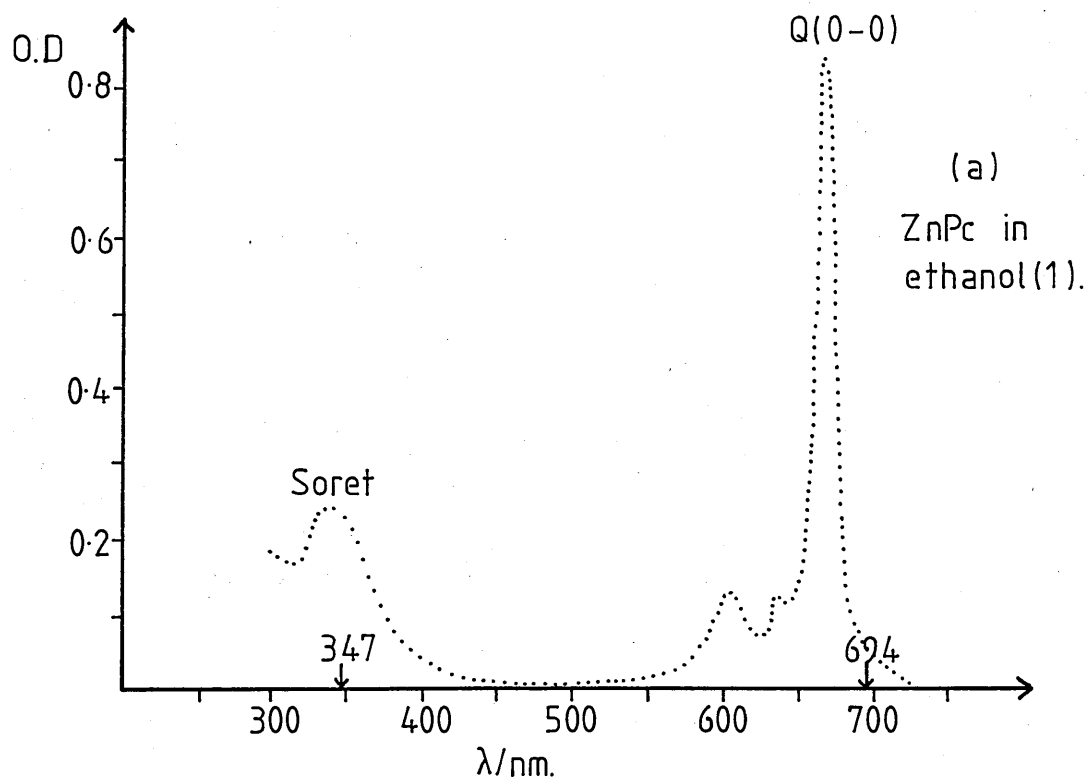


Fig.4.36:Ground-state absorption spectra.

Fig. 4.37

Transient difference spectra of ZnPc in ethanol (1).

Spectra plotted at $t = 0$: --x--x--x--

$t = 20\text{ns}$:●.....●.....●.....

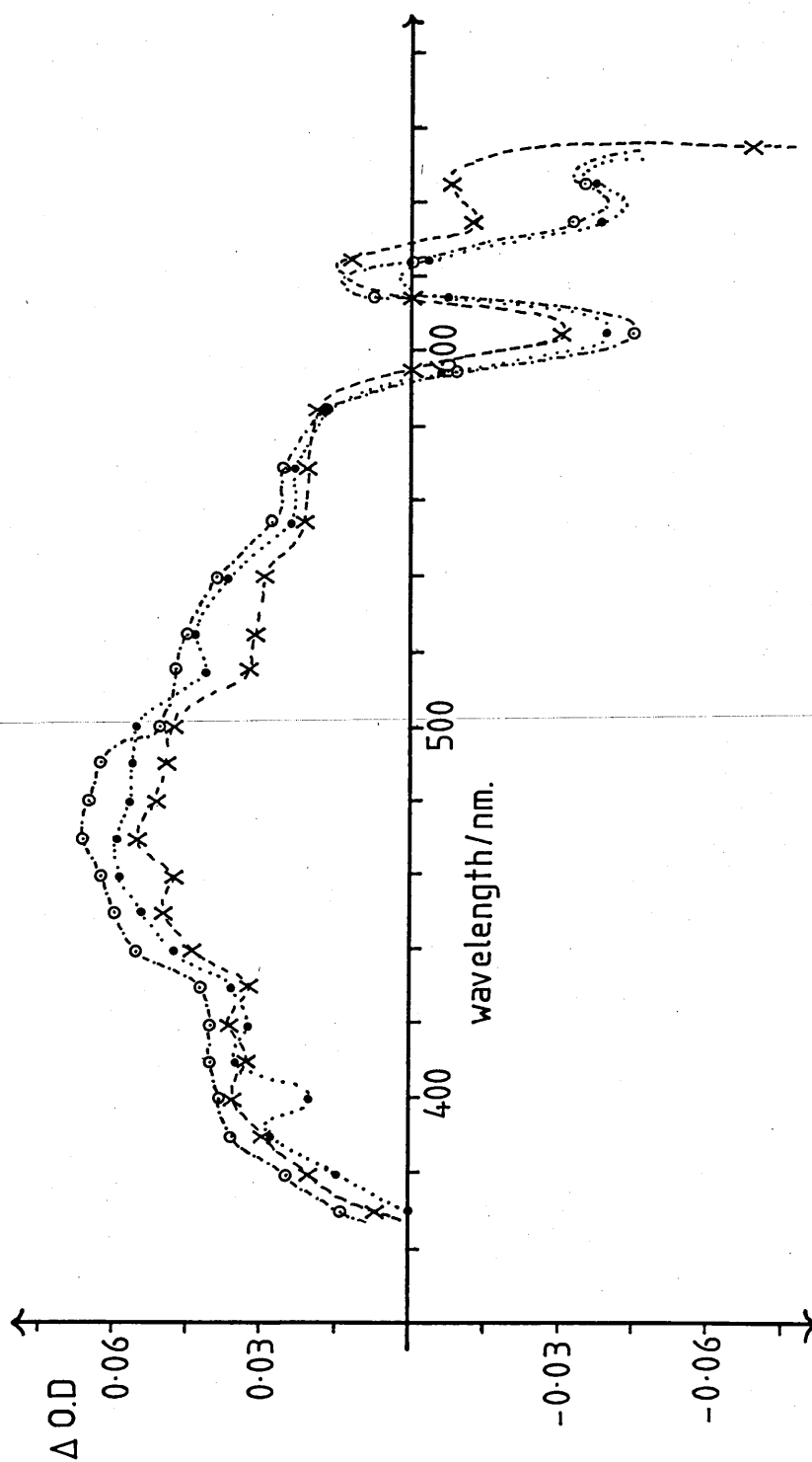
$t = 350\text{ns}$ $\cdots \circ - \cdots \circ - \cdots \circ - \cdots$

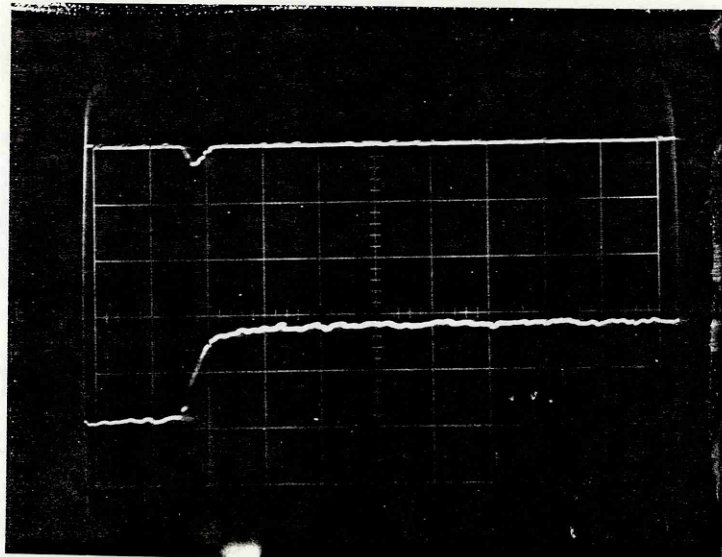
$$\lambda_{ex} = 347\text{nm}$$

Monochromator resolution = 1.04nm

Photomultiplier tube bias = -826V

Fig.4.37

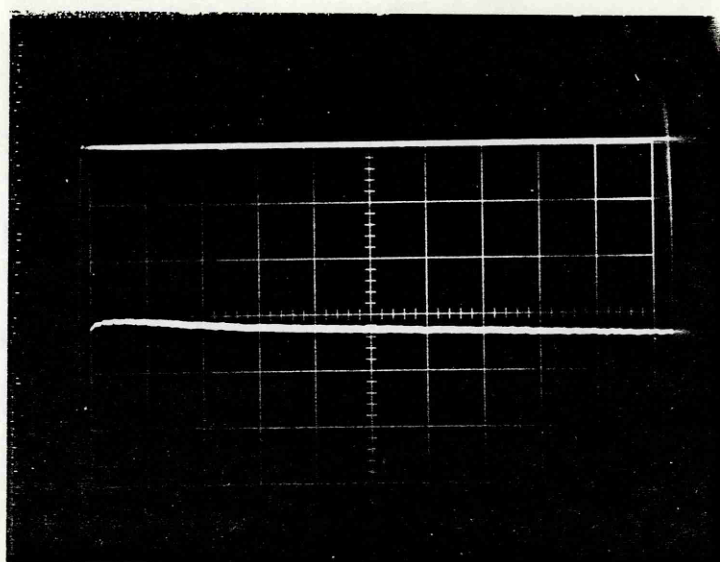




470nm

20mv/div

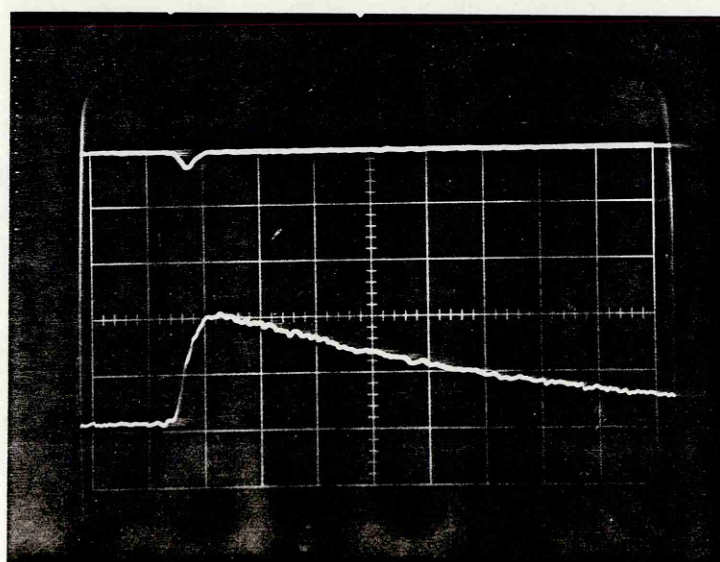
50ns/div



470nm.

1 μ s/div

20mv/div



470nm.

20mv/div

50ns/div

not
outgassed

Fig.4.38: ZnPc in ethanol. λ_{ex} 347nm. # 1

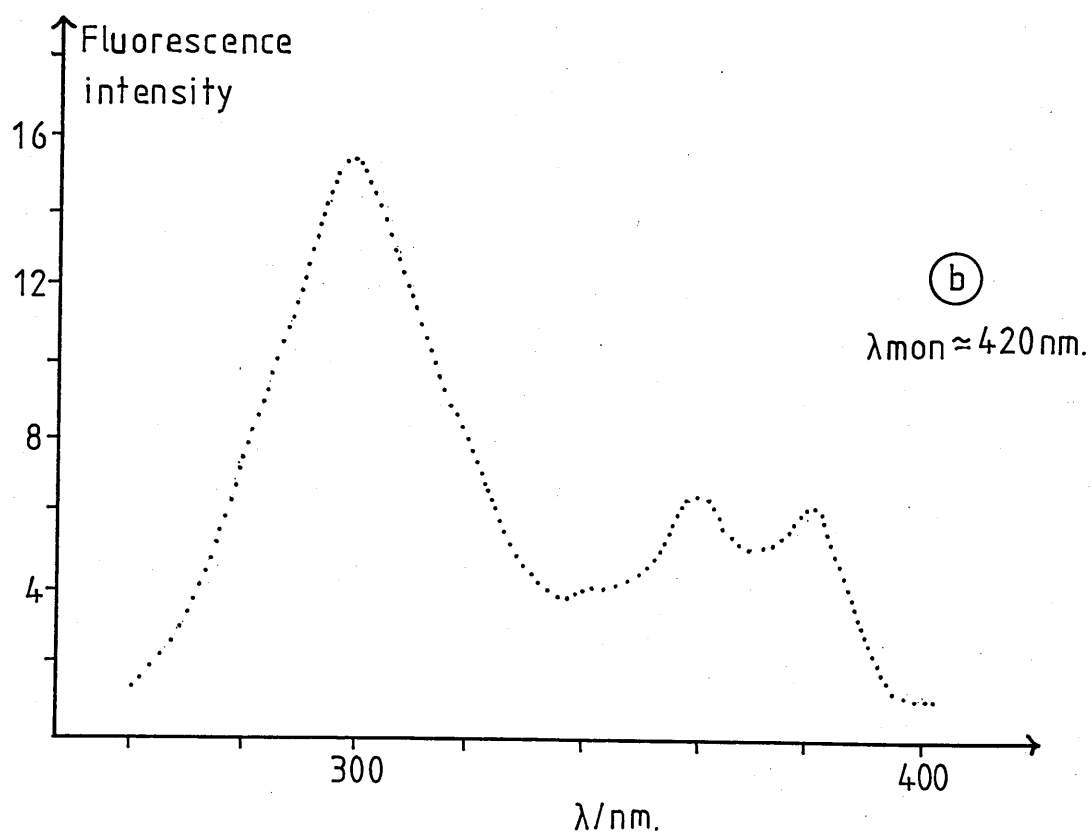
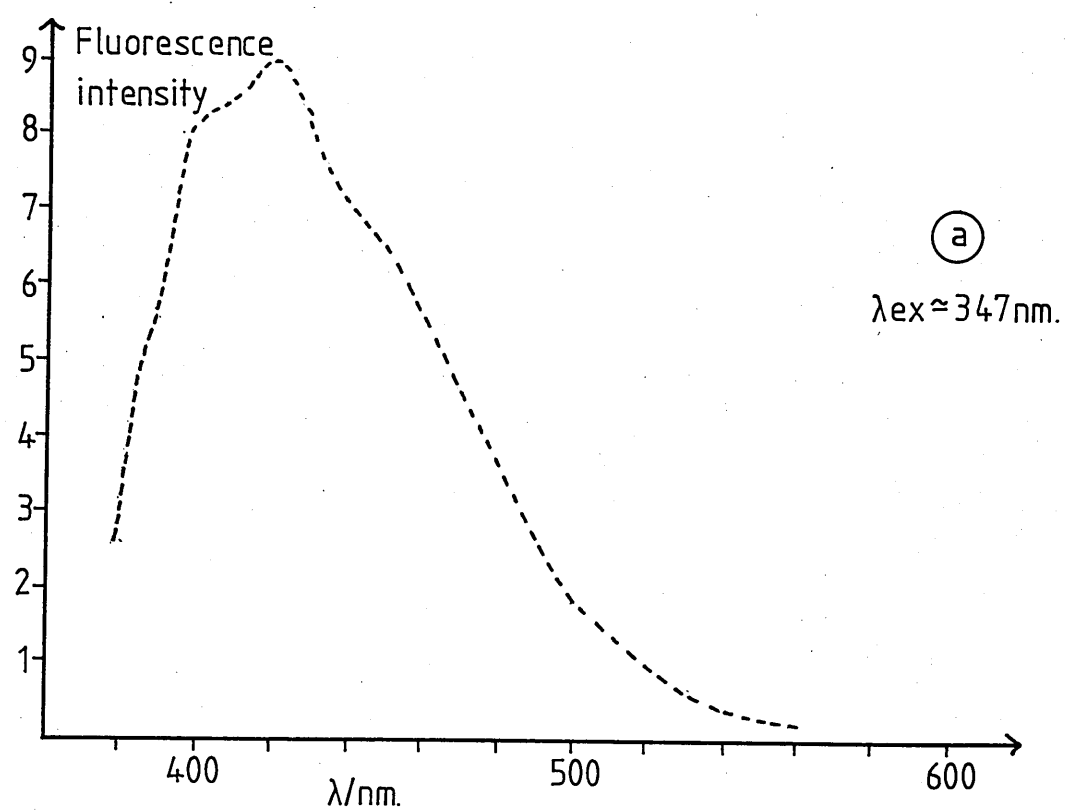


Fig.4.39: Fluorescence of ZnPc in ethanol (1)

can be seen that the presence of oxygen has a marked effect upon the kinetics.

Depletion of the absorption bands yields a bleaching effect at wavelengths shorter than 370 nm and longer than 595 nm. The intensity of this effect in the red band at $t = 0$ appears slightly less than at later times.

A fluorescence emission is recorded between 625 nm and 670 nm with a decaying edge only slightly longer than that of the excitation. Also a weak 'blue' fluorescence is recorded over the broad region 370 - 585 nm and has a maximum intensity at ≈ 420 nm.

4.5(iii) Fluorescence spectra

The fluorescence emission spectrum of this solution obtained using arc-lamp excitation at 347 nm is shown in Fig.4.39(a) to consist of a broad band centred on 420 nm. An excitation spectrum monitored at this wavelength shows [Fig.4.39(b)] a main peak at ≈ 300 nm with two smaller peaks at 360 nm and 380 nm.

4.5(iv) ZnPc in ethanol . λ_{ex} 347 nm # 2

The transient spectra of solution (2) of ZnPc in ethanol at times $t = 0$, 20 ns and 350 ns after the peak of the 347 nm laser pulse are shown in Fig.4.40. As with solution (1), the

Fig. 4.40

Transient difference spectra of ZnPc in ethanol (2).

Spectra plotted at $t = 0$: ---x---x---x---

$t = 20\text{ns}$:•.....•.....

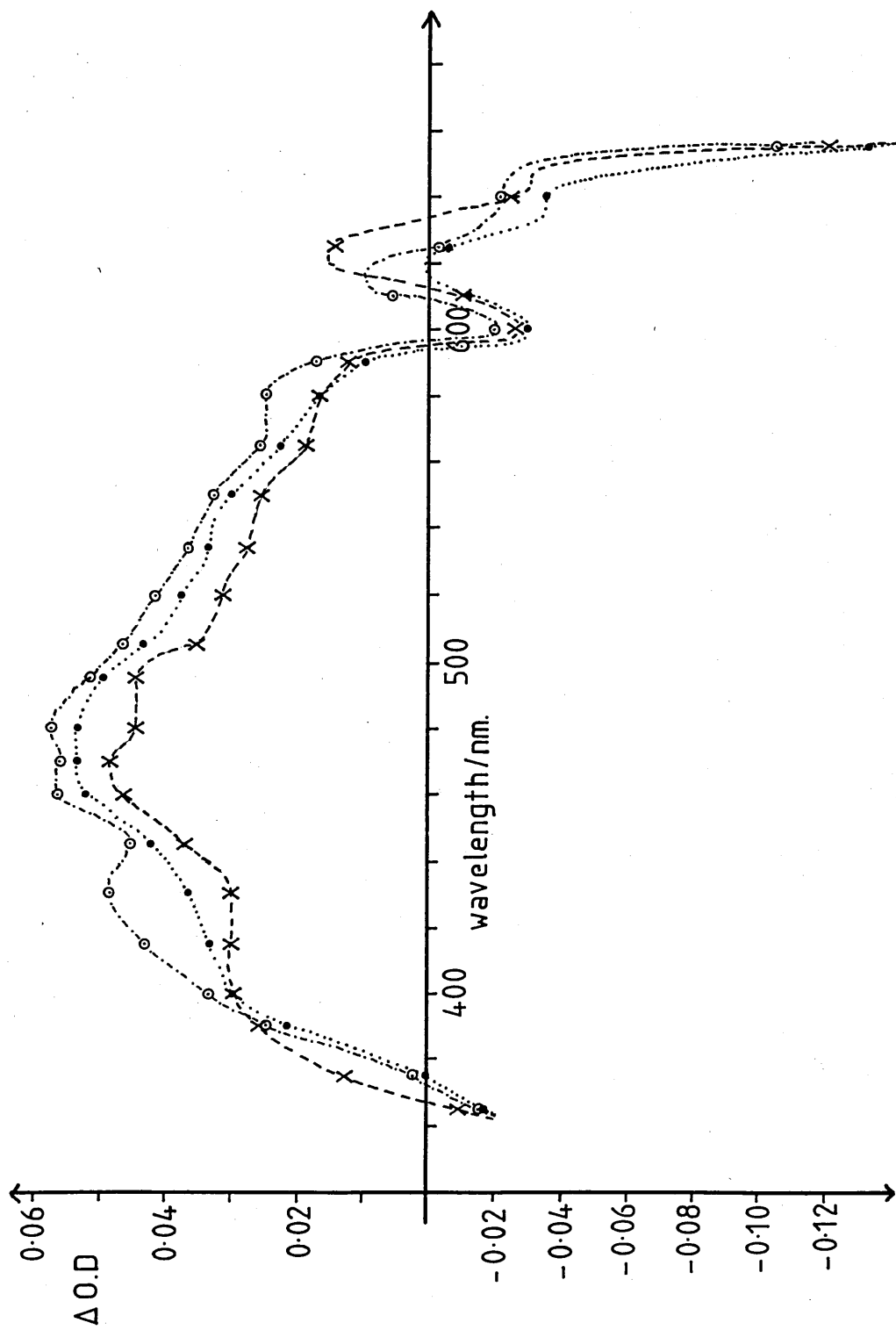
$t = 350\text{ns}$: -o---o---o---

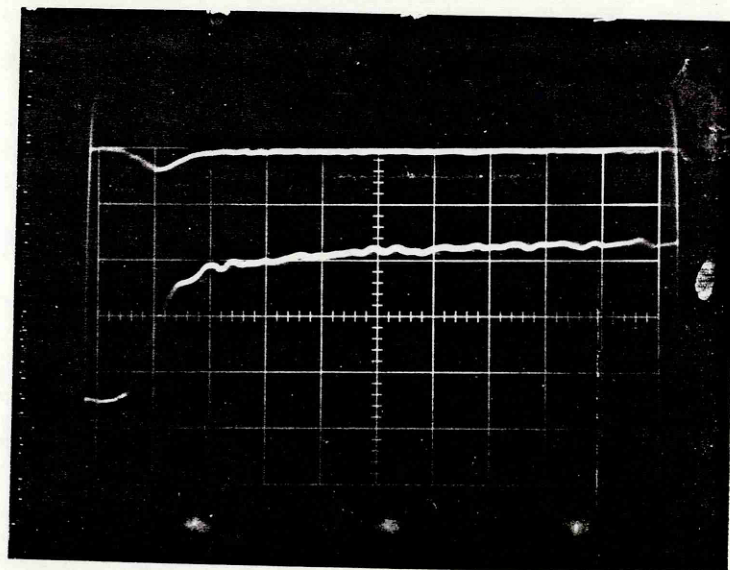
$\lambda_{\text{ex}} = 347\text{nm}$

Monochromator resolution = 1.17nm

Photomultiplier tube bias = -820V

Fig. 4.40

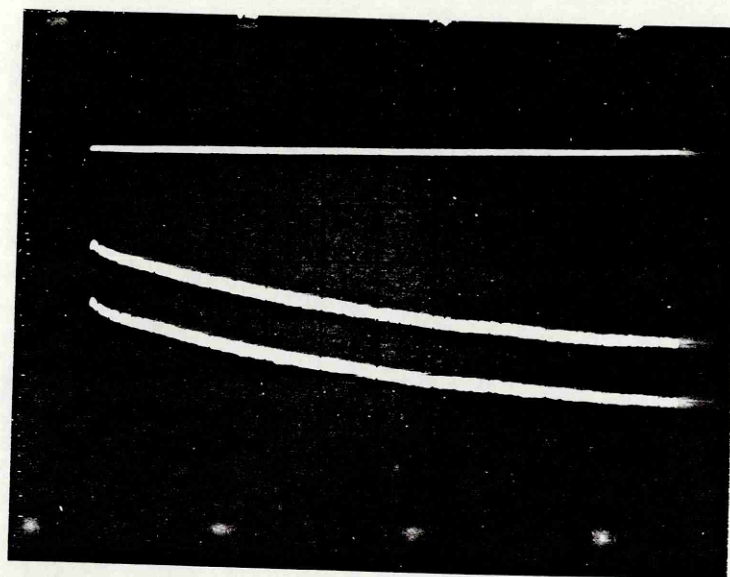




475nm.

10mv/div

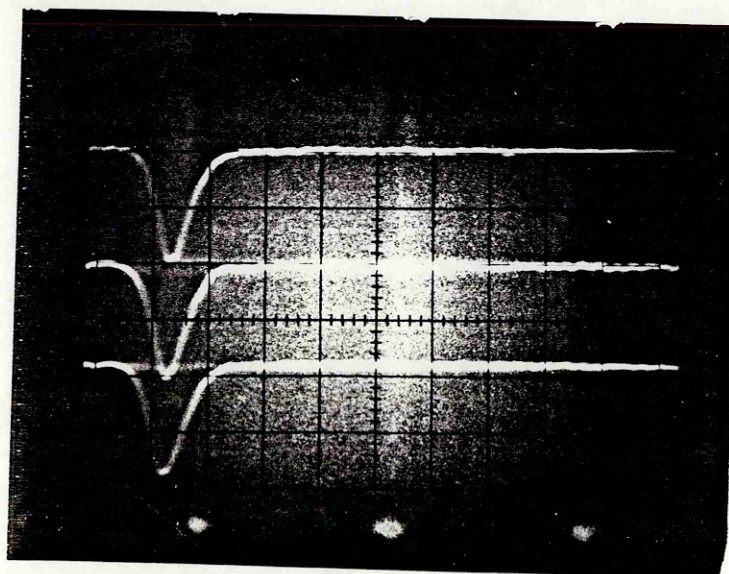
20ns/div



475 nm.

10mv/div

10 μ s/div



660 nm.

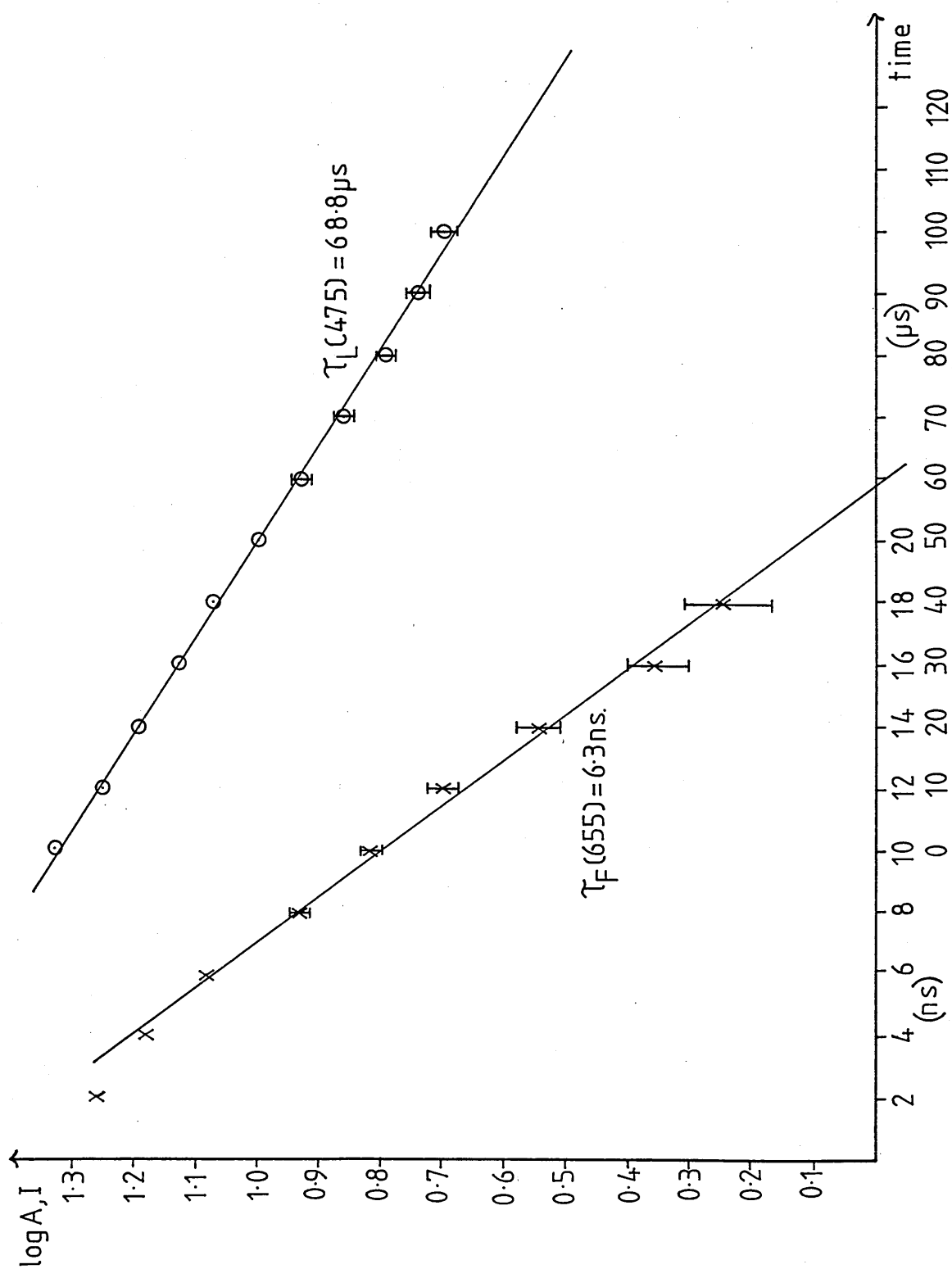
10mv/div

20ns/div

Fig. 4.41: ZnPc in ethanol. λ_{ex} 347nm # 2.

Fig. 4.42

Semi-log plots of ZnPc in ethanol.(2) λ_{ex} 347nm



spectrum at $t = 0$ has the lowest intensity of transient absorption and contains the nearest thing to structure. There is a shoulder at ≈ 400 nm and a broad absorption across the visible with a maximum at 470 nm. The spectra at $t = 20$ ns and 350 ns show a similar overall shape with a maximum at 480 nm and ground-state depletion at wavelengths shorter than 370 nm and longer than 595 nm.

The lifetimes of the longest-lived decay component at 475 nm and the fluorescence decay at 655 nm, which are shown in Fig.4.41, are calculated from the graphs of Fig.4.42 to be:

$$\tau_F(655) = 6.3 \pm 0.3 \text{ ns}$$

$$\tau_L(475) = 68.8 \pm 3.6 \text{ } \mu\text{s}$$

4.5(v) Summary

The two sets of transient spectra compare well with each other. In both cases, the spectrum at $t = 0$ shows a lower amplitude of absorption than at subsequent times. Also this spectrum is slightly more structured than the later ones which have a consistently "smooth" absorption band. There is evidence that the transient species absorbs light in the near u-v, a behaviour masked by the depletion of the Soret absorption band. The shape of the spectra is the same as that reported by Tsvirko et al.⁽¹⁰³⁾ which they assigned to the lowest triplet state of ZnPc in propanol. However, the response can be seen not to follow simple kinetics - there is a rapid rise in absorption followed by a slight increase over

the subsequent 500 ns. This then decays to form a longer-lived transient which has a lifetime calculated to be 68.8 μ s, although the decay appears not to be a perfectly smooth exponential.

The red fluorescence was recorded in a spectral region which corresponds to energies higher than that of the lowest excited electronic singlet state. A decay time of 6.3 ns of this emission is calculated, which at best can only be an upper limit to the fluorescence lifetime due to the convolution of the laser pulse.

The 'blue' fluorescence of solution (2) is of much lower intensity than that of solution (1) indicating a different effect upon the solute of the purification procedures.

4.6 MAGNESIUM PHTHALOCYANINE

4.6(i) Ground-state absorption

The ground-state absorption spectra of two solutions of MgPc in ethanol are shown in Fig.4.43. Solution (1) was purified by method A, solution (2) by method B.

4.6(ii) MgPc in ethanol . λ_{ex} 347 nm # 1

Transient spectra of solution (1) of MgPc in ethanol at times $t = 0, 20$ ns and 350 ns after the maximum of the 347 nm laser

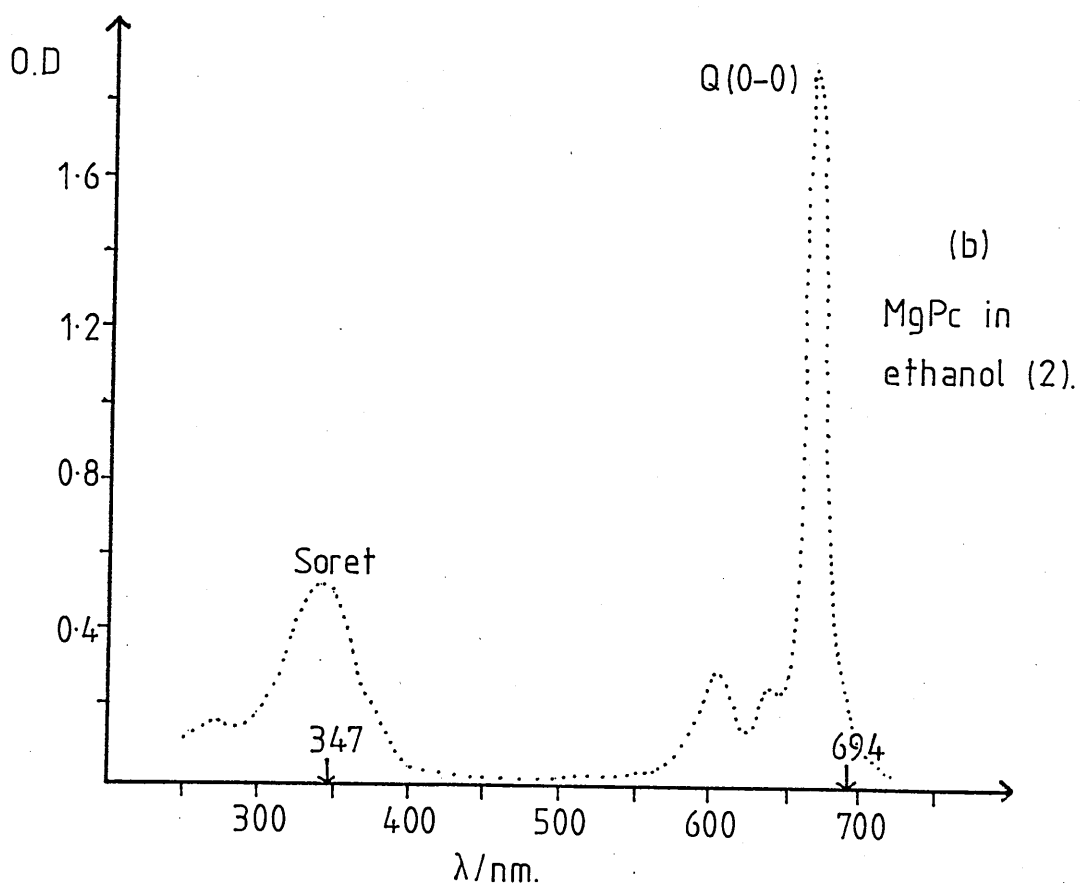
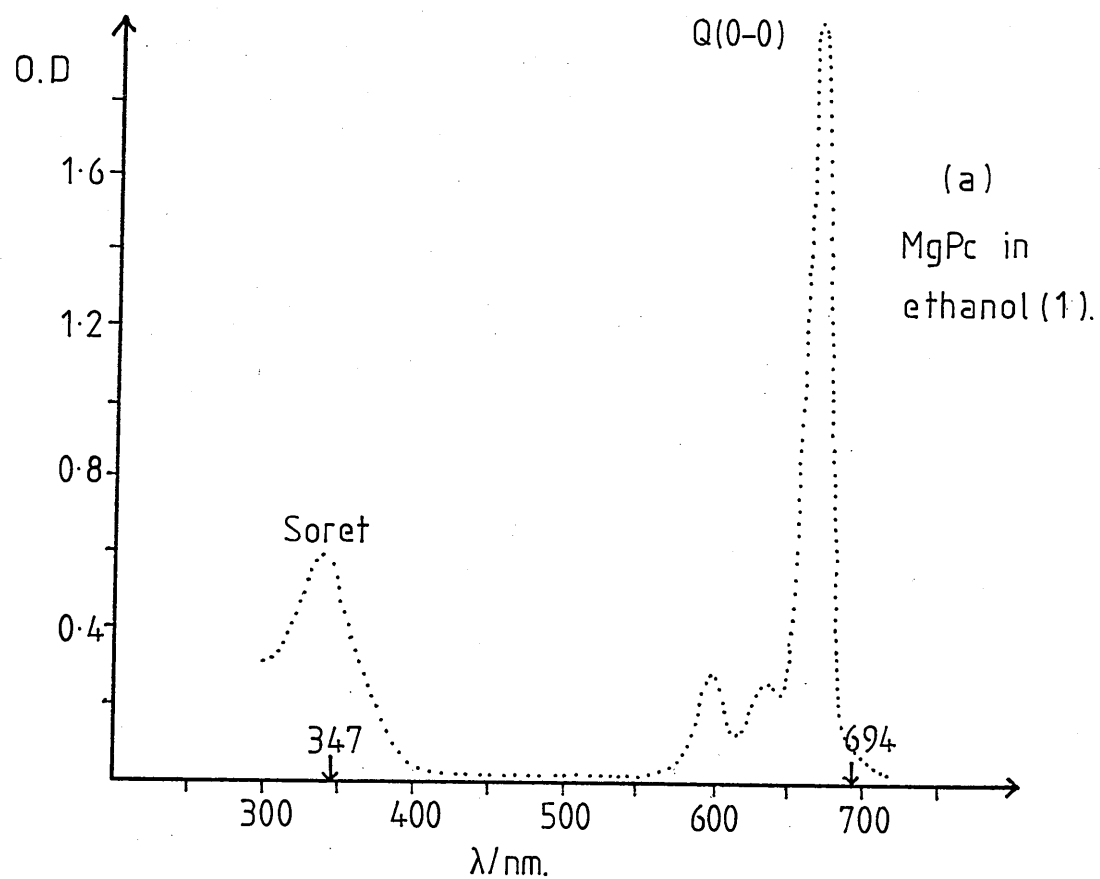


Fig.4.43: Ground-state absorption spectra.

excitation are shown in Fig.4.44. The spectrum at $t = 0$ displays a strong, structured absorption throughout the visible with a local peak at 390 nm and a maximum amplitude at 480 nm. The absorption falls off sharply to longer wavelengths until, approaching the red part of the spectrum the amplitude begins to increase and would constitute a large peak at ≈ 620 nm were it not for strong ground-state depletion. At 20 ns the absorption is neither so structured nor so intense - in particular the red response is much reduced. The overall shape of the spectrum remains the same at 350 ns with a maximum at 470 nm and ground-state depletion at wavelengths shorter than 370 nm and beyond 595 nm. No change in absorption is induced at 720 nm.

The transient kinetics at 470 nm can be seen (Fig.4.45) to include a long-lived decay component. Also the fluorescence recorded at 650 nm shows a falling edge longer than that of the exciting light. The intensity of this red fluorescence prevented measurements between 650 nm and 720 nm and it could be detected at wavelengths as short as 630 nm.

A weak blue fluorescence was also emitted - across a broad band with a maximum intensity at 450 nm.

4.6(iii)Fluorescence spectra

The fluorescence spectrum of solution (1) of MgPc in ethanol using arc-lamp excitation at 347 nm is shown in Fig.4.46.

Fig. 4.44

Transient difference spectra of MgPc in ethanol (1).

Spectra plotted at $t = 0$: --X--X--X--

$t = 20\text{ns}$:●.....

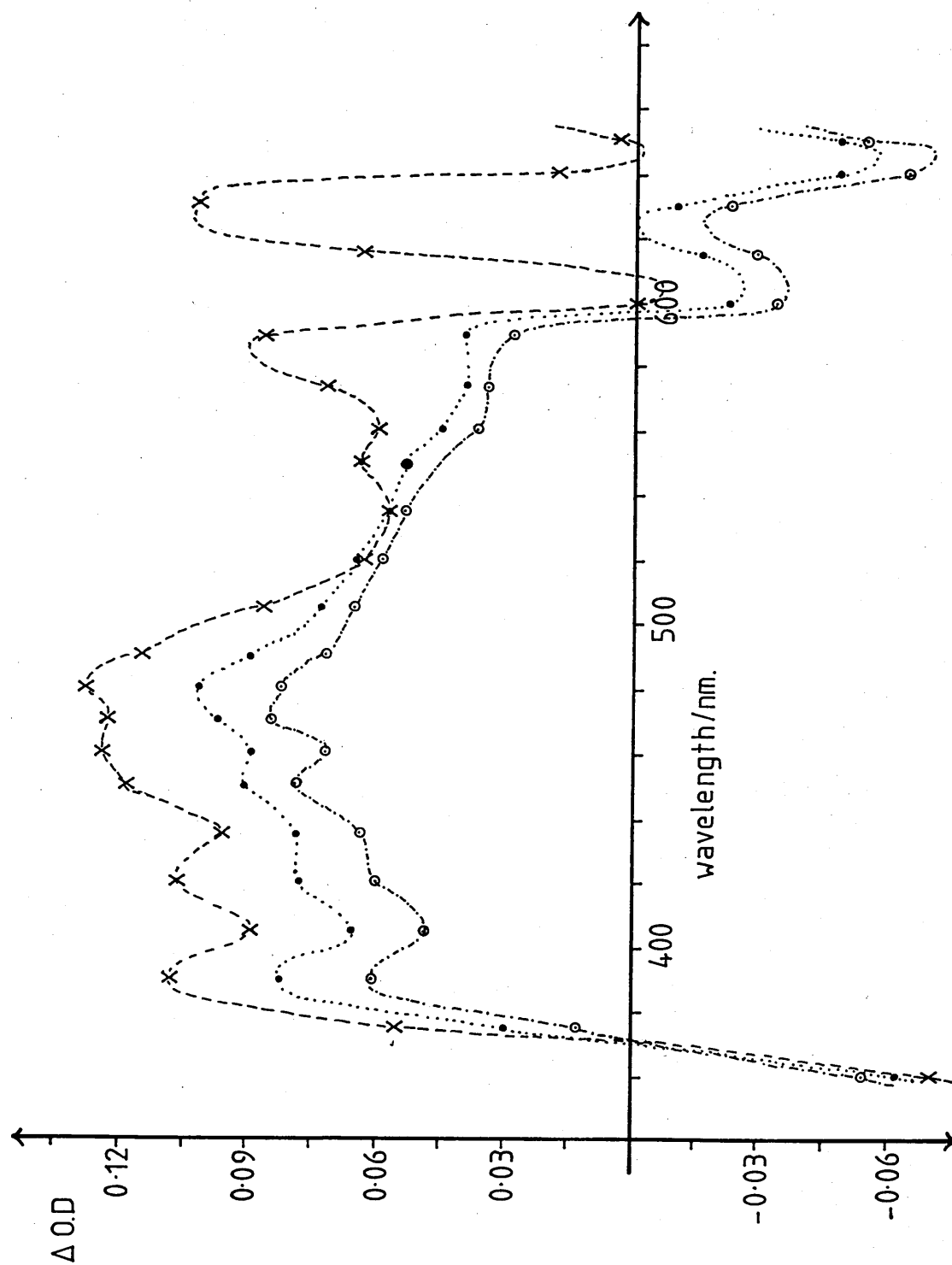
$t = 350\text{ns}$: -○- -○- -○- -○-

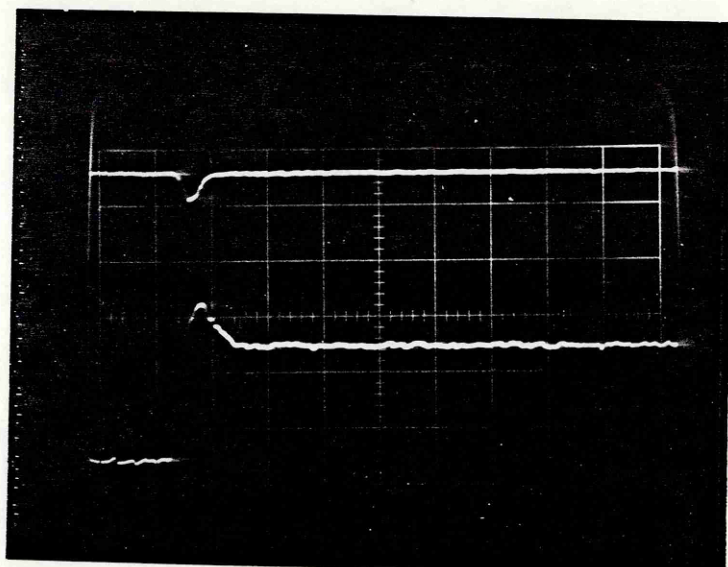
$\lambda_{\text{ex}} = 347\text{nm}$

Monochromator resolution = 1.04nm

Photomultiplier tube bias = -822V

Fig. 4.44

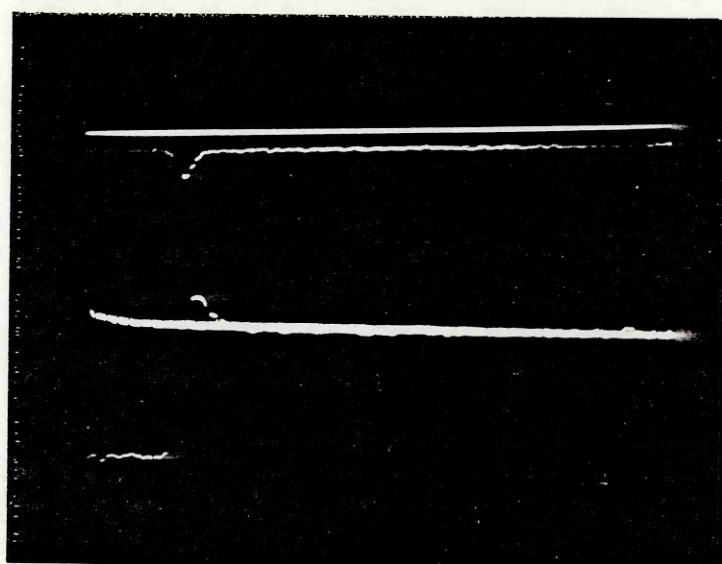




480nm.

20mv/div

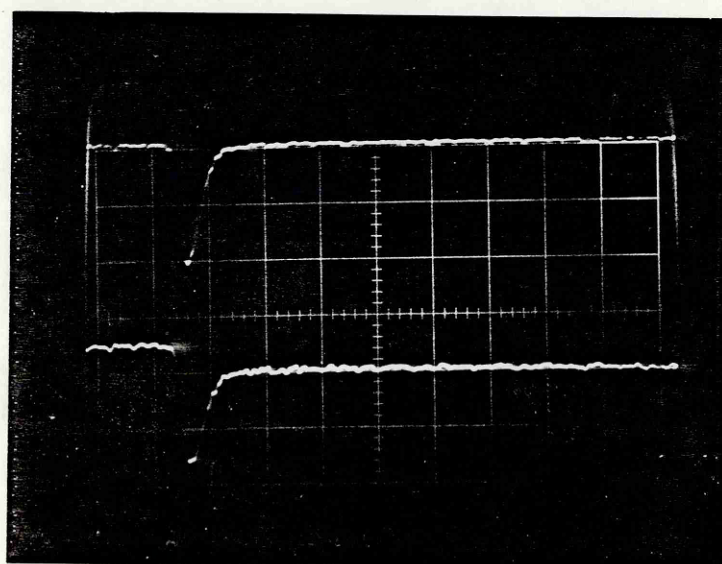
50ns/div



470nm

20mv/div

50ns,
2 μ s/div



650nm.

10mv/div

50ns/div

Fig.4.45: MgPc in ethanol. λ_{ex} 347nm. #1

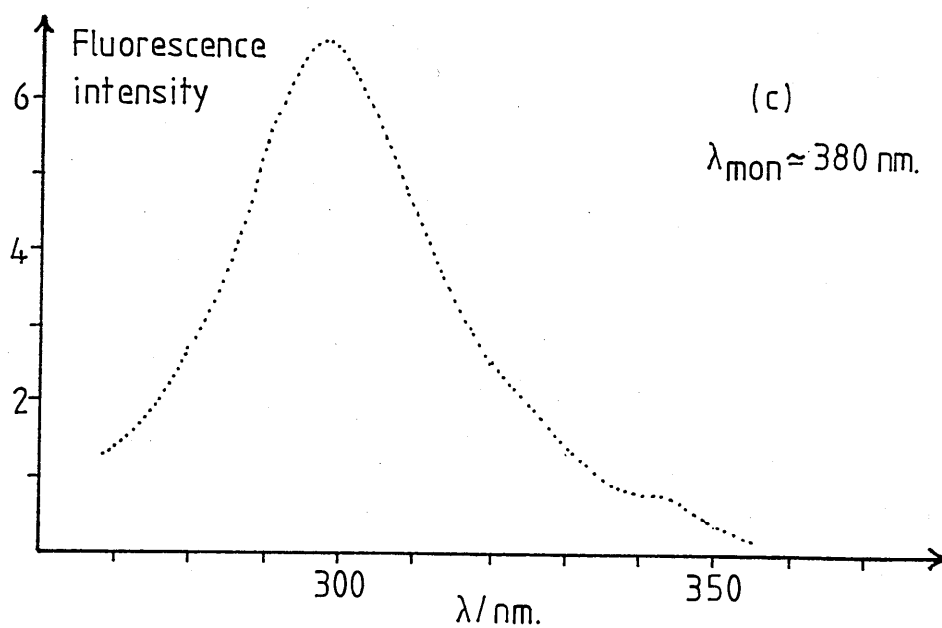
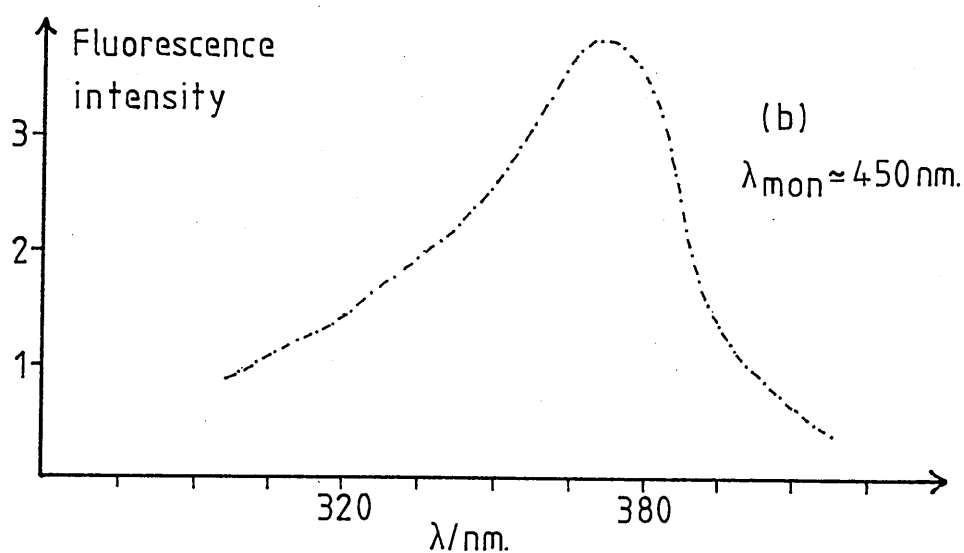
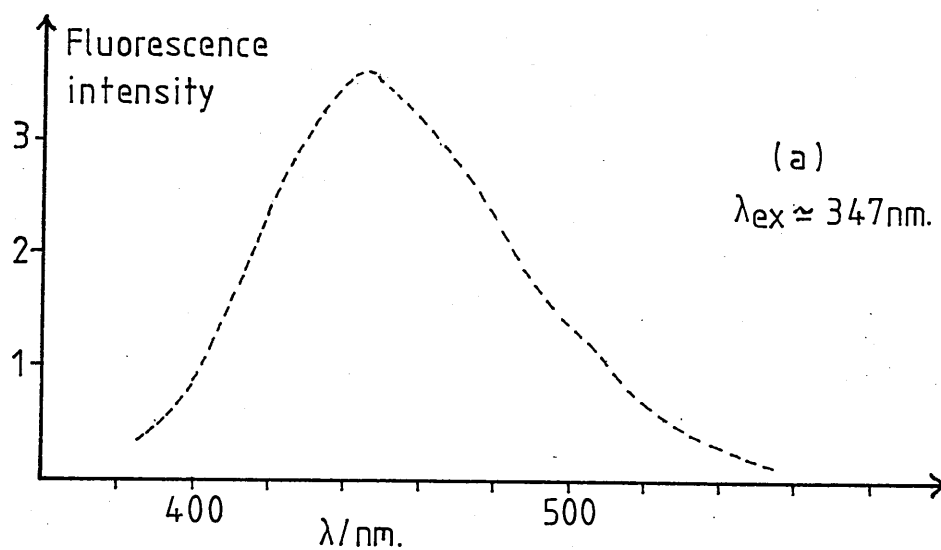


Fig.4.46: Fluorescence spectra of MgPc in ethanol(1).

The emission is broad-band and centred on 450 nm. An excitation spectrum monitored at this wavelength shows a diffuse band with a slight peak at ≈ 375 nm. When monitored at 380 nm the excitation spectrum shows a well-defined peak at 300 nm.

4.6(iv) MgPc in ethanol . λ_{ex} 347 nm # 2

The transient spectra of solution (2) of MgPc in ethanol at times $t = 0, 20$ ns and 350 ns after the maximum of the 347 nm excitation are shown in Fig.4.47. These spectra show the same features as described for solution (1).

Fig.4.48 show the transient absorption profile at 490 nm and the fluorescence response at 675 nm in outgassed and non-outgassed solution. The average lifetime of the decay is calculated from the graph of Fig.4.49 to be:

$$\tau_F 675 \text{ (outgassed)} = 7.3 \pm 0.2 \text{ ns}$$

$$\tau_F 675 \text{ (non-outgassed)} = 6.7 \pm 0.4 \text{ ns}$$

The 'blue' fluorescence emitted from this solution is of a lower intensity than that from solution (1).

The amplitude of transient absorption at 490 nm was recorded as a function of laser intensity and the results are shown in Fig.4.50.

Fig. 4.47

Transient difference spectra of MgPc in ethanol (2).

Spectra plotted at $t = 0$: --X---X---X--

$t = 20\text{ns}$:●.....

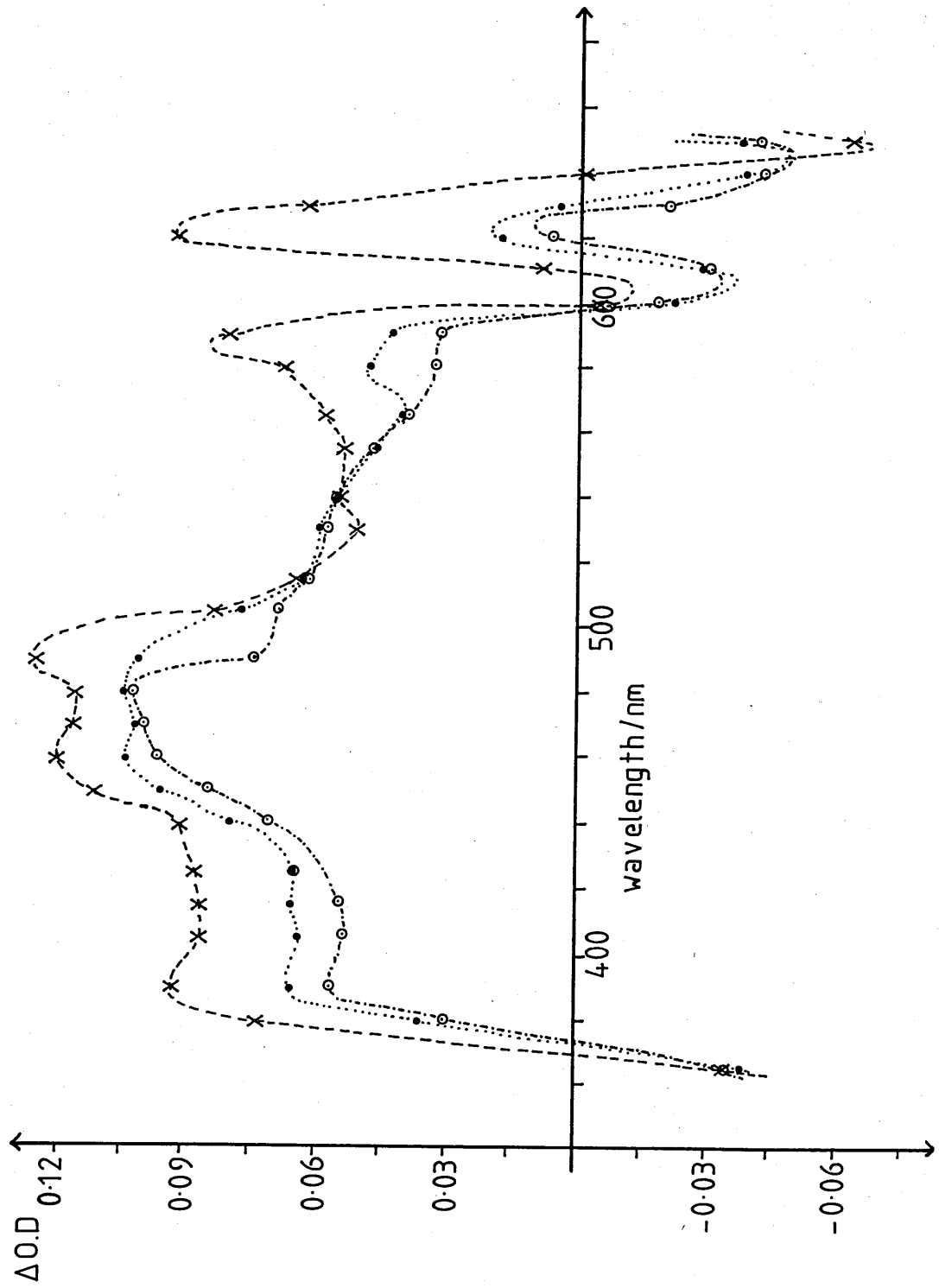
$t = 350\text{ns}$: --○---○---○--

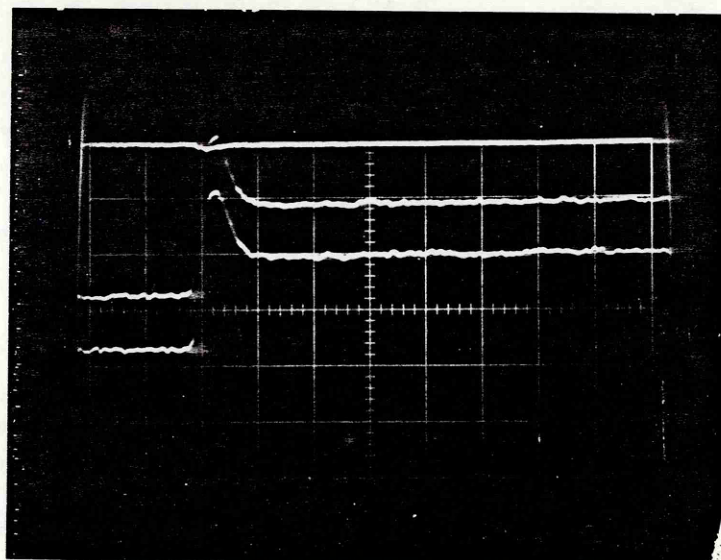
$\lambda_{\text{ex}} = 347\text{nm}$

Monochromator resolution = 1.04nm

Photomultiplier tube bias = -820V

Fig. 4.47

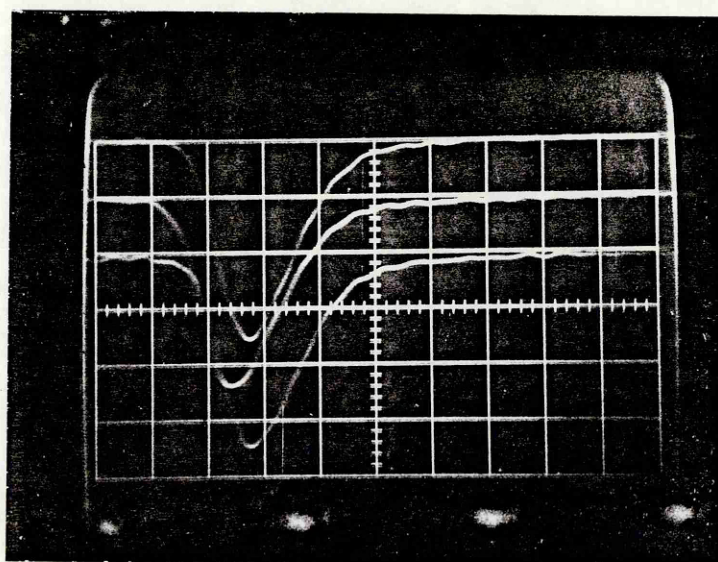




490 nm.

20mv/div

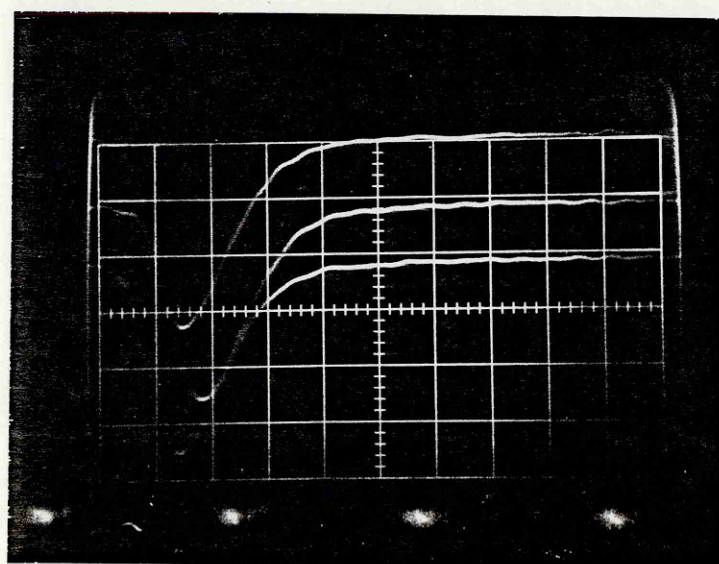
50ns/div



675 nm.

10mv/div

10ns/div



675 nm.

10mv/div

10ns/div

not
outgassed

Fig.4.48: MgPc in ethanol. λ_{ex} 347nm #2

Fig. 4.49

Semi-log plots for MgPc in ethanol (2). $\lambda_{ex}=347\text{nm}$.

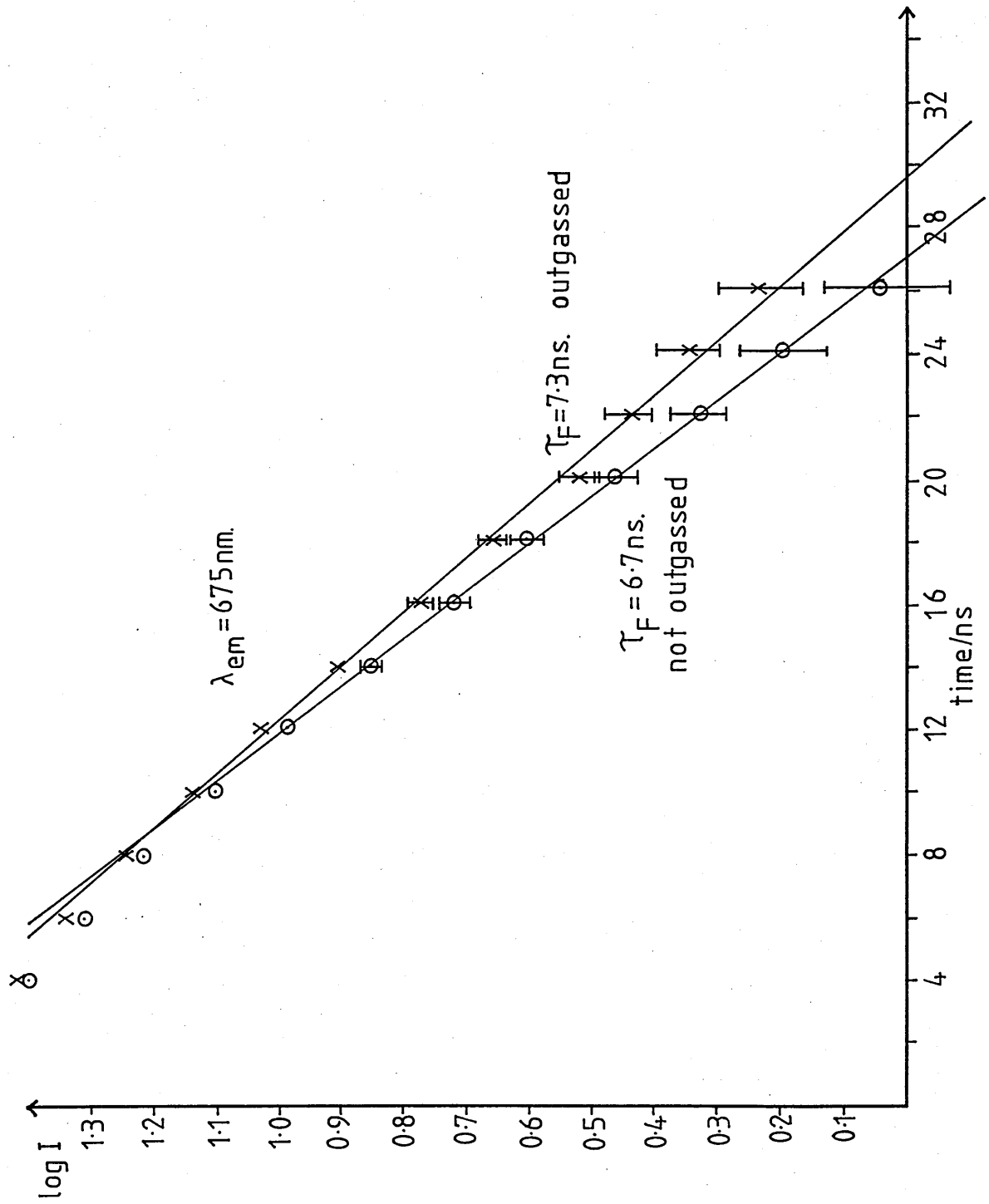
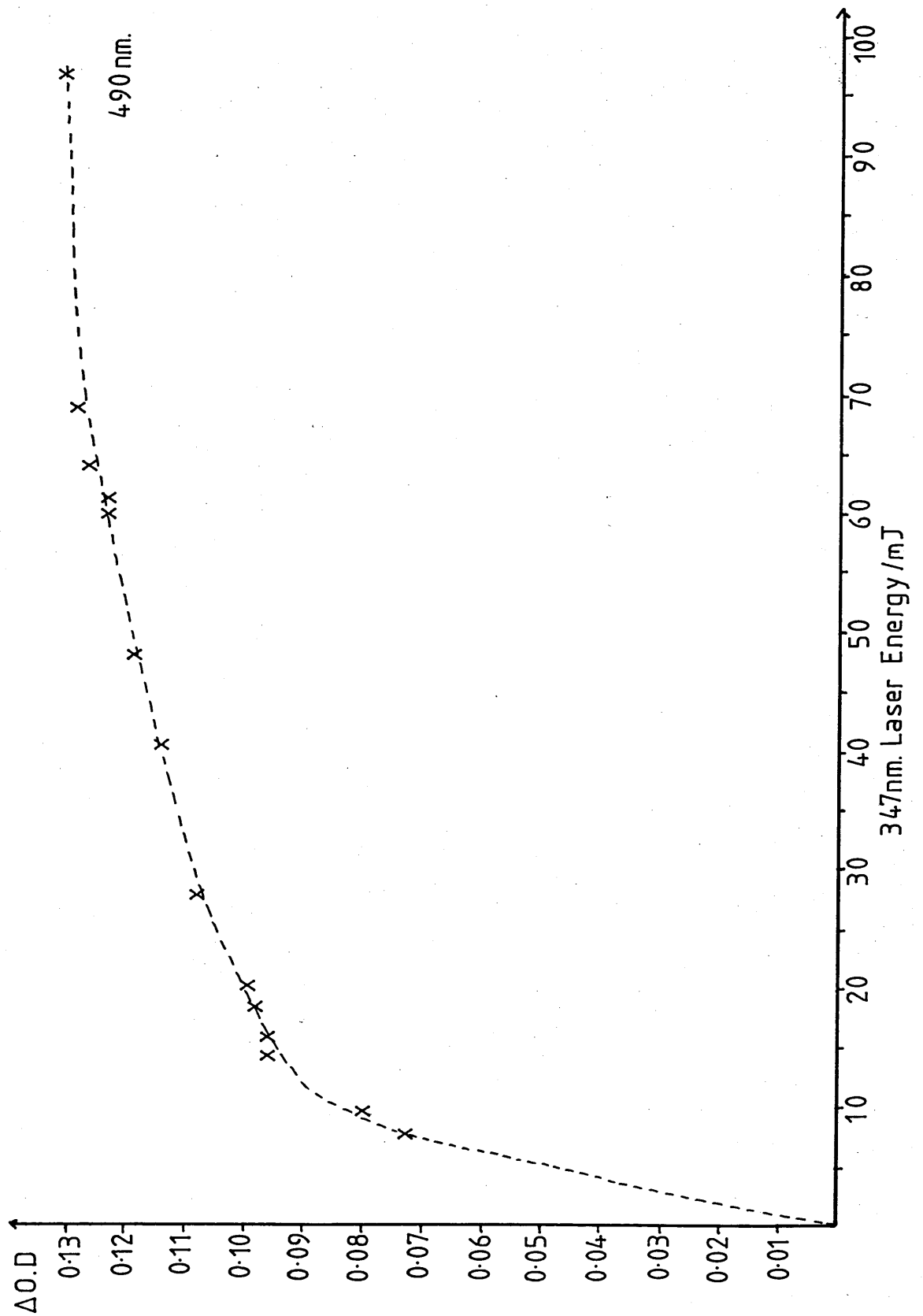


Fig.4.50

MgPc in ethanol: saturation of transient absorption.



4.6(v) Summary

The shape of the transient spectra are in agreement with those reported by Livingston and Fujimori⁽¹⁰¹⁾ and Tsvirko et al.⁽¹⁰³⁾ as being due to absorption from the lowest excited triplet state. The peak at 390 nm may be the long wavelength segment of an absorption in the near u-v part of the spectrum. The kinetics in the visible region show a rapid initial rise in absorption followed by a slight growing-in of absorption over the subsequent 500 ns which then decays into a longer-lived component.

At zero-time, the difference spectrum implies an intense absorption in the red part of the spectrum. This short-lived component has a decay-time of similar magnitude to that of the red fluorescence. Such an observation for this compound was also made by Muller.⁽¹⁰⁶⁾ It is clear that both the fluorescence and the short-lived transient absorption in this region are of much shorter duration than the initial short-lived transient in the visible part of the spectrum.

This red fluorescence is recorded in a region that corresponds to energies greater than the lowest excited electronic singlet state. The decay-time of 7.3 ns is an upper limit to the fluorescence lifetime and compares to previous observations.^(83,84)

The fact that the 'blue' fluorescence of solution (2) is of

lower intensity than that of solution (1) indicates a different effect of the purification procedures upon the solute.

The saturation of transient absorption at 490 nm is shown to occur at moderate laser intensities (Fig.4.50).

4.7 METAL-FREE PHTHALOCYANINE

4.7(i) Preamble

Although the results obtained using this compound are presented last in the sequence, the experiments from which they derive were performed earlier than those described previously in this chapter. No transient spectra are presented because the solutions were deoxygenated by purging with nitrogen and the transient decays show evidence that the technique was not completely efficient. However, the data do contain certain features worth describing; discussed below are the data obtained for metal-free phthalocyanine,

- (a) in 1-chloronaphthalene - excited at 694 nm.
- (b) in toluene - excited at 347 nm.
- (c) in o-xylene - excited at 694 nm.
- (d) in o-xylene - excited at 347 nm.

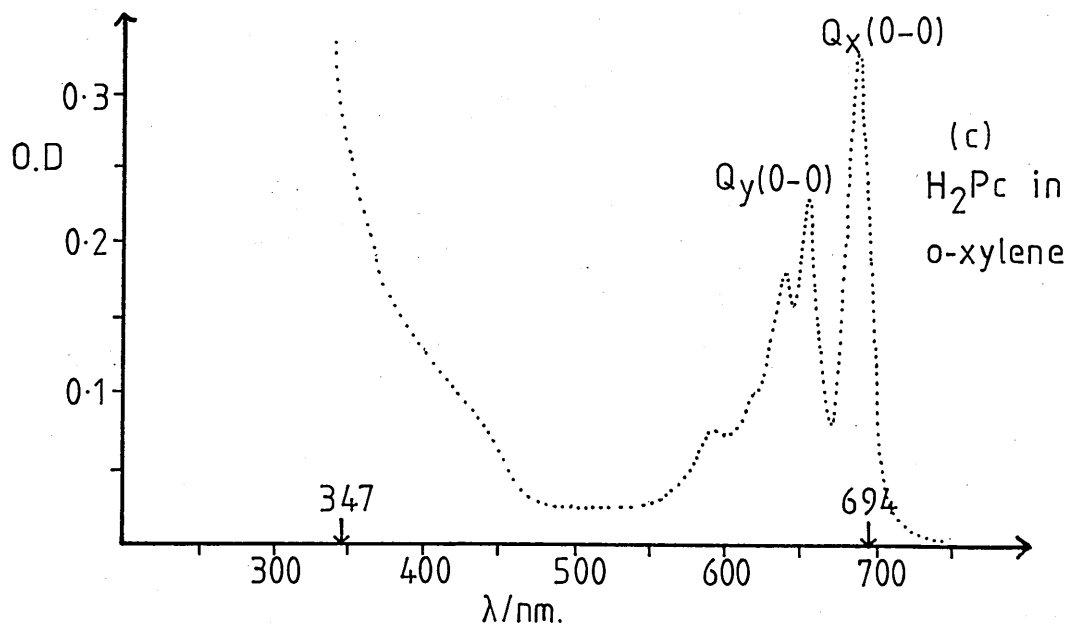
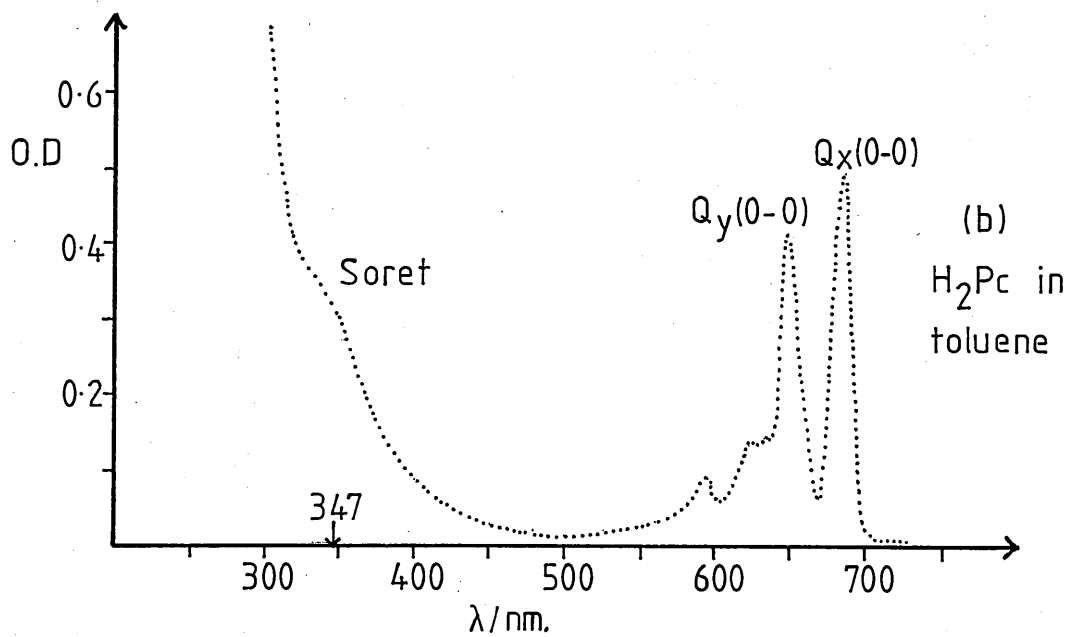
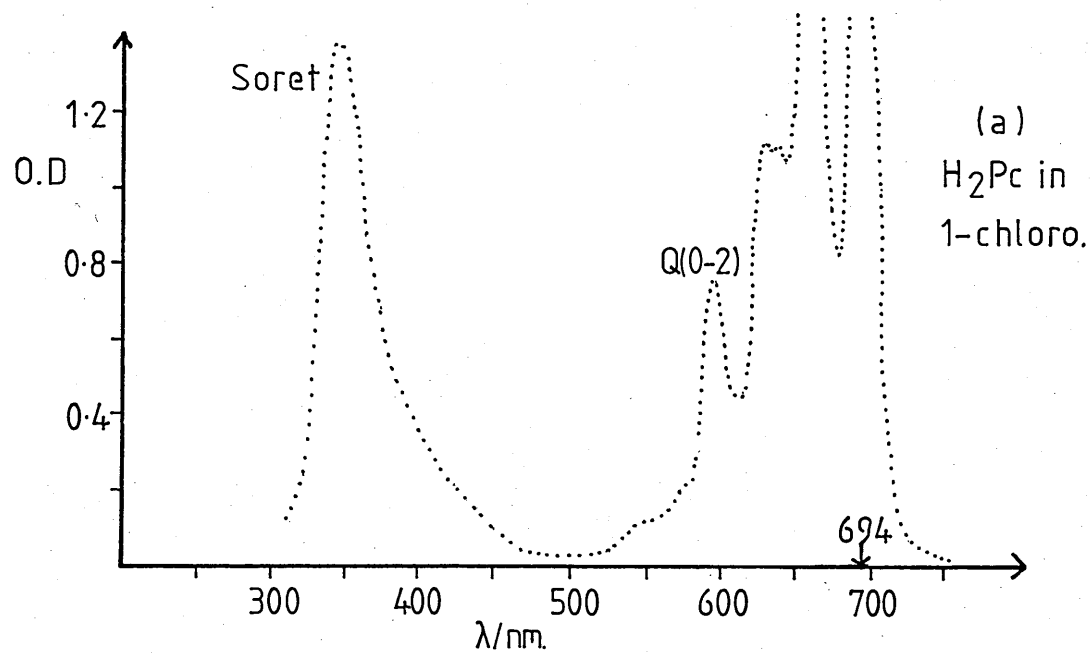


Fig.4.51: Ground-state absorption spectra.

4.7(ii) Ground-state absorption

Ground-state absorption spectra of three solutions of H₂Pc are shown in Fig.4.51. None of these solutions were purified.

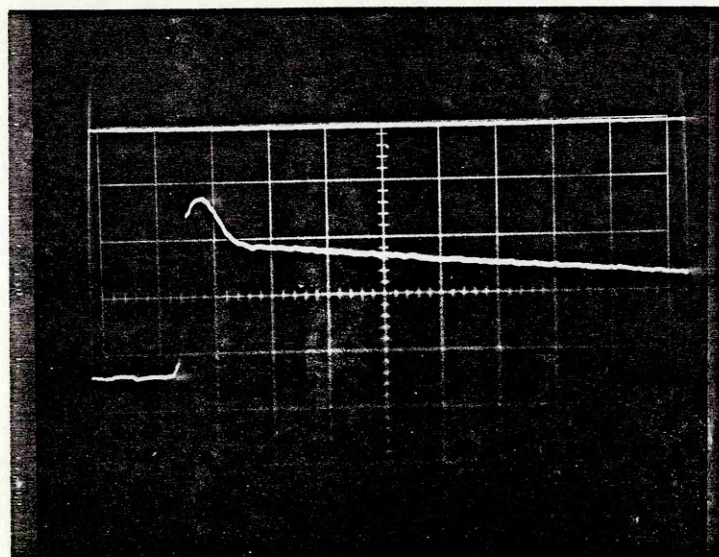
4.7(iii) H₂Pc in 1-chloronaphthalene . λ_{ex} 694 nm

Transient absorption was monitored between 655 nm and 420 nm and the decay profiles (Fig.4.52) indicate several transient components. In the visible region, there is a long-lived absorption with a maximum at 470 nm, as well as a shorter-lived transient which has a maximum amplitude at 490 nm. Between 550 nm and 630 nm, there is a very short-lived positive absorption that is intense relative to the long-lived component, with evidence of a local maximum at \approx 610 nm.

The decay profiles at long wavelengths show strong ground-state depletion over the entire red absorption band. Also, red fluorescence is recorded between 655 nm, where it is very intense, and 600 nm. The decay of this fluorescence is longer than that of the exciting laser pulse.

4.7(iv) H₂Pc in toluene . λ_{ex} 347 nm

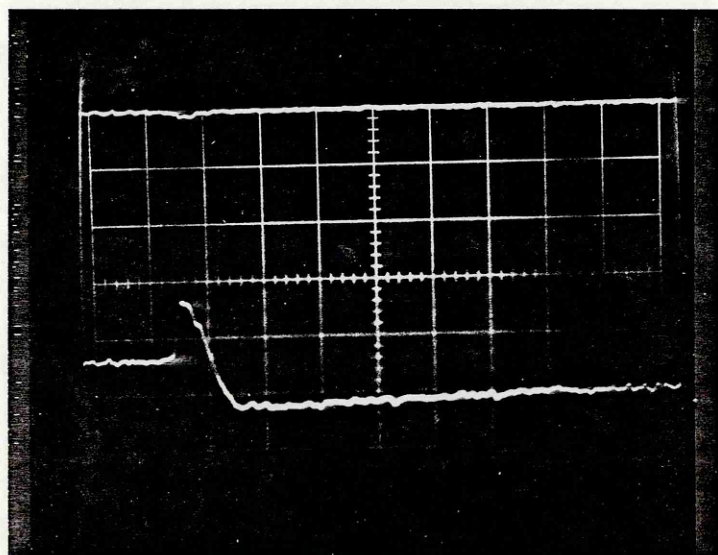
Transient absorption was monitored between 680 nm and 420 nm. The size of the signal (Fig.4.53) is limited by the low



470nm.

50mv/div

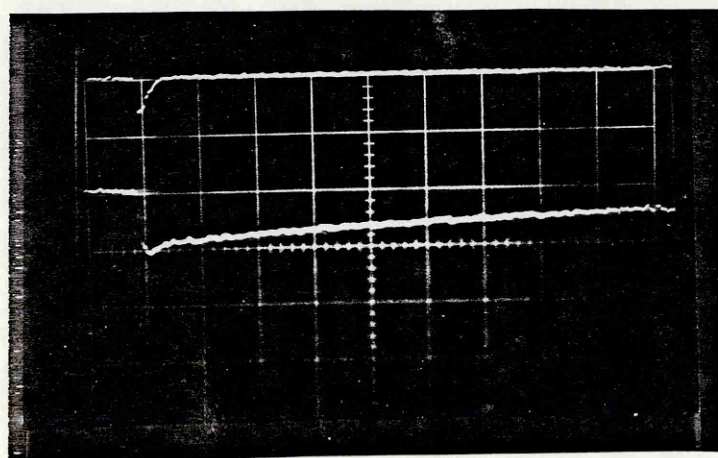
50ns/div



605nm.

10mv/div

50ns/div

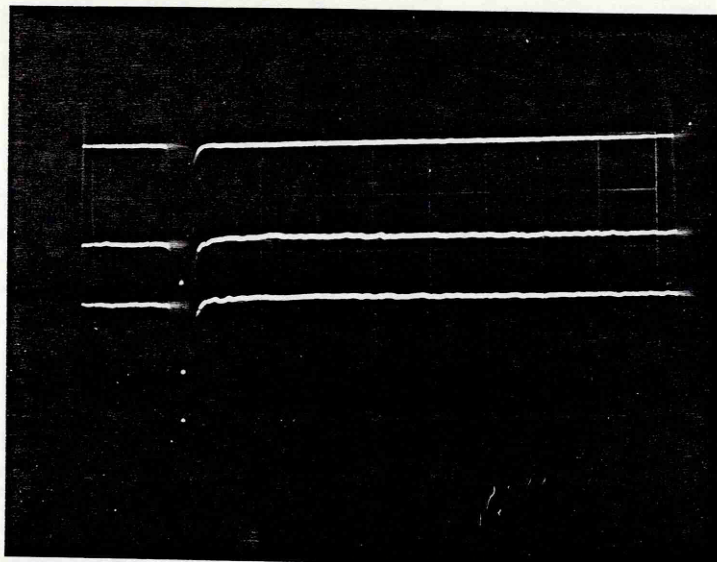


645nm.

10mv/div

50ns/div

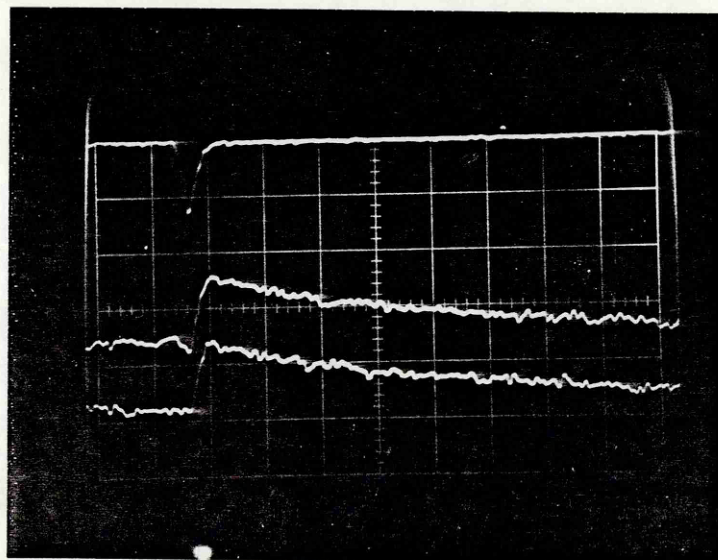
Fig.4.52: H_2Pc in 1-chloronaphthalene. λ_{ex} 694 nm.



420 nm.

50 mv/div

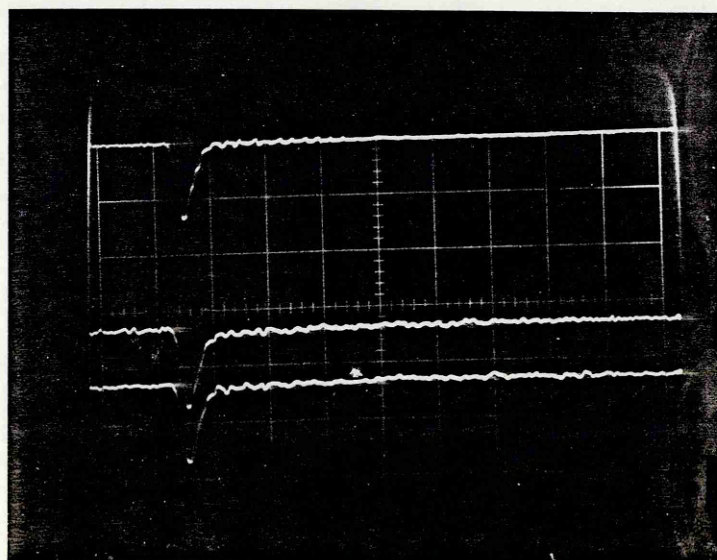
50 ns/div



500 nm.

10 mv/div

50 ns/div



670 nm.

10 mv/div

50 ns/div

Fig.4.53: H_2Pc in toluene. λ_{ex} 347 nm.

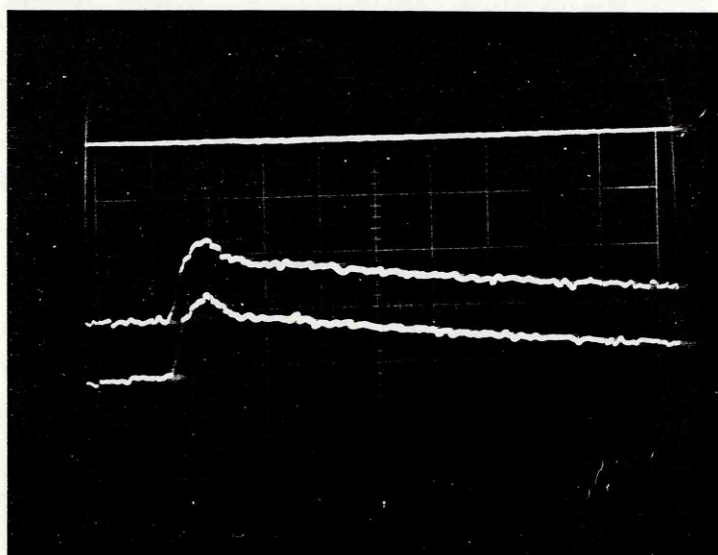
solubility of H₂Pc in this solvent. However, in the visible region of the spectrum there is evidence of short and long-lived decay components, both having a maximum amplitude at 475 nm. At 610 nm there is a small amount of short-lived absorption.

Red fluorescence is recorded between 680 nm and 640 nm, with a decaying edge slightly longer than that of the laser pulse. There is also a fairly strong 'blue' fluorescence which has a broad spectral width and reaches a maximum at a wavelength less than or equal to 420 nm.

4.7(v) H₂Pc in o-xylene . λ_{ex} 694 nm

Transient absorption was monitored between 715 nm and 420 nm. Short-lived and long-lived decays are evident in both the transient absorption and recovery from ground-state depletion (Fig.4.54). The long-lived depletion begins at \approx 590 nm whereas the signal determined by a short-lived component does not turn negative until about 640 nm. This may indicate a short-lived transient absorption in this spectral region.

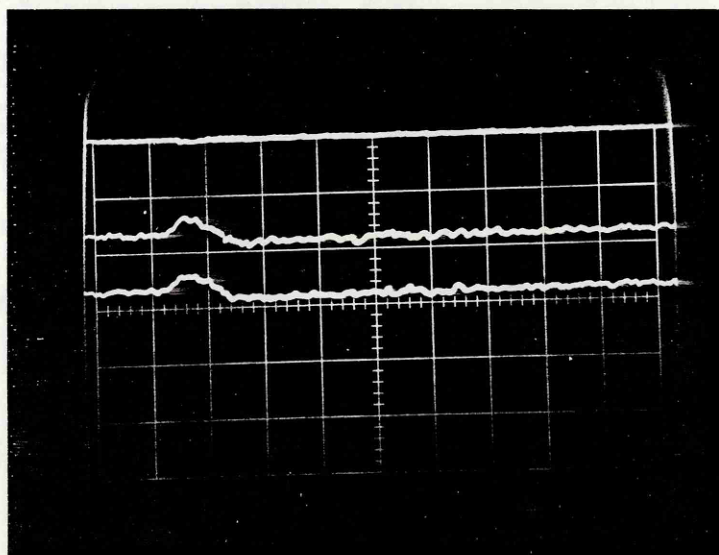
At 715 nm there is no transient absorption or bleaching but there is a strong fluorescence emission which is detected in the visible as far as \approx 635 nm. The decaying edge of this fluorescence is fairly long and does not appear to be a simple exponential.



495 nm.

20mv/div

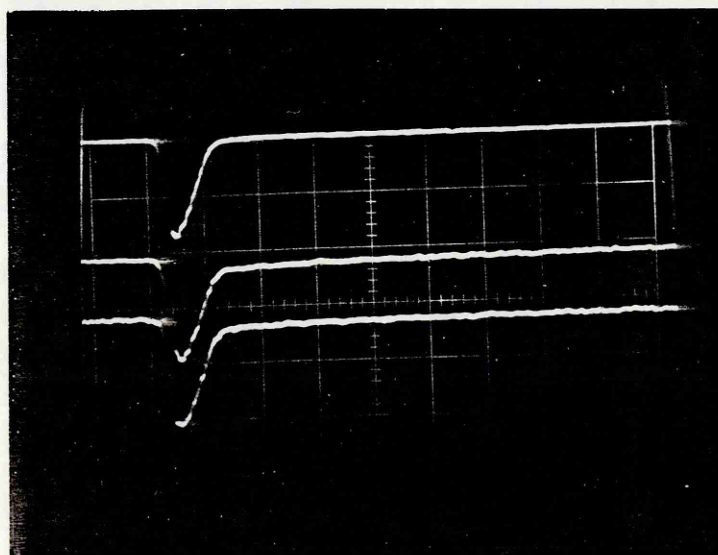
50ns/div



605 nm.

10mv/div

50ns/div

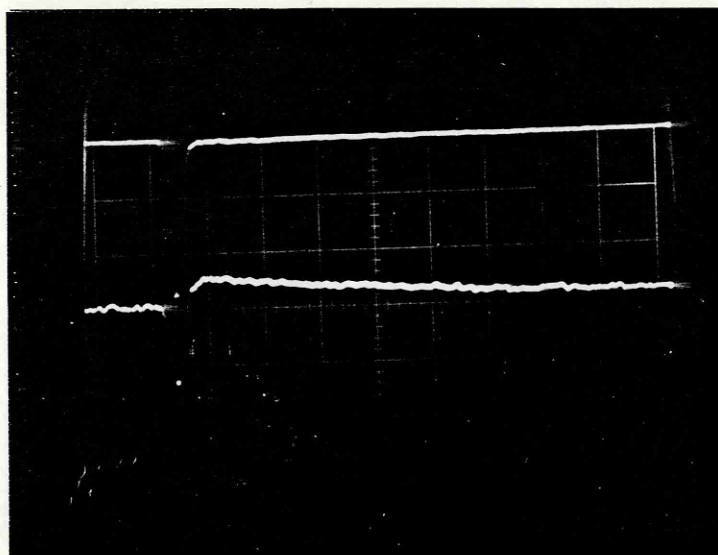


675 nm.

20mv/div

50ns/div

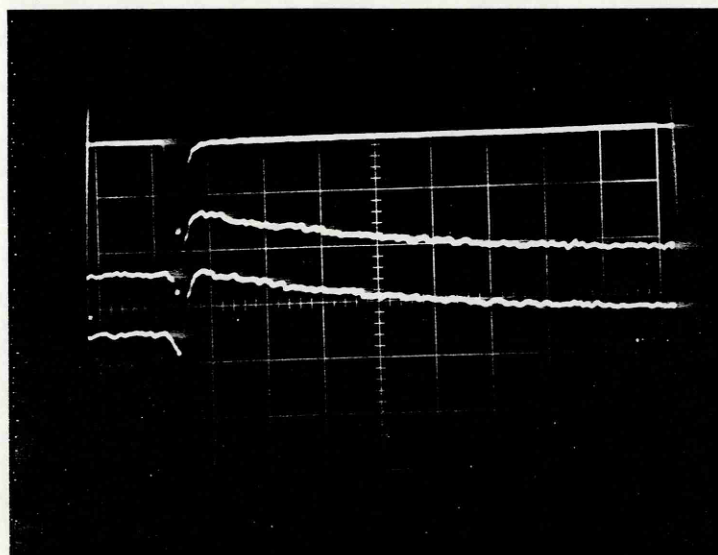
Fig.4.54: H_2Pc in o-xylene. $\lambda_{ex}=694nm$.



440nm.

20mv/div

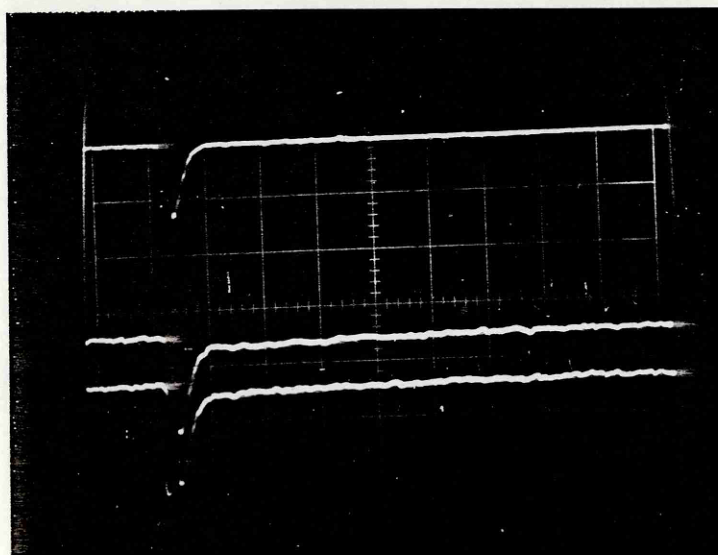
50ns/div



490nm.

20mv/div

50ns/div



660nm.

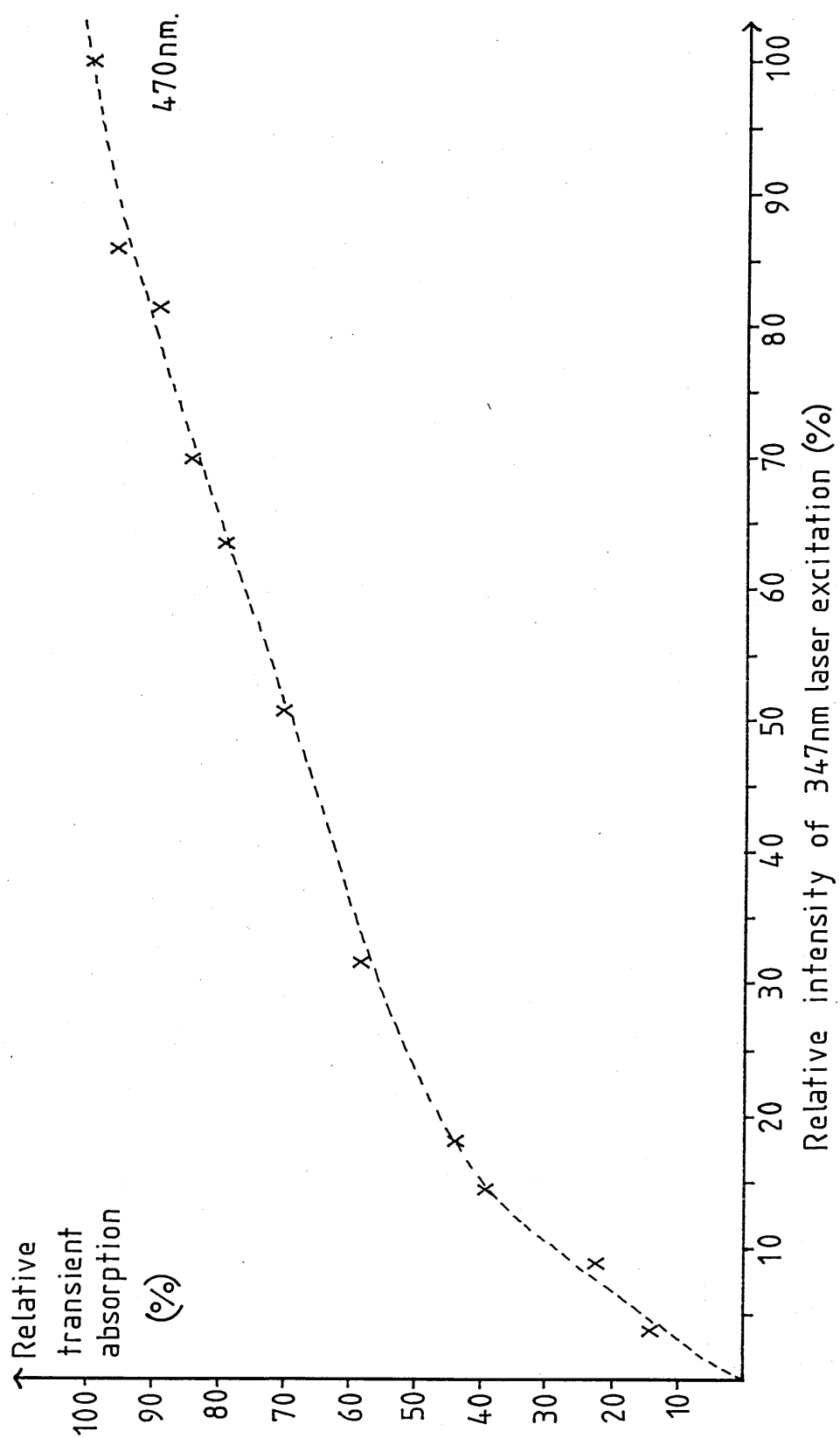
10mv/div

50ns/div

Fig.4.55: H_2Pc in o-xylene. $\lambda_{ex}=347nm$.

Fig. 4.56

H₂Pc in o-xylene: saturation of transient absorption.



4.7(vi) H₂Pc in o-xylene . λ_{ex} 347 nm

Transient absorption was monitored between 740 nm and 430 nm and it is noted that no change in absorption is induced beyond 720 nm. The longer-lived transient has a maximum absorption at about 485 - 490 nm and depletion is evident across the whole red absorption band.

Fig.4.55 shows that the fluorescence emission, which is recorded between 740 nm and 640 nm, has a decaying edge only marginally longer than that of the laser pulse, assuming the latter to be symmetrical with the rising edge of the fluorescence.

Laser-induced 'blue' fluorescence is strong and has a maximum yield at a wavelength shorter than or equal to 430 nm.

The amplitude of transient absorption at 470 nm was recorded at different intensities of 347 nm laser irradiation. A graph of laser intensity Vs relative transient absorption is shown in Fig.4.56.

4.7(vi) Summary

Although the transient absorption of H₂Pc was monitored in different solvents and at different wavelengths of excitation, there are marked similarities in response. All of the solutions show a positive transient absorption in the

visible part of the spectrum which consists of two components, as well as strong ground-state depletion across the Q-absorption band. The two decay components have a maximum amplitude in the same region of the spectrum - 470 - 500 nm - but they are not always exactly coincident.

The short-lived transient absorption centred at ≈ 610 nm that is particularly evident using 694 nm excitation is seen to have a much faster decay than the initial component evident in the visible band. The existence of such an absorption is in agreement with the work of Muller⁽¹⁰⁶⁾ who observed a transient in the red part of the spectrum with a decay time similar to that of the fluorescence emission.

No decay times of these transients are presented since the solutions show evidence of incomplete deoxygenation. This correlates further with the evidence of Muller - that the decay of the long-lived absorption component has a time dependence that is strongly sensitive to the presence of oxygen.

Fluorescence is emitted from all solutions at wavelengths extending from the near infra-red into the visible part of the spectrum. Not only does this emission occur at wavelengths shorter than 694 nm, but also at those corresponding to energies higher than that of the first excited singlet state of this compound. The fluorescence decay is longer than that of the laser pulse - emphatically

so using 694 nm irradiation. This emission appears similar to the 'delayed' fluorescence from H₂Pc in 1-chloronaphthalene reported by Harrison and Kosonocky(88) and Guiliano and Hess.(89)

Subject to 347 nm excitation, H₂Pc in toluene and o-xylene exhibits a 'blue' fluorescence which is moderately intense and, from data obtained using the fluorimeter, has a peak at \approx 395 nm. This wavelength does not correspond to the energy of the excited electronic states of singlet or triplet character. In addition, the decay of this emission can be seen to be more rapid than that of the 'red' fluorescence.

4.8 MISCELLANY

4.8(i) Effect of temperature upon the ground-state absorption of H₂Pc in toluene

Ground-state absorption spectra of a purified solution of H₂Pc in toluene were recorded at temperatures between ambient and 64°C. The values of optical density at the main absorption peaks are listed in Table 4.1

Table 4.1
Absorption peaks of H_2Pc in toluene -
effect of temperature

Optical density $\pm 5 \times 10^{-4}$					
λ (nm)	24°C	32°C	41°C	53°C	64°C
691	0.1076	0.1066	0.1040	0.1012	0.0973
655	0.0870	0.0850	0.0824	0.0790	0.0764
640	0.0332	0.0336	0.0338	0.0337	0.0337
628	0.0284	0.0282	0.0280	0.0277	0.0268
593	0.0144	0.0142	0.0138	0.0136	0.0132
340	0.0573	0.0559	0.0559	0.0588	0.0560

4.8(ii) Effect of temperature upon the ground-state
absorption of $AlPcCl$ in ethanol

Ground-state absorption spectra of solution (2) of $AlPcCl$ in ethanol were recorded at temperatures between ambient and 50°C. The values of optical density at the main absorption peaks are listed in Table 4.2

Table 4.2
Absorption peaks of $AlPcCl$ in ethanol -
effect of temperature

Optical density $\pm 5 \times 10^{-3}$					
λ (nm)	23°C	30°C	40°C	50°C	23°C
688	1.665	1.649	1.600	1.560	1.665
637	0.230	0.230	0.226	0.226	0.235
602	0.262	0.262	0.252	0.244	0.270
350	0.492	0.480	0.470	0.472	0.492

4.8(iii) Effect of temperature upon the ground-state
absorption of $ZnPc$ in ethanol

Ground-state absorption spectra of $ZnPc$ in ethanol were recorded at temperatures between ambient and 65°C. The

values of optical density at the main 'red' absorption peaks are listed in Table 4.3.

Table 4.3
Absorption peaks of ZnPc in ethanol -
effect of temperature

Optical density $\pm 1 \times 10^{-3}$					
$\lambda(\text{nm})$	21°C	30°C	40°C	52°C	65°C
655	0.412	0.410	0.395	0.382	0.370
634	0.052	0.055	0.055	0.055	0.053
600	0.055	0.058	0.057	0.056	0.053

4.8(iv) Effect of concentration upon the ground-state
absorption of ZnPc in ethanol

Ground state absorption spectra of ZnPc in ethanol were recorded for increasingly dilute solutions. The values of optical density at the main 'red' absorption peaks are listed in Table 4.4.

Table 4.4
Absorption peaks of ZnPc in ethanol -
effect of concentration

Optical density						
$\lambda(\text{nm})$	(a)	(b)	(c)	(d)	(e)	(f)
	$\pm 2 \times 10^{-3}$	$\pm 2 \times 10^{-3}$	$\pm 1 \times 10^{-3}$	$\pm 1 \times 10^{-3}$	$\pm 1 \times 10^{-3}$	$\pm 2 \times 10^{-4}$
655	0.843	0.691	0.482	0.352	0.218	0.0655
634	0.117	0.101	0.063	0.046	0.028	0.0074
600	0.123	0.102	0.068	0.049	0.029	0.0077

4.8(v) Effect of concentration upon the ground-state
absorption of MgPc in ethanol

Ground-state absorption spectra of Mg in ethanol were recorded for increasingly dilute solutions. The values of

optical density at the main 'red' absorption peaks are listed in Table 4.5.

Table 4.5
Absorption peaks of MgPc in ethanol -
effect of concentration

$\lambda(\text{nm})$	Optical density					
	(i)	(ii)	(iii)	(iv)	(v)	(vi)
	$\pm 4 \times 10^{-3}$	$\pm 4 \times 10^{-3}$	$\pm 4 \times 10^{-3}$	$\pm 2 \times 10^{-3}$	$\pm 2 \times 10^{-3}$	$\pm 1 \times 10^{-3}$
667	1.895	1.570	1.182	0.955	0.723	0.390
637	0.245	0.205	0.152	0.124	0.094	0.049
602	0.280	0.225	0.172	0.138	0.106	0.055

4.8(vi) Summary

The effect of temperature on the intensity of absorption relative to that at room temperature is shown in Table 4.6. It can be seen that all three solutions studied in this way show a response to increasing temperature that is different for each absorption transition. Furthermore, the two main peaks that constitute the doublet of H_2Pc both suffer a reduction in amplitude of optical density with increasing temperature, but the effect is the more pronounced for the shorter wavelength component [$\text{Qy}(0-0)$]. This differs with McVie's⁽⁴²⁾ observation that the two absorption peaks of H_2Pc in 1-chloronaphthalene are replaced by a single peak of enhanced intensity at 670 nm, upon heating to 40°C.

Table 4.6
Relative intensity of absorption - effect of temperature

Solution	Wave-length (nm)	Transition	Relative intensity of absorption				
			24°C	32°C	41°C	53°C	64°C
H ₂ Pc in toluene	691	Qx(0-0)	1.0000	0.9907	0.9665	0.9405	0.9043
	655	Qy(0-0)	1.0000	0.9770	0.9471	0.9089	0.8782
	640	Qx(0-1)	1.0000	1.0120	1.0180	1.0151	1.0151
	628	Qy(0-1)	1.0000	0.9930	0.9859	0.9754	0.9477
	593	Q (0-2)	1.0000	0.0861	0.9583	0.9444	0.9167
	340	SORET	1.0000	0.9756	0.9756	1.0262	0.9773
			23°C	30°C	40°C	50°C	
AlPcCl in ethanol	688	Q (0-0)	1.000	0.990	0.961	0.937	
	637	Q (0-1)	1.000	0.989	0.972	0.972	
	602	Q (0-2)	1.000	0.985	0.947	0.917	
	350	SORET	1.000	0.976	0.955	0.959	
			21°C	30°C	40°C	52°C	65°C
ZnPc in ethanol	665	Q (0-0)	1.000	0.995	0.050	0.927	0.898
	634	Q (0-1)	1.000	1.115	1.115	1.115	1.019
	600	Q (0-2)	1.000	1.055	1.036	1.018	0.964

It is apparent that the vibronic transitions $S_{00} \rightarrow S_{11}$, $S_{00} \rightarrow S_{12}$ do not suffer as great a reduction in absorption probability as the "purely electronic" transition ($S_{00} \rightarrow S_{10}$) of the compounds. In fact the results show specific instances of an increase in vibronic absorption intensity following an increase in temperature. Also the Soret absorption shows only a relatively moderate reduction in intensity.

A comparison of the values of optical density at the absorption peaks of AlPcCl in ethanol before and after heating to 50°C show that the effect of temperature upon this

solution is reversible.

The relative intensities of absorption transition within the Q-band of ethanol solutions of ZnPc and MgPc at different concentrations are shown in Table 4.7. It can be seen that, for both solutions, the optical densities corresponding to the three transitions do not decrease in the same proportion upon dilution. Although it is not possible to deduce a pattern of behaviour from a sample of two, the effect of concentration will be discussed in Chapter 5.

Table 4.7
Relative intensity of absorption - effect of concentration

Solution	Wave-length (nm)	Transition	Relative intensity of absorption					
			(a)	(b)	(c)	(d)	(e)	(f)
ZnPc in ethanol	665	Q (0-0)	1.000	0.820	0.572	0.418	0.259	0.078
	634	Q (0-1)	1.000	0.863	0.539	0.393	0.239	0.063
	600	Q (0-2)	1.000	0.829	0.553	0.398	0.236	0.063
MgPc in ethanol			(i)	(ii)	(iii)	(iv)	(v)	(vi)
	667	Q (0-0)	1.000	0.829	0.624	0.504	0.382	0.206
	637	Q (0-1)	1.000	0.837	0.620	0.506	0.384	0.200
	602	Q (0-2)	1.000	0.804	0.614	0.493	0.379	0.196

CHAPTER 5

DISCUSSION AND CONCLUSIONS

5.1 SATURATION

A combination of the low concentrations ($\approx 10^{-5}$ M) of many of the solutions investigated and the high light intensity of the laser excitation makes certain that most measurements were recorded under conditions of 'saturation'. This is shown to be the case by the plots of laser intensity vs. transient absorption/fluorescence. For this reason, most of the transient spectra reported in this work are not normalised to account for shot to shot variations in laser intensity - in the region of saturation, a slight increase or decrease in laser intensity incident upon the sample cell is not accompanied by a significant change in transient response.

This argument does not apply to those solutions of 1-chloronaphthalene (with and without CuPc) excited at 347 nm. Since the strong absorption of the laser light here results from the concentration of the solvent rather than from a large absorption cross-section, the region of saturation appears not to have been reached. Therefore the transient spectra are normalised to a laser energy of 90 m J. It is possible, as evidenced by fig 4.56, that there is also incomplete saturation of transient response in the solution of H₂Pc in o-xylene. Again, this may be due to the participation of the solvent in the absorption of u-v laser-light.

It is unfortunate that the large noise spike that accompanies the firing of the laser, and/or the insensitivity of the laser energy monitor in its present operating mode, prevented the recording of 2nd harmonic laser energy of magnitude ≤ 7 mJ. This low-intensity region remains potentially the most interesting in the light of Jacques and Braun's claim (108) that a deviation from the predicted transient response occurs when the 694 nm excitation wavelength contains more than 2 mJ of energy.

5.2 TRANSIENT RESPONSE

It is clear, from the evidence of previous flash photolysis studies of phthalocyanines, that the data presented in this work displays many of the characteristics of molecular triplet states. There is good agreement between the various spectra obtained using each of the ruby laser excitation wavelengths; there is also good agreement between spectra of solutions that have been prepared following different purification procedures. In addition, all of these spectra agree with the published spectra shown in Appendix 3.

Therefore, the results support the assertion of Pyatosin and Tsvirko(107) that identical triplet spectra are obtained following either 694 nm or 347 nm excitation. The inference that the lowest triplet state can be populated via Q-band and Soret band absorption, is in itself significant. However, it is the immediate response of a solution that can provide a

means of following the pathways of energy redistribution, and this work provides some evidence that the intense transient absorption, which occurs at wavelengths shorter than ≈ 550 nm, is 'absorption band dependent'; at least during the period of excitation. This is displayed by a more gradual growing-in of response to 694 nm pumping than to 347 nm.

Although the ground-state absorption transitions populate the first and second excited singlet states respectively, it is not obvious that the transient absorption proceeds from these states - particularly as the shape of this region of the transient spectra recorded at the peak of the laser pulse ($t = 0$) is so similar to that at later times. In addition, the unusual decay kinetics displayed by many of the solutions indicates an initial component that is too long-lived to be of singlet origin.

Transient response more characteristic of excited singlet absorption is evident between 580-640 nm (with a peak at 620 nm) in solutions of H_2Pc , $MgPc$, $AlPcCl$, and to a lesser extent, $ZnPc$ - compounds that are either metal-free, or contain central metal atoms in which the electrons are paired. It is concluded that a lack of such absorption in solutions of $VOpc$ and $CuPc$ is due to an efficient quenching of the lowest excited singlet states of these compounds - induced by the presence of unpaired electrons. The effect of the central metal atom is also displayed by the decay of the longer-lived transient species. For $VOpc$ in toluene, this decay is rapid and, within experimental error,

proceeds at the same rate in both of the solutions tested, irrespective of the wavelength of pumping. However, there is a difference between the calculated time of recovery from ground-state depletion (average = 8.7 ns) and the decay of the transient absorption at 490 nm (average = 11.0 ns). The existence of this effect is confirmed by the response of CuPc in 1-chloronaphthalene to 694 nm irradiation (ground-state recovery = 34.2 ns, transient decay = 45.6 ns). This presents the apparent paradox that the ground-state recovery is complete while the transient species are still actively absorbing visible light.

The only way that such behaviour can be explained is by the convolution of more than one absorbing component in a particular spectral region. If this region is one of strong ground-state depletion, an additional positive transient absorption component would be necessary to reduce the measured recovery-time. It is emphasised that such an additional component must behave with kinetics that are different from those of the 'dominant' triplet states, since the co-existence of triplet absorption and ground-state depletion in a particular spectral region has the effect of reducing the amplitude of response, but does not affect the rate parameter of triplet decay.

The existence of such an additional absorbing component in a region of strong transient absorption would have the effect of lengthening the decay time.

Since it has not been possible to determine whether such a component is absorbing light in only one of these two spectral regions, or in both (and in which proportion), the values of decay of transient absorption for these solutions of VOPc in toluene and CuPc in 1-chloronaphthalene are assumed to be upper limits, while those for ground-state recovery are assumed to be lower limits.

The solutions that contain phthalocyanine compounds with central atoms that have a totally paired electron arrangement exhibit a transient response which includes a long-lived component. However, the kinetics are not simple - particularly evident is an increase in amplitude of absorption over the initial 500 ns or so. That this gradual increase shows up in the spectral region that includes the Q-absorption bands of these compounds is indicative of a positive absorption component occurring across the whole of the spectral range studied. Indeed it is possible that such behaviour is a manifestation of the type of transient component that perturbed the decay times of VOPc and CuPc solutions.

It is not clear what in the nature of the transient species causes so devious a deviation from the 'simple' photophysical processes illustrated by the Jablonski diagram (Fig. 1.4), yet still exhibits a spectrum that resembles that of the triplet state of phthalocyanine compounds. It may be convenient to invoke the observations of Jacques and Braun

that the tendency of phthalocyanine compounds to form molecular aggregates affects their transient response to high-intensity laser excitation in such a way as to behave in the manner of colloids.(108) However, the presence of aggregates is not evident from the ground-state absorption spectra and there is not significant indication of deviation from Beers law upon change of solution concentration (table 4.7).

Therefore it seems likely that a combination of excited states and perturbing species is induced by laser irradiation.

The effect of the CuPc chromophore in quenching the excited state of 1-chloronaphthalene, as demonstrated by the overall reduction in amplitude of transient absorption and fluorescence emission by the solvent, is representative of a simple energy-transfer process. Although it is not possible to accurately resolve the decay times of the laser-induced light emission, a qualitative assessment of fig. 4.33 indicates that, as would be expected in such a quenching process, the addition of the chromophore effects a reduction in emissive lifetime. It is clear that since the concentration of CuPc relative to that of the solvent molecules is small, the process by which energy is transferred to the phthalocyanine compound must be efficient.

5.3 'RED' FLUORESCENCE

The use of the fluorimeter in recording the 'red' fluorescence from phthalocyanine solutions was found to be impractical, due to the low sensitivity of the photomultiplier tube cathode material to light in this wavelength region. Therefore the discussion refers only to laser-induced emission.

Like the transient absorption assigned to the lowest excited singlet state, this fluorescence was found to be a property of only those phthalocyanine compounds that are either metal-free, or contain "electron-paired" central metal atoms. In common with previous reports (66,74,77), no such emission was recorded from solutions of VOPc and CuPc. The observation that the fluorescence and transient absorption can proceed from state S_1 , even with pumping of the Soret band, indicates an efficient internal conversion process ($S_2 \rightarrow S_1$).

The spectral distribution of the light emitted from H_2Pc and $AlPcCl$ is identical for either wavelength of excitation, and includes photons more energetic than those of the ruby laser fundamental wavelength. This suggests that high-intensity pumping at 694 nm induces biphotonic absorption, with subsequent relaxation to the emitting state.

Although fluorescence from H_2Pc , $AlPcCl$, $ZnPc$ and $MgPc$ occurs in a spectral region which includes wavelengths shorter than

the peak of the purely electronic absorption transition, the emission is much lower in intensity than that corresponding to the peaks of highly allowed $S_{10} \rightarrow S_{0n}$ transitions and there is no vibronic evidence with which to categorise it as 'hot-band' fluorescence.

The magnitudes of the calculated fluorescence decay times when excited at 347 nm [AlPcCl in ethanol = 10.4 ns, ZnPc in ethanol = 6.3 ns, MgPc in ethanol = 7.3 ns], which are upper limits to the fluorescence lifetimes, are in good agreement with previous observations.^(83,85) The effect of high-intensity red excitation appears to be to lengthen the emissive lifetime. This occurs in AlPcCl [14 ns] and is most apparent for H₂Pc in o-xylene. It has previously been suggested⁽⁸⁸⁾ that this effect may be due to a 'delayed' fluorescence, following triplet-triplet absorption of laser light during the period of excitation, with subsequent inter-system crossing to the singlet manifold. Although all indications are that the triplet extinction coefficient at 694 nm is small, and mindful of the fact that such a process is biphotonic, the high intensity of the ruby laser makes such an effect feasible.

5.4 'BLUE' FLUORESCENCE

While it is recognised that dual fluorescence (the simultaneous emission from two different excited singlet states) is becoming a well documented property of

tetrabenzporphins(112,113), the 'anomalous blue fluorescence' reported in this and previous studies from phthalocyanine compounds (tetrazatetrabenzporphins) clearly does not originate from the excited singlet states. This is shown by the occurrence of peaks in the emission spectra at wavelengths that correspond to energies lower than the Soret transition. Also, the intensity of emission is too great to be compared to that reported as fluorescence from vibrational levels of the lowest electronic singlet state ($S_{1n} \rightarrow S_{0n}$). (75,76)

This observation ties-in with those of Muralidharan et al., (81,82) although their claim that the emission occurs within the triplet manifold bears further investigation, particularly as the two variants of the technique of purification adopted here produced solutions that show markedly different yields of this type of emission.

It is possible that the effect of purification method B, which chiefly differs from method A by the increased thoroughness of washing with HCl (Appendix 4), could be to perturb the phthalocyanine ring in such a way as to prevent emission. However, such a chemical change would also be expected to affect the transient absorption spectrum, and no such effect is observed.

If the emission originates from an impurity, it seems unusual that, although the overall character of the emission is

similar for all of these compounds, the peaks vary slightly in position (390 nm - 430 nm). Yet the absorption responsible for populating the emissive state is shown by the excitation spectra to peak within the narrow wavelength range of 300 nm - 310 nm. No deduction regarding the nature of any such impurity is made.

5.5 SUMMARY AND TIPS FOR FUTURE WORK

This work shows that a short-lived transient absorption, which can be assigned to absorption from the lowest excited singlet state, and an intense 'allowed' fluorescence transition occurs following excitation in either the Soret band or the Q-band of phthalocyanine dyes. This provides evidence of a rapid degradation of energy from the electronic state S_2 . However, a complete picture, i.e. one that exhibits the processes occurring across the entire visible spectrum, is not so easy to interpret because of the complex kinetics that are displayed - kinetics that are not characteristic of excited-state absorption. Therefore it must be emphasised that in order to monitor the intramolecular relaxation processes within these compounds, it is imperative that the effects of dimer or aggregate formation - whether in equilibrium, or laser-induced - are avoided. The difficulties of such a requirement are illustrated not only in this work, but also in several of the studies outlined in Chapter 3.

One particular method that is reported to be successful in physically separating the chromophores is their inclusion in micelles: Darwent(114) has shown that both ZnPc and its sulphonated derivative can be included in a cationic or neutral micelle solution, with no evidence of the presence of dimers or oligomers at a molecular concentration of 2×10^{-5} M.

A further demand upon the choice of solvent or host medium is that, in order to be able to excite dye molecules in different regions of the spectrum, the solvent should transmit light across the whole of the spectral range involved. The relative insolubility of phthalocyanine dyes in solvents that allow excitation at 347 nm has, in this work, allowed a comparative study (i.e. of 694 nm and 347 nm-induced spectra) to be made for two compounds only (VOPc and AlPcCl). The absorption of pump-light by 1-chloronaphthalene has precluded a kinetic analysis of 347 nm-induced response in CuPc and has allowed only an indirect method of obtaining transient spectra.

A recent development, that has already been applied to both conventional and time-resolved spectroscopic studies(115,116) is the use, as a solvent, of Xenon in the liquid state. The large polarisability of molecular Xenon allows an interaction with the solute that is not chemically or structurally disruptive. In addition, the transmission of light across a spectral range that stretches from the vacuum ultra-violet

into the infra-red means that deleterious features of solvent interference can be avoided.

The types of molecule that have been found to be soluble in Xenon include hydrocarbons, organic acids and, to a lesser extent, certain biological compounds. It is considered (117) that the phthalocyanine dyes are also suitable for inclusion in this medium.

It is clear that not all metal phthalocyanine solutions possess an absorption band that is conveniently located to allow excitation at 694 nm - for example the principal absorption band in ethanol solutions of ZnPc and MgPc is centred on 665 nm and 666 nm respectively. Thus, even though the ruby laser has been, and still is, an important tool in many studies involving phthalocyanine compounds, the fixed output wavelength can be a limitation.

For this reason, and because of the limitation upon time-resolution imposed both by the output of the ruby laser in the Q-switched mode and by the detection system, it is concluded that the experimental arrangement used in this study is not the most suitable with which to monitor the primary energy redistribution processes.

As mentioned in Chapter 2, the synchronously-pumped, mode-locked dye laser provides a source of excitation that is wavelength tunable and which consists of a continuous train

of low energy pulses, a number of picoseconds in duration. Therefore several advantages might be gained by applying picosecond techniques to the study of phthalocyanines.

Finally, the results presented in this work serve to emphasise that, in order to be able to categorise the 'blue' fluorescence as a real property of these compounds, it is imperative that the level of impurity should be minimized. For this reason, the reader is referred to the recent report by Wagner et al.(118) which deals specifically with the purification of phthalocyanine dyes.

Appendix 1

Phthalocyanines in use

The physical properties of phthalocyanine compounds have allowed a wide variety of uses in both applied science and industry. The scientific uses have been realised mainly as a consequence of the type of spectroscopic studies touched upon in Chapter 3. For example, the suitability of certain metal phthalocyanine solutions as repeatable Q-switch elements is directly related to the high absorptivity of many such solutions at the ruby laser fundamental wavelength.

The same research group that developed this form of passive Q-switching - that led by Peter Sorokin at the Watson Research Centre of I.B.M. - also made the first discovery of laser emission from organic dye molecules. This discovery was initially a fortuitous one in that a solution of AlPcCl in ethyl alcohol was subject to high-intensity giant-pulse ruby laser irradiation in an attempt to observe Stimulated Raman Scattering. However, an unexpected type of emission was observed in the near infra-red, which, when the dye cell was incorporated into a suitable resonant cavity was shown to consist of an intense laser line at 755.5 nm. Although the phthalocyanines were subsequently found to be of limited use as laser dyes (they require a high pumping intensity to achieve threshold and they emit only over a narrow bandwidth), this discovery led to the investigation of many

other fluorescent dyes as potential laser media. The result has been the development of the dye laser, a source of coherent light that is tunable over the entire visible spectrum and beyond.

A novel use of a solution of AlPcCl in ethanol is the pseudoholographic effect described by Sawatari and Shupe.(119) They report the use of the dye solution for wavefront multiplication in which two halves of a Q-switched frequency-doubled ruby laser pulse are recombined at a cell containing the dye. This recombination generates a spatial gain and index of refraction distribution which is used to modulate the amplitude and phase of an optical field in the amplification band of the dye in order to form a new wavefront.

As early as 1941, Vartanyan and Terenin(120) were able to demonstrate the presence of electron and hole photoconductivity in various organic molecular crystals such as photographic sensitizers, polyacenes, phthalocyanines and biological pigments. Since this time a number of phthalocyanine compounds have been found to exhibit a potential use as organic photovoltaic cells (121-124) - they have been shown to produce efficient photogeneration in response to light from 400 - 700 nm.(125)

A group at Durham University(126) have developed the use of phthalocyanine compounds as Langmuir-Blodgett films for use

on the surface of various semi-conductors. The aim is to fabricate simple structures that may be an improvement on existing devices or which could find applications as sensitive and selective transducers.

An area of solar energy research that is currently very attractive is the photolysis of water by sunlight into hydrogen and oxygen. Since water is translucent, such a reaction must be sensitized by a visible light absorber. A group at the Royal Institution are just one of several that have been working on the photo-oxidation and photo-reduction of water with metal porphyrins and phthalocyanines as sensitizers.(127) One form of such an artificial photosynthetic process is the hydrogen generating system consisting of a sensitizer, an electron relay, a colloidal platinum catalyst and a sacrificial electron-donor, all suspended in water.(128) On exposure to visible light, hydrogen is released and the electron donor consumed. Harriman et al.(129) have studied the photoreduction of the solution often used as electron-relay (methyl viologen) following singlet-state sensitization from a MgPc^{4+} (a tetra[N-methylazaphthalocyanine]). The phthalocyanine skeleton was chosen because of the favourable absorption spectrum and the magnesium derivative since it has a fairly long S_1 lifetime. Also, this compound is water soluble and is estimated to have a potential for collecting up to 45% of the solar spectrum. Emphasis should be placed upon the word "potential" however, since to date, success with such systems

has been limited.

Information storage is another area in which the light absorption by phthalocyanines is exploited. The use of a narrow line-width, tunable dye laser to bleach a molecule located at a particular molecular site has been discussed.⁽¹³⁰⁾ The spectral width of the absorption band is broad in comparison to the laser line-width and the laser is able to 'burn holes' in the absorption band, corresponding to bleaching at slightly different frequencies. The 'hole' may then be probed by a weaker laser beam in order to generate a simple digital code. It is estimated that H₂Pc dissolved in PMMA can store 1000 bits of information and in polyethelene, 10,000 bits. A barrier to the immediate progress of such optical computer memories is that the material must be kept at very low temperatures in order to prevent a reversal of the bleaching process.

Kivits et al.⁽¹³¹⁾ describe the use of a thin layer of VOPc on the surface of PMMA to provide a high density optical storage material that is stable against oxidation and corrosion and that absorbs light in the spectral region of semiconductor lasers. The ablation of the dye layer is said to be easily varied with laser power and exposure time.

The principal commercial use of a phthalocyanine compound is that of CuPc and its derivatives as pigments and dyes. The disulphonated copper derivative is used to dye cotton a shade

of turquoise blue, and more complex derivatives of copper and other metal phthalocyanines have been patented for use as dyes. Non-colourant applications of phthalocyanines include their use as thickening agents in silicones or stable oils to form greases, and an addition of between 0.1% to 10% of H_2Pc to polyphenyl coolants in nuclear reactors improves their resistance to neutron-induced deterioration. Such applications are a consequence of the high thermal and chemical stability that these compounds possess.

This work, like many others before it, justifies the study of phthalocyanine compounds partly on the basis of their structural similarity to the naturally occurring porphyrin compounds. While comparison of the properties of these compounds is valuable, the much-vaunted role of the phthalocyanines as 'stable model compounds' for the porphyrins is doubtful and, in the light of the large amount of experimental procedure to which the porphyrins have been subject in their own right, unnecessary.

Appendix 2

Intensity dependence of transient optical density

From equation 2.6, page 41, the transient optical density at wavelength, λ , and with excitation intensity, I , is given by:

$$\Delta O.D_t(\lambda, I) = C_t(I)l(\epsilon_t(\lambda) - \epsilon_g(\lambda)) \quad (1)$$

It has been shown by Lachish et al. (132) that C_t may be written as a function of the excitation intensity:

$$C_t(I) = C_0 [1 - \exp(-2.3 \Phi \epsilon_g(\lambda') I)] \quad (2)$$

where Φ = quantum yield of the excited state analysed.

I = excitation intensity (einstein/dm²).

$\epsilon_g(\lambda')$ = molecular extinction coefficient of the ground state at the wavelength of excitation.

Combining (1) and (2):

$$\Delta O.D_t(\lambda, I) = a (1 - e^{-bI}) \quad (3)$$

$$\text{where } a = [\epsilon_t(\lambda) - \epsilon_g(\lambda)] C_0 l \quad (4)$$

$$b = 2.3 \Phi \epsilon_g(\lambda) \quad (5)$$

In most cases the output of the laser is measured in mJ per pulse thus:

$$\Delta O.D_t = a (1 - e^{-BI}) \quad (6)$$

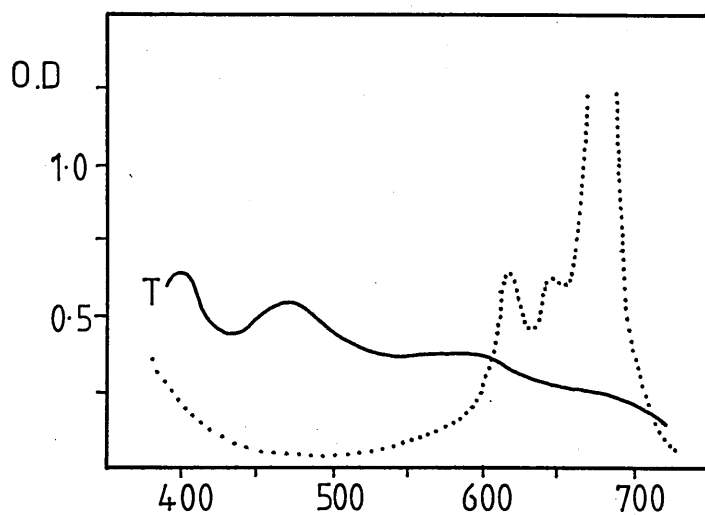
where $B = kb$, k being a constant relating to the experimental conditions.

'a' and 'B' may be determined by fitting an experimental set of values $\Delta O.D_t$, I , to equation (6) and from these the parameters $\epsilon_t(\lambda)$ and Φ may be determined, provided the

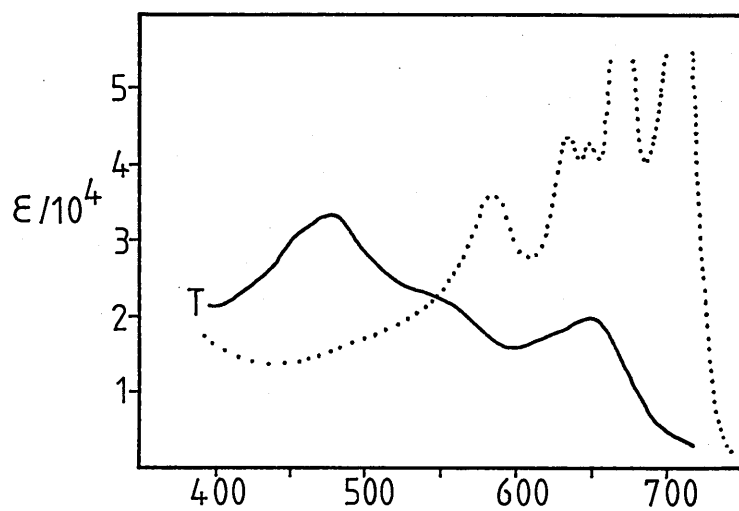
initial ground-state concentration (C_0) is known.

Appendix 3Phthalocyanines - a collection of transient absorption
spectra

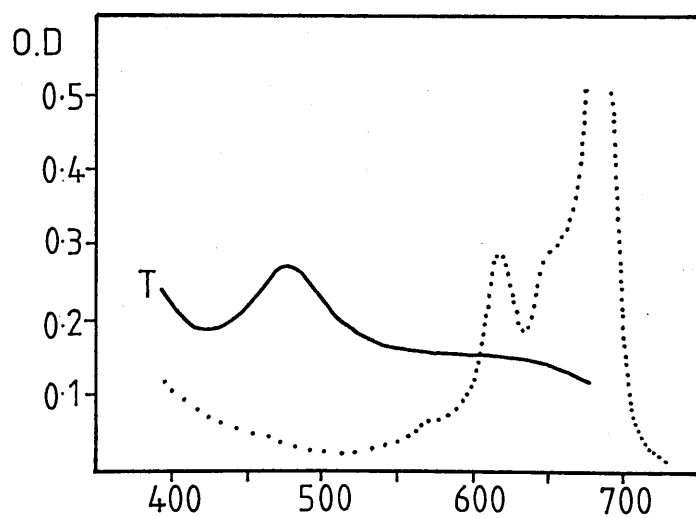
- (1) MgPc in pyridine - Livingston and Fujimori. ref. 101.
- (2) H₂Pc in 1-chloronaphthalene - Villar and Lindquist.
ref. 102.
- (3) MgPc in pyridine - Tsvirko, Sapanov and Solov'ev.
- (4) ZnPc in pyridine ref. 103
- (5) VOPc in nitrobenzene - Hodgkinson. ref. 34.
- (6) H₂Pc in toluene - Da-Silva.
- (7) VOPc in toluene Ref. 35.
- (8) CuPc in 1-chloronaphthalene
- (9) H₂Pc in 1-chloronaphthalene
- (10) VOPc in 1-chloronaphthalene - McVie. ref. 42.
- (11) CuPc, H₂Pc in 1-chloronaphthalene
- (12) H₂Pc in 1-chloronaphthalene
- (13) AlOHPC in 1-chloronaphthalene - Pyatosin and Tsvirko.
- (14) GaPcCl in chlorobenzene ref. 107
- (15) VOPc in chlorobenzene



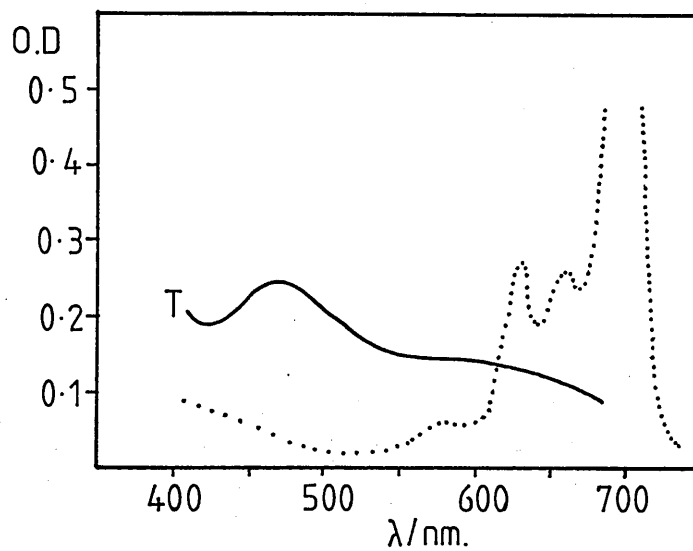
①



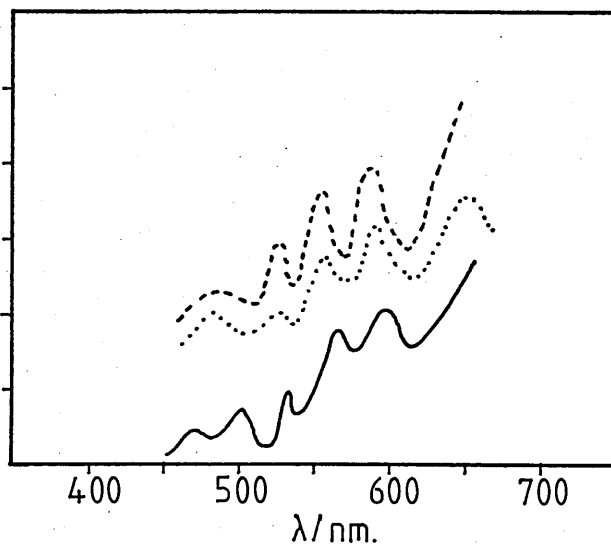
②



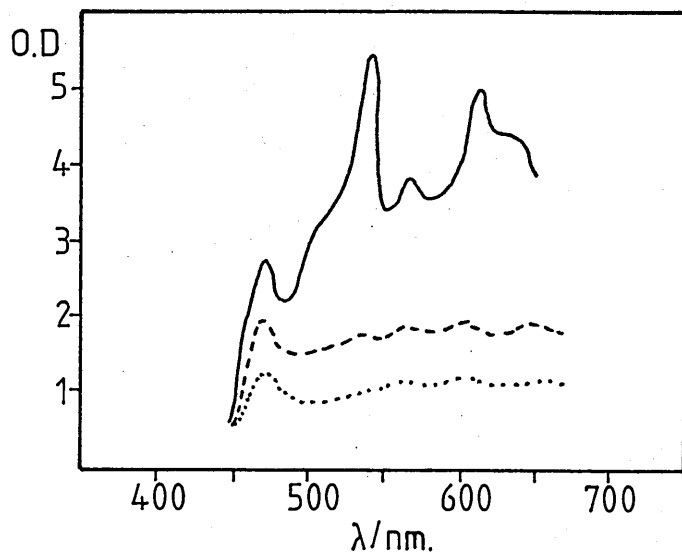
③



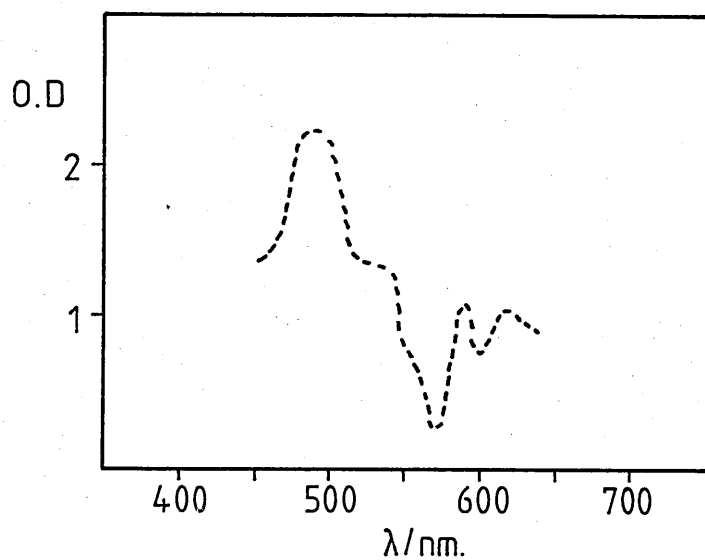
④



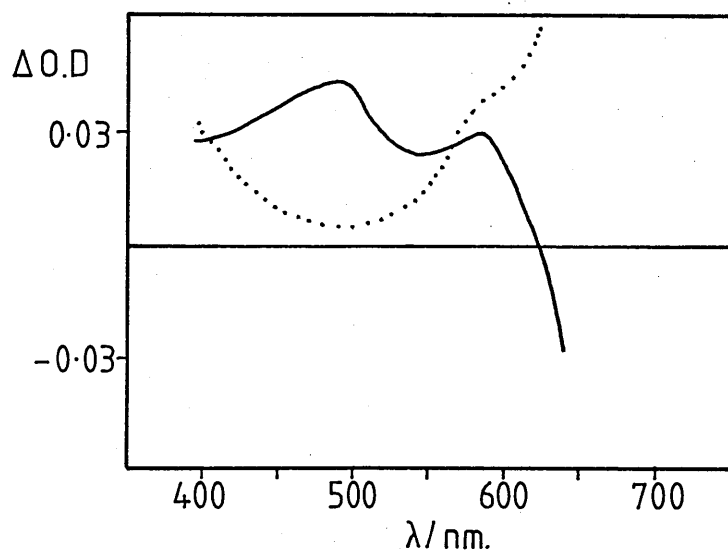
⑤



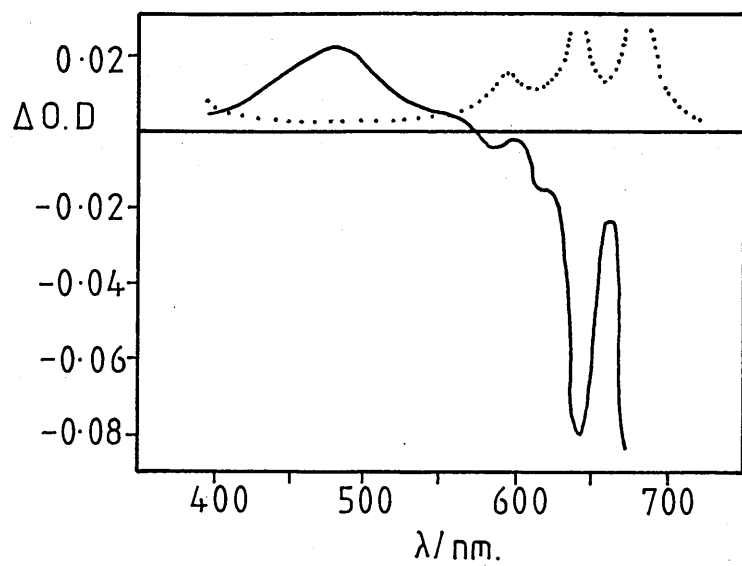
⑥



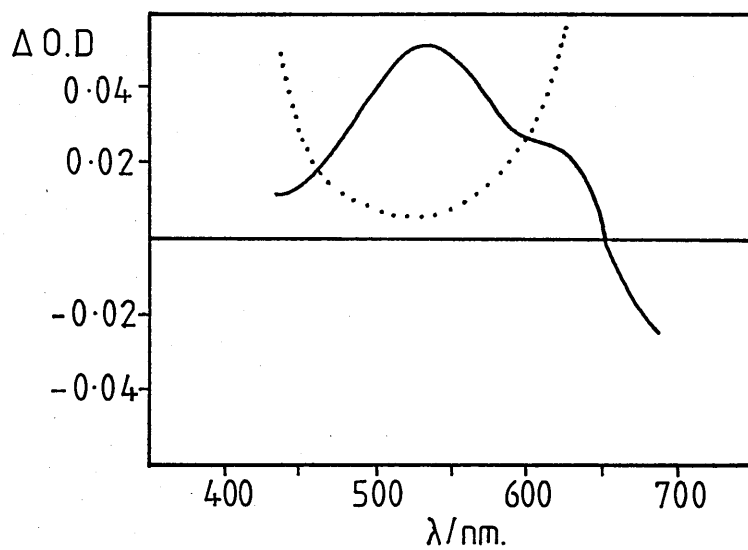
⑦



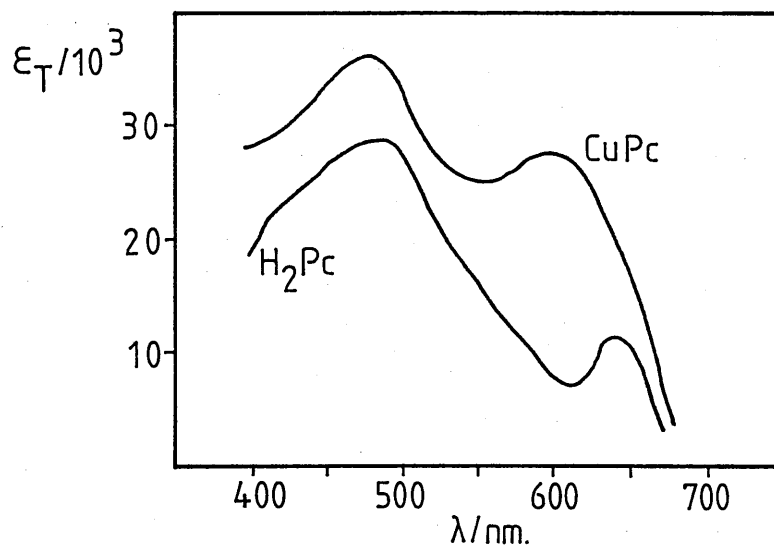
⑧



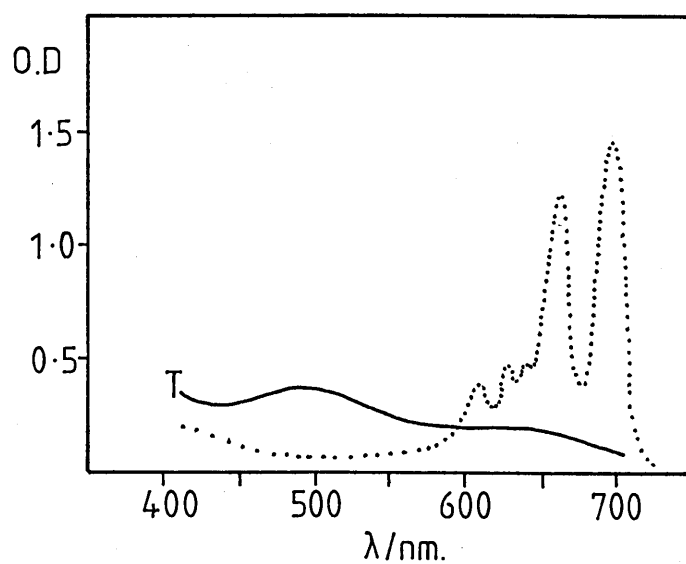
⑨



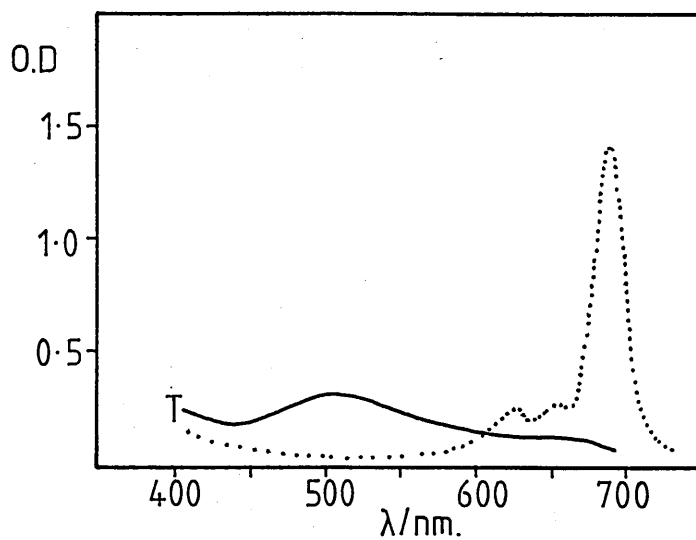
⑩



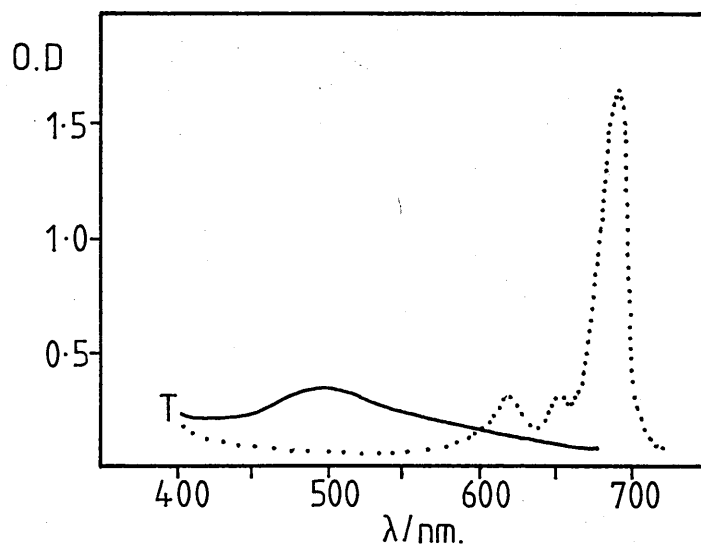
⑪



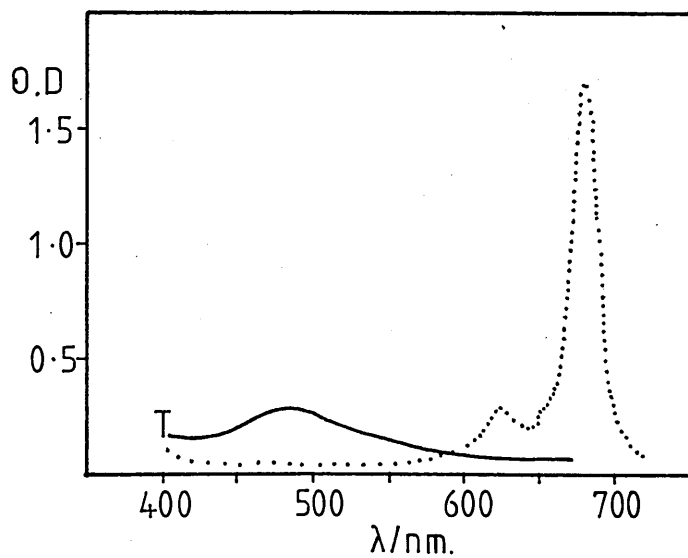
⑫



⑬



⑭



⑮

Appendix 4

Solute purification

Two methods of purification of the phthalocyanine compounds were attempted; referred to in Chapter 4 as methods A and B. Both involve using a scintered glass filter/water filter pump arrangement to wash the compounds with a sequence of solvents.

Method A

- (1) Place compound in scintered glass filter
- (2) Rinse with 5M HCl
- (3) Rinse with distilled water
- (4) Rinse with dimethyl formamide
- (5) Rinse with distilled water
- (6) Rinse with ethanol
- (7) Pour mixture of compound and ethanol into a beaker
- (8) Boil off ethanol

Method B

- (1) Soak compound in 5M HCl for several hours
- (2) Rinse with distilled water
- (3) Rinse with ethanol
- (4) Soak in a beaker of ethanol - allow excess solute to settle
- (5) Pour/boil off ethanol

The rationale for using these techniques is that the HCl solution should be effective in removing base impurities, and the dimethyl formamide (D.M.F) and ethanol solvents should remove organic impurities. The distilled water is used in an attempt to remove residual deposits of the HCl and D.M.F.

There are two reasons why method A is judged as being the less successful. Firstly, rinsing with HCl is not as effective as 'a good soak'. Secondly, there were, in some instances, an indication that the D.M.F solvent was difficult to completely remove.

Fig.A4.1 shows the absorption spectra of ethanol solutions of non-purified MgPc and ZnPc. It can be seen that, compared to the spectra of the purified solutions (shown in Chapter 4), there are extra absorption regions. In the case of MgPc in ethanol the impurity shows up as a very intense absorption to the short wavelength side of the phthalocyanine Soret band, with a maximum optical density at ≈ 250 nm. That in the solution of ZnPc in ethanol shows up as a broad absorption of moderate intensity from ≈ 500 nm into the near u-v. It is notable that the impurity level of the compound is so high and that the impurity is different in these two cases. An analysis of the method of preparation of these compounds may yield the nature of such impurities, but such an analysis is beyond the scope of this work.

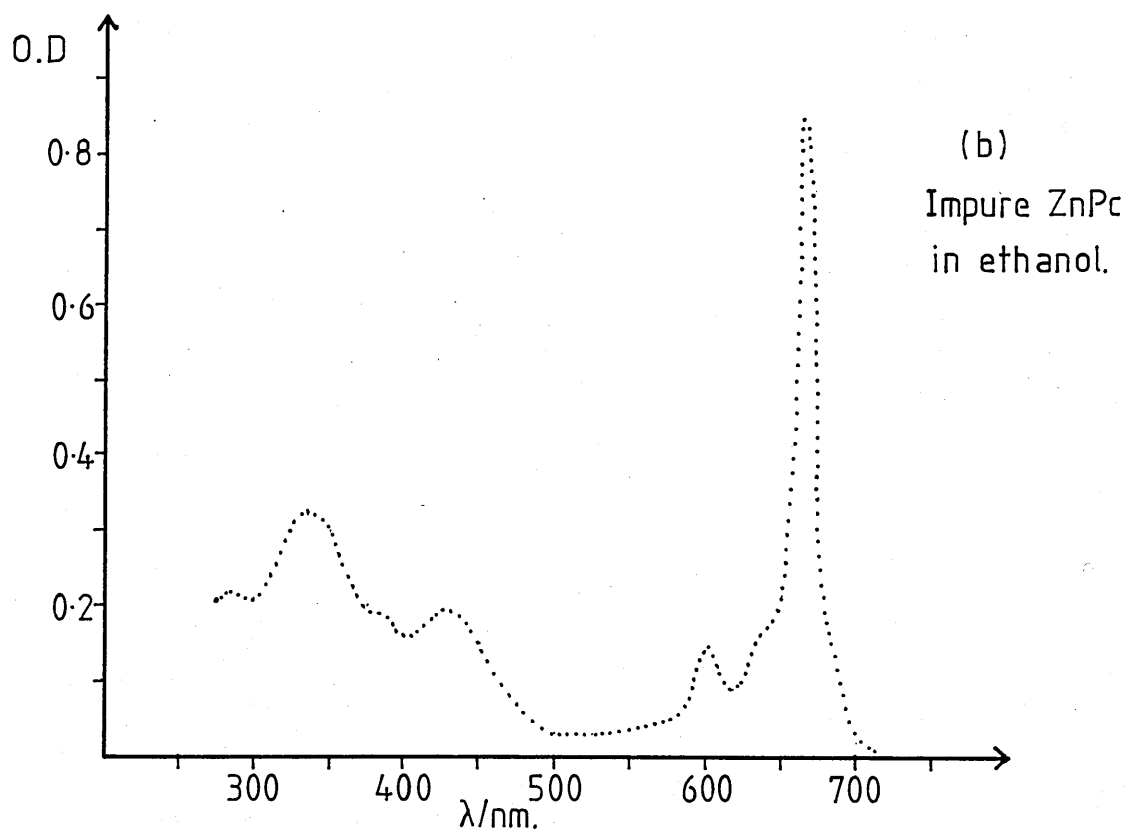
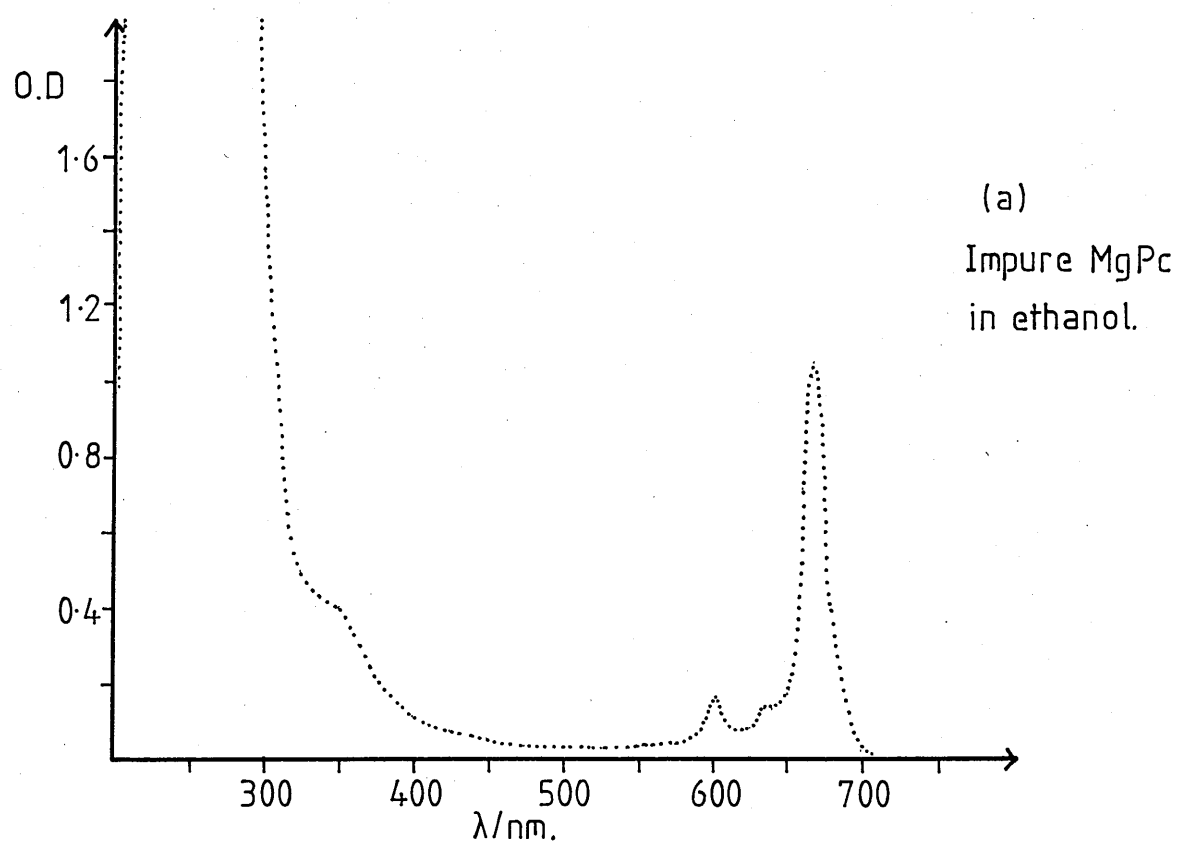


Fig.A4.1: Ground-state absorption spectra.

REFERENCES

- (1) L. Pauling. J.Am.Chem.Soc. 53,1367. 1931.
- (2) E.g.: B.P. Straughan and S. Walker. "Spectroscopy 3". Chapman and Hall. 1976.
- (3) E.g.: W. West in "Technique of Organic Chemistry" vol.IX, part I. Wiley. 1968.
- (4) E.g.: B.J. Snavely in "Organic Molecular Photophysics" vol.1. Wiley. 1973.
- (5) E.g.: J.B. Birks. "Photophysics of Aromatic Molecules". Wiley. 1970.
- (6) F. Hund. Z. Physik. 40,742. 1927.
- (7) M. Kasha. Disc. Faraday Soc. 9,14. 1950.
- (8) M. Beer and H.C. Longuet-Higgins. J.Chem.Phys. 23,8,1890. 1955.
- (9) E.g.: J.A. Barltrop and J.D. Coyle. "Excited States in Organic Chemistry". Wiley. 1975.
- (10) J.B. Birks and D.J. Dyson. Proc.Roy.Soc. A275,135. 1963.
- (11) G.N. Lewis and M. Kasha. J.Am.Chem.Soc. 67,994. 1945.
- (12) G.N. Lewis, M. Calvin and M. Kasha. J.Chem.Phys. 17,804. 1949.
- (13) J.F. Rabek. "Experimental methods in Photochemistry and Photophysics." Wiley. 1982.
- (14) G.C. Pimentel and K.C. Herr. J.Chim.Phys. 61,1509. 1964.
- (15) R.G.W. Norrish and G. Porter. Nature. 164,658. 1949.

- (16) G. Porter. Proc.Roy.Soc. A200,284. 1950.
- (17) H. Linschitz and K. Sarkanen. J.Am.Chem.Soc. 80,4826. 1958.
- (18) L. Pekkarinen and H. Linschitz. J.Am.Chem.Soc. 82,10,2407. 1959.
- (19) L. Hundley, T. Coburn, E. Garwin and L. Stryer. Rev.Sci.Inst. 38,488. 1967.
- (20) G. Porter and M.W. Windsor. J.Chem.Phys. 21,2088. 1953.
- (21) G. Porter and M.W. Windsor. Proc.Roy.Soc. A245,238. 1958.
- (22) F.J. McClung and R.W. Hellwarth. J.App.Phys. 33,3,828. 1962.
- (23) P.P. Sorokin, J.J. Luzzi, J.R. Lankard and G.D.Pettit. I.B.M. Journal. 8.182. 1964.
- (24) J.R. Novak and M.R. Windsor. J.Chem.Phys. 47,3075. 1967.
- (25) G. Porter and M.R. Topp. Nature. 220,1228. 1968.
- (26) R. Bonneau, J. Faure and J. Joussot-Dubien. Chem.Phys.Letts. 2,65. 1968.
- (27) H.W. Mocker and R.J. Collins. App.Phys.Letts. 7,270. 1965.
- (28) A.J. De-Maria, D.A. Stetser and H. Heynau. App.Phys.Letts. 8,7,174. 1966.
- (29) Y. Suzuki, Y. Tsuchiya, K. Kinoshita, M. Sugiyama, E. Inuzuka. Phil.Trans. R.Soc.Lond. A298,295. 1980.
- (30) T. Doust in "Picosecond Chemistry and Biology" Science Reviews Ltd. 1984.

- (31) D. Von der Linde }
 K.B. Eisenthal }
 A.J. Campillo } In "Topics in Applied Physics
 vol.18. Ultra-short light
 pulses" Springer. 1977.
- (32) E.g.: "Springer series in Chemical Physics, vol 3:
 Advances in Laser Chemistry" Springer. 1978.
- (33) P.M. Rentzepis. Science. 202,174. 1978.
- (34) K.A. Hodgkinson. Ph.D. Thesis. University of
 Manchester. 1972.
- (35) M.F. Da-Silva. Ph.D. Thesis. University of
 Manchester. 1976.
- (36) G. Porter and M.A. Topp in "Techniques in Chemistry,
 vol.VI. part II. Wiley. 1974.
- (37) R.S. Adhav and A.D. Vlassopoulos. Laser Focus. 47.
 May 1974.
- (38) W.F. Kosonocky, S.E. Harrison and R. Stander.
 J.Chem.Phys. 43,3,205. 1964.
- (39) D. Bebelaar. Chem.Phys. 3,205. 1974.
- (40) B.W. Hodgson and J.P. Keene. Rev.Sci.Inst. 43,3,493.
 1972.
- (41) T.R. Evans in "Techniques in Chemistry, vol.XVII."
 Wiley. 1982.
- (42) J. McVie. Ph.D. Thesis. Paisley College. 1979.
- (43) S.J. Formosinho, G. Porter and M.A. West.
 Chem.Phys.Letts. 6,1,7. 1970.
- (44) J.W. Hunt and J.K. Thomas. Radiation Research.
 32,149. 1967.
- (45) G. Beck. Rev.Sci.Inst. 47,5,537. 1976.
- (46) J.W. Hunt, C.L. Greenstock and M.J. Bronskill.
 Int.J.Radiat.Phys.Chem. 4,87. 1972.

- (47) A. Fenster, J.C. Leblanc, W.B. Taylor and H.E. Johns.
Rev.Sci.Inst. 44,6,689. 1973.
- (48) B. Amand and R.V. Bensasson. Chem.Phys.Letts.
34,1,44. 1975.
- (49) I.A. Ramsay. Ph.D. Thesis. University of Manchester.
1966.
- (50) A. Braun and J. Tcherniac. Ann.Ber. 40,2709. 1907.
- (51) H. de Diesbach and E. Von der Weid. Helv.Chim.Acta.
10,886. 1927.
- (52) A.G. Dandridge. H.A. Drescher and J. Thomas.
Brit.Pat. 332. 169. 1929.
- (53) R.P. Linstead. Brit.Assoc.Adv.Science Report. 465.
1933.
- (54) R.P. Linstead. J.Chem.Soc. 106. 1934.
- (55) G.T. Byrne, R.P. Linstead and A.R. Lowe. J.Chem.Soc.
1017. 1934.
- (56) J.M. Robertson. J.Chem.Soc. 615. 1935.
- (57) J.M. Robertson and I. Woodward. J.Chem.Soc. 219.
1937.
- (58) H. Kuhn. J.Chem.Phys. 16.840. 1948.
- (59) H. Kuhn. Prog.Chem.Org.Nat.Prod. 16,169. 1958.
- (60) A. Chikayama, Y. Ooshika, R. Itoh and I. Oshida.
J.Phys.Soc.Japan. 12,1316. 1957.
- (61) I. Chen. J.Mol.Spectrosc. 23,131. 1967.
- (62) A. Henriksonn and M. Sundbom. Theor.Chim.Acta.
27,213. 1972.
- (63) J.S. Anderson, E.F. Brabrook, A.H. Cook and R.P.
Linstead. J.Chem.Soc. 1151. 1938.

- (64) V.B. Estigneev and A.A. Krasnovskii. D.A.N. S.S.R. 58,1399. 1947.
- (65) J.M. Assour and S.E. Harrison. J.Am.Chem.Soc. 87,3,651. 1965.
- (66) D. Eastwood, L. Edwards, M. Gouterman and J. Steinfield. J.Mol.Spect. 20,381. 1966.
- (67) L. Edwards and M. Gouterman. J.Mol.Spect. 33,292. 1970.
- (68) O.L. Lebedev and V.S. Nasonov. Opt.Spectrosc. 23,170. 1967.
- (69) A.D. Britt and W.B. Moniz. Appl.Spectrosc. 31,2,104. 1977.
- (70) M. Abkowitz and A.R. Monohan. J.Chem.Phys. 58,6,2281. 1973.
- (71) R.S. Becker and M. Kasha. J.Am.Chem.Soc. 77,3669. 1955.
- (72) J.B. Allison and R.S. Becker. J.Chem.Phys. 32.5.1410. 1960.
- (73) A.N. Sidorov and I.P. Kotlyar. Opt.Spectrosc. 11,92. 1962.
- (74) P.S. Vincett, E.M. Voigt and K.E. Rieckhoff. J.Chem.Phys. 55,8,4131. 1971.
- (75) E.R. Menzel, K.E. Rieckhoff and E.M. Voigt. Chem.Phys.Letts. 13,6,604. 1972.
- (76) K. Yoshino, M. Hikida, K. Kaneto and Y. Inuishi. J.Phys.Jap. 1105,171. 1972.
- (77) K.E. Rieckhoff and E.M. Voigt. Proc.Int.Conf.Lumin. 295. 1968.

- (78) T.H. Huang and J.H. Sharp. Chem.Phys. 65,205. 1982.
- (79) W.E.K. Gibbs. Appl.Phys.Letts. 11,4,113. 1967.
- (80) A. Szabo and L.E. Erickson. J.App.Phys. 40,9,3574. 1969.
- (81) S. Muralidharan, G. Ferraudi and L.K. Patterson. Inorg.Chim.Acta. 65,L235. 1982.
- (82) G. Ferraudi and S. Muralidharan. Inorg.Chem. 22,1369. 1983.
- (83) O.D. Dmetrievsky, V.L. Ermolaev and A.N. Terenin. D.A.N. S.S.S.R. 114,4,468. 1957.
- (84) P.W.A. Bowe, W.E.K. Gibbs and T. Tregellas-Williams. Nature. 5018,65. 1966.
- (85) M.E. Mack. J.Appl.Phys. 39,2483. 1968.
- (86) A.S. Pine. J.Appl.Phys. 39,1,106. 1968.
- (87) J.H. Brannon and D. Magde. J.Am.Chem.Soc. 102,1,62. 1980.
- (88) S.E. Harrison and W.F. Kosonocky. Proc.Int.Conf.Lumin. 237. 1967.
- (89) C.R. Guiliano and L.D. Hess. I.E.E.E. J.Quantum Elec. Q.E.3,8,358. 1967.
- (90) P.P. Sorokin and J.R. Lankard. I.B.M. Journal. 10,162. 1966.
- (91) P.P. Sorokin, J.J. Luzzi, J.R. Lankard and G.D. Pettit. I.B.M. Journal. 11,130. 1967.
- (92) W.E.K. Gibbs and H.A. Kellock. I.E.E.E. J.Quantum Elect. 419. 1967.
- (93) B.I. Stepanov, A.N. Rubinov and V.A. Mostovnikov. Zh.Et.Pis'ma. 5,5,144. 1967.

- (94) C. Lin. I.E.E.E. J.Quantum Elect. 61. 1975.
- (95) R. Kugel, A. Svirmicks, J.J. Katz and J.C. Hindman.
Optics Comm. 23,2,189. 1977.
- (96) K.N. Solov'ev, V.A. Mashentzov and T.F. Kachura.
Opt.Spectrosc. R27,1,24. 1969.
- (97) J.A. Armstrong. J.App.Phys. 36,2,471. 1965.
- (98) M. Hercher, W. Chu and D.L Stockman. I.E.E.E.
J.Quantum Elec. Q.E.4,11,954. 1968.
- (99) Y.M. Gryaznov, O.L. Lebedev and A.A. Chastov.
Sov.Phys. J.E.P.T. 503, 1965.
- (100) S.P. Batashev, V.A. Gorbachev, L.D. Derkacheva, O.L.
Lebedev, N.G. Mek-hryakova, V.M. Mizia and V.A.
Petukhov. Sov.Journ.Quant.Elect. 9,11,1431. 1979.
- (101) R. Livingston and E. Fujimori. J.Am.Chem.Soc.
80,5610. 1958.
- (102) J.G. Villar and L. Lindquist. C.R. Hebd. Seances
Acad.Sci. 264,1807. 1967.
- (103) M.P. Tsvirko, V.V. Sapunov and K.N. Solov'ev.
Opt.Spect. 34,6,635. 1973.
- (104) W.F. Kosonocky and S.E. Harrison. J.Appl.Phys.
37,13,4789. 1966.
- (105) M.L. Spaeth and W.R. Sooy. J.Chem.Phys. 48,5,2315.
1968.
- (106) A. Muller. Z. Naturforsch. 23a,946. 1968.
- (107) V.E. Pyatosin and M.P. Tsvirko. Zh.Prikl.Spect.
33,2,320. 1980.
- (108) P. Jacques and A.M. Braun. Helv.Chim.Acta.
64,6,169,1800. 1981.

- (109) D.H. Levy. *Ann.Rev.Phys.Chem.* 31,197. 1980.
- (110) O.N. Koromaev and R.I. Personov. *Opt.Spectrosc.* 37,5,507. 1974.
- (111) G. Nouchi. *J.Chim.Phys.* 66,554. 1969.
- (112) L. Bajema. M. Gouterman and C.B. Rose. *J.Mol.Spect.* 39,421. 1971.
- (113) J. Aaviksoo, A. Freiberg, S. Savikhin, G.F. Stelmack and M.P. Tsvirko. *Chem.Phys.Letts.* 111,3,275. 1984.
- (114) J.R. Darwent. *J.Chem.Soc.Chem.Comm.* 805. 1980.
- (115) P.M. Rentzepis and D.C. Douglass. *Nature.* 293,165. 1981.
- (116) D.F. Kelley and P.M. Rentzepis. *Chem.Phys.Letts.* 85,1,85. 1982.
- (117) P.M. Rentzepis. Private Communication.
- (118) H.J. Wagner, R.O. Loutfy and C.K. Hsiao. *J.Mat.Sci.* 17,2781. 1982.
- (119) T. Sawatari and D.M. Shupe. *Appl.Phys.Letts.* 24,2,95. 1974.
- (120) A.T. Vartanyan and A.N. Terinin. *Zh.Fiz.Khium.* 15. 1941.
- (121) E.K. Putseiko and I.A. Akimov. *Iz.Akad.Nauk. S.S.S.R.* 301. 1959.
- (122) A. Ghosh, D. Morel, T. Feng, R.F. Shaw and C.A. Rowe. *J.Appl.Phys.* 45,230. 1974.
- (123) R.O. Loutfy. *J.Phys.Chem.* 86,3302. 1982.
- (124) R. Branston, J. Duff, C.K. Hsiao and R.O. Loutfy. *A.C.S.SYMP. S.* 220,437. 1983.
- (125) S. Grammatica and J. Mort. *Appl.Phys.Letts.*

38,6,445. 1981.

- (126) S. Baker, M.C. Petty, G.G. Roberts and M.V. Twigg.
Thin Solid Films. 99,53. 1983.
- (127) G. Porter. J.Photochem. 17,193. 1981.
- (128) L. Milgrom in 'New Scientist' 26. Feb.1984.
- (129) A. Harriman, G. Porter and M.C. Richoux.
J.Chem.Soc.Farad.Trans.2. 77,1175. 1981.
- (130) 'New Scientist' 295. May 1983.
- (131) P. Kivits. R. de Bont and J. Van der Veen.
Appl.Phys. A26,101. 1981.
- (132) U. Lachish, A. Shafferman and G. Stein. J.Chem.Phys.
64,2405. 1976.